# STABILITY PROFILING OF CERTAIN ACTIVE PHARMACEUTICAL INGREDIENTS

*A Thesis submitted in partial fulfillment for the Degree of*

**DOCTOR OF PHILOSOPHY**

**IN PHARMACY**

**GOA UNIVERSITY**

**By**

**RAHUL SUVARN CHODANKAR**
**Goa College of Pharmacy**
**Panaji-Goa**

**May 2023**

## DECLARATION

I, Rahul Suvarn Chodankar hereby declare that this thesis represents work which has been carried out by me and that it has not been submitted, either in part or full, to any other University or Institution for the award of any research degree.

Place: Panaji, Goa
Date : 22/05/2023

Rahul Suvarn Chodankar

## CERTIFICATE

I hereby certify that the above declaration of the candidate, name of the candidate is true, and the work was carried out under my supervision.

Dr. Anand A. Mahajan
Professor
Department of Pharmaceutical Analysis
Goa College of Pharmacy
Panaji, Goa, 403001

## ACKNOWLEDGMENT

Completing this thesis, a product of several years work, I feel deeply indebted to many people who have greatly inspired and supported me during my Ph.D. study at Goa College of Pharmacy and the writing of this thesis.

I want to thank my research guide, **Professor (Dr.) Anand A. Mahajan** for his invaluable guidance, encouragement, intellectual stimulus, and generous help from the inception to the completion of the research work. I consider it my destiny to do my dissertation under his guidance. I will not forget those enjoyable and illuminating discussions with him at each stage of my writing, which always turned out to be several hours long.

I am indeed obliged to **Dr. Gopal Krishna Rao**, principal and head of the research centre, Goa College of Pharmacy, for providing me with the opportunity, research facilities at every stage, and his constant encouragement to complete work on time.

My gratitude also goes to Professor **(Dr.) Sanjay Pai P.N.**, head of the department, of pharmaceutical chemistry, for his critical observations and suggestions for improving my research work. I am grateful to him for allowing me to use the departmental facilities on weekends and lending me HPLC columns for my research work.

I owe a huge debt of gratitude to Professor **(Dr.) Sudheer Moorkoth.**, head of the department, Department of Pharmaceutical Quality Assurance, Manipal College of Pharmacy, for his valuable feedback throughout the completion of my work. His calm and soothing demeanor reminded me of the importance of humility and good nature. He always provided help and support.

I'd like to show great thanks to **Dr. Vivek Kamat**, director, Directorate of Technical Education, Porvorim, Goa, for allowing me to enroll in the Ph.D. program and granting the required approvals.

I would like to express my thanks to the teaching members of Goa College of Pharmacy, for directly or indirectly extending their help at various stages of my work. Their guidance and encouragement infused me with confidence and enthusiasm. Special mention to **Dr. Madhusudan Joshi, Dr. Prashant Bhide. Dr. Rupesh Shirodkar, Dr. Shailendra Gurav, Dr. Raghuvir Pissurlenkar, Dr. Adison Fernandes, Rohan Prabhu, and Saba Jamadar.**

I would like to acknowledge the non-teaching staff of the college for their help in different ways during the duration of my research work, Sham Kharwat and Arlette Barreto need special mention.

I am thankful to Cadila Healthcare, Intas Pharmaceutical, and MSN laboratories for providing gift samples of the active pharmaceutical ingredients.

Finally, but not least, I express my gratitude to my family, friends, and well-wishers for their constant love, understanding, and encouragement.

Rahul Suvarn Chodankar

# Table of Contents

## Chapter 1



## Chapter 2

## Chapter 3



## Chapter 4



## Chapter 5

## Chapter 6

## Chapter 7



## Chapter 8

# List of tables

## Chapter 2



## Chapter 4



## Chapter 5

## Chapter 6



## Chapter 7

# Chapter 8

# List of figures

## Chapter 4

# Chapter 5

# Chapter 6

# Chapter 7

# List of abbreviations

| Abbreviation | | Definition |
|---|---|---|
| API | : | Active Pharmaceutical Ingredient |
| % RSD | : | Percentage Relative Standard Deviation |
| ~ | : | Approximate |
| ACN | : | Acetonitrile |
| amu | : | Atomic Mass Unit |
| ANDA | : | Abbreviated new drug application |
| BBB | : | Blood brain barrier |
| BP | : | British Pharmacopoeia |
| CAS | : | Chemical Abstracts Service |
| CDER | : | Centre for drug evaluation and research |
| CHMP | : | Committee for medicinal products for human use |
| DMF | : | Drug master file |
| DPs | : | Degradation products |
| ELSD | : | Evaporative light scattering detector |
| EP | : | European Pharmacopoeia |
| ESI | : | Electro Spray Ionization |
| FMTE | : | Felbamate |
| $H_2O_2$ | : | Hydrogen Peroxide |
| HALO | : | Haloperidol |
| HCl | : | Hydrochloric Acid |
| HPLC | | High Performance Liquid Chromatography |
| HPTLC | : | High Performance Thin Layer Liquid Chromatography |
| ICH | : | International Conference on Harmonization of Technical Requirements for Registration of Pharmaceuticals for Human Use |
| ID | : | Internal Diameter |
| IP | : | Indian Pharmacopoeia |
| *k'* | : | Capacity factor |
| LC-MS | : | Liquid Chromatography – Mass Spectrometry |
| LC-MS/MS | : | Tandem Mass Spectrometry |
| mg | : | Milligram |
| µg | : | Microgram |
| mL | : | Milliliter |

| | | |
|---|---|---|
| µm | | Micrometer |
| mM | : | Millmolar |
| mmu | : | Milli mass unit |
| N | : | Normality |
| n | : | Number of Sample |
| NaOH | : | Sodium Hydroxide |
| NDA | : | New drug application |
| nm | : | Nanometer |
| NTP | : | Number of theoretical plates |
| $^{o}C$ | : | Degree Centigrade |
| OECD | : | Organization for economic cooperation and development |
| OPA | : | Ortho Phosphoric Acid |
| PDA | : | Photo Diode Array Detector |
| PDE | : | Permitted Daily Exposure |
| PgP | : | P-glycoprotein |
| PIMO | : | Pimozide |
| QSAR | : | Quantitative structure-activity relationship |
| RDB | : | Ring double bond equivalent |
| RH | : | Relative Humidity |
| RID | : | Refractive index detector |
| RIO | : | Riociguat |
| RPC | : | Reversed Phase Chromatography |
| RRT | : | Relative Retention Time |
| Rs | : | Resolution |
| RSD | : | Relative Standard Deviation |
| RT | : | Room Temperature |
| SD | : | Standard Deviation |
| sGC | : | Soluble guanylate cyclase |
| SMILES | : | Simplified Molecular Input Line Entry System |
| TEA | : | Triethylamine |
| $T_f$ | : | Tailing Factor |
| TFA | : | Trifluoracetic acid |
| TLC | : | Thin layer chromatography |
| $t_R$ | : | Retention Time |
| TTC | : | Threshold for toxicological concern |
| US-FDA | : | United States Food and Drug Administration |
| USP | : | United States Pharmacopeia |
| UV | : | Ultraviolet |
| V | | Volts |

# Chapter 1

# Introduction

The pharmaceutical industry is expanding daily intending to develop new drugs extracted from natural substances or synthesized chemically. But one thing always remains constant, the products obtained or manufactured must be as pure as possible. Consequently, purity has always been regarded as crucial in ensuring drug quality[1].

During manufacturing processes such as chemical synthesis, extraction of natural products, isolation from cell culture or during storage of drug substances, impurities may be formed[2]. Impurity is "any part of a pharmaceutical product that is not the chemical entity defined as the active pharmaceutical ingredient (API) or the excipient"[3]. The International Council for Harmonisation of Technical Requirements for Pharmaceuticals for Human Use (ICH) categorizes impurities broadly into three groups: organic impurities, inorganic impurities, and residual solvents. They may be produced during production or storage and mainly comprise of starting material, by-products, and degradation products (DPs)[4].

Impurities are detrimental to the patient and can have adverse effects, e.g., they can act as inhibitors of the cytochrome P450 family of enzymes essential for detoxification or can be hepatotoxic, causing liver damage. Additionally, certain impurities (genotoxic) may cause mutations in genetic material. Genotoxic impurities have been suggested to play a crucial role in carcinogenesis and mutagenesis. The mutagenic carcinogen is detected using bacterial reverse mutation (mutagenicity ) assay[5-10].

Because the drug impurities significantly threaten public safety. Regulatory agencies have developed specific guidelines to address concerns about them. Guidlines Q3A(R2), Q3B(R2), and Q3C(R7) are developed by ICH for controlling impurities in the products for human use. These guidelines explain the various thresholds for reporting, identifying, and qualifying impurities in new drug substances and products. Qualifying an impurity involves

evaluating the biological safety of the impurity through clinical studies. Higher or lower qualification thresholds for a compound can be set based on the level of concern and scientific rationale. For instance, a lower qualification threshold may be required if the impurity present has the propensity to cause adverse drug reactions. However, these guidelines don't specifically mention genotoxic impurities[11-13].

The issue pertaining to genotoxic impurities is addressed separately in the ICH M7 guideline [14]. This guideline segregates the synthetic impurities and the degradation products into separate classes (I-IV) based on mutagenic and carcinogenic potential. The guidelines state that for impurity qualification, computational toxicology must be performed using QSAR (quantitative structure-activity relationship). Ideally, two QSAR methods should be used for predictions in combination for the best results. One methodology must be expert rule based while the second should be statistical based. These QSAR models should be validated based on the tenets set by Organisation for Economic Co-operation and Development (OECD). The absence of structural alerts from the complementary QSAR methods is sufficient to pass the impurity as one of no mutagenic concerns. The committee for medicinal products for human use (CHMP) of the European Medicine Agency had also established a guideline for limiting genotoxic impurities, which was in force from 1st January 2007 to 31st January 2018. At present, the ICH M7 guideline has superseded it[15].

The Centre for Drug Evaluation and Research (CDER) of the US Food and Drug Administration (US-FDA) has developed its guideline to address the issue of genotoxic impurities in commercially available drug formulations for human use [16]. This guideline states that the Drug Master File (DMF) holder or the Abbreviated New Drug Application (ANDA) applicant should give a sound rationale for selecting an acceptance criterion for an impurity. It further states that any impurity present in the drug substance that meets the USP specification or has been evaluated by in-vitro genotoxicity studies or evaluated with an acceptable QSAR database program is deemed qualified for ANDAs. This guideline classifies impurities based on their ability to cause genotoxicity: Class 1 impurities are those that are known to be both genotoxic and carcinogenic; Class 2 impurities are those that are known to be genotoxic but may not be carcinogenic; Class 3 an alerting structure that is unconnected to the API's structure and has an undetermined level of genotoxicity. Class 4 an alerting structure that is connected to the API. Class 5 no alerting structure or sufficient proof that there is no genotoxicity. The US-FDA guideline also offers a qualification

technique based on the threshold for toxicological concern (TTC) concept and the permitted daily intake (PDI).

Impurity profiling is a method for identifying, characterizing, and qualifying drug impurities[17]. This technique separates the drug from impurities using high-performance liquid chromatography (HPLC) or thin-layer chromatography (TLC). The RP-HPLC is the most widely used analytical tool for separating and quantifying impurities and is frequently coupled with a UV detector. At the same time, nuclear magnetic resonance (NMR) studies and mass spectrometry[18] are used for characterization. With the advent of the hyphenated techniques liquid chromatography can be conjugated with mass (LC-MS, LC-MS/MS) and NMR (LC-NMR), making the characterization of impurities a less tedious process.

According to ICH guideline Q1A (R2), stress studies or forced degradation studies can assist in identifying potential degradation pathways. It involves exposing the drugs to various stress conditions specified in the guideline, such as hydrolytic (acid, base, neutral), oxidative, thermal, and photolytic, to simulate environmental stress conditions the drug may be exposed throughout its life cycle[19-20].

According to the FDA guidelines, the stability-indicating method (SIM) is an analytical technique used to quantify degradation. A stability-indicating method is a validated quantitative analytical technique that can be used to determine how the stability of drug substances and drug products changes over time. Additionally, a stability-indicating approach is precisely used to monitor changes in the concentration of the active components, even if there is no involvement of additional degradation products, contaminants, or excipients[21].

Various in-silico tools can be used to evaluate the absorption, distribution, metabolism, excretion, and toxicity (ADMET) of a drug due to the rapid increase in the processing power of computers. Many computational approaches have been developed for predicting compounds' pharmacokinetic and toxicity properties based on the chemical structure like QSAR (major approach), similarity search, ligand-protein docking, and pharmacophore modelling. However, many of these tools are not free, limiting their utility for the scientific community. However, some are freely available for predicting ADME properties like pkCSM and SwissADME.

To predict mutagenicity there are two categories of tools 1) Rule-based or empirical expert systems and 2) statistical or QSAR-based systems. The DEREK and ToxTree (open-source) software packages employ the former method, whereas MultiCase and SciQSAR employ the latter. Ideally, both methods should be employed to validate potential mutagenic structural alerts in the chemical structures of impurities[22-24].

# 1.0. Prelude to the thesis

This thesis has eight chapters

**Chapter 1: Introduction**

This chapter mainly provides an overview of the drug impurities and the various regulatory guidelines pertaining to impurities. The overview also extends to other subjects like impurity profiling, forced degradation studies, stability-indicating assay methods and the *in-silico* approaches to predict ADMET properties.

**Chapter 2: General Literature Survey**

This chapter discusses impurity profiling, the role of stress studies in impurity profiling, and regulatory requirements. It also emphasizes developing and validating a stability-indicating HPLC method, characterization of degradant products by LC-MS and LC-MS/MS, and use of *in-silico* methods in predicting ADMET properties.

**Chapter 3: Research Envisage**

This chapter presents the aim and comprehensive plan of the current research work.

**Chapter 4, Chapter 5, Chapter 6 and Chapter 7**

Chapters 4 to 7 describes designing and development of research work related to impurity profiling of four drugs - pimozide, felbamate, haloperidol, and riociguat. Each of the four chapters represents the development and optimization of stability-indicating assay method using forced degradation studies, characterization of the degradation products (DPs) using LC-MS and LC-MS/MS, and their in-silico ADMET predictions.

**Chapter 8**

This chapter provides a summary and discussion of entire research work.

# Chapter 2

# General literature survey

General literature survey is segregated into the following parts.

2.0. Impurity profiling.

2.1. Introduction to stability indicating assay method (SIAM).

2.2. Instrumentation, parameters related to HPLC method development, mass and tandem mass spectrometry.

2.3. *In-silico* methods for predicting ADMET.

## 2.0. Impurity profiling

According to the ICH, impurity profiling is defined as “description of the known and unknown impurities present in a new drug substance. Impurity profiling involves the analytical activities that are used in detecting, identifying, or characterizing the chemical structure and quantitatively estimating the inorganic, organic impurities and the residual solvents present in the bulk drug and the finished dosage form.

Drug impurities are often termed as “pollutants” of the pharmaceutical world. During the synthesis of API, many starting material, intermediates, or reagents makes its way into ultimate drug substance. Few of these remain in the drug substance as impurities in low levels. These impurities may possess toxic properties and may pose safety risks. Impurities may also arise during storage when exposed to environmental conditions. The quality of the drug substance is considered compromised in purity even if the impurity present has better

pharmacological or toxicological properties. Any foreign material present in the drug substances has to be considered as impurity, whether inert or having superior pharmacological properties.

ICH has formulated practical guidelines for impurity control. Different compendias have already established acceptable impurity levels for APIs and formulations. This has increased the demand for impurity reference standards and API reference standards among regulatory authorities and pharmaceutical companies. Interestingly, quite a few companies have begun the synthesis and marketing pharmacopoeia-reference impurity standards.

ICH in their guideline Q3A(R2) have segregated impurities and have provided threshold for reporting, identification, and qualification based on the daily dose of the drug. Reporting threshold is a limit above which the presence of the impurity must be reported. Identification threshold is the limit above which the impurity must be identified whereas, qualification threshold defines the limit above which the biological safety of the impurity has to be established. This guideline has provided the essential framework to establish the impurity profile of a drug substance.

Historically, the purity of a drug was determined by the percentage of the labelled amount of API found in it using a suitable analytical method. Nowadays, the purity of a drug is determined by monitoring impurities, even if they do not affect the labelled content. As a result, everyone is required to perform impurity profiling for drugs and drug products in order to ensure their purity and comply with regulatory requirements[6, 25-27].

## 2.0.1. Impurity

The ICH guideline Q3A (R2) states under glossary that an impurity as “any component of the new drug substance that is not the chemical entity defined as the new drug substance. This definition of impurity is considered broad enough to encompass degradation products (DPs) as impurities. However, ICH to make matters explicit in its guideline Q3B(R2) has defined degradation product as “an impurity that is formed due to a chemical transformation in the drug substance during manufacturing or storage of the finished dosage forms by exposure to light, temperature, pH, water or by reaction with excipients or the immediate container closure system.

## 2.0.2. General terminologies used to describe impurities

Impurities have been called by different names by the several groups of scientists who have come across them. Some of the general terms used to describe impurities are mentioned below[28-29].

**By-products**

By-products are the unsolicited compounds that are formed during the chemical synthesis of an API.

**Degradation products**

This are the compounds that are formed due to decomposition of the API due to exposure to the environmental conditions, excipients, or the container closure system.

**Interaction products**

Interaction products are formed due to deliberate or inadvertent interactions between the various chemical involved.

**Intermediates**

The planned compounds formed while the synthesizing an API are called as intermediates.

**Penultimate intermediates**

Penultimate intermediates are the last preceding compounds to the final desired compound in the chemical synthesis process.

**Related products**

Related impurities have chemical structure similar to the drug substance and may possess potentially similar biological activities.

**Transformational products**

They are the theorized and the non-theorized products that may be formed during chemical reactions. Transformational products are more comparable to the by-products.

## 2.0.3. Compendial terminologies used to describe impurities

The USP-NF mentions impurities under various sections:

- Impurities in official articles.
- Ordinary impurities.
- Organic volatile impurities (OVI).

The idea of purity varies from one time period to another. This is due to the advancement in the analytical chemistry. What is deemed as pure now might be considered impure in the future if new methodology is established to determine the minute quantities of other components like inorganic, organic, biochemical or polymeric substances. Pharmacopeia uses the following terms for impurities.

**Concomitant components**

Concomitant impurities are the geometric or the optical isomers of the API. These isomers might have different pharmacological and toxicological properties.

Thalidomide was sedative hypnotic that was used in the treatment of morning sickness in pregnant women. However, its use resulted in a condition called as phocomelia (limb malformation) in infants. Investigations revealed that thalidomide exist as a racemic mixture of *(R)* and *(S)*- enantiomers. The *(R)*- isomer had sedative effect while the *(S)*- isomer was teratogenic.

**Foreign substances**

They are contaminants or adulterants that present in the API.

**Ordinary impurities**

These impurities are present in bulk drug but they do not have any adverse biological activity.

**Organic volatile impurities**

Organic volatile impurities are the organic solvents which are used in the chemical synthesis that remain in trace amounts in the final product.

**Signal impurities**

Signal impurities must be identified and quantified. They can be either process impurities or DPs that provides a great deal of information about the process.

**Toxic impurities**

These impurities have adverse effects and hence, requires identification and quantification by explicit tests.

## 2.0.4. ICH terminologies used to describe impurities

ICH classifies impurities into three categories.

**Organic impurities**

Organic impurities include process impurities, starting material, DPs and the reaction intermediates.

**Inorganic impurities**

Inorganic impurities include salts, catalyst, ligands, heavy metals or residual metals.

**Residual solvents**

These includes the organic and the inorganic solvents used during the chemical synthesis, Purification, or recrystallization. The organic solvents are classified in the ICH Q3C(R8) into the following types.

**Class I**

These includes Environmental hazards, known human carcinogens, and strongly suspected human carcinogens.

**Class II**

Animal carcinogens that are not genotoxic or potential agents of other irreversible toxicity, such as neurotoxicity or teratogenicity.

**Class III**

Solvents with low toxicity to humans; no exposure limit based on health is required. Class 3 solvents have PDE levels of at least 50 mg per day.

## 2.0.5. Identification and qualification threshold for impurities

ICH addresses the questions pertaining to drug stability and impurities in the following guidelines.

Q1A(R2) Stability testing of new drug substances and products.

Q1B Stability testing: photostability testing of new drug substances and products.

Q3A(R2) Impurities in new drug substances.

Q3B(R2) Impurities in new drug products.

Q3C(R8) Impurities: Guideline for residual solvents.

Q6A Specifications: test procedures and acceptance criteria for new drug substances and new drug products: chemical substances.

In the Q3A (R2) and Q3B (R2) guidelines, ICH specifies the identification and qualification thresholds for impurities and degradation products. The specifications are listed in the table below.

**Table 2.1.4.1:** Different Thresholds for impurities in drug substance

| Maximum daily dose[1] | Reporting Threshold[2, 3] | Identification threshold [c] | Qualification threshold [c] |
|---|---|---|---|
| ≤ 2 g/day | 0.05% | 0.10 % or 1.0 mg/day intake (whichever is less) | 0.15 % or 1.0 mg/day intake (whichever is less) |
| > 2 g/day | 0.03% | 0.05% | 0.05% |

[1] The amount of drug substance administered per day
[2] Higher reporting thresholds should be scientifically justified
[3] Lower thresholds can be appropriate if the impurity is unusually toxic

**Table 2.1.4.2:** Different Thresholds for Degradation Products in New Drug Products

| Maximum daily dose[1] | Reporting threshold [2,3] |
|---|---|
| ≤1g | 0.1% |
| > 1g | 0.05% |
| Maximum daily dose[1] | Identification threshold [2,3] |
| < 1 mg | 1.0% or 5µg TDI, whichever is lower |
| 1 mg – 10 mg | 0.5% or 20µg TDI, whichever is lower |
| > 10 mg – 2 mg | 0.2% or 2mg TDI, whichever is lower |
| > 2 mg | 0.10% |
| Maximum daily dose[1] | Qualification threshold [2,3] |
| < 10 mg | 1.0% or 50µg TDI, whichever is lower |
| 10 mg – 100 mg | 0.5% or 200µg TDI, whichever is lower |
| >100 mg – 2 g | 0.2% or 3 mg TDI, whichever is lower |
| > 2 g | 0.15% |

[1] The amount of drug substance administered per day
[2] Thresholds for degradation products are expressed either as a percentage of the drug substance or as total daily intake (TDI) of the degradation product. Lower thresholds can be appropriate if the degradation product is unusually toxic.
[3] Higher thresholds should be scientifically justified.

## 2.0.6. Isolation of impurities[28]

The best strategy for separation depends on the type and complexity of the impurities. Resolution of all the target impurities is the main objective of an effective separation technique. The following techniques are mainly used in separation of impurities and the degradation products.

- Capillary electrophoresis (CE)
- Chiral separations
- Gas chromatography (GC)
- High-performance liquid chromatography (HPLC)

- Supercritical fluid chromatography (SFC)
- Thin-layer chromatography (TLC)

Impurities can be isolated using chromatographic and non-chromatographic techniques. Basic isolation techniques should be prioritised because they can result in significant time savings and make it easier to create bigger quantities of materials. A chromatographic approach needs to be used initially if the component of interest needs to be separated from a complicated mixture.

Several factors, including the complexity of the mixture, the impurity's chemical makeup, and the needed amount of the impurity, must be taken into account while choosing the best method for impurity isolation. Liquid-liquid extraction can be used as the initial option when a small number of impurities are present and their polarity or pKa is sufficiently different from that of API. Aqueous solutions make up one phase of a liquid-liquid extraction, while nonpolar organic phases make up the other. Acidic, basic, or neutral impurities can be removed by properly adjusting the pH of the aqueous solution.

Due to their higher separation effectiveness, chromatographic techniques including thin layer chromatography (TLC) and column chromatography can be utilised successfully for the isolation of impurities. Preparative HPLC is the technique of choice for isolation when the impurities and API are closely related and present in low quantities. Little quantities of chemicals can also be produced through capillary electrophoresis. This method has, however, been applied in micro-preparative applications.

In certain cases, supercritical fluid chromatography has shown its merit in resolving impurities thus its application as an isolation technique. As the mobile phase is gaseous, It can be easily removed from the separated fractions.

## 2.0.7. Characterization of impurities[28]

According to the ICH guidelines identification of impurities are essential when it crosses the identification threshold. Characterization of impurities can be done by various spectroscopic methods like Ultraviolet spectrophotometry (UV), Infrared (IR), Mass spectrometry (MS) and Nuclear magnetic resonance (NMR).

UV spectrophotometry (UV) at a single wavelength provides the least amount of analysis selectivity; but, with the availability of diode array detectors nowadays, it is possible to acquire enough information simultaneously at different wavelengths to ensure improved accuracy.

Infrared spectrophotometry (IR) provides detailed information about some functional groups that enable selectivity,

The measurement of dispersed electromagnetic radiation brought on by irradiating materials is the foundation of Raman spectroscopy. Raman spectroscopy is seen as complementary to IR spectroscopy. The two methods give a complete vibrational image of a material. Due of its relative complexity, and high instrumentation costs, Raman spectroscopy is not as frequently utilised for identification as IR spectroscopy. Raman spectroscopy is a very potent method for identifying the presence of polymorphs.

NMR spectroscopy is a useful method for the characterization of low-level impurities and degradation products since it is non-destructive and non-invasive. NMR can also be viewed as being almost a universal detector for hydrogen, carbon, and other magnetically active nuclei.

Mass spectrometry provides information about the molecular weight of the substance which can help estimate the structure of a molecule based on fragmentation patterns.

New options for monitoring, characterization, and quantifying drugs and impurities from pharmaceutical goods have been made possible by improvements in the design and effectiveness of the interfaces that directly connect separation techniques with NMR and mass spectrometers. hyphenated approaches like LC-NMR, LC-MS/MS, and LC-DAD-NMR-MS significantly reduce the amount of time required for characterization.

## 2.1. Introduction to stability indicating assay method (SIAM)[30-32]

With the introduction of ICH, USP-NF US-FDA, WHO, Japanese pharmacopoeia (JP), National health surveillance agency (ANVISA), and European medicines agency (EMA) guidelines, the requirement for establishing stability-indicating assays became more explicit. These guidelines require the execution of forced degradation studies under a variety of

conditions, including pH, light, oxidation, dry heat, etc., as well as the separation of drug substance from degradation products.

Stability indicating assay method is defined as "a validated quantitative analytical procedure that can detect the changes with time in pertinent properties of drug substance and drug product. Generally, there are two stages in validating a stability-indicating method. First stage is during the initial development of the drug substance. During this stage, the drug is subjected to stress studies and based on the drug degradation behaviour a stability indicating assay method is established. The focus of validation in this stage is determination of specificity/ selectivity, accuracy, range and robustness. The method developed during this stage is frequently used in the analysis of the stability samples of the bulk drug. In the second stage, the developed stability-indicating method is extended to the analysis of formulations. The purpose of this, is to prove the validity of the method in presence of excipients and other formulation constituents. Important validation parameters such as selectivity, specificity, accuracy, and precision are revalidated here.

### 2.1.1. Forced degradation Studies[30-32]

Forced degradation studies are also referred to as stress studies or stress degradation studies. Forced degradation studies involves exposing the API to conditions like light, heat, hydrolysis, and oxidation to facilitate its degradation by chemical or physical means. Formal Stress (stability) studies are mainly classified into three types; long term, intermediate and accelerated. Long term studies are carried for 12 months while intermediate and accelerated for 6 months. However, the main issue with these studies is that it takes a substantial amount of time. Forced degradation studies provides an alternative approach for faster generation of degradation products. Further, the stability indicating method developed during the forced degradation studies can be used for analysis of the stability samples.

Forced degradations studies are usually carried out to achieve the following objectives:

- It helps in determination of the drug degradation pathways.
- It aids in segregation of DPs that are formed from the API from those that are formed from the excipients in the formulation.
- To characterize the structure of DPs

- It reveals the susceptibility of the API to conditions like the hydrolysis, oxidation, thermolysis and photolysis.
- It is used to develop stability indicating assay method.
- It helps in formulation of better dosage forms.
- It aids in the formal stability studies.

According to the FDA guidelines, stress testing must be performed in the Phase III of the regulatory submission process. However, doing stress studies during the preclinical or Phase I of the clinical studies is beneficial as it provides sufficient time for optimizing the stress condition and characterization of the DPs. Moreover, an early stress study provides opportunity to give feedback for the improvement in the manufacturing process and selecting the ideal stability-indicating assay method.

### 2.1.2. Practical approach for the conduct of forced degradation studies[30-33]

Forced degradation studies should be performed in a manner to produce 5 % to 20% degradation. This can be achieved by varying the intensity and the duration of these studies. It not mandatory for the forced degradation studies to form DPs. The study can be stopped if no DPs are observed after the API or the drug formulation have been exposed to the stress conditions than those mentioned in the accelerated stability studies as this is more or less indicative of the stability of API. Overstressing the API may form secondary degradation products that might not be actually seen during the long term or the accelerated stability studies. On the other hand, under stressing can result in little degradation of API due to which no DPs are observed. The conditions mostly used to conduct the forced degradation studies is seen in the table 2.1.2.1.

**Table 2.1.2.1:** Recommended conditions for conduct of forced degradation studies

| Degradation type | Experimental conditions | Storage | Sampling time (days) |
|---|---|---|---|
| **Hydrolysis** | Control API (no acid or base) | 40 ℃, 60 ℃, | 1,3,5 |
| | 0.1 N / 1 N HCl | 40 ℃, 60 ℃, | |
| | 0.1 N/ 1 N NaOH | 40 ℃, 60 ℃, | |
| | Acid control (no API) Base | 40 ℃, 60 ℃, | |
| | control (no API) pH: 2,4,6,8 | 40 ℃, 60 ℃, | |
| **Oxidation** | 3% H2O2 | 25 ℃, 60 ℃, | 1,3,5 |
| | Peroxide control | 25 ℃, 60 ℃, | |
| | Azobisisobutyronitrile (AIBN) | 40 ℃, 60 ℃, | |
| | AIBN control | 40 ℃, 60 ℃, | |
| **Photolytic** | ICH Q1B mandated dose of light. | NA | 1,3,5 |
| | Light control | NA | |
| **Thermal** | Heat chamber | 60 ℃ | 1,3,5 |
| | Heat chamber | 60 ℃/75% RH | |
| | Heat chamber | 80 ℃ | |
| | Heat chamber | 80 ℃/75% RH | |
| | Heat control | RT | |

Few chemists have found it to useful to begin with extreme conditions like using higher strength of acids or bases and using higher temperature (80 ℃ or higher temperature) and testing for shorter durations (2, 5, 8, 24 h).

In a different approach, degradation is initiated by considering the drug substance to be labile and carrying out degradation under the conditions listed in table 2.2.2.1. Then, the level of stress would be increased or decreased to achieve adequate degradation. This strategy is superior to the harsher conditions and shorter time approach for the following reasons: There is a practical difficulty in neutralising or diluting every sample that contains a high concentration of reactants, e.g., acid or base, before an injection can be made on the HPLC column, as harsh conditions may alter the mechanism of reaction. Both of these arguments are sufficient to suggest that the drug should be degraded under conditions as close to natural as possible.

It is very important to carry out stress studies at a proper drug concentration. Its recommended that the degradation studies should be conducted at a concentration of 1 mg/ mL in order to get even minor DPs in the range of detection.

## 2.1.3. Degradation conditions[30-33]

### Hydrolytic conditions

Hydrolysis is one of the most prevalent chemical reactions of degradation over a broad pH range. Hydrolysis is a chemical process involving the disintegration of a chemical compound through its reaction with water. Ionizable functional groups present in the molecule are catalysed during hydrolytic study under acidic and basic conditions. Acid or base stress testing involves the forced degradation of a drug substance through exposure to acidic or basic conditions, which generates desirable levels of primary degradants. The choice of acid or base type and concentration depends on the drug substance's stability. Suitable reagents for hydrolysis include hydrochloric acid or sulfuric acid (0.1 N/ 1 N) for acid hydrolysis and sodium hydroxide or potassium hydroxide (0.1 N/ 1 N) for base hydrolysis. If the compounds to be subjected to stress testing are insoluble in water, co-solvents can be utilised to dissolve them in HCl or NaOH. The selection of co-solvent depends on the structure of the drug substance. Normal stress testing begins at room temperature, and if there is no degradation, elevated temperatures (50–70 °C) are applied. The duration of stress testing

should not exceed seven days. The degraded sample is neutralised with an appropriate acid, base, or buffer to prevent further degradation.

**Oxidation conditions**

The first-choice stressor to carry out the oxidative degradation stress study is hydrogen peroxide. However, other oxidising agents, such as metal ions, oxygen, and radical initiators (e.g., azobisisobutyronitrile) can also be utilised for the oxidation of drug substances in forced degradation studies. The selection of an oxidising agent, its concentration, and conditions depend on the active pharmaceutical ingredient. Ideally, subjecting the drug solution to 0.1–3.0% hydrogen peroxide at neutral pH and room temperature for seven may generate relevant degradation products. Oxidative degradation of a drug substance occurs via an electron transfer mechanism which results in formation of anions and cations. The electron transfer oxidation of amines, sulphides, and phenols produces N-oxides, hydroxylamine, sulfones, and sulfoxide. The functional group containing labile hydrogen, such as benzylic carbon, allylic carbon, and tertiary carbon, or positions relative to the hetero atom, has propensity for oxidation to form hydro peroxides, hydroxide, or ketone.

**Photolytic conditions**

The photostability testing of pharmaceutical substances must demonstrate that exposure to light does not result in an unacceptable change. Photostability studies involves exposing the drug to UV or fluorescent light to form the DPs. The ICH (Q1B) guideline specifies a minimum of 1.2 million lux h and 200 W h/m2 of light must be applied to a drug substance in solid or liquid state. The most accepted range of light wavelengths for photolytic degradation is between 300 and 800 nanometres. Conditions of light stress can induce photo-oxidation via the free radical mechanism. Carbonyls, nitroaromatics, N-oxides, alkenes, aryl chlorides, weak C–H and O–H bonds, sulphides, and polyenes are functional groups that are likely to introduce drug photosensitivity.

**Thermal degradation**

Thermal degradation (e.g., dry heat and wet heat) should be conducted under more rigorous conditions than those recommended by ICH Q1A. Solid drug substances and drug products should be exposed to both dry and moist heat, whereas liquid drug products should be exposed to only dry heat. The Arrhenius equation used to study the effect of temperature on the thermal decomposition of a substance is as follows.

$$K = Ae^{\frac{-Ea}{RT}}$$

Where *k* is the reaction rate, *A* is frequency factor, $E_a$ is activation energy and *R* is gas constant. Ideally, the thermal degradation study has to be conducted in-between 40–80 ℃.

## 2.1.4. Development of a stability indicating method[31,34]

Various titrimetric, spectrophotometric, and chromatographic methods are reported in the literature for analysing stability samples.

The objective of the majority of titrimetric and spectrophotometric techniques is to analyse the drug of interest separately from excipients, additives, DPs, and impurities. The only advantages of these methods are their low cost and ease of use. However, due to limitations in specificity, stability-indicating methods are scarcely reported.

Because of their superior accuracy and sensitivity in the separation of multiple components, chromatographic methods have surpassed conventional methods of analysis. Thin-layer chromatography (TLC), high-performance thin-layer chromatography (HPTLC), gas chromatography (GC), and high-performance liquid chromatography (HPLC) are some of the chromatographic techniques that have been utilised. Among these TLCs is straightforward method. However, its variable and non-quantitative nature limit its use as a foundational technique for SIAM development. Nonetheless, it is used extensively in the early stages of development to determine the number of degradation products formed, to identify degradants by comparing them to a standard, and to even isolate these products.

HPTLC eliminates the drawbacks associated with TLC. It is dependable, quick, and precise for quantitative drug analysis. In addition, many samples can be analysed simultaneously using a small amount of mobile phase, which reduces the time and cost associated with analysis. Due to these benefits, a substantial number of publications based on this technique have been published in the last decade[35-37].

GC can be utilised in the development of SIAM, but it is not a versatile or suitable technique for the analysis of volatile and thermostable substances. Due to this significant limitation, there are very few SIAM methods that utilise GC[38-39].

In comparison to the aforementioned methods, HPLC is the most prevalent technique employed in the development of SIAM. Due to its high resolution, sensitivity, and specificity, it has become a widely used technique. Additionally, HPLC is capable of analysing thermally unstable, polar, and ionic compounds. Consequently, the majority of SIAMS have been developed using HPLC. It is also possible to increase the sensitivity of HPLC analysis by coupling it with a mass detector (LC-MS or LC-MS/MS) and NMR (LC-NMR), which aids in the structural elucidation of unknown impurities. A small number of additional techniques, such as nuclear magnetic resonance spectroscopy (NMR) and capillary electrophoresis (CE), have been reported for the development of SIAM.

## 2.1.5. Steps involved in development of SIAM[30-32]

HPLC is the most predominant technique used in the development of SIAM. development of a SIAM requires good foresight along with systematic approach. It involves gathering of the physio chemical data for the drug, carrying out stress studies, developing and optimizing HPLC method for separation of DPs, and validation of the method as per the regulatory guidelines. The various steps involved in the development of SIAM is as follows.

**Step 1:** An analysis of the drug's structure to determine its likely decomposition routes. Many of the new drugs are derivatives of a prototype drug molecules. Based on the reported degradation profile of the prototype drug, it is simple to predict the chemistry of degradation for the drugs derived from it. In case of a new chemical entity, depending upon the functional groups present, the most likely degradation products can be predicted.

**Step 2:** Gathering information pertaining to the physio-chemical properties

Before developing a HPLC method, it is essential to understand various physicochemical parameters, such as pKa, log p, solubility, absorptivity and wavelength of maximum absorbance.

Knowledge of pKa is crucial because it affects the retention pattern of the drug whenever the pH of the mobile phase changes by ± 1.5 pKa units. Knowledge of the log p value for the drug and its degradants facilitates the selection of the ideal stationary phase. Solubility data in aqueous, organic, and commonly used HPLC solvents, as well as their combinations, is extremely useful for designing mobile phase. As most HPLC analyses are performed using UV detectors. The knowledge of the maximum wavelength and extinction of the drug and

degradation products in different solvents and at different pH levels aids in the development of absorbance-optimized chromatographic method. If the degradation product is unknown, with the aid of a photo diode array (PDA) detector, the wavelength maxima can be determined.

**Step 3:** Forced degradation studies.

Stress studies are conducted to produce potential degradation products. The ICH guidelines suggest the subsequent conditions for stress studies:

1) Thermal condition – 10 $^0$C increments above accelerated temperatures (50$^0$C, 60$^0$C etc)

2) Humidity – 75% RH or greater when applicable

3) Hydrolysis – over an extensive pH range

4) Oxidation

5) Photolysis – as per ICH Q1B guidelines

**Step 4: Development of RP-HPLC SIAM and its optimization**

The stress sample can be analyzed by employing the reverse phase octadecyl column and mobile phase used in the development of the drug's assay method. This run can be used to determine the number and type of degradation products. The final method is devised using the mixture of DPs formed during all the stress conditions. If there are problems with peak shape or separation, the mobile phase can be altered. The majority of the time, degradation results in the formation of both polar and non-polar degradants. Using a gradient-based program, these types of degradants can be separated. The wavelength for detection is determined by the spectral behavior of degraded samples. Adjusting the injection volume, column temperature, and flow rate can improve resolution. The retention time (RT) and relative retention time (RRT) are determined after proper separation. Special consideration is given to components whose RT or RRT are very close. These components' PDA spectra or LC-MS profiles are evaluated critically to determine whether the degradants are identical or distinct.

**Step 5: Identification and characterization of degradation products**

According to ICH, degradation products must be identified and qualified if they meet the thresholds for identification and qualification. Identifying degradants also aids in the

establishment of degradation pathways. Once the structure of the degradant has been determined, it can be synthesized and purified in order to serve as an impurity standard.

In the past, degradant products were identified by isolating and characterizing them. The compound is characterized by subjecting it to spectral (UV, IR, NMR, and MS) and elemental analysis. Nonetheless, this method is laborious and time-consuming when multiple degradation products are produced. The modern strategy is to employ LC techniques coupled with mass spectrometry (LC-MS or LC-MS/MS) and nuclear magnetic resonance spectroscopy (LC-NMR). It offers a reasonable understanding of the chemical structure of degradants.

**Step 6: Validation of SIAMs**

The guidelines framed by the US-FDA, United States Pharmacopeia and the ICH are mainly followed for the HPLC method validation. According to the ICH Q2(R1) guideline, an SIAM has to be validated for accuracy, precision (repeatability and intermediate precision), specificity, linearity and range.

**2.1.5.1. Specificity and selectivity**

Developing a separation for chromatographic methods requires demonstrating specificity, which is the method's ability to accurately measure the analyte response in the presence of all potential sample components.

However, there is lack in clarity in distinguishing the methods that measure quantitatively the analyte of interest in sample matrix without separation, and the methods where separation is achieved of the drug and the DPs. The former approach is called as the stability specific while the latter is called stability-indicating. Unfortunately, sometime stability specific methods are referred to as stability indicating.

Specific stability indicating methods is defined as “a method that can quantitate drug clearly in presence of impurities, excipients and additives that are expected to be present in the dosage form”. On the other hand, selective stability indicating method is “a method that can clearly quantitate the drug and the impurities in presence of the excipients and the additives that are present in the dosage form. Selective stability indicating method is both selective as well as specific while, specific method is usually not selective.

Specificity is measured by the resolution between the closely eluting peaks while the methods selectivity is expressed as the peak purity. Peak purity is mostly calculated by the data acquisition software by comparing the UV spectra obtained on the upslope, the apex, and the downslope. If the spectrums match then its deemed that the peak is pure.

**2.1.5.2. Accuracy**

The accuracy of an analytical method is the degree to which its test results correspond to the actual value. The accuracy of the method can be determined by using one of the following approaches.

In the first approach, accuracy is determined by analyzing the sample and a known concentration of reference standard and comparing the measured value to the true value.

The second approach is to compare the test results from the new method to those of an alternative, well-defined, and known-accurate procedure.

The third approach involves spiking analyte into blank matrices and calculating the recovery (%). The analyte concentrations in the spiked samples are determined using the assay method.

The fourth approach is called as the standard addition method. It is used to determine the recovery of an analyte that has been spiked. This method is utilized when it is not possible to prepare a sample matrix devoid of the analyte.

In the case of SIAM, accuracy is typically determined by adding a known amount of drug to placebos or formulations and calculating the percent recovery. However, a more accurate method of determining accuracy is to determine the percentage of drug recovery by spiking the degradant sample.

**2.1.5.3. Precision**

Precision is a measure of closeness of results of an analytical method under normal circumstances to the true value. It is expressed in terms of percent relative standard deviation (% RSD). According to the ICH, precision studies must be ideally carried out at three levels: repeatability, intermediate precision, and reproducibility.

Repeatability (intra-day precision) measures the closeness of the results of the method over a short duration. Intra-day precision is calculated from a minimum of nine determinations

within a specified range (for instance, three concentration levels, three repetitions for each level). Intraday precision can also be calculated from a minimum of six determinations at 100 % of the target concentration.

Intermediate precision considers Variations within the laboratory due to random events, such as different days (inter-day precision), analysts, equipment, etc. In order to monitor the effects (if any) of the individual variables, an experimental design must be utilized when determining intermediate precision.

Reproducibility is obtained by testing homogeneous samples in multiple laboratories and is frequently included in cross-laboratory studies. The evaluation of reproducibility results frequently places a greater emphasis on measuring bias than on identifying differences in precision alone.

#### 2.1.5.4. Linearity and range

Linearity is the capacity of a method to generate test results proportional to analyte concentration within a given range, either directly or through a well-defined mathematical transformation. In addition to specifying a minimum of five concentration levels, the ICH guidelines also outline certain ranges.

In practice, the linearity study should be tailored to the intended analytical technique. Linearity data is analyzed by regression analysis wherein area under curve of the analyte peak is plotted against the concentration. In general, a correlation coefficient of 0.999 indicates an acceptable fit of the data to the regression line.

Range is the interval between the highest and lowest levels of analyte which can can be established with precision, accuracy, and linearity using a suitable method. The Minimum specified range for assay is 80 to 120% of the target concentration. The minimum range for an impurity test is between the reporting level of each impurity and 120% of the specification. For content uniformity testing, the minimum range is between 70 and 130% of the test or target concentration, whereas for dissolution testing, the minimum range is 20% over the specified test range.

#### 2.1.5.5. Robustness

A method's robustness is its ability to remain unaffected by small, deliberate changes to its parameters. The robustness of a method is evaluated by varying method parameters such as

percentage of organic solvent, pH of buffer, column temperature, flow -rate, wavelength, etc. As stated in the ICH guidelines, robustness must be considered early on in the method development process. Moreover, if the results of a method or other measurements are susceptible to variations in method parameters, these parameters should be adequately controlled and a warning statement should be included in the method documentation.

## 2.2. Instrumentation, parameters related to HPLC method development, mass, and tandem mass spectrometry

### 2.2.1. High performance liquid chromatography (HPLC)[40-42]

HPLC was developed sometime in later half of the nineteen century from the knowledge of other chromatographic techniques prevalent during that period especially, column chromatography. HPLC is based on similar mode of separation as column chromatography, i.e. adsorption, gel permeation, ion exchange, partition (including reverse-phase partition). However, it diverges from column chromatography in that the liquid phase is pumped through the stationary phase in high pressure. The primary advantage of the HPLC over the classical gravity fed column chromatography is the improved resolution, faster analysis, increased accuracy and precision with which the separated analytes can be quantified.

#### 2.2.1.1. Components of HPLC

A modern HPLC system mainly consist of the following parts.

**Solvent reservoir**

Solvent reservoir is used for storage of sufficient quantities of HPLC solvents for continuous system operation. It can also be outfitted with an online degassing system and specialised filters to isolate the solvent from environmental influences.

**Pump**

Pump ensures the constant and continuous flow of the mobile phase throughout the system; the majority of modern pumps permit the controlled mixing of different solvents from separate reservoirs.

**Injector**

Injector permits the introduction (injection) of the analytes mixture into the mobile phase stream before it enters the column; the majority of modern injectors are autosamplers, which permit the programmed injection of different sample volumes withdrawn from vials in the autosampler tray.

**Column**

The analytical column is the central component of an HPLC system. Generally, HPLC separation columns are composed of stainless steel and range in length from 50 to 250 mm with an internal diameter of 2 to 4.6 mm. The HPLC column packing particles are composed of silica or porous polymer. There are three available particle types for HPLC separations. (a) Microspeares that are completely porous, (b) micropellicular particles, and (c) perfusion particles. Particle size of HPLC column packing plays a crucial role in separation efficiency. For the majority of HPLC separations, micro spherical columns with a particle sizes of 3 to 5 µm are sufficient.

It is possible to coat, or graft, chromatographic support with another material to serve as the stationary phase. This is referred to as the bonded phase. The three most common bonded phases are C1, C4, and C18. The most popular of these are octyl (C8) and octadecyl (C18) modified adsorbents. With these adsorbents, nearly 80% of all HPLC separations have been developed.

**Detector**

This is a device for the continuous monitoring of specific physical (and sometimes chemical) properties of the effluent from a column. UV (ultraviolet) is the most common detector used in pharmaceutical analysis, as it permits monitoring and continuous registration of UV absorbance at a selected wavelength or across a range of wavelengths (diode array detection). Changes in absorbance are caused by the presence of analyte in the detector flow cell. A positive signal is obtained when the analyte absorbs more light than the background (mobile phase).

Besides UV-visible detectors, other optical detectors used with HPLC include: refractive index detector (RID), evaporative light scattering detector (ELSD), luminescent and fluorescence/ phosphorescence.

### 2.2.1.2. Design and development of HPLC method

The current discussion focuses on the design and development of reversed-phase methods for the analysis of small organic molecules, as reversed-phase HPLC accounts for 60–80 percent of these applications.

### 2.2.1.3. Considerations before method development

New analytical method development and validation is expensive and time-consuming. A thorough literature search should be done to find any current techniques for the intended analytes or related compounds before beginning the laborious process. Computerized searches of chemical abstracts and other pertinent databases, including compendial monographs, journal articles, manufacturer material, and the Internet, should be part of this process. Even though this search might not turn up a method that can be used right away, it frequently yields a starting point for method development or at the very least some helpful references.

New analytical methods are needed because of the following:

- Methods are not available, e.g., In the case of a new chemical entity (NCE)
- Methods are not reliable, sensitive, or cost efficient.
- New technique or instrumentation has better performance due to ease of use, automation, higher sensitivity and quicker turnaround.
- Due to regulatory compliance an orthogonal method is required.

### 2.2.1.4. Approach for Method Development

A simple approach frequently used for HPLC development is as follows:

1) Defining the method type (quantitative, qualitative, or preparative) and separation goals.
2) Gather physiochemical properties of analyte of interest as well as other components (e.g., buffers, solvents, etc.)
3) Initial “exploratory” or “scouting” runs to obtain the first chromatogram.
4) Optimization of the HPLC method
5) Method validation

#### 2.2.1.4.1. Best practices for HPLC method development in pharmaceutical analysis

Some of the evolving trends in HPLC method development is listed below:

- Use of modern instruments consisting of quaternary pumps, PDA detectors, modelling software, automated development systems and multicolumn selector valves.
- Use of MS- compatible mobile phases for impurity analysis.
- Use of a combined method for assay and impurity testing.
- Phase-appropriate HPLC method development and method.
- Use of secondary methods for complete separation of all impurities (process impurities and DPs).
- Use of a single method for product of different strengths.
- LC/MS/MS methods for trace analysis.

#### 2.2.1.4.2. Defining the method type and separation goals

HPLC method developed can be categorized into three categories.

- Qualitative
- Quantitative
- Preparative

A qualitative method serves as an identification test that confirms the presence or absence of certain analytes in samples by comparing the retention time and the UV spectra of the reference standard. Qualitative method is used to evaluate whether the level of the analyte is above or below a certain limit or to develop a chromatographic profile for comparative analysis.

A quantitative method determines the concentration of the analyte in the sample. System calibration using an external standard is required. A quantitative method can also serve as qualitative method and used for identification of analytes in a sample. A quantitative method takes a lot of time and effort for development and validation.

A preparative method finds application during isolation of analytes. This method uses a large diameter column with high flow rates. Method validation is not required for preparative method as their objective is isolation of purified compounds or enriched fractions.

#### 2.2.1.4.3. Method objectives

Defining the method objectives are paramount in designing the ideal HPLC method. Parameters considered while designing the HPLC methods include resolution, precision, specificity, and sensitivity. Ideally a pharmaceutical method should have a resolution of ≥ 1.5 from the closest eluting peak. Precision for retention time and area under peak should be less than 2. Linearity for the method has to be established in range of 50 to 150%. The other ideal characteristics of the method include analysis time (approx. 5-10 min), robustness, and low cost of analysis.

#### 2.2.1.4.4. Collecting physiochemical properties of analyte and other components

Literature survey should be caried out to obtain information pertaining to physiochemical properties of analyte like the molecular weight solubility, pKa, chromophore data, and log P. To develop appropriate guidelines on safe handling procedures, toxicology information and Material Safety Data Sheets (MSDS) should be gathered, if they are available. Any reference standard materials should have availability and purity verified. Certificates of analysis (COAs) should be obtained. Vendors can be a very useful source of relevant data, such as spectral data and reference chromatograms.

Besides, information of the other components like the buffers, organic solvents must be gathered. Buffering capacity of the buffers used in mobile phase, UV-cut-off values are pertinent to developing a robust HPLC method.

#### 2.2.1.4.5. Initial method development

##### 2.2.1.4.5.1. Generating initial chromatogram

The preferred condition for generating the initial chromatogram is described in the table 2.2.1.4.5.1.1

##### 2.2.1.4.5.2. Selection of detector

For analytes with a reasonable UV absorbance, the UV / Vis detector (or the PDA detector) is the preferred option. Typically, the monitoring wavelength is set to the $\lambda_{max}$ ( wavelength of maximum absorbance) of the analyte. For nonchromophoric analytes (with low or no UV-Vis absorbance), only refractive index (RI) detectors and evaporative light scattering detectors can be used (ELSD). For ionizable analytes mass spectrometry can be used. For bioanalytical assay MS or MS/MS is the standard detector.

**Table 2.2.1.4.5.1.1 :** Ideal chromatographic conditions for scouting runs.

| **Separation variable** | **Preferred initial choice** |
|---|---|
| **Column** | |
| **Dimension** | 150 mm × 4.6 mm |
| **Particle size** | 5 µm / 3 µm |
| **Stationary phase** | $C_{18}$ or $C_8$ |
| **Mobile phase** | |
| **Solvents A and B** | Buffer-acetonitrile |
| **% B** | 80-100% (gradient elution) |
| **Buffer (compound, pH, concentration)** | 80 |
| **Additives (e.g., ion pair reagents)** | Not to be used during initial runs |
| **Flow rate** | 1.5-2.0 mL/min |
| **Column temperature** | |
| T**emperature** | 35-45 ℃ |
| **Sample size** | |
| **Volume** | < 25 µL |
| **Weight** | < 100 µg |

### 2.2.1.4.6. HPLC method optimization

The fundamental objective of the vast majority of chromatographic techniques is to achieve adequate resolution of all key analytes with sufficient precision and sensitivity in a reasonable amount of time. After determining the initial separation conditions, the next step is to fine-tune each parameter to achieve all of the necessary objectives. The method's specificity is evaluated by confirming the absence of interference from the procedural blank (diluent) or placebo sample (sample containing all formulation components except the active ingredient). In the case of impurity testing or forced degradation, peak purity of API is given significant consideration. Typically, peak purity is evaluated using PDA or MS. Often, an experienced method developer invests more time at this stage to reduce problems during method validation. The parameters modified at this stage include:

- Mobile phase parameters — Percentage organic solvent (%B), buffer type and concentration, pH, solvent type

- Operating parameters — Flow (F), temperature (T), gradient range (ΔΦ), gradient time ($t_G$)
- Column — Bonded phase type, length (L),column diameter (dc),particle size (dp)
- Detector setting (monitoring wavelength) and sample amount

In high-performance liquid chromatography, the mobile phase influences the retention and selectivity of the separation and is easily and continuously adjustable for method improvement. Lowering the percentage of organic phase typically improves retention and resolution. In isocratic separations, the analyte peaks are typically maintained within the capacity factor range of 2–20 to preserve the sensitivity of late eluting peaks. As a result of the insolubility of the analytes in the lower-strength mobile phases, a decrease in solvent strength may cause peak shape distortion. Reducing % B below 3–5% can also be problematic due to the phase collapse or "dewetting" of the hydrophobic bonded groups of the stationary phase.

Ion pairing or the use of polar-embedded or lower-coverage bonded phases are typical techniques for enhancing retention and resolution of highly polar compounds. For controlling separations of acidic or basic analytes, buffers in the mobile phase are required. 10–25 mM buffer concentrations are typically sufficient. For MS-compatible methods, volatile buffers (formate, acetate, carbonate, bicarbonate, ammonia) are required.

Trifluoroacetic acid (TFA) and heptafluorobutyric acid (HFBA) are both effective volatile acidifiers with ion-pairing properties. Considerable progress has been made with the introduction of silica-based bonded phases compatible with high pH levels. Traditionally, organic modifiers in RPC (methanol, acetonitrile and THF) are used to adjust selectivity. Since THF is unstable and toxic, some analysts prefer to use methyl-t-butyl ether (MTBE) in small quantities instead.

When mobile phase adjustments do not produce the required resolution, column switching is often the final step to be implemented. Choose a column with a selectivity that differs from the original column. $C_8$, cyano, and phenyl exhibit the most dissimilar selectivity. As it is difficult to predict which column will provide the best separation of a given mixture, it is problematic to select the optimal column. It is recommended to test a variety of columns under optimized mobile phase conditions or to optimize the mobile phase for the most promising candidate column. Additionally, column dimensions can be optimized to improve

performance, speed, or sensitivity. In general, increasing column temperatures (T) in reverse phase chromatography (RPC) reduces retention and can have some effect on selectivity.

In the concluding step, the settings for the detector and sample loading (sample concentration and injection volume) are finalised. The objective is to maximise sensitivity (increase signal-to-noise ratio) while preserving linearity and peak shapes. For impurity methods and trace analysis, sensitivity is essential. For large-volume injections (i.e., >20 L), the sample solvent strength should be equal to or weaker than the starting mobile phase to prevent chromatographic anomalies. Clearly, the maximum sample amount depends heavily on column size.

#### 2.2.1.5. System suitability parameters/ or HPLC descriptors

**Retention time**

Every analyte is represented by a peak in a chromatogram. In case strong analyte interactions are absent with stationary phase and at low analyte concentration, peaks obtained are symmetrical and looks like gaussian curve.

The distance from the injection point to the peak maxima is called as retention time ($t_R$) and it acts like an identifier for a given analyte of interest. Retention time is the most often used and most readily quantifiable measure for describing the behaviour of an analyte. It is the least ubiquitous parameter but being the most easily measurable.

**Void volume**

Even if the analyte of interest has no affinity towards the stationary phase, its peak will not immediately appear after the injection. This is because an HPLC column is filled with small porous material which has a significant amount of liquid phase in-between and inside them. Therefore, any noninteracting analyte has to pass though this volume before its detected. This volume of liquid phase is named as "Void volume ($V_0$).

Void volume is referred by several other names like "hold up volume," "dead volume," and "retention volume of non-retained component.

**Capacity factor**

Its also referred to as retention factor. Retention of an analyte consists of two parts 1) The time analyte spends in the mobile phase as it moves through the column and 2) the time

analyte spends in the column. The capacity factor (*K'*) is the ratio of difference of the retention time and void volume to void volume. Its value can be calculated by using the following equation.

$$K' = \frac{(t_R - t_0)}{t_0}$$

Where, $t_R$ is the retention time and $t_0$ is the void volume. Capacity factor is not dependent on the flow rate and the column dimension hence, it provides a valid comparison of the data obtained using different chromatographic systems in different laboratories.

**Selectivity**

The ability to discriminate the various analytes by the chromatographic system is called as the selectivity **(*α*)**. Selectivity is defined as the ratio of the capacity factors of two analytes and is given by the following equation.

$$\alpha = \frac{K_2'}{K_1'} = \frac{t_{R2} - t_0}{t_{R1} - t_0}$$

Where, $t_{R2}$ and $t_{R1}$ is the retention time of the components and $t_0$ is the void volume, Selectivity is mainly dependent upon the nature of the analyte and its interaction with immobile phase. Besides, eluent type, composition of mobile phase and ionization also affects the selectivity.

**Efficiency**

An analyte when injected into the stationary phase forms a very small zone. The analyte is distributed evenly within this area. As the mobile phase flows though the stationary phase this zone undergoes band broadening. The degree of band-broadening is called as efficiency. Martin and synge brought to fore the plate theory to evaluate the column efficiency.

The plate theory is based on the belief that the stationary phase is divided into several hypothetical plates and the analyte is in constant equilibrium with the stationary phase. Each of these plates have finite height (height of the effective theoretical plates, HETP), and an analyte spends finite amount of time in the column. This time is sufficient for equilibration of the analyte in both the phases. Smaller the plate height, greater is the number of plates which translates into better separation. Hence, efficiency of the column is measured by the

number of theoretical plates. The number of theoretical plates (*N*) is given by the following formula.

$$N = 16\left(\frac{t_R}{w}\right)^2$$

Where, $t_R$ is the retention time of the analyte and *w* is peak width calculated in time units as the distance between the intersections of tangents to the analyte peak.

The kinetic parameters of the chromatographic system, such as molecular diffusion, mass-flow dynamics, characteristics of the packing bed in the column, flow rate, etc., are the key determinants of column efficiency. The efficiency increases with particle size and with uniformity of packing within the column. The amount of time analyte molecules has to undergo diffusive band-broadening decreases with flow rate. Moreover, the analyte molecules are further away from the thermodynamic equilibrium with the stationary phase with the faster flow rate.

This demonstrates that for a particular column, there should be an ideal flow rate that enables the achievement of an ideal efficiency.

**Resolution**

The separation between the peak maxima reveals the system's selectivity. The selectivity increases with increasing distance. The width of the analyte peak gives the efficiency of the system. Resolution ($R_s$) relates efficiency and selectivity and is defined as the ratio of the distance between the two peaks to the average width of the peaks at the baseline and is given by the equation

$$R_s = 2\left(\frac{t_{R2}-t_{R1}}{w_2+w_1}\right)$$

Substituting for peak width and by considering the retention of the second analyte the above equation can be modified to

$$R_S = \left(\frac{t_{R2}-t_{R1}}{t_{R2}}\right)\times\frac{\sqrt{N}}{4}$$

Simple algebraic conversion gives the master resolution equation which is as follows

$$R_s = \frac{\alpha-1}{\alpha}\times\frac{K_2}{1+K_2}\times\frac{\sqrt{N}}{4}$$

The resolution of poorly resolved analytes could then be improved in one of two ways: either by boosting efficiency or by boosting selectivity.

**Peak symmetry**

Under the ideal circumstance the peak shapes should be gaussian with perfect symmetry. For such peak the asymmetry factor ($A_s$) is equal to one. However, in practise most peaks are not symmetrical and either peak fronting or tailing is observed. If $A_s$ is less than 1 then it indicates fronting and if more than 1 it indicates tailing. Ideally tailing should be curtailed to a value less than 2.

## 2.2.2. Liquid chromatography-mass spectrometry (LC-MS)[40, 43-44]

In pharmaceutical product development, structural characterization of impurities and DPs in bulk drug substances is essential. Since, LC-MS combines the high-resolution separation capability of HPLC with the detection and characterization capabilities of MS, LC-MS plays a crucial role in the overall product development process.

### 2.2.2.1. Interfaces used in LC-MS

The interface that connects an HPLC system to a mass spectrometer is a critical component of the LC-MS system. The development of atmospheric pressure ionisation (API) interfaces, such as electro spray ionization (ESI), atmospheric pressure chemical ionization (APCI), and atmospheric pressure photo ionization (APPI) is largely responsible for the immense popularity of LC-MS systems.

ESI is a soft ionization technique. It is a very gentle process that produces predominantly molecular ions with minimal fragmentation. Single-charged molecular ions typically dominate the mass spectrum of small molecules. The other characteristic of ESI is the simplicity of the source design and its operation at atmospheric pressure, which enables ESI to be coupled with HPLC with relative ease. To maintain a stable spray in ESI, a low flow rate of the sample solution (0.2 mL/min) is required. Consequently, flow splitters are frequently employed in ESI-LC/MS applications.

In APCI, sample solution is introduced into a nozzle spray device comparable to that used in ESI, but without the application of a high electrical potential to the nozzle. Typically, the nebulizing gas (typically nitrogen) is added to aid in the desolvation/ionization process.

Although a 400–500°C heater is used to vaporise solvents, the sample is not significantly compromised. A high-voltage (3–5kV) corona discharge needle is responsible for producing a discharge current and inducing solvent ionisations. Through gas-phase ion/molecule reactions, the solvent reagent ions generated react with analyte molecules to produce analyte ions. low-polarity solvents generally used in normal-phase chromatography can be evaporated for APCI ionization.

APPI is used in analysis of non-polar and neutral analytes that are not properly ionized by ESI and APCI. This technique is based on photoionization. Ion formation involves the absorption of a photon by the molecule and the expulsion of an electron to form the radical cation. The photon energy must be greater than the ionisation potential of the target molecule for ionisation to occur.

#### 2.2.2.2. Mass analyzers

A mass analyzer measures the mass-to-charge ratios (*m/z*) of ions (charged particles) and provides a method for separating the ions. Mass analyzers rely on the interactions of charged particles with electrical or magnetic fields for their operation. Magnetic sector, quadrupole, ion trap, time-of-flight (TOF), and Fourier transform ion cyclotron resonance are typical mass analyzers (FT-ICR). The combination of multiple mass analyzers can enhance the structural characterization capabilities of mass spectrometry/mass spectrometry (MS/MS) or tandem MS experiments. The table 2.2.2.2.1 explain the characteristics of the various mass analyzers.

#### 2.2.2.3. Tandem mass spectrometry

In a classic MS/MS experiment, two mass analyzers are used to determine the parent and product ions. Typically, the first mass analyzer is set to select the desired ion (i.e., the parent ion), which then dissociates and generates product ions. The second mass analyzer is used to evaluate the product ions. Collisions with a target gas introduced into the mass spectrometer (collision-induced dissociation, CID), collisions with a surface (surface-induced dissociation, SID), or photodissociation can dissociate ions in MS/MS experiments. CID is the most common dissociation method due to its ease of implementation. Argon and nitrogen are the typical collision gases.

**Table 2.2.2.2.1:** Description of the mass analyzers.

| Mass Analyzer | Quantity Being Measured | Mass Range (Da) | Mass Resolution[a] | Dynamic range[b] |
|---|---|---|---|---|
| **Magnetic sector** | Momentum per charge | $> 10^4$ | $> 10^4$ | $> 10^6$ |
| **Quadrupole** | Path stability | $> 10^3$ | Unit resolution | $> 10^4$ |
| **Ion trap** | Path stability | $> 10^3$ | Unit resolution | $> 10^3$ |
| **Time-of-flight** | Time | $> 10^5$ | $> 10^4$ | $> 10^3$ |
| **FT-ICR** | Frequency | $> 10^5$ | $> 10^5$ | $> 10^4$ |

[a]Mass resolution is defined as $m/\delta m$, where $\delta m$ is defined as mass difference at full width at half-maximum (FWHM).

[b]Dynamic range is defined as the range of either ion counts or sample concentration over which a linear response is obtained.

MS/MS experiments can be conducted with a variety of tandem-in-space or tandem-in-time instruments. Multiple mass analyzers, such as triple quadrupole (QQQ) and quadrupole-TOF (Q-TOF), constitute the tandem-in-space instruments. The majority of tandem-in-time instruments are ion-trapping devices, such as the ion trap and FT-ICR. They operate sequentially in the scan function to generate MS/MS data; no additional mass analyzer is necessary.

A hybrid of tandem-in-space and tandem-in-time devices, such as the Q-trap (QQ-2D-linear trap) and the ion trap-FT-ICR instruments (2D-linear ion trap-FT-ICR), is the third type of MS/MS. The Q-trap has a triple quadrupole configuration, with the third quadrupole replaced by a 2D-linear ion trap. It is suitable for qualitative and quantitative research. Ion Trap-FT-ICR combines the ion accumulation and $MS^n$ characteristics of a 2D-linear ion trap with the superior mass analysis capability (mass resolution, mass accuracy, and sensitivity) of FT-ICR.

### 2.3.2.4. Effect of instrumental parameters on ionization efficiency in LC-MS

The rate at which a substance ionises molecules into charged particles (ion) is known as ionisation efficiency. It directly impacts the mass spectrometer's sensitivity and detection limit in an LC-MS system. There are number of instrumental factors that are crucial to a compound's ability to ionise. The names of these parameters are typically vendor specific.

**Ionization mode**

Before LC-MS analysis can begin, the mode of ionization (positive or negative) must be selected. The mode of ionization depends upon the structure of the analyte. A positive ion mode can be employed to generate a protonated or cationized molecule for basic substances (such as amines). Whereas a deprotonated molecule forms in the negative ion mode for acidic substances. As only a small number of molecules may be ionised in this mode, the negative ion MS provides selectivity and sensitivity. To gain structural information, it could be essential to conduct both positive ion and negative ion LC/MS investigations on a chemical if it can be found as salts (for example, quaternary ammonium salts).

The choice of ionisation method—ESI or APCI—is another way to choose the ionisation mode. In addition, complex structures have a role in this. Most polar compounds respond best to ESI, whereas low to moderately polar molecules respond better to APCI. It is possible to detect unknown substances by switching between ESI and APCI modes, allowing the optimal ionisation technique to be chosen for signal optimisation.

**Ionization voltage**

A high voltage employed in both ESI and APCI, including capillary voltage and corona discharge voltage. In LC-ESI-MS, a capillary voltage, typically 4 to 5 kV, is supplied to create a powerful electrical field. A lower voltage, often 2.5 to 3kV, is frequently provided to a corona pin in LC-APCI-MS. The sensitivity can be increased by adjusting these high voltages. Moreover, the placement of the ESI capillary or the APCI probe should be optimised as it may affect the ion signal.

**Cone voltage (orifice voltage)**

Cone (orifice) voltage is a third instrumental parameter that can be employed to create some in-source fragmentation in structural determination. It is used to extract ions from the atmospheric pressure region of the ion source into the vacuum region of the mass spectrometer using a sample cone or orifice. The ions are driven swiftly through this area as the cone voltage rises, colliding with solvent vapour and desolvation gas and experiencing some fragmentation as a result. Even though there is no mass selection of the parent ions during cone voltage fragmentation, some fragment ions can still be successfully produced. Cone voltage can be changed in real-world applications to either detect molecular ions of a substance (low cone voltage) or get fragmentation data (high cone voltage).

**Desolvation gas flow and temperature settings**

Desolvation gas flow and temperature setting are two important instrumental factors that determine a compound's ability to ionise. A nebulizing gas ($N_2$) going through the ESI probe for LC-ESI-MS is typically set between 70 and 90 L/hr to help with the production of liquid droplet aerosol from the sample solution. Depending on the solvent flow rate and water content of the solvent, the temperature of the ion source block is typically set between 100°C and 150°C.

Using the ion source, a hot desolvation gas ($N_2$) is given to aid in the solvent's evaporation and removal. By using a larger flow rate of solvent, a higher flow rate of desolvation gas is frequently required.

**2.2.2.5. Effect of flow rate**

The separation and functionality of a mass spectrometer are both impacted by the flow rate in LC-MS. Different flow rates are used, depending on the type of column used for separation. On a 4.6-mm-i.d. column, the ideal flow rate might be used at 1.0 mL/min. The ideal flow rate for a 2.1-mm-i.d. column is 0.2 mL/min. LC capillary columns and traditional analytical columns are both compatible with LC-ESI-MS. For flow rates between 0.5 and 1.0 mL/min, a flow splitting could be necessary for the ESI to perform at its best. The concentration dependence is one of ESI's distinctive features.

The concentration of the sample in solution, not the total amount of sample introduced into the source, determines the ESI response. The ESI signals are not diminished because of flow splitting. The optimal flow rate entering the ESI source with the flow splitting, however, may increase sensitivity, as the desired flow rate for stable ESI spray is about 0.2 mL/min or less.

**2.2.2.6. Effect of mobile-phase composition on ionization efficiency in LC-MS**

**Choice of solvents**

The best reversed-phase LC solvents for LC-MS include water, acetonitrile, and methanol. To keep ion signals stable during LC-MS analysis, all reversed-phase solvents must be degassed. Sonification, helium sparging, or vacuum membrane degassing can all be used to accomplish this.

The source and probe temperatures should be elevated to aid in desolvation in the ion source when using solvents with a high water content. Because ESI requires a polar mobile phase for ionisation, normal-phase solvents including dichloromethane, hexane, toluene, and other hydrocarbons are not appropriate for ESI-MS. These solvents for the normal phase and the typical solutes they contain are sufficiently volatile for APCI analysis and are compatible with APCI-MS**.**

**Choice of mobile phase additives.**

In HPLC, mobile-phase additives are employed to regulate pH and achieve effective separations. Also, they need to work under ESI or APCI circumstances. Acetic acid and formic acid, with typical concentrations ranging from 0.1% to 1%, are the most ideal additions in LC-MS if the pH of the mobile phase needs to be decreased for improved LC separations. Remember that adding acids will prevent ionization from occurring in the negative ion mode. Under acidic conditions, weakly acidic chemicals might not generate deprotonated ions. Ammonium hydroxide (0.1% to 1%) is appropriate if the pH of the mobile phase needs to be raised to improve LC separations. In the negative ion mode, weakly acidic substances can be ionized successfully. Another addition, triethylamine, is basic and may help to improve the ionization of other substances in the negative ion mode. Triethylamine should be avoided because it may prevent other chemicals from ionizing in the positive ion mode.

Ammonium acetate (0.1 M) is a typical volatile salt used in LC/MS to buffer mobile phases. It is employed in place of nonvolatile salts like phosphates because these salts have a propensity to precipitate in the ion source, block the source, and prevent analytes from ionizing.

Inorganic acids and surfactants/detergents are a couple of other additions that are inappropriate for LC-MS (sulfuric acid or phosphoric acid). While the latter can lead to corrosion of metal components in the source, the former tend to restrict the ionisation of other chemicals. Trifluoroacetic acid (TFA) acts as an ion-pairing agent, reducing ESI signals in the positive ion mode and possibly suppressing ionisation entirely in the negative ion mode. TFA is frequently used for protein and peptide analysis at concentrations lower than 0.1%.

**Adduct formation.**

Impurities in the sample solution and mobile phase additives can complicate the LC-MS mass spectral analysis. Common examples of noncovalent complexes include protonated dimeric ions [2M + $H^+$]. Other frequent adduct ions include multimeric ions ([3M + $H^+$], [2M + $Na^+$], etc.), complex cations ([M + $NH_4^+$], [M + $Na^+$], [M + $K^+$], etc.), solvent adduct ions ([M + $H_2O$ + $H^+$], [M + $CH_3OH$ + $H^+$], [M + $CH_3CN$ + $H^+$], [M + Cl], [M + $CH_3COO$], etc.). This adducts ions creation can offer extra details on how to determine the molecular weight of unknowns. However, extra alkali metal cations may need to be eliminated before analysis since they can prevent other compounds from ionising. If protonation does not happen easily in particular circumstances, it could be essential to introduce a tiny amount of cation source to the sample to promote complex cations.

**Effect of analyte concentration**

The ESI response is concentration-dependent. Up to a maximum concentration of around $10^{-5}$ M, there is a linear response to concentration. The ESI response plateaus once the analyte concentration crosses this threshold. This is because ESI intensity is inversely related to ion surface concentration. Higher concentrations will not result in an increase in the total number of surface charges available for ion production since the droplet surface is totally saturated at about $10^{-5}$M. This will influence the high concentration end of LC-ESI-MS quantitation. The sensitivity of the LC-MS system, which includes effective ion transfer/detection and reduction of chemical noise in the system, determines the detection limit for the low concentration end**.**

## 2.3. *In-silico* methods for prediction of ADMET[45-49]

Animal testing is the practise of using nonhuman animals in research. The number of vertebrate animals used in animal studies each year is thought to be in the tens of millions on a global scale. In vivo models, also known as animal testing in toxicity, provide doses for specific species and are used to extrapolate findings to human health or the environment. As previously stated, it is not always clear how to extrapolate data from one species to another. For instance, there can be significant differences between the lethal doses for mice and rats.

Even before computers became widely available, researchers looked at how to build a model that connects a chemical structure to the action. As computers are used and have silicon in their hardware, the phrase "*in silico"* currently refers to the techniques devoted to achieving this goal. The most popular *in silico* techniques are the QSAR (Quantitative Structure Activity Relationships) techniques, which are based on the idea that all actions are controlled by the molecular structure.

## 2.3.1. QSAR

The construction of a QSAR model using quantitative data aims to correlate the response variable of interest with chemical descriptors computed or even measured from the molecules themselves. In the 1940s, Corwin Hansch developed what are now known as QSAR approaches by analysing congeneric sequences of compounds and formulating the QSAR equation:

$$\boldsymbol{log\frac{1}{c} = ap + bs + c\mathrm{Es} + \mathrm{const}}$$

Where, C is effect concentration, P=octanol-water partition coefficient, S= Hammett substituent constant (electronic) and Es= Taft's substituent constant.

The QSAR techniques occasionally go by more precise names, such as QSPR (quantitative structure property relationship) or QSTR (quantitative structure toxicity relationship). For physicochemical parameters such the boiling point, solubility, and logP, QSPR is utilised.

They all establish a relationship between a collection of independent variables (often calculated attributes or descriptors) and a dependent variable (the effect or response). These are statistical models that can be used to completely *in silico* anticipate the outcomes for unobserved data items. Instead of from an experiment, it is feasible to compute them from a model.

### 2.3.1.1. Molecular descriptors

Since statistical analyses of the molecules frequently involve molecular structures, the production of useful data from these structures is crucial to cheminformatics. Calculating molecular descriptors which describe the local or global prominent properties of the molecule—can be done in a variety of ways. Many categories of descriptors include the following.

**Constitutional descriptors**

They are based upon the number and types of atoms, bonds, and functional groups.

**Geometric descriptors**

They give molecular surface area and volume, moments of inertia, shadow area projections, and gravitational indices.

**Topological indices**

They are dependent upon the topology of the molecular graph. The description is produced using only the structural data. Examples include the Randic index (a measure of a molecule's branching) and the Wiener index (the total number of bonds between all nodes in a molecular network).

**Physiochemical descriptors**

The physical properties of molecules are estimated using physicochemical descriptors. Molecular weight, hydrogen bond acceptors, donors, and partition coefficients, expressed as logP, are a few examples. The calculation of logP determines the general lipophilicity (or hydrophobicity) of the material and predicts the logarithm of the partition coefficient between octanol and water.

**Electrostatic descriptors**

Electrostatic descriptors like partial atomic charges and other depends upon the likelihood of formation of hydrogen bonds.

**Quantum chemical descriptors**

These descriptors are related to the molecular and orbitals and their characteristics.

**2.3.1.2. Model construction**

Classification and regression are two extensively used supervised learning techniques for creating models in cheminformatics and toxicology. By using classification methods, new items, in this case molecules, are divided into two or more categories, often physiologically active or inactive. Regression approaches make an effort to link molecules with continuous data, such as a measured biological response variable, in order to develop a model that can be used to predict a continuous numeric value for new and unidentified molecules.

Partial Least Squares, Linear Discriminant Analysis, Naive Bayesian Classifier, Decision Trees, Recursive Partitioning, and Support Vector Machines are the techniques most frequently used for classification modelling, while Multiple Linear Regression, Partial Least Squares, Support Vector Machines, and Artificial Neural Networks are the techniques most frequently used for regression modelling.

#### 2.3.1.3. Model acceptability

The leave-one-out cross-validation method is frequently used in published QSAR models, which also compute the cross-validated determination coefficient $R^2$, or $q^2$. The determination coefficient is defined as follows, if $y_{pi}$ and $y_i$ are the expected and observed property values, and *ypim* and *yim*, respectively, are the average values of the predicted and observed property values.

$$R^2 = 1(\frac{sum(y_{pi} - y_i)^2}{sum(y_{pi}^2 - y_i^m)^2})$$

An indication or even the strongest evidence that the model is highly predictive is a high value of $q^2$ (for example, $q^2 > 0.5$).

#### 2.3.1.4. Model interpretation

The approaches used in interpretation of QSAR are classified into two categories; machine learning (ML) dependent and ML-agnostic. Further based on the level of interpretation, approaches are classified as feature or structure based. Commonly used QSAR interpretation approaches are described in the following table:

**Table 2.3.1.4.1:** QSAR interpretation approaches

| | **ML-dependent** | **ML-agnostic** |
|---|---|---|
| **Feature-based** | Regression coefficients Rule extraction Layer-wise relevance propagation (LRP) CAM, GRAD-CAM | Sensitivity analysis Partial derivatives Feature importance by permutation Integrated gradients Shapley sampling values |
| **Structural** | Attention weights of attention-based (graph) neural networks | Universal approach of structural Interpretation Similarity maps Computational matched molecular pairs/series |

*Page intentionally left blank.*

# Chapter 3

# Research Envisaged

The ICH and the US-FDA have issued a number of guidelines for registration applications pertaining to the content and qualification of impurities that may be present in drug substances and drug products.

The ICH considers degradation products to be an impurity and has developed practical guidelines for the content and qualification of degradation products. The guidelines Q1A (R2), Q3A(R2), and Q3B(R2) require the execution of forced decomposition studies under a variety of stress conditions, such as pH, light, oxidation, and dry heat, in order to determine the degradation pathways that support the inherent stability of the drug and the suitability of the proposed validated SIAM for analysing stability samples.

ICH guidelines were initially pertinent only to New Drug Applications (NDA). However, the FDA has extended this to include generic products. Due to this, impurity profiling became a primary activity for all pharmaceutical companies engaged in the regulatory and generic drug industries.

## 3.1. Objectives of the proposed research work

The research work carried out can be broadily segregated into three parts;

First part involves development of HPLC method to monitor the drug degradation behaviour, stress studies as per the ICH guidelines, optimization of HPLC method (if necessary), and validation of HPLC method.

Second part involves characterization of the DPs by using LC-MS and LC-MS/MS techniques.

Lastly, *in-silico* approaches were used to predict the ADMET properties of the DPs.

### 3.1.1. Pimozide

Pimozide is an official drug as per European Pharmacopoeia (EP) and United States Pharmacopeia and National Formulary (USP-NF). Literture survey showed couple of bioanalytical methods, a HPLC method for estimation of pimozide in bulk and tablet dosage form and a stability-indicating HPTLC method. However, there was a research gap regarding a systematic development of SIAM, characterization of DPs by LC-MS and LC-MS/MS and *in-silico* ADMET predictions of DPs. Hence, the work is carried out to address the research gap.

### 3.1.2. Felbamate

Felbmate is an official drug in USP-NF. There are HPLC, LC-MS, capillary electrophoresis and gas chromatography methods available for analysis of felbmate in plasma and formulation. There was also a single UHPLC method for separation of process impurities of felbamate. However, the said method lacks in stress studies, identification of degradation studies and *in-silico* ADMET prediction. Hence, attempts were made to address these issues.

### 3.1.3. Haloperidol

Haloperidol is official in the USP-NF, British, European, and Indian pharmacopoeia. There are HPLC methods avaiaible for estimation of haloperidol in dosage forms as a single entity or in combination with other active pharmaceutical ingredients and biological fluids. However, none of the methods have systematically carried out stability testing of HALO under ICH-mandated stress conditions, structural characterization of the degradation products by LC-MS and LC-MS/MS and *in-silico* ADMET prediction. Hence, the work is carried out to fill the research gaps.

### 3.1.4. Riociguat

Riociguat is not yet official in any compendia. However, Literature shows some bioanalytical methods for estimation of RIO in plasma, few HPLC methods for estimation of RIO in formulation and a single method for estimation of riociguat by UV. Literature also revealed a single stability indicating assay method for RIO. However, it lacks in systematic approach in SIAM development, toxicity studies and a comparative binding study with target receptor. Hence, attempts were made to to address these issues.

## Chapter 3

# Chapter 4

# Characterization and *in-silico* toxicity prediction of degradation products of pimozide

## 4.0. Introduction

Pimozide is an official drug as per European Pharmacopoeia (EP)[50] and the United States Pharmacopeia and National Formulary (USP-NF).[51] Its drug Profile is also available in Clark's analysis of drugs and poisons. [52]

Pimozide treatment is efficacious in managing schizophrenia[53]. Also, it is approved by United States Food & Drug Administration (US-FDA) for relieving the vocal tics experienced by a person suffering from Tourette's Disorder[54-55]. Moreover, recently a report is published related to use of pimozide for treatment of intracellular bacterial infections. [56]

The work presented herein focuses on the following objectives:

1. Conduct of forced degradation studies on pimozide as per the ICH-mandated stress conditions.
2. Development of a stability-indicating assay method (SIAM) for pimozide.
3. Validation of the SIAM as per the ICH guidelines.
4. Structural characterization of the degradation products by liquid chromatography coupled with mass and tandem mass spectrometry.

5. Prediction of absorption, distribution, metabolism, excretion, and toxicity (ADMET) profiling using *in-silico* studies.

# 4.1. Drug profile[52]

## 4.1.1 Pimozide (PIMO)

**Chemical structure:**

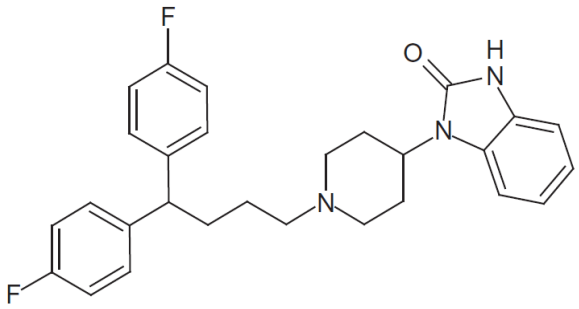


**IUPAC name:** 1-[1-[4,4-Bis(4fluorophenyl) butyl] piperidin-4-yl]-1,3-dihydro-2H-benzimidazole- 2-one.

**Molecular formula:** $C_{28}H_{29}F_2N_3O$.

**Melting point:** 214-218℃

**pKa:** 7.3

**LogP:** 5.349

**Description:** A colorless microcrystalline powder.

**Solubility:** Insoluble in water, soluble 1 in 1000 parts of ethanol, methanol, ether, 1 in 10 parts of chloroform, and 1 in 100 parts of acetone.

**Drug category:** Neuroleptic.

**Listed impurities of pimozide in monograph:** EP, USP-NF

A. 1-(piperidin-4-yl)-1,3-dihydro-2H-benimidazole-2-one.

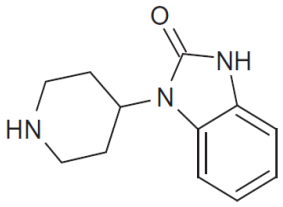


B. 1-[1-[(4RS)-4-(4-flurophenyl)-4-phenylbutyl]piperidin-4-yl]-1,3-dihydro-2H-benzimidazol-2-one.

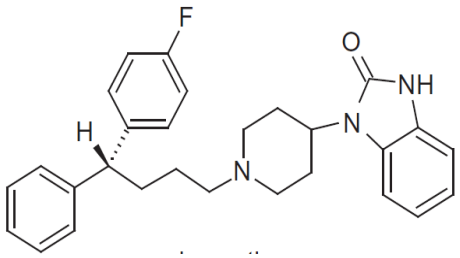


C. 1-[1-[(4RS)-4-(2-flurophenyl)-4-(4-flurophenyl)butyl]piperidin-4-yl]-1,3-dihydro-2H-benimidazol-2-one.

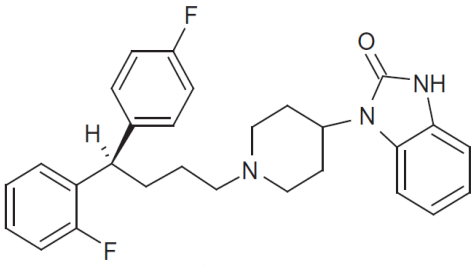


D. 1-[1-[4,4-bis(4-flurophenyl)butyl]-1,2,3,6-tetrahydropyridin-4-yl]-1,3-dihydro-2H-benzimidazol-2-one.

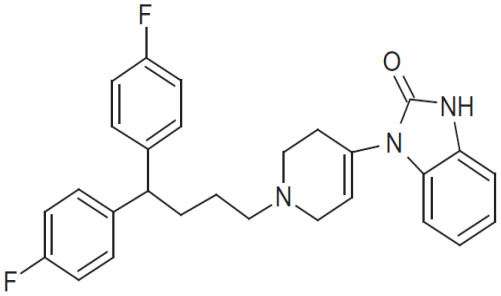

E. 1-[1-[4,4-bis(4-flurophenyl0butyl]piperidin-4-yl-1-oxide]-1,3-dihydro-2H-benimidazol-2-one.

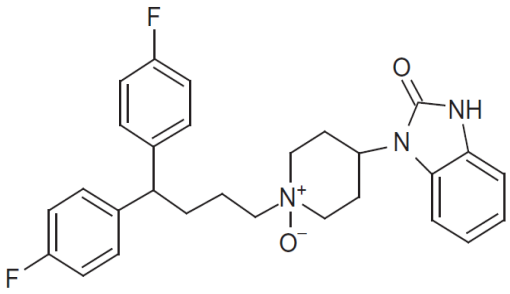


**Clinical Pharmacology:**

Dopamine is a neurotransmitter that controls several cerebral functions like mood, reward, locomotive function, learning, and motivation.[57]

The primary action of most antipsychotic drugs, including PIMO is to attach to the D2 receptor making it unavailable for dopamine. After PIMO attaches to the receptor, its dissociation from the receptor takes longer time due to the higher dissociation constant. This result exhibhits inhibitory activity towards the receptor.

**Pharmacokinetics:**

PIMO has good absorption through the gastrointestinal tract (GIT). Once absorbed, studies have revealed that its hepatic first-pass metabolism is very high resulting in reduced systemic availability. Its volume of distribution is very high with an apparent elimination half-life of 24 h. The elimination of PIMO is through the renal route without formation of any active metabolite[57-58].

**Toxicity:**

PIMO is a known inhibitor of specific isoforms of the cytochrome P450 enzyme system, namely, CYP3A, CYP1A2, and CYP2D6. Administration of PIMO with other CYP3A inhibitors like clarithromycin can result in fatal cardiac arrhythmias.

## 4.2 Literature survey

A thorough search was conducted to check for the various analytical methods available for PIMO. Information about various physiochemical properties was collected and is listed under section 4.1 (drug profile ). European Pharmacopoeia mentions five process impurity for pimozide (A-E). The process impurity E (N-oxide) is a known degradation product of PIMO.

Besides the compendial methods, there were a few bioanalytical methods reported for the estimation of PIMO in plasma.[59-61] There was also an HPLC method for estimating PIMO in bulk and tablet dosage form[62] and a couple of stability-indicating methods using HPTLC and UV.[63-64] However, none of the methods had extensively carried out stability testing of PIMO under ICH-mandated stress conditions and subsequent structural characterization of the degradation products.

The following table summarizes the chromatographic conditions used by various analytical methods using HPLC.

**Table 4.2.1:** Summary of HPLC methods available for determination of PIMO by HPLC

| | Type of method | Column Type | Mobile Phase composition | Flow rate | Detector used | References |
|---|---|---|---|---|---|---|
| 1 | **USP-NF and EP.** | | | | | |
| | HPLC | C18, 100mm × 4.6mm, 3 µm | Mixture of ammonium acetate (32mM) and tetrabutylammonium hydrogen sulfate (32 mM) in water [A]: acetonitrile[B], ($T_{min}$/A:B (v/v) - $T_0$/80:20;$T_{10}$/70:30;$T_{15}$/70:30;$T_{20}$/80:20;$T_{25}$/80:20 ) | 2.0mL /min | UV, 280nm | 50,51 |
| 2 | **Title: Quantitative determination of pimozide in human plasma by liquid chromatography-mass spectrometry and its application in a bioequivalence study** | | | | | |
| | LC-MS | Thermo Hypersil-HyPURITY C18,150mm×4.6mm, 5 µm | ammonium acetate (5 mM, pH adjusted to 3.5 with acetic acid):methanol:acetonitrile, 39:5:56 (v/v/v) | 0.22 mL/min | MS | 60 |
| 3 | **Title: Sensitive assay for pimozide in human plasma using high-performance liquid chromatography with fluorescence detection application to pharmacokinetic studies** | | | | | |
| | HPLC | Vydac C18, 150mm× 4.6mm, 5 µm | sodium dihydrogen phosphate (50mM, pH adjusted to 3.0 with 1% phosphoric acid):acetonitrile | 1.0 mL/min | Fluorescence, excitation wavelength-285nm, emission wavelength 320nm | 61 |
| 4 | **Title: RP-HPLC method for estimation of an antipsychotic drug - pimozide** | | | | | |
| | HPLC | Grace Smart RP-18 column, 250mm× 4.6mm, 5 µm | Acetonitrile: Disodium Hydrogen phosphate (50 mM, pH adjusted to 6.2 with 1 % orthophosphoric acid), 60:40, (v/v) | 1.0 mL/min | UV, 280nm | 62 |

# 4.3. Present work and discussion

## 4.3.1. Development of HPLC method to monitor drug degradation behavior of pimozide

### 4.3.1.1. Selection of chromatographic methods

All the published HPLC methods including compendial methods employ reverse-phase chromatography (RPC) approach for detection and quantification of PIMO. Due to this, it was decided to develop the HPLC method using RPC approach.

### 4.3.1.2. Selection of stationary phase

The compendial and the reported HPLC methods preferred use of a C18 column as a stationary phase for PIMO. C18 is the most popular column for the initial exploratory run for a drug molecule. It's got the highest carbon load among the RPC column resulting in stronger retention[42]. So, Phenomenex C18 (150mm ×4.6mm, 5µm) column was selected as a stationary phase due to availability.

### 4.3.1.3. Selection of wavelength for analysis

During the initial HPLC runs, the diode array detector (DAD) was set to scan the entire UV range (200-400nm) to determine the wavelength of maximum absorbance ($\lambda_{max}$) of PIMO. The UV spectrum obtained is depicted in figure 4.3.1.3.1. The UV spectrum showed two wavelength maxima, one at 210 nm and other at 280 nm. The wavelength maxima at 280 nm was selected for further analysis. The preference was given to the higher wavelength to obtain stable baseline during the HPLC analysis.

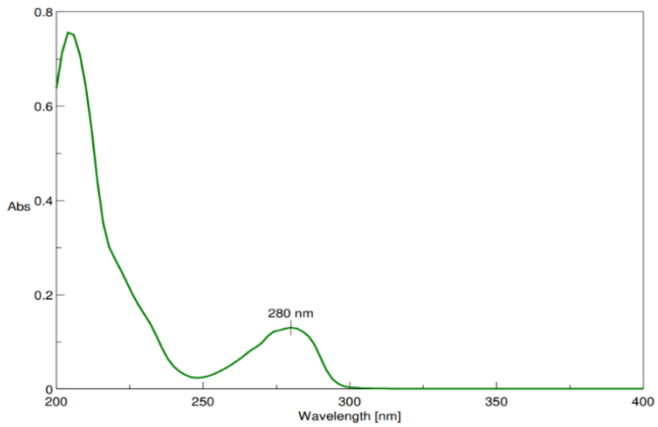


**Figure 4.3.1.3.1:** UV spectrum of PIMO having concentration (10 µg/mL in acetonitrile)

### 4.3.1.4. Selection and optimization of mobile phase for monitoring degradation of PIMO

The primary objectives were to develop a simple, robust, isocratic, and mass-friendly RP-HPLC (reverse-phase high-performance liquid chromatography) method to monitor the drug degradation behaviour. The method was also required to have a capacity factor (*K'*) in the range of 4-10 [65,31]. The selection of stated range of *K'* allows efficient separation of polar and non-polar DPs and enhances the robustness of the method.

The reported methods for PIMO used isocratic elution with the most preferred organic component of the mobile phase being acetonitrile. The aqueous component of the mobile phase mainly consisted of phosphate or acetate buffer with a pH in range of 3.5 to 6.

The pKa of PIMO is 7.3. In acidic pH, PIMO exists in an ionized form. Generally, it is advised to set the pH of the mobile phase ± 1.5 units away from the pKa of the drug to convert the drug predominantly into one of its ionic form. Taking this as a guideline, initial exploratory runs were taken at acidic pH away from the pKa of the drug to observe the retention behaviour of the drug . Ammonium acetate (10 mM, pH 3.7, adjusted with acetic acid) was selected as the aqueous component along with acetonitrile. Moreover, ammonium acetate is a volatile buffer having compatibility with mass detector. It is a salt of weak acid and weak base, its solution has pH 7. The buffer does not have significant buffer capacity at pH 7 but it exhibit buffer capacity near pH 4.75 ± 1 (pKa of acetic acid) and pH 9.25 ± 1 (pKa of ammonia).[66]

The preliminary trial was taken by using a mobile phase ratio (70:30, v/v) of acetonitrile and ammonium acetate buffer (10 mM, pH 3.7). The chromatogram obtained is shown in figure 4.3.1.4.1.

The above trial resulted in a very sharp peak close to the void volume. Early elution of the drug was attributed to higher composition of the organic component. To get desired retention time, subsequent trials were conducted with gradual decrease in the organic phase composition.

Trials involving a change in organic phase from 70 to 50 % did not yield desired retention. However, when organic phase was reduced to 45 %, a significant change in retention time was observed. The chromatogram obtained is seen in figure 4.3.1.4.2

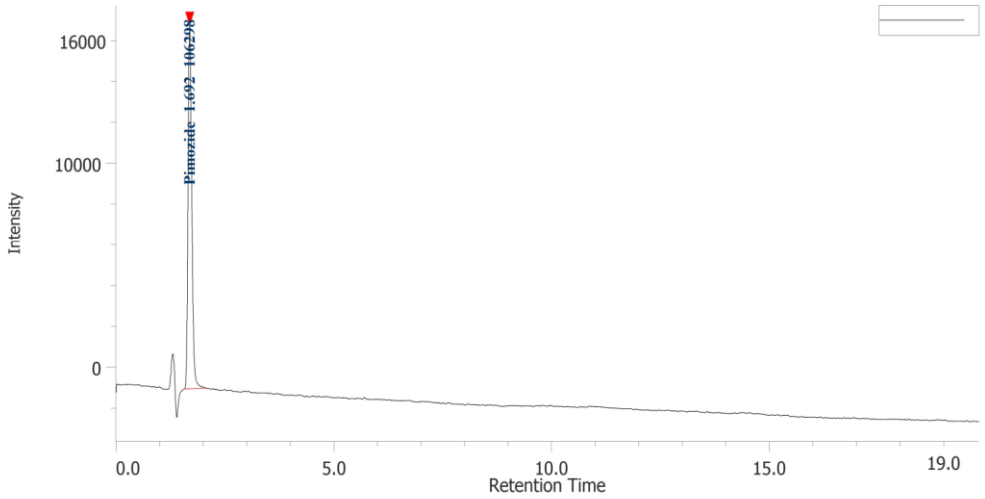


**Figure 4.3.1.4.1: Chromatogram of PIMO (10µg/mL)** (Mobile phase, acetonitrile: ammonium acetate buffer (pH 3.7, adjusted with acetic acid), 70:30 (v/v), flow rate: 1mL/min; wavelength: 280nm, Column: Phenomenex C18 (150mm ×4.6mm, 5µm))

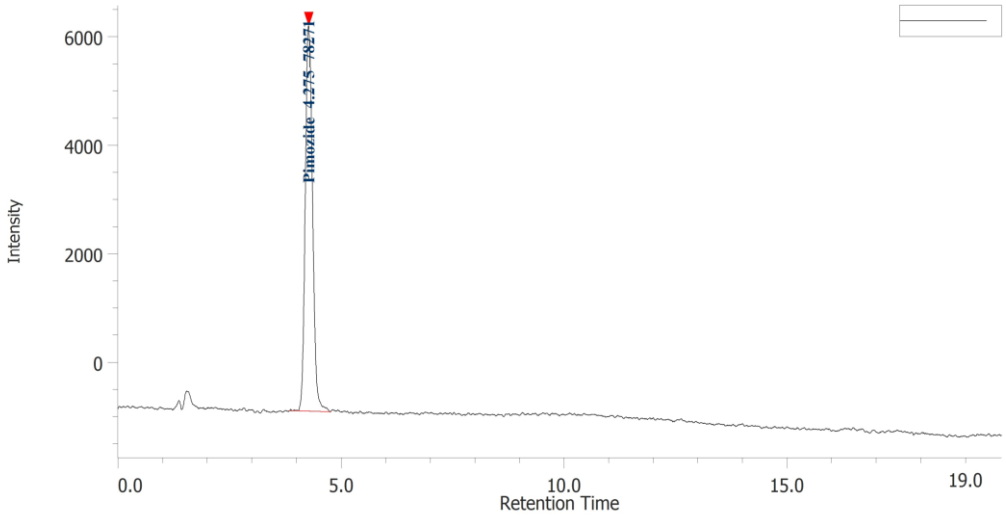


**Figure 4.3.1.4.2: Chromatogram of PIMO (10µg/mL)** (Mobile phase, acetonitrile: ammonium acetate buffer (pH 3.7, adjusted with acetic acid), 45:55 (v/v); flow rate: 1mL/min; wavelength: 280nm; Column: Phenomenex C18 (150mm ×4.6mm, 5µm))

The said modification did not result in desired value of *K'*. Due to this, the mobile phase percentage was further decreased to 40%. The resulting chromatogram is depicted in figure 4.3.1.4.3.

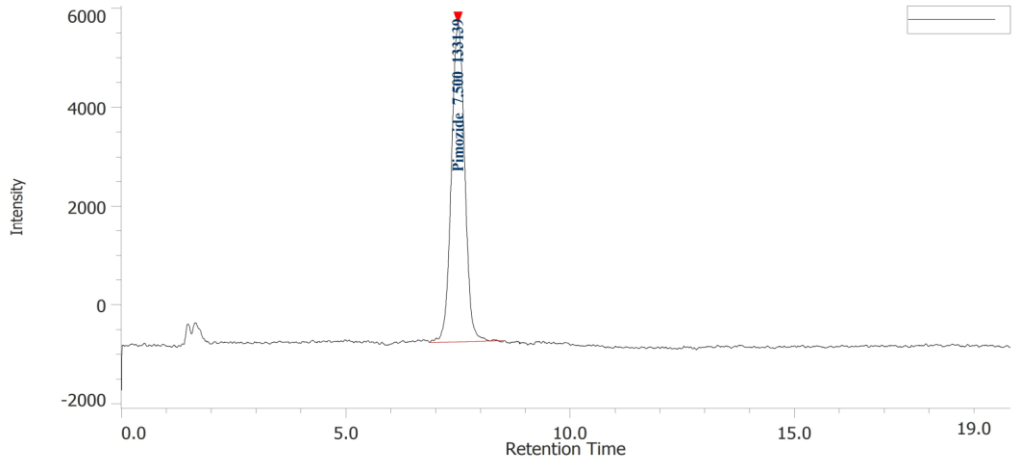


**Figure 4.3.1.4.3: Chromatogram of PIMO (10µg/mL)** (Mobile phase, acetonitrile: ammonium acetate buffer (pH 3.7, adjusted with acetic acid), 40:60 (v/v); flow rate: 1mL/min; wavelength: 280nm; Column: Phenomenex C18 (150mm ×4.6mm, 5µm))

This modification resulted in the desired value of *K'* (4.5). The peak had a retention time of 7.5 min, number of theoretical plates (NTP) > 3000, and symmetry factor was < 2. The summary of the chromatographic conditions adopted for the developed HPLC method to monitor the drug degradation behavior was as follows;

**Mobile phase:** Acetonitrile: ammonium acetate buffer (pH = 3.7, adjusted with acetic acid), 40:60 (v/v).

**Column:** Phenomenex C18 (150 mm ×4.6 mm, 5µm).

**Wavelength:** 280 nm.

**Flow rate:** 1 mL/min.

## 4.3.2. Forced degradation studies

The stability of the drug was probed as per the guidance provided in the ICH Q1A(R2) guideline. The drug was tested under hydrolytic (acidic, basic, and neutral), oxidative,

thermal, and photolytic conditions. The stressed samples were subjected to HPLC analysis using optimized chromatographic conditions, and the chromatogram obtained was compared with blank stored under normal condition (blank untreated), blank subjected to stress conditions like the drug (blank treated), and the drug solution stored under normal condition (standard untreated)

#### 4.3.2.1. Hydrolytic degradation

Hydrolytic degradation was performed using acidic, basic, and neutral conditions. The degradation studies were carried out at room temperature in order to get desired degradation of the drug. The degradation studies were also carried out at higher temperature ( 70 ℃, 7 h), in case, no degradation was observed at room temperature. The concentration of the stressors was also optimized from low to high depending upon the degradation behaviour of the drug. Periodically, samples were withdrawn, neutralized, and diluted to the desired concentration and injected into HPLC using optimized chromatographic conditions.

**Acid degradation**

Acid degradation was carried out at room temperature by exposing drug solution to 0.1 N /1 N HCl for 48 hours in a volumetric flask to get desired degradation of the drug. The studies were repeated using 1 N HCl at 70℃ for 7 hours since no degradation was observed at room temperature. After applying the stress conditions, the samples were neutralized by using equal strength of base (NaOH). The neutralized samples were diluted to get the desired concentration and injected into HPLC using optimized chromatographic conditions.

The drug showed resilience to degradation under acidic conditions, and no degradation was observed.

**Base degradation**

Base degradation was carried out at room temperature by exposing drug solution to 0.1 N /1 N NaOH for 48 hours in a volumetric flask to get desired degradation of the drug. The studies were repeated using 1 N NaOH at 70℃ for 7 hours since no degradation was observed at room temperature. After applying the stress conditions, the samples were neutralized by using equal strength of acid (HCl). The neutralized samples were diluted to get the desired concentration and injected into HPLC using optimized chromatographic conditions.

The drug showed resilience to degradation under basic conditions, and no degradation was observed.

**Neutral degradation**

Neutral degradation was carried out at room temperature by exposing drug solution to water for 48 hours in a volumetric flask to get desired degradation of the drug. The studies were repeated by heating the drug solution with water at 70℃ for 7 h since no degradation was observed at room temperature. Samples were diluted to get the desired concentration and injected into HPLC using optimized chromatographic conditions.

The drug showed resilience to degradation under neutral basic condition, and no degradation was observed.

**4.3.2.2. Oxidative degradation**

Oxidative degradation was carried out at room temperature by exposing drug solution to 15% $H_2O_2$ for 48 hours in a volumetric flask to get desired degradation of the drug. The studies were repeated by heating the drug solution with 15% $H_2O_2$ at 70℃ for 7 hours to enhance the concentration of DPs. However, it led to formation of secondary DPs. Samples were diluted to get the desired concentration and injected into HPLC using optimized chromatographic conditions.

The drug was susceptible towards degradation under oxidative stress. The drug degraded ~ 27% at room temperature for 48 h and led to formation five degradation products. The representative chromatogram is shown in figure 4.3.2.2.1.

**4.3.2.3. Thermal degradation**

Thermal degradation was carried out by exposing the drug in sealed ampoule to dry heat at 70 ℃ for 7 days using hot air oven. A control sample was maintained by placing drug into a separate glass ampoule stored at room temperature. After the stress period, the sample was diluted with diluent to get the desired concentration and injected into HPLC using optimized chromatographic conditions.

The drug did not show degradation under thermal conditions

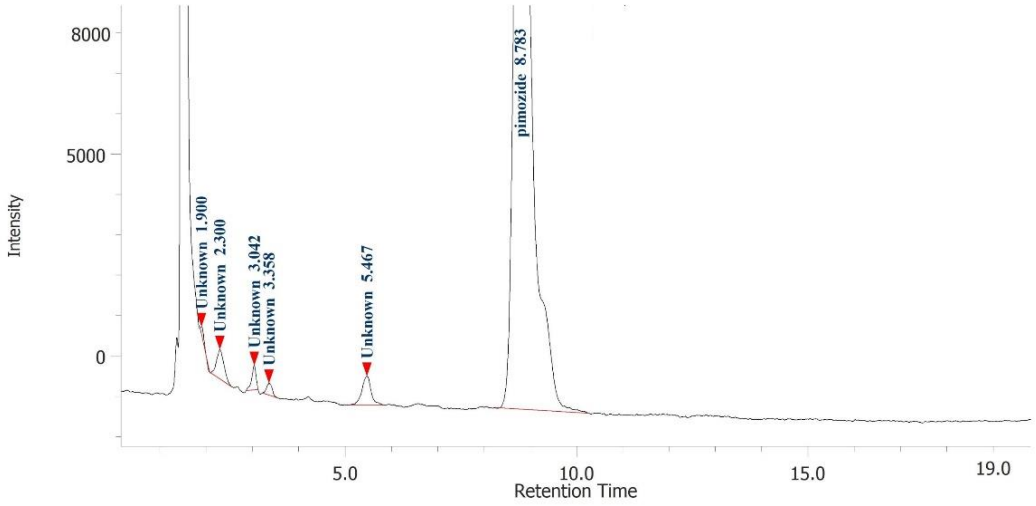


**Figure 4.3.2.2.1: Chromatogram of Pimozide (100 µg/mL) treated with 15% $H_2O_2$ at room temperature for 48 h (isocratic). (**mobile phase, Acetonitrile: ammonium acetate buffer (pH 3.7, adjusted with acetic acid), 40:60 (v/v); flow rate: 1mL/min; wavelength: 280nm; Column: Phenomenex C18 (150mm ×4.6mm, 5µm))

### 4.3.2.4. Photolytic degradation

Photolytic degradation studies were carried out in the solid and liquid states using photostability chamber. Solid state stress studies were carried out by spreading the drug as a thin layer inside a petri dish while, liquid state stress studies were carried out by placing drug solution inside a volumetric flask. Both the samples were exposed to ICH Q1B mandated dose of light. In addition, solid-state studies were also carried out by exposing the drug placed inside a volumetric flask to sunlight for 7 days.

The chromatogram obtained from photolytic stressed samples did not show degradation.

## 4.3.3. Development and Optimization of the stability-indicating assay method

During the stress studies, it was observed that the unknown peak 1 ($t_R$ = 1.9 min) eluted very close to the void volume with peak symmetry value of 2.67. The unknown peak 2 ($t_R$ = 2.3 min) had NTP < 1000. Moreover, $R_s$ of unknown peak 2 and 3 ($t_R$ = 3.0 min) was < 0.75, which made it a critical band pair.

All the above problems were resolved by changing the elution mode form isocratic to gradient. The obtained chromatogram and the details of the gradient program is depicted in figure 4.3.3.1.

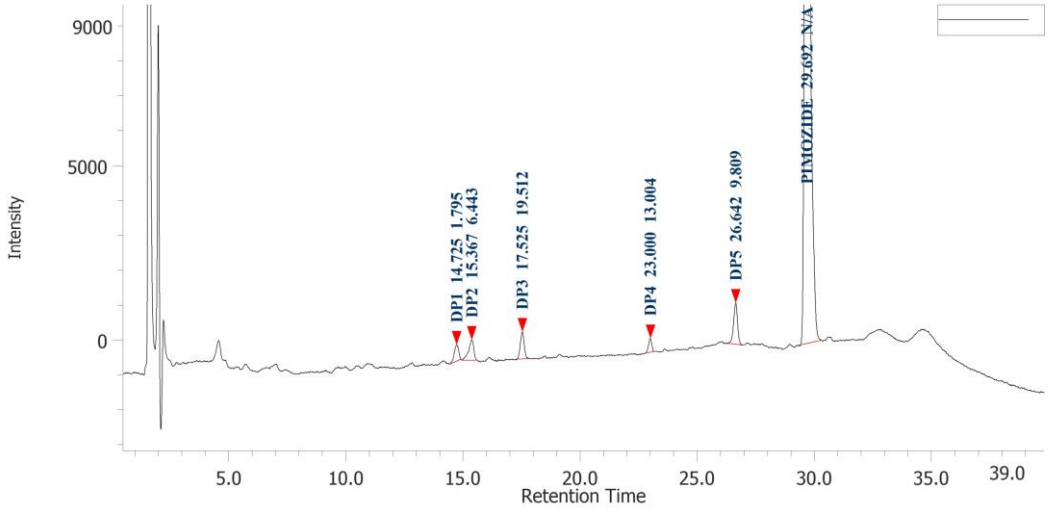


**Figure 4.3.3.1: Chromatogram of Pimozide (100 µg/mL) treated with 15% $H_2O_2$ at room temperature for 48 h. (**Mobile phase, acetonitrile(A): ammonium acetate buffer(B) (pH=3.7, adjusted with acetic acid), ($T_{min}$/A:B (v/v) - $T_0$/15:85;$T_{30}$/45:55;$T_{35}$/15:85;$T_{40}$/15:85); flow rate: 1mL/min; wavelength: 280nm; Column: Phenomenex C18 (150mm ×4.6mm, 5µm))

The UV spectra of the individual degradation products was recorded using the diode array detector and overlain with the UV spectra of the drug as shown in 4.3.3.2.

The summary of the chromatographic conditions of the optimized HPLC method was as follows

**Mobile phase:** Acetonitrile(A): ammonium acetate buffer(B) pH 3.7, adjusted with acetic acid, $T_{min}$/A:B (v/v) - $T_0$/15:85;$T_{30}$/45:55;$T_{35}$/15:85;$T_{40}$/15:85.

**Column:** Phenomenex C18 (150 mm ×4.6 mm, 5 µm).

**Wavelength:** 280 nm.

**Flow rate:** 1 mL/min.

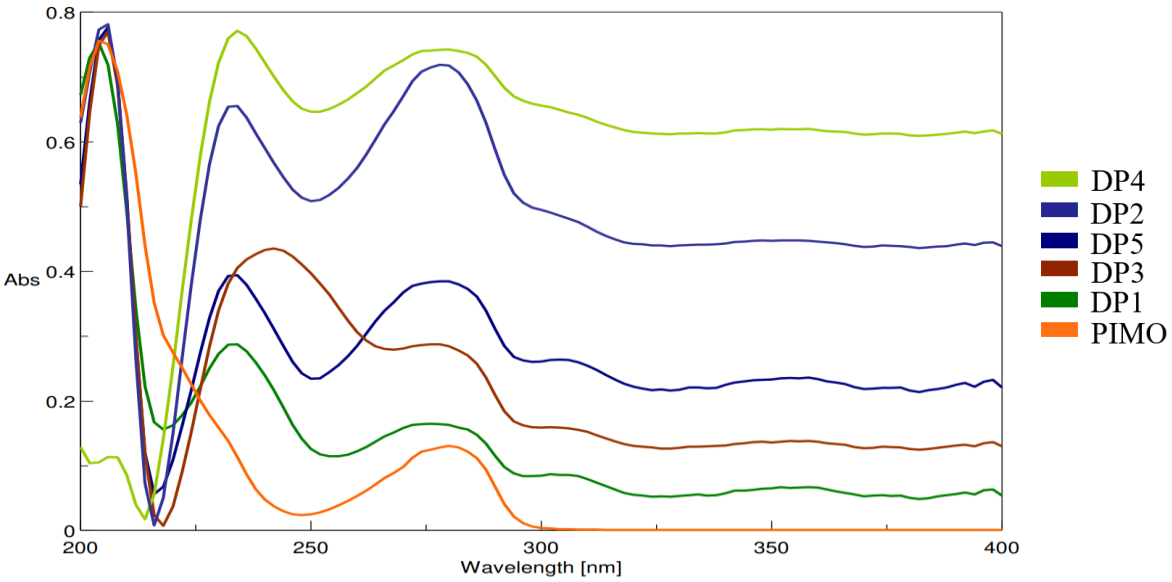


**Figure 4.3.3.2:** Overlain of UV spectra of PIMO with its oxidative DPs.

## 4.3.4. Validation of the developed stability-indicating assay method (SIAM)

HPLC method validation is required to ensure that the method achieves an adequate standard of specificity, accuracy, and precision. The developed SIAM was validated as per the guidance of the ICH Q2 guideline. The parameters considered during the validation process is summarized in table 4.3.4.1.

### 4.3.4.1. Specificity and selectivity

The specificity of the HPLC method was expressed in terms of resolution between the closely eluting peaks. It is evident from figure 4.3.3.1 that the peaks were well resolved with a resolution value greater than one which confirms the specificity of the method. The method's selectivity was determined by measuring % peak purity value acquired using data acquisition software. The peak purity(%) was > 99% which indicates that the method is selective.

**Table 4.3.4.1:** Validation parameters and acceptance criteria

| Sr.No | Validation Parameters | Acceptance Criteria |
|---|---|---|
| **1** | **Specificity** | Resolution > 1 |
| **2** | **Selectivity** | Peak purity (%) > 99 |
| **3** | **Linearity** | Correlation coefficient not less than 0.999 |
| **4** | **Accuracy (across the specified range)** | Recovery (%) between 98.0 to 102% |
| **5** | **Precision (intraday & interday)** | RSD (%) of replicate injections not more than 2.0 |
| **6** | **Robustness** | 1) Resolution between adjacent peak should not be less than 1.0<br>2) Numbers of theoretical plates of analyte peak should not be less than 2000.<br>3) Asymmetry of peak should not be more than 2.0 |

### 4.3.4.2. Linearity and range

The linearity was established in triplicate by taking five incremental concentrations in a range of 10-100 µg/mL. The graph was plotted between the average area under peak v/s concentration. The data obtained was subjected to regression analysis. The calculated value of the corelation coefficient ($r^2$) was 0.999. The linearity plot and the data pertaining to linearity is given in figure 4.3.4.2.1 and table 4.3.1.2.1. The representative chromatogram at each concentration level is seen in figure 4.3.4.2.2.

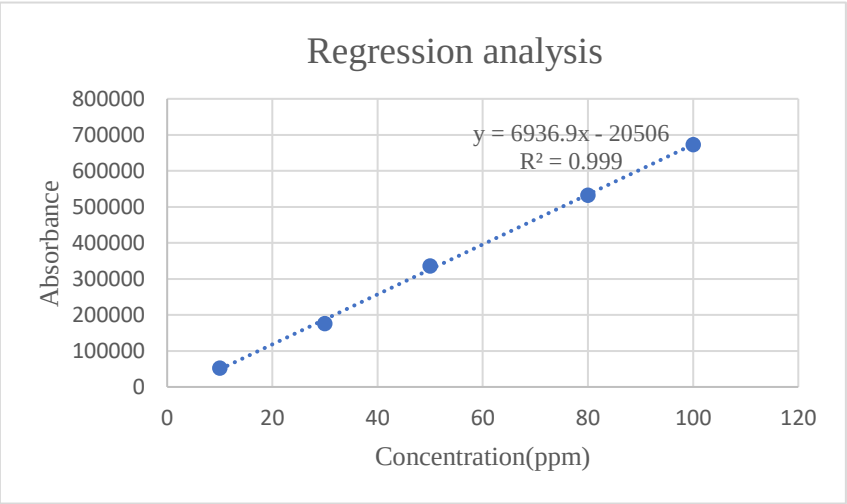


**Figure 4.3.4.2.1:** Linearity graph of PIMO

**Table 4.3.1.2.1:** Linearity data for PIMO

| Sr. No. | Concentration (µg/mL) | Peak area | | | | RSD(%) |
|---|---|---|---|---|---|---|
| | | Injection 1 | Injection 2 | Injection 3 | Average | |
| 1 | 10 | 52393 | 52168 | 53301 | 52621 | 1.13 |
| 2 | 30 | 178008 | 174202 | 176127 | 176112 | 1.08 |
| 3 | 50 | 341701 | 333421 | 333892 | 336338 | 1.38 |
| 4 | 80 | 530609 | 534444 | 533177 | 532743 | 0.36 |
| 5 | 100 | 671200 | 674701 | 671944 | 672615 | 0.27 |

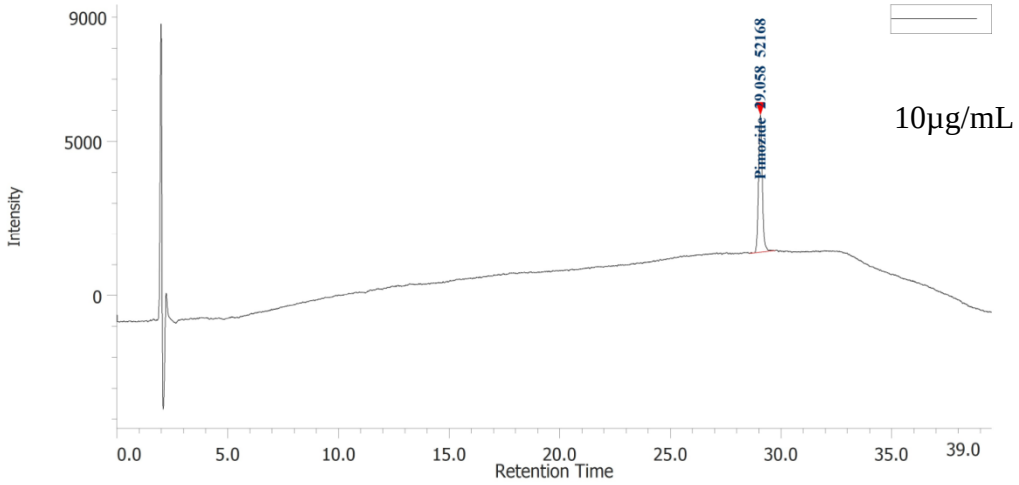


**Chromatogram no 1**

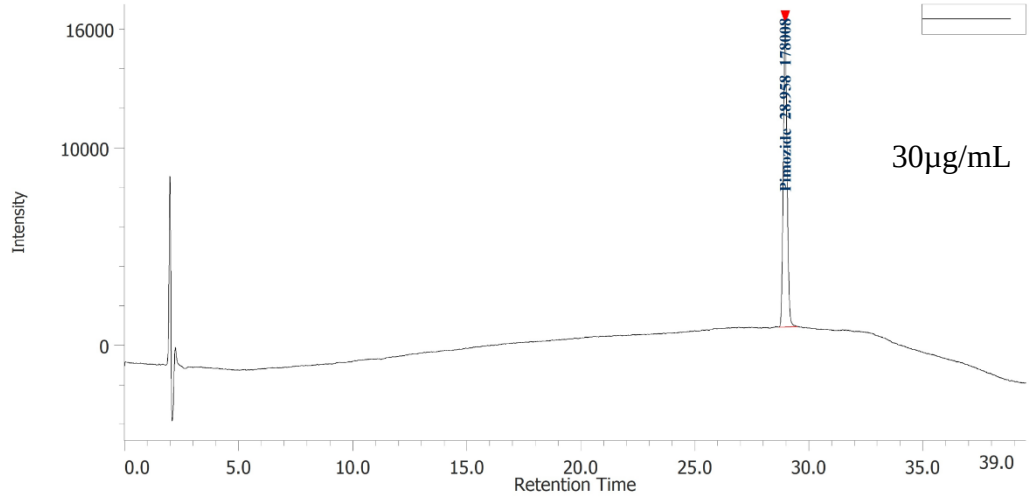


**Chromatogram no 2**

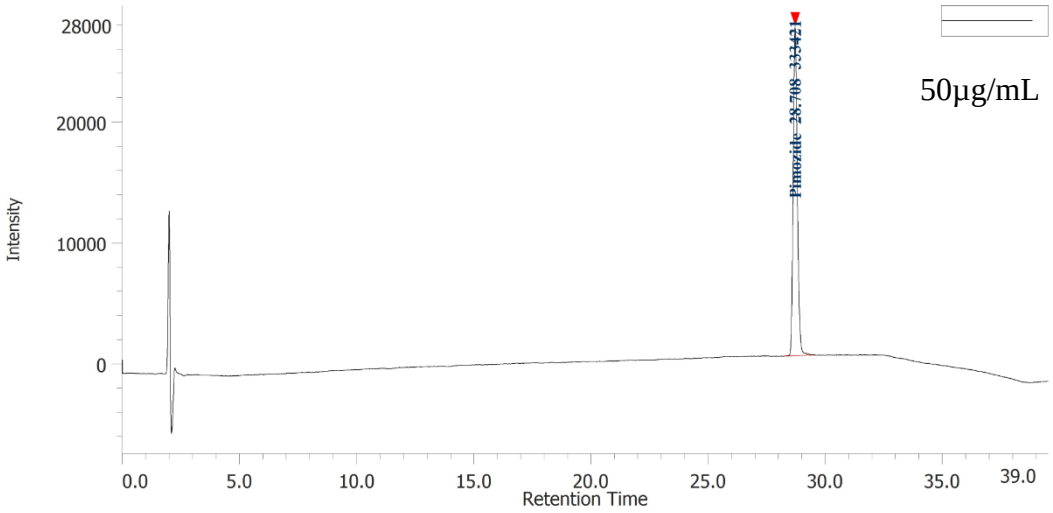


**Chromatogram no 3**

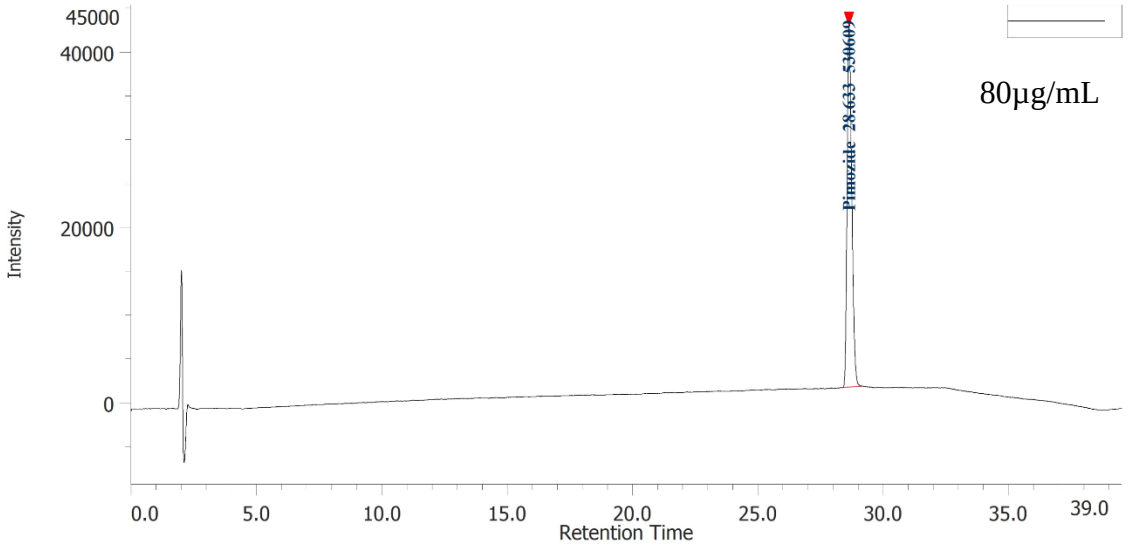


**Chromatogram no 4**

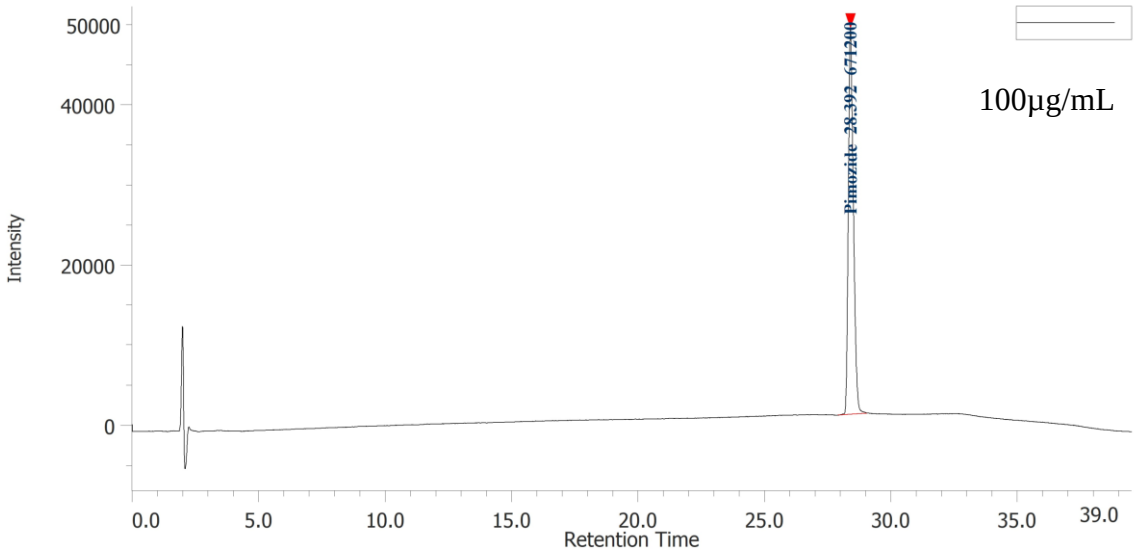


**Chromatogram no 5**

**Figure 4.3.4.2.2:** Representative chromatograms at concentration level 10, 30, 50, 80 and 100 µg/mL.

### 4.3.4.3. Accuracy

The accuracy was expressed in terms of recovery (%) of the spiked standard drug and was done by the standard addition method The stressed sample were separately spiked with standard drug with concentrations 40 µg/mL (80%), 50 µg/mL (100%) and 60 µg/mL (120%) of the target assay concentration (50 µg/mL) and injected in triplicate. The average recovery at each level was between 98 to 102 %, with the mean recovery of 101.3 %. The data of recovery studies is shown in table 4.3.4.3.1.

**Table 4.3.4.3.1:** Recovery studies for PIMO (n=3)

| Spiked drug concentration (µg/mL) | Recovered concentration (µg/mL) ± S. D, % R.S.D. | Recovery (%) |
|---|---|---|
| 40 | 40.6 ± 0.26, 0.64 | 101.5 |
| 50 | 50.8 ± 0.10, 0.19 | 101.6 |
| 60 | 61.1 ± 0.19, 0.31 | 101.8 |

The representative chromatogram obtained at each level of accuracy study is shown in figure 4.3.4.3.1.

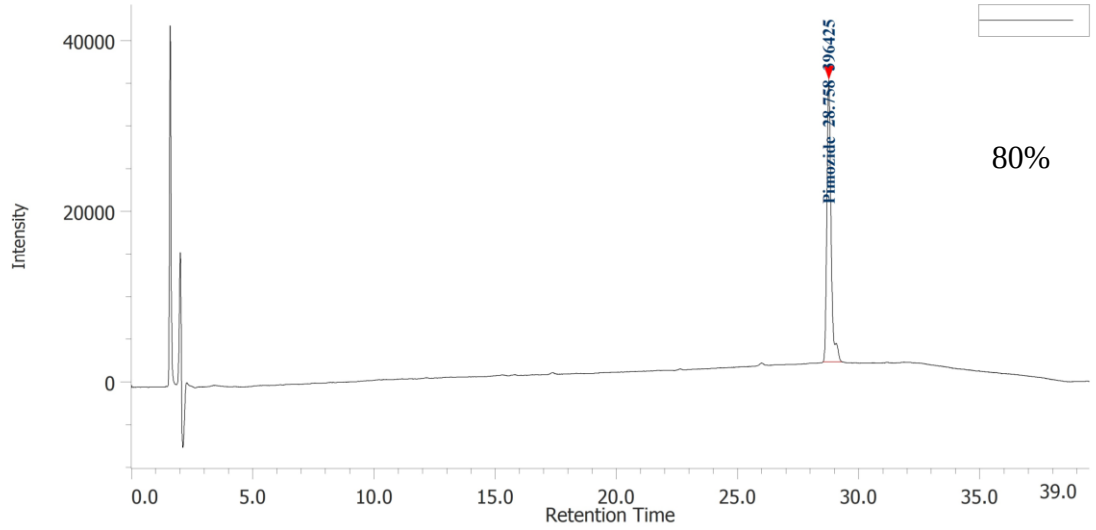


**Chromatogram no 6**

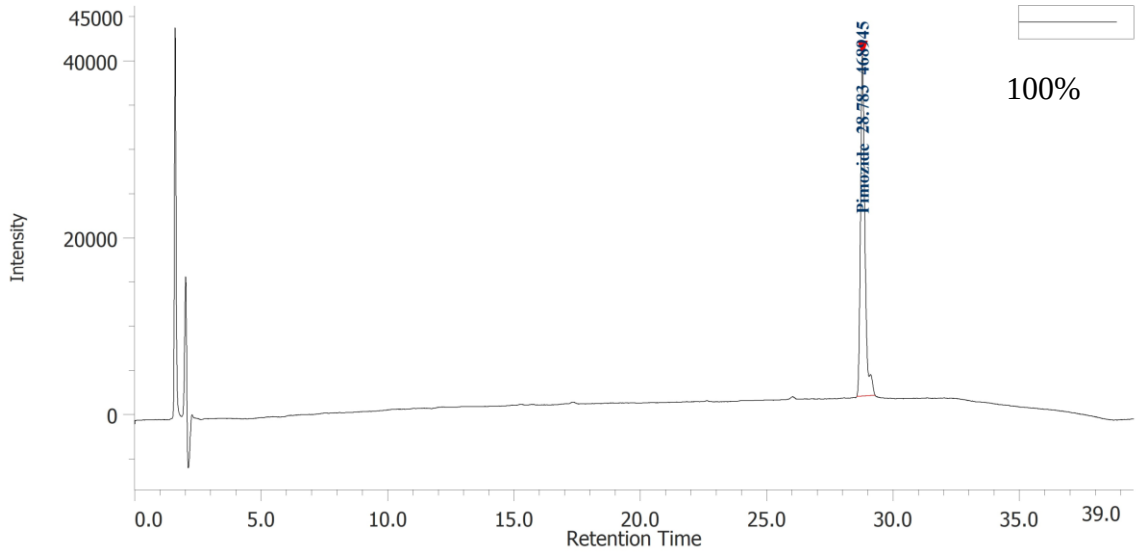


**Chromatogram no 7**

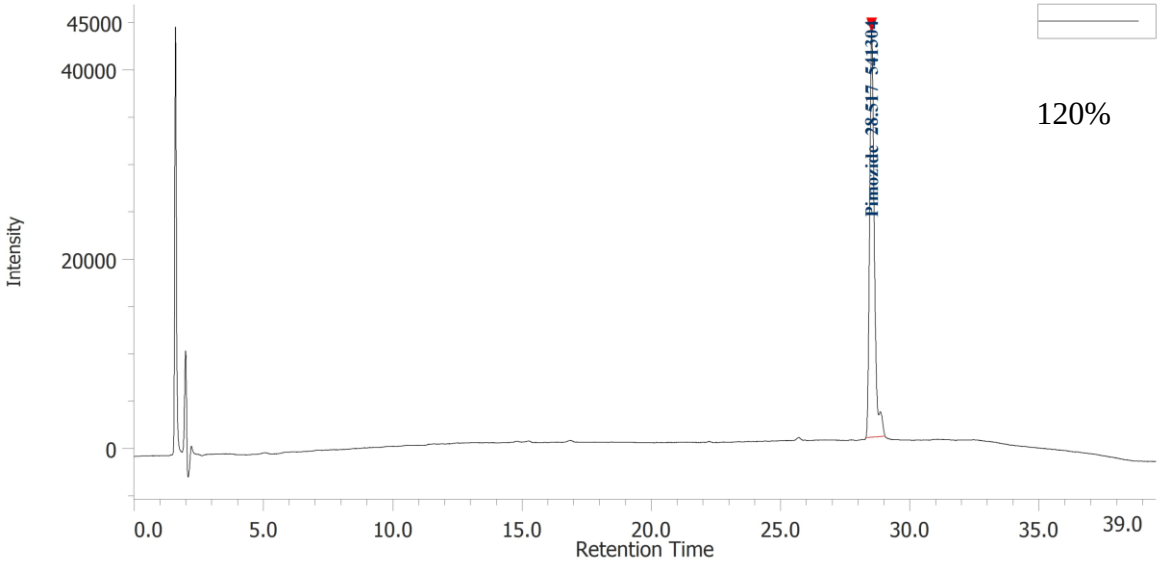


**Chromatogram no 8**

**Figure 4.3.4.3.1:** Representative chromatograms obtained at each level of accuracy studies at 80, 100, and 120%

### 4.3.4.4. Precision

Intra and inter-day precision studies were performed at three concentration levels of 30, 50, and 100 µg/mL in triplicate. The % RSD at each level was found to be < 2% inferring that the method was precise. The precision data is seen in the following table.

**Table 4.3.4.4.1:** Precision data obtained during intra-day and inter-day studies

| Concentration (µg/mL) | Intraday (n=3) Mean peak area ± SD; %RSD | Inter-day (n =3) Mean peak area ± SD; %RSD |
|---|---|---|
| 30 | 178008 ± 1906;1.1 | 168221 ± 3111 ;1.8 |
| 50 | 336338 ± 4650.5;1.4 | 343607 ± 1021.7;0.3 |
| 100 | 672615 ± 1844.4;0.3 | 676497 ± 4107.9;0.6 |

### 4.3.4.5. Robustness

The robustness of the HPLC method was established to understand the HPLC methods tolerance to deliberate change in the chromatographic parameters. For this purpose, the following changes were carried out to observe its effect on the developed method.

1) The pH of the mobile phase (± 0.5 of the optimized value.)
2) Flow rate (± 0.1ml of the optimized flow rate)
3) Mobile phase composition (± 1% strength of the optimized ratio)
4) Wavelength (± 3 units of the optimized wavelength)

The results of the robustness studies are depicted in the tables below.

**Table 4.3.4.5.1:** Data pertaining to robustness studies

| Peak | Theoretical plates | Asymmetry | Resolution |
|---|---|---|---|
| | **pH 3.2** | | |
| DP1 | 28064 | 0.91 | 1.22 |
| DP2 | 43810 | 0.95 | 4.65 |
| DP3 | 39349 | 0.87 | 18.21 |
| DP4 | 126640 | 0.91 | 13.29 |
| DP5 | 146292 | 0.97 | 10.33 |
| PIMO | 149392 | 1.69 | -- |
| | **pH 4.2** | | |
| DP1 | 33083 | 1.04 | 1.52 |
| DP2 | 45994 | 0.82 | 4.83 |
| DP3 | 40786 | 0.92 | 18.40 |
| DP4 | 120756 | 1.03 | 13.30 |
| DP5 | 146518 | 0.97 | 10.39 |
| PIMO | 147768 | 1.70 | -- |

| Peak | Theoretical plates | Asymmetry | Resolution |
|---|---|---|---|
| | **Flow rate 0.9ml/min** | | |
| DP1 | 23134 | 0.95 | 1.70 |
| DP2 | 46073 | 0.74 | 5.06 |
| DP3 | 40643 | 0.90 | 17.46 |
| DP4 | 123731 | 0.95 | 12.84 |
| DP5 | 135825 | 1.06 | 10.17 |
| PIMO | 152135 | 1.72 | -- |

| | | | |
|---|---|---|---|
| **Flow rate 1.1ml/min** | | | |
| DP1 | 21780 | 1.02 | 2.43 |
| DP2 | 32666 | 0.79 | 4.94 |
| DP3 | 45794 | 0.99 | 18.50 |
| DP4 | 96548 | 1.05 | 11.99 |
| DP5 | 112473 | 1.08 | 9.79 |
| PIMO | 144714 | 1.52 | -- |

| **Peak** | **Theoretical plates** | **Asymmetry** | **Resolution** |
|---|---|---|---|
| **Organic phase +1% of the optimized ratio** | | | |
| DP1 | 24397 | 0.89 | 1.56 |
| DP2 | 28041 | 0.85 | 6.67 |
| DP3 | 50469 | 1.03 | 19.56 |
| DP4 | 106723 | 0.84 | 12.82 |
| DP5 | 118570 | 1.03 | 9.96 |
| PIMO | 133233 | 1.37 | -- |
| **Organic phase -1% of the optimized ratio** | | | |
| DP1 | 32194 | 0.84 | 1.80 |
| DP2 | 45331 | 1.01 | 7.14 |
| DP3 | 65199 | 1.13 | 18.97 |
| DP4 | 109297 | 1.01 | 12.64 |
| DP5 | 143908 | 0.93 | 10.07 |
| PIMO | 147957 | 1.40 | -- |

| **Peak** | **Theoretical plates** | **Asymmetry** | **Resolution** |
|---|---|---|---|
| **Wavelength (277 nm)** | | | |
| DP1 | 28748 | 0.91 | 1.79 |
| DP2 | 28553 | 0.79 | 6.50 |
| DP3 | 53082 | 1.01 | 19.42 |
| DP4 | 124440 | 0.92 | 13.03 |
| DP5 | 126591 | 0.92 | 9.87 |
| PIMO | 136265 | 1.34 | -- |
| **Wavelength (283 nm)** | | | |
| DP1 | 26643 | 0.90 | 1.79 |
| DP2 | 28893 | 0.84 | 6.48 |
| DP3 | 52598 | 1.02 | 19.35 |
| DP4 | 124716 | 1.01 | 13.03 |
| DP5 | 125739 | 0.93 | 9.85 |
| PIMO | 136076 | 1.34 | -- |

## 4.3.5. Characterization of the degradation products by mass and tandem mass spectrometry

The structural characterization of the DPs was carried out using LC-MS and LC-MS/MS. The LC-MS and LC-MS/MS spectra were recorded in positive electro spray ionization mode(+ESI). The optimized parameters of LC-MS/MS studies are depicted in table 4.3.5.1

**Table 4.3.5.1:** The optimized parameters of LC-MS/MS studies.

| Parameter | Value |
|---|---|
| **Dying, sheath, and nebulizing gas** | Nitrogen |
| **Vcap** | 4000 V |
| **Fragmentor** | 50 V |
| **Skimmer** | 45 V |
| **Octopol RF peak** | 750 V |
| **Drying gas flow** | 11 L/min |
| **Sheath gas flow** | 11 L/min |
| **Nebulizing gas** | 25 psi |
| **Sheath gas temp** | 400°C |

Based on the MS and the MS/MS data the most probable structure for degradation products was postulated along with its fragmentation pathway.

### 4.3.5.1. PIMO

The molecular weight of PIMO is 461.2351 g/mole. The LC-MS spectra recorded in the +ESI mode showed molecular peak ion at *m/z* 462.2380. The MS/MS spectra of PIMO showed peaks at *m/z* 328.1889 and 201.1028. PIMO loses $C_7H_6N_2O$ fragment with theoretical mass 134.0480 (1,3-dihydro-*2H*-benzo[*d*]imidazol-2-one) to yield fragment with *m/z* 328.1889. Further cleavage of this fragment forms the fragment with m/z 109.0452 ((4-fluorophenyl) methylium). This fragment forms a tropylium carbocation which confers stability due to the conjugation of positive charge with pi electrons[67]. The radical cation with *m/z* 201.1028 is formed due to loss of bis-4-flurophenyl-butyl moiety from the drug and subsequent collapse of the piperidine ring.

The MS, MS/MS spectra, and the fragmentation pattern for PIMO is shown in the following figures.

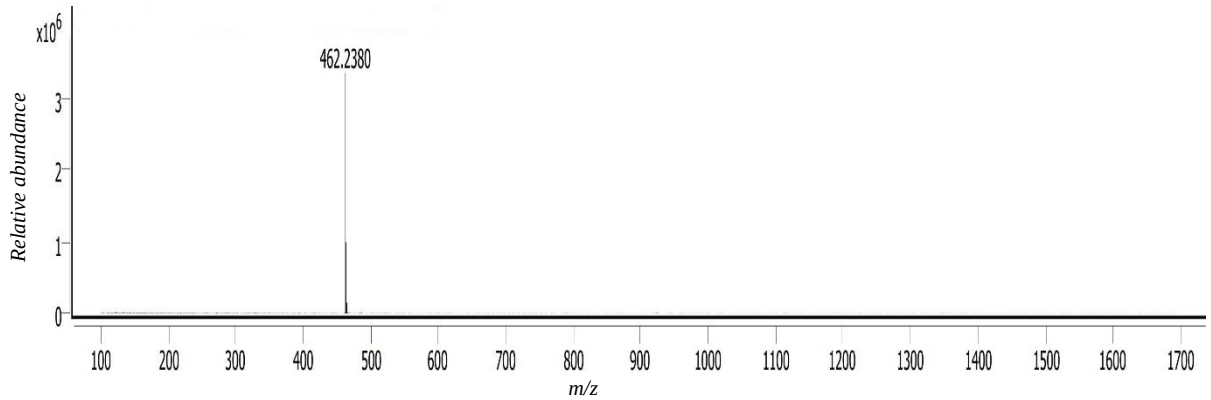


**Figure 4.3.5.1.1:** MS spectra of PIMO

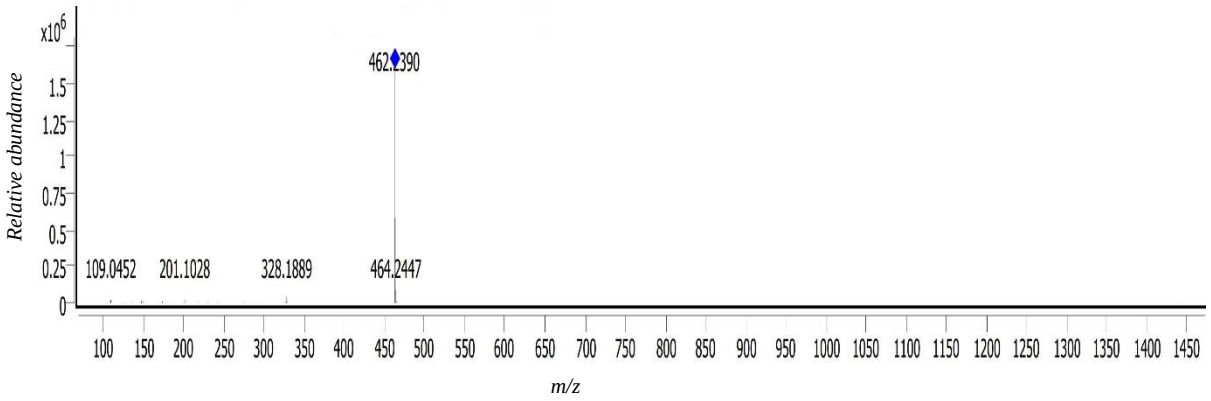


**Figure 4.3.5.1.2:** MS/MS spectra of PIMO

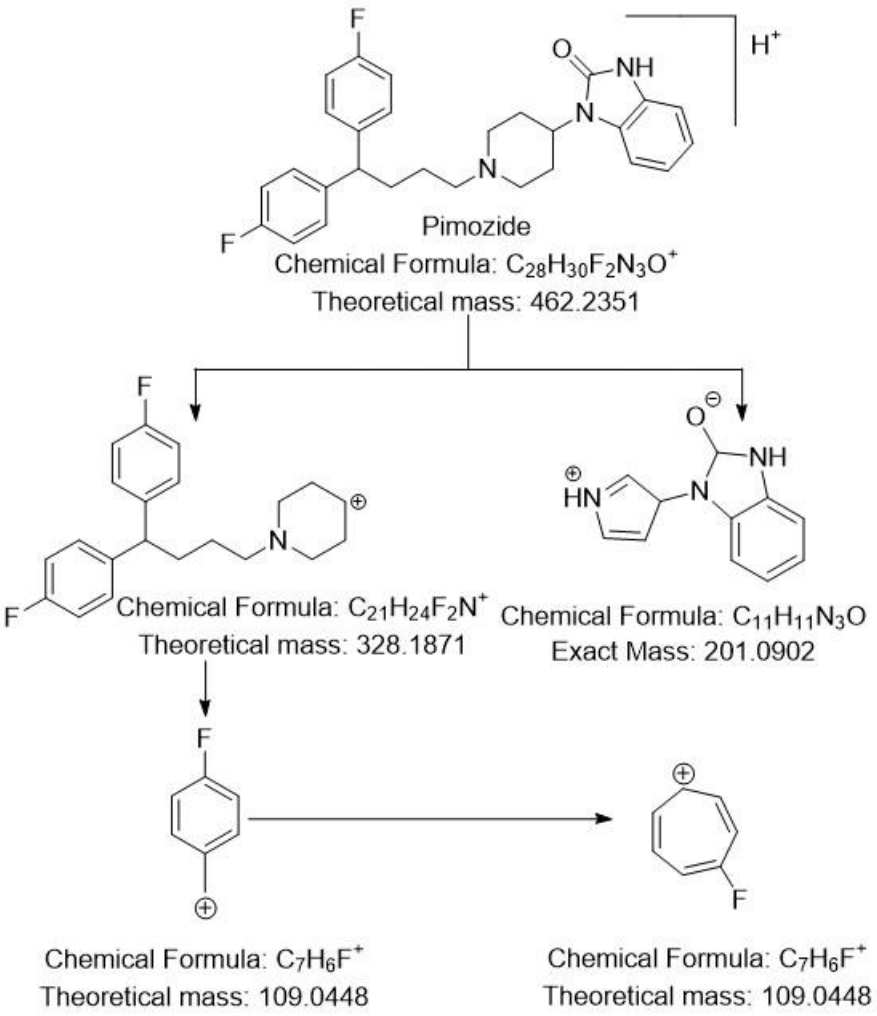


**Figure 4.3.5.1.3:** MS/MS fragmentation pattern of PIMO

**4.3.5.2. DP1**

The protonated ion peak for DP1 was seen at *m/z* 428.1978. The MS/MS spectra showed three fragment ion peaks at *m/z* 276.1383, 230.1279, and 201.1008. The fragment with *m/z* 276.1383 is created due to the loss of the benzimidazole fragment and the formation of the 5-membered heterocyclic pyrrolidine from piperidine. The loss of $C_{15}H_{18}$ from DP1 forms the fragment with *m/z* 230.1279. The fragment at *m/z* 201.1008 is seen in the fragmentation of the drug and is formed via a similar mechanism. This fragment loses the pyrrole ring to form a fragment with *m/z* 149.0754.

The most likely mechanism for the formation of DP1 is the loss of both fluorine moieties followed by the reduction of a ketone to form secondary alcohol.

DP1 of PIMO was identified as 1-(1-(4,4-diphenylbutyl) piperidin-4-yl)-2,3-dihydro-1H-benzo[d]imidazole-2-ol. The RDB value for the proposed structure was 13.5, and the error in mmu was -7.18 . The MS, MS/MS spectra, and the fragmentation pattern for DP1 is shown in the following figures.

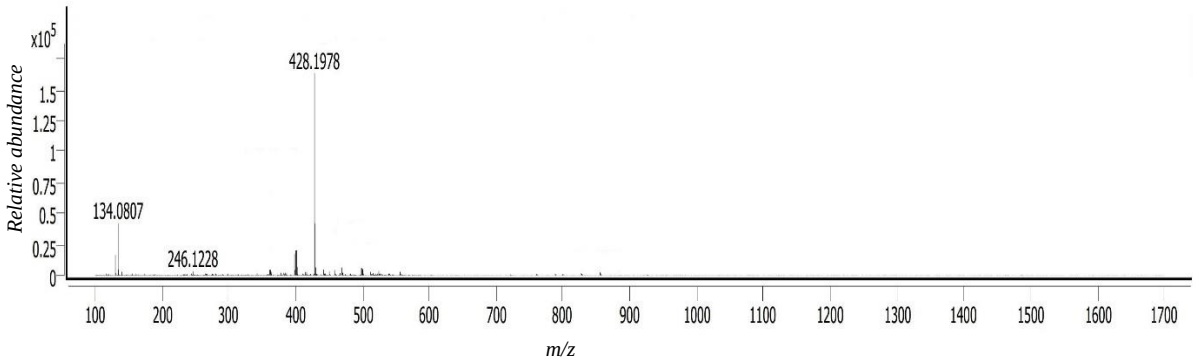


**Figure 4.3.5.2.1:** M.S. spectra of DP1.

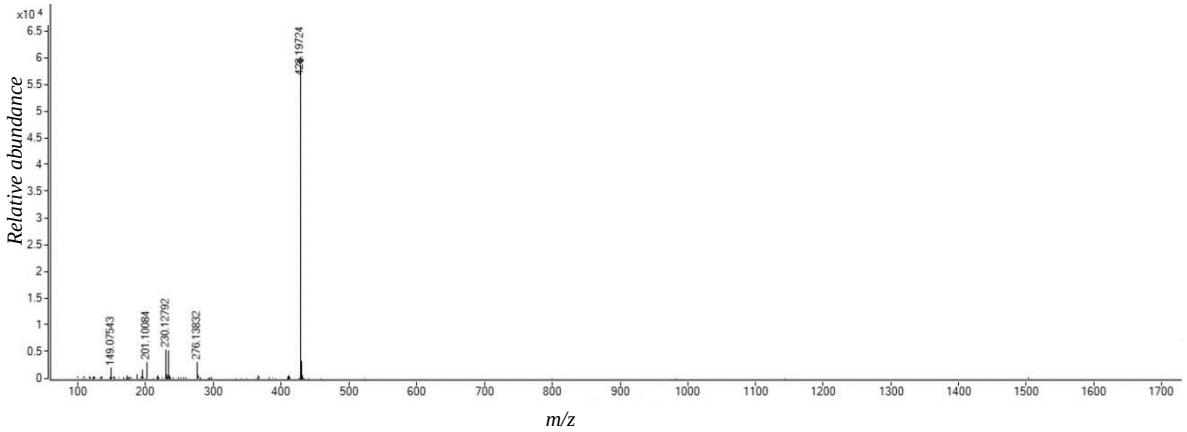


**Figure 4.3.5.2.2:** MS/MS spectra of DP1.

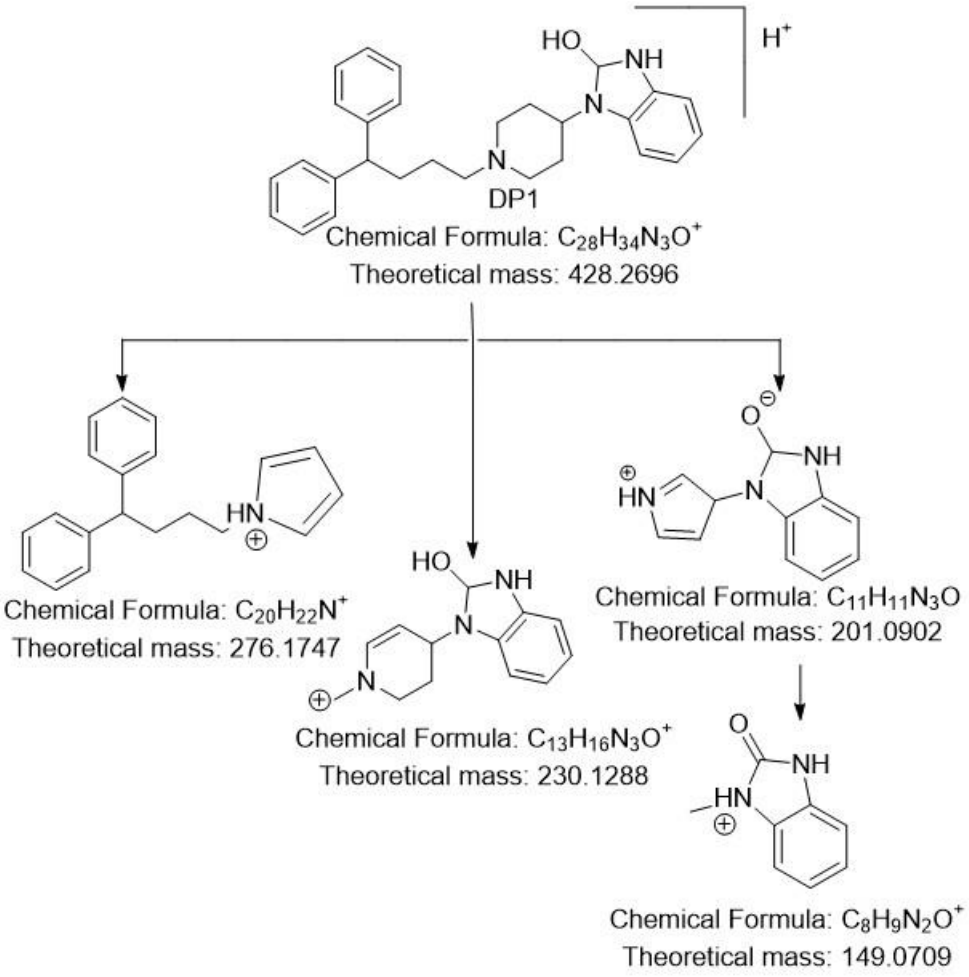


**Figure 4.3.5.2.3:** MS/MS fragmentation pathway of DP1.

### 4.3.5.3. DP2

The molecular ion peak for DP2 was seen at *m/z* 404.2140. DP2 showed fragment ion peaks at *m/z* 326.1704 and 387.1868. The fragment with *m/z* 326.1704 is formed due to the loss of $C_6H_6$ (theoretical mass = 78.0470).

The fragment with *m/z* 387.1868 is formed due to conversion of five membered ring to four membered ring along with loss of a nitrogen. The Loss of $C_2H_2$ from this fragment creates a secondary fragment with *m/z* 361.2073.

Based on the structure DP2 was assigned the name as 1-(1-(4,4-diphenylbut-1-en-1-yl)-1,4-dihydropyridin-4-yl)-1H-benzo[d]imidazole. The RDB value and error in mass was calculated to be 17.5 and 0.19 respectively.

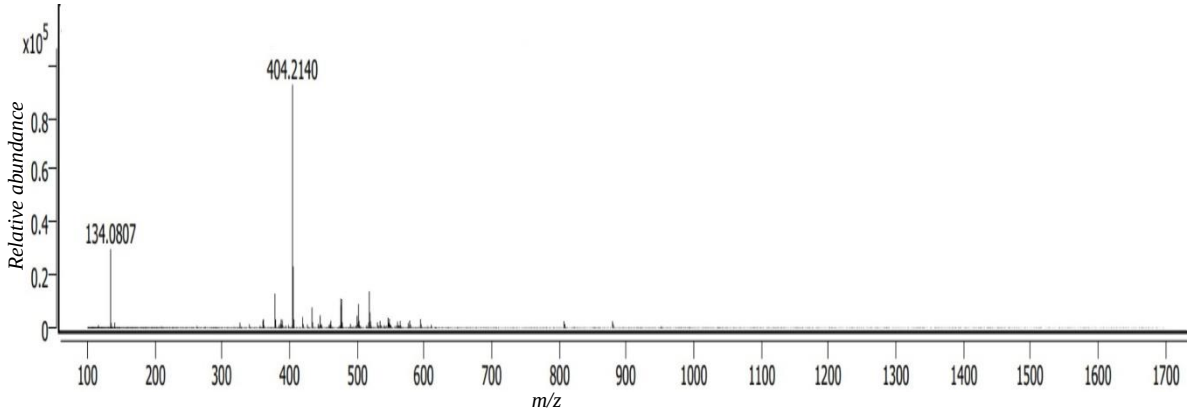


**Figure 4.3.5.3.1:** MS spectra of DP2.

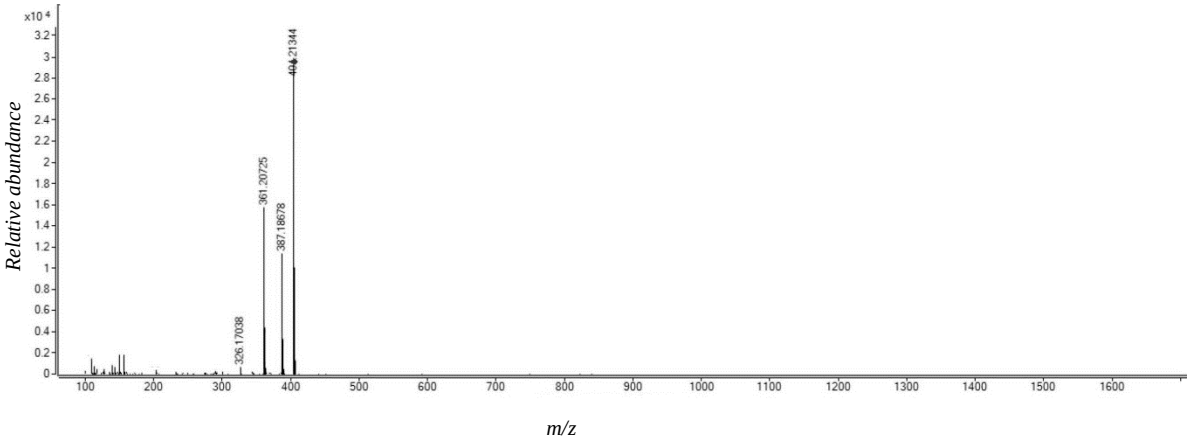


**Figure 4.3.5.3.2:** MS spectra of DP2.

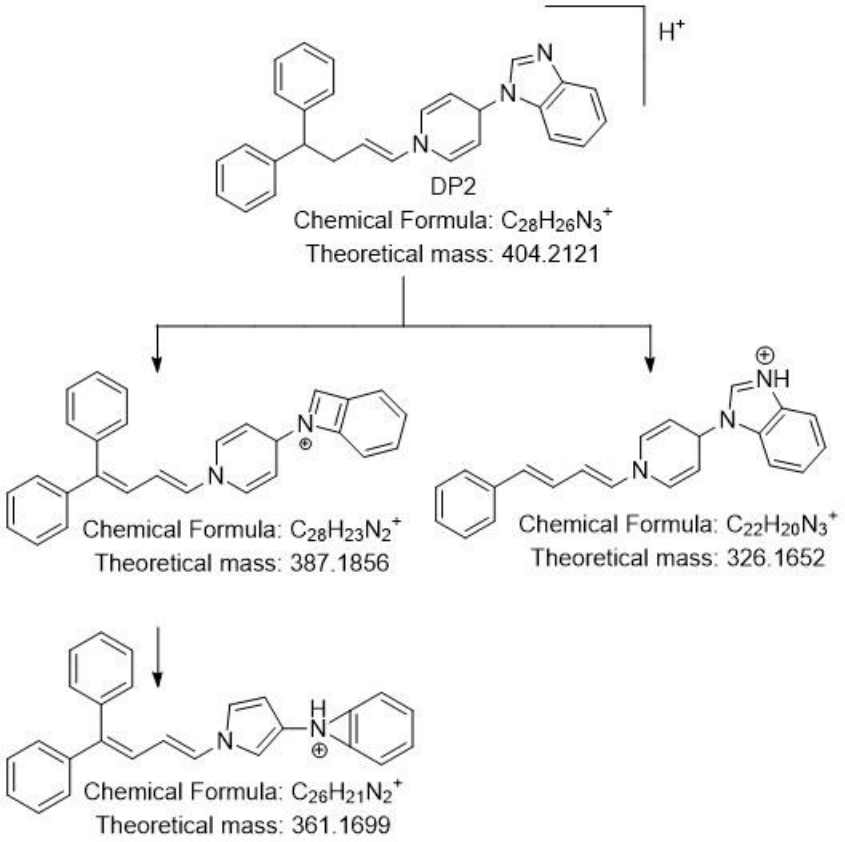


**Figure 4.3.5.3.3:** MS/MS fragmentation pathway of DP2.

**4.3.5.4. DP3**

The molecular ion peak for DP3 was seen at *m/z* 444.2088. The formation of DP3 was attributed to the dehalogenation of a single fluorophenyl moiety. The MS/MS spectra showed peaks at *m/z* 427.2042, 326.1699, 149.0750, and 109.0444. The formation of the tropylium cation (*m/z* 109.0444) is like that of the drug.

The fragment with *m/z* 427.2042 was formed due to cleavage of imidazole ring. Loss of a fluorophenyl moiety from DP3 forms the fragment with *m/z* 326.1699. This fragment further loses but-3-en-1-ylbenzene ($C_{10}H_{10}$) to form a secondary fragment with *m/z* 196.1072.

At the same time, the fragment with *m/z* 149.0750 is formed due to the cleavage of the bond connecting benzimidazole moiety to piperidine. DP3 was identified as the process impurity B (EP) having IUPAC name 1-(1-(4-(4-flurophenyl)-4-phenylbutyl) piperidie-4-yl)-1,3-dihydro-2H-benzo[d]imidazole-2-one. The RDB value for the predicted structure was 13.5

and error in mmu was -3.58. The MS, MS/MS spectra and the proposed fragmentation pathway for DP3 are seen in the figures below.

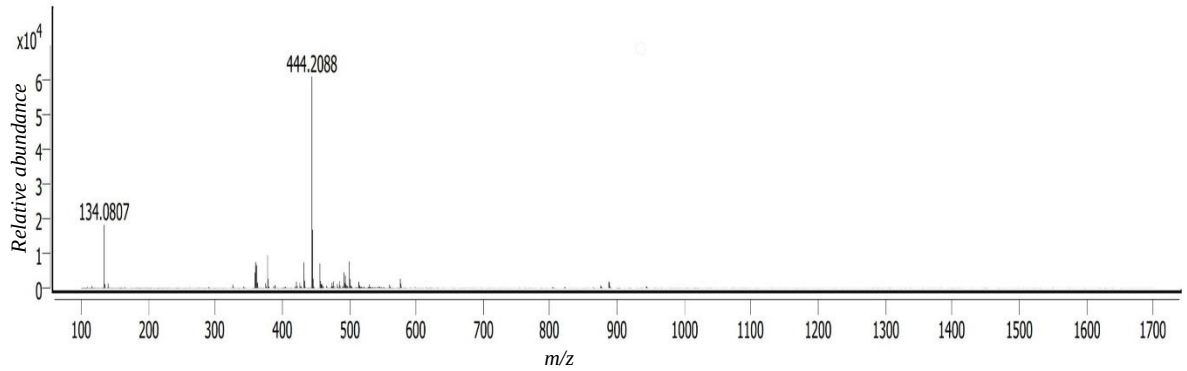


**Figure 4.3.5.4.1:** MS spectra of DP3.

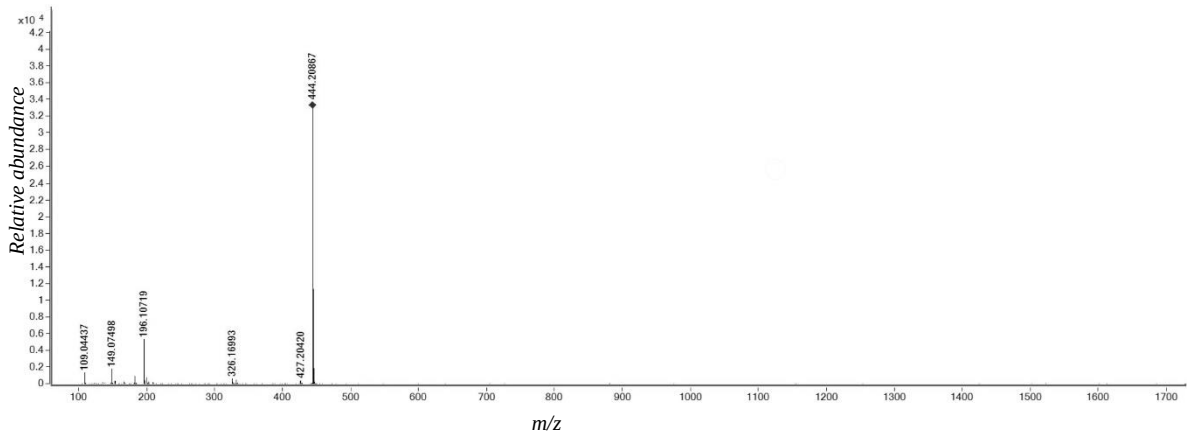


**Figure 4.3.5.4.2:** MS/MS spectra of DP3.

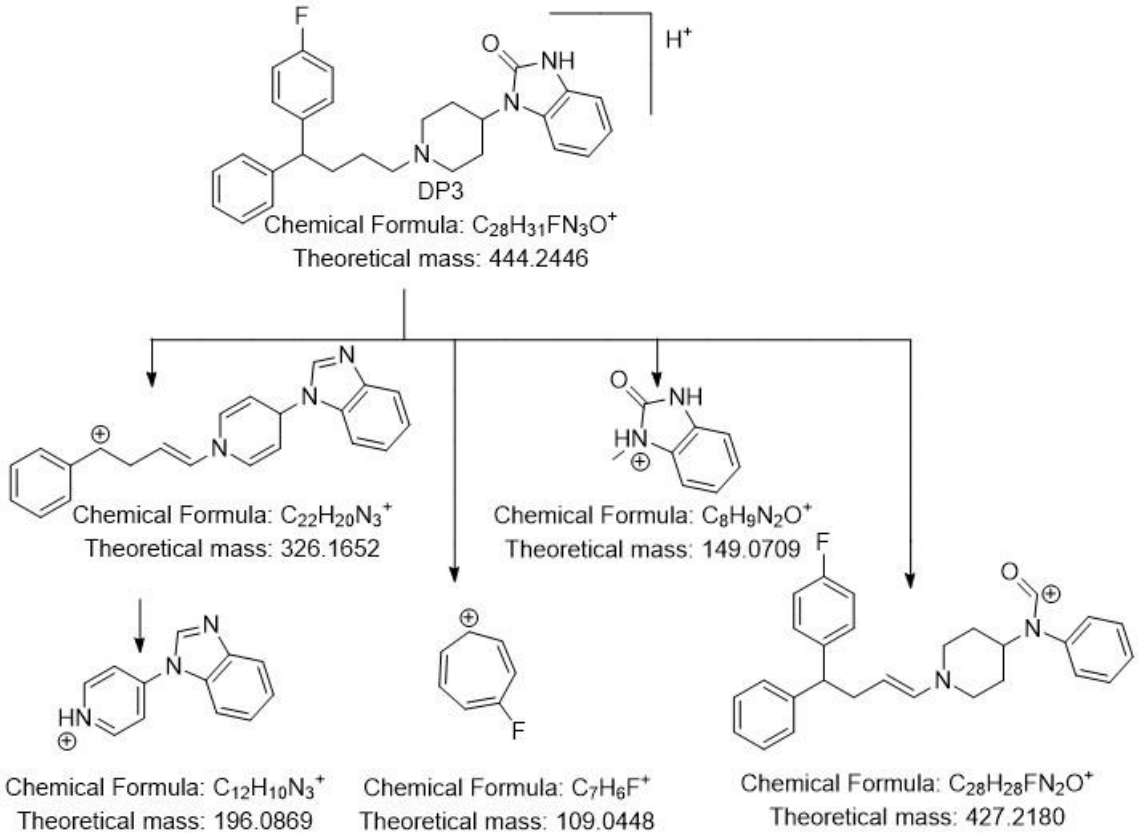


**Figure 4.3.5.4.3:** MS/MS fragmentation pathway of DP3.

### 4.3.5.6. DP4

The molecular ion peak for DP4 was observed at *m/z* 324.1552. The CID-MS/MS spectra showed three major fragments with *m/z* 203.0658, 135.0596, and 109.0442.

The fragment with *m/z* 203.0658 is formed due to the loss of a fragment with a theoretical mass of 121.0892 and molecular formula $C_8H_{11}N$. This fragment further loses a fluorobenzene moiety to create a fragment with *m/z* 109.0442.

The radical cation with *m/z* 135.0596 has formed due to the loss of Bis-(4-fluorophenyl) moiety.

DP4 is formed by the degradation of N-oxide (DP5) by cope's reaction in which an amine oxide undergoes cleavage to yield an alkene and hydroxylamine. The intermediate formed

undergoes peroxide-mediated dehydrogenation to yield DP4. The proposed route for formation is depicted in figure 4.3.5.6.4.

DP4 was designated IUPAC name as 1-(4,4-bis(4-fluorophenyl) but-1-en-1-yl)-1,2-dihydropyridine. The RDB value for the predicted structure was 11.5 and error in mmu was -0.06. The MS, MS/MS spectra, and the fragmentation pathway is shown in the figures below

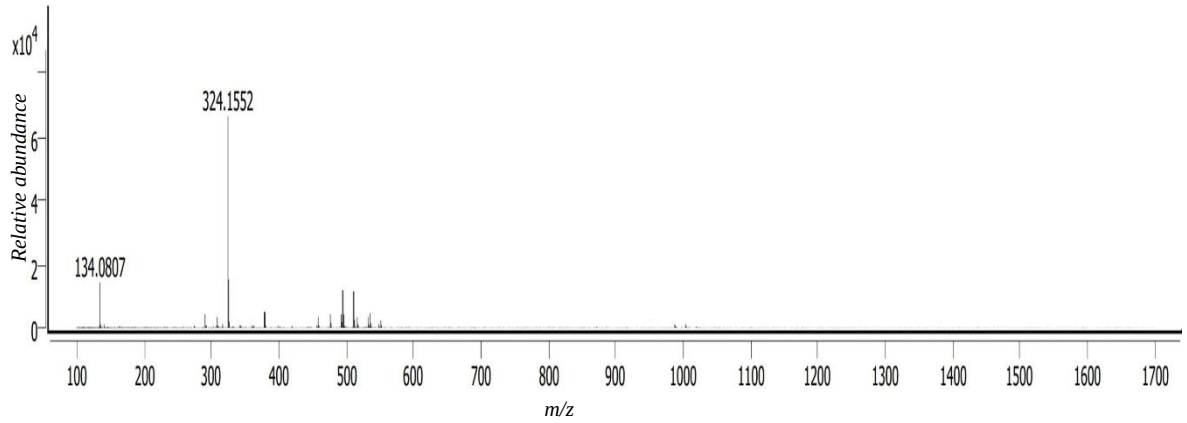


**Figure 4.3.5.6.1:** MS spectra of DP4

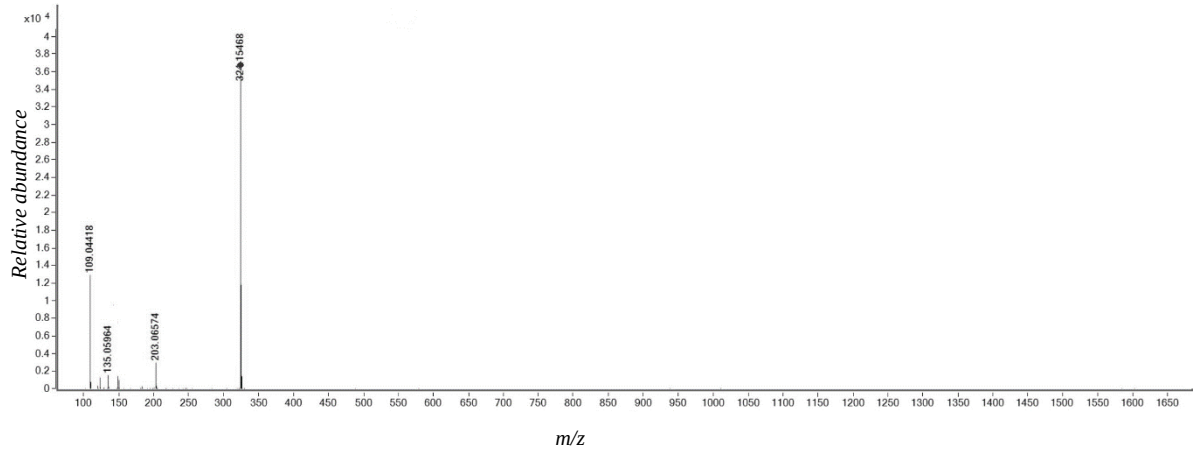


.

**Figure 4.3.5.6.2:** MS/MS spectra of DP4.

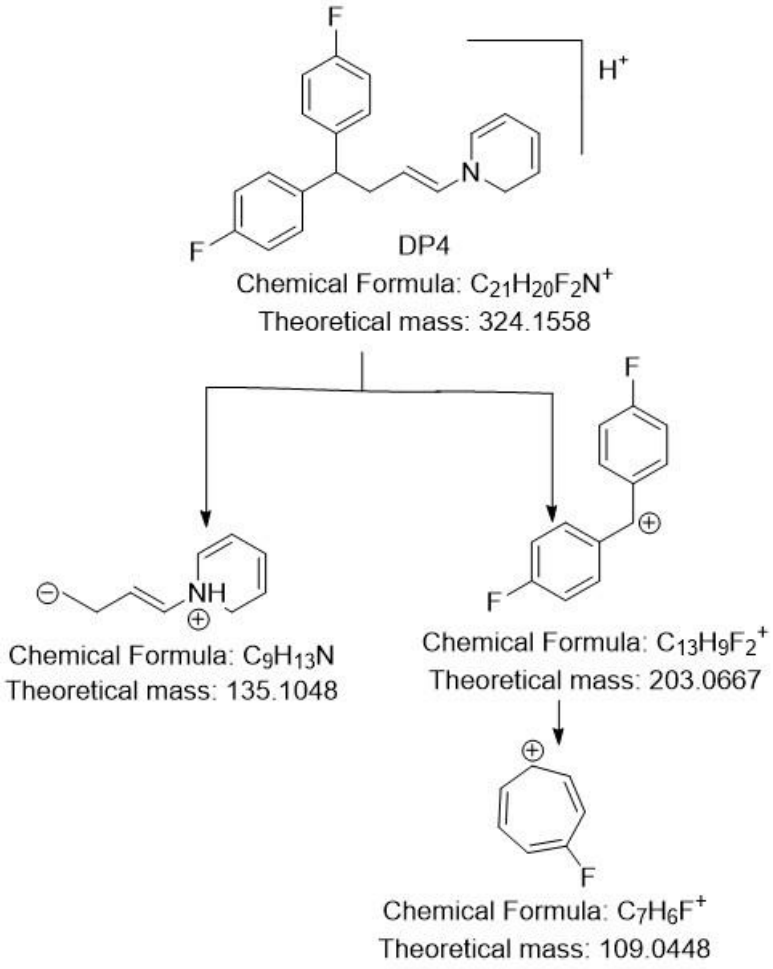


**Figure 4.3.5.6.3:** MS/MS fragmentation pathway of DP4.

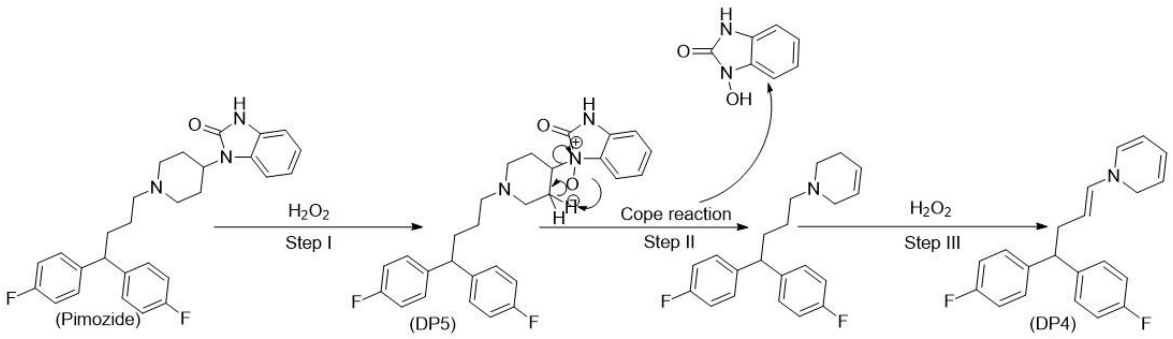


**Figure 4.3.5.6.4:** Proposed mechanism form formation of DP4.

### 4.3.5.7. DP5

The quasi-molecular ion peak for DP5 was seen at *m/z* 478.2298. It had a molecular weight of sixteen amu higher than PIMO, indicating the formation of N-oxide. Tertiary amines are

known for their propensity to form N-oxides. The MS/MS spectra showed two major fragments at *m/z* 326.1709 and 230.1276.

The fragment with *m/z* 326.1709 is formed due to loss of benzimidazole moiety from PIMO. This fragment further breaks down to give fragment with *m/z* 109.0438. The loss of 4,4′-Bis(fluorophenyl) propyl moiety fragment creates the fragment with *m/z* 230.1276. This fragment undergoes cleavage to form a radical cation with *m/z* 201.1009 which, further fragments to produce another fragment with *m/z* 149.0754.

DP5 was identified as the impurity E (EP) having IUPAC name 1-(4,4-bis(4-fluorophenyl)butyl)-4-(2-oxo-2,3-dihydro-1H-benzo[d]imidazol-1-yl)piperidine-1-oxide. The RDB value of the proposed structure was 14.5, and error in mmu was -0.03. The MS, MS/MS spectra, and fragmentation pattern are depicted in the figures below.

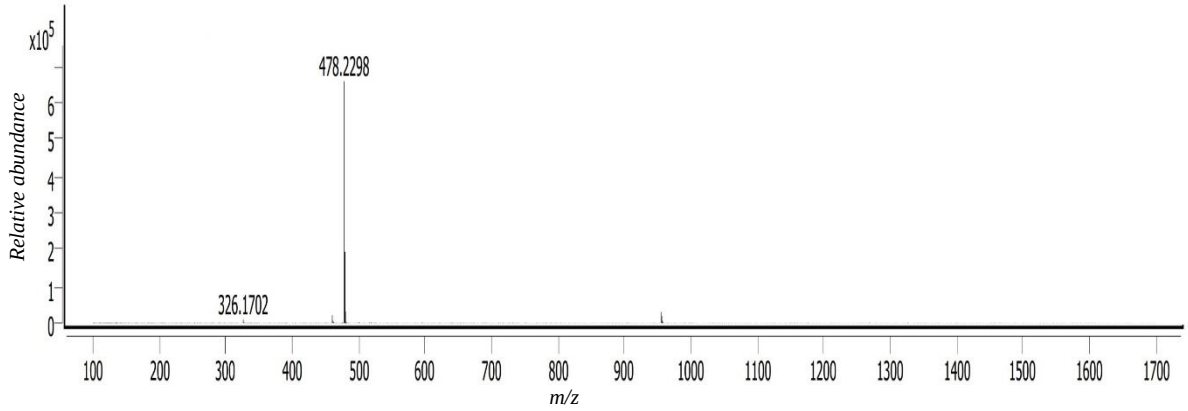


**Figure 4.3.5.7.1.** MS spectra of DP5.

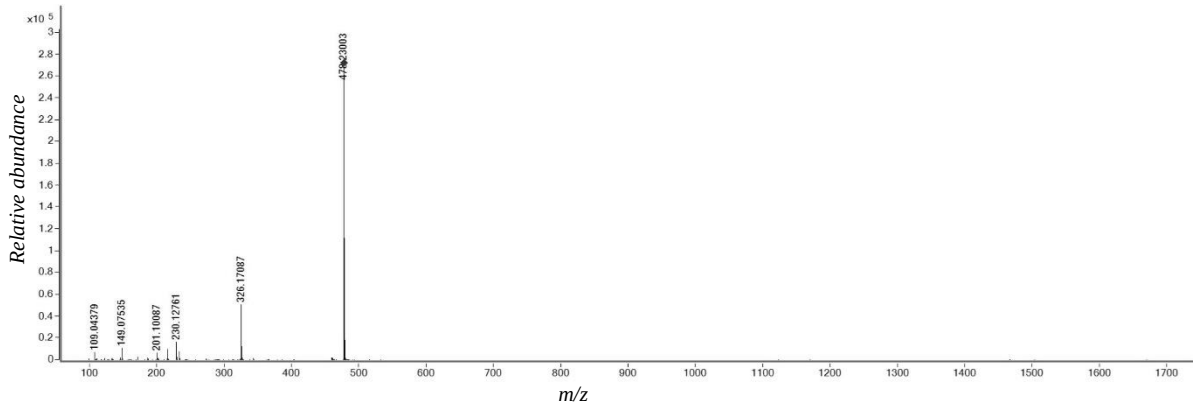


**Figure 4.3.5.7.2.** MS/MS spectra of DP5.

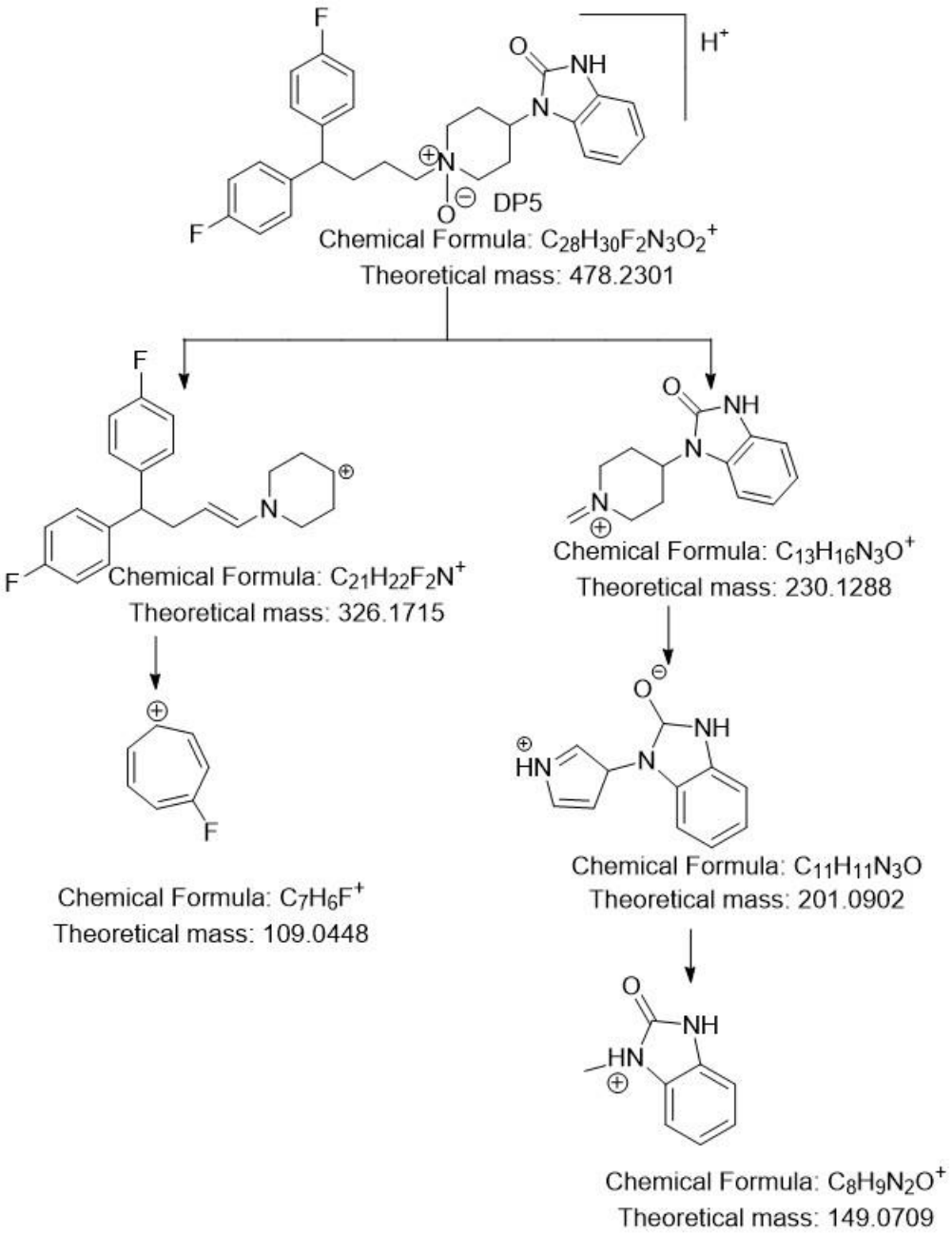


**Figure 4.3.5.7.3.** MS/MS fragmentation pathway of DP5.

The Summary of the MS and MS/MS data along with other attributes is summarized in table 4.3.5.1.

**Table 4.3.5.1:** Summary of Mass data of PIMO and its degradation products

| Compound | Experimental mass | Most likely molecular formulae | Theoretical mass | R.D.B | Error in mmu | Fragments | | Most probable molecular formulae for fragments. |
|---|---|---|---|---|---|---|---|---|
| | | | | | | Experimental mass | Theoretical mass | |
| DP1 | 428.1978 | $C_{28}H_{34}N_3O^+$ | 428.2696 | 13.5 | -7.18 | 276.1383 | 276.1747 | $C_{20}H_{22}N^+$ |
| | | | | | | 230.1279 | 230.1288 | $C_{13}H_{16}N_3O^+$ |
| | | | | | | 201.1008 | 201.0902 | $C_{11}H_{11}N_3O$ |
| | | | | | | 149.0754 | 149.0709 | $C_8H_9N_2O^+$ |
| DP2 | 404.2140 | $C_{28}H_{26}N_3^+$ | 404.2121 | 17.5 | 0.19 | 387.1868 | 387.1856 | $C_{28}H_{23}N_2^+$ |
| | | | | | | 361.2073 | 361.1699 | $C_{26}H_{21}N_2^+$ |
| | | | | | | 326.1704 | 326.1652 | $C_{22}H_{20}N_3^+$ |
| DP3 | 444.2088 | $C_{28}H_{31}FN_3O^+$ | 444.2446 | 13.5 | -3.58 | 427.2042 | 427.2180 | $C_{28}H_{28}FN_2O^+$ |
| | | | | | | 326.1699 | 326.1652 | $C_{22}H_{20}N_3^+$ |
| | | | | | | 196.1072 | 196.0869 | $C_{12}H_{10}N_3^+$ |
| | | | | | | 149.0750 | 149.0709 | $C_8H_9N_2O^+$ |
| DP4 | 324.1552 | $C_{21}H_{20}F_2N^+$ | 324.1558 | 11.5 | -0.06 | 109.0444 | 109.0448 | $C_7H_6F^+$ |
| | | | | | | 203.0658 | 203.0667 | $C_{13}H_9F_2^+$ |
| | | | | | | 135.0596 | 135.1048 | $C_9H_{13}N$ |
| | | | | | | 109.0442 | 109.0448 | $C_7H_6F^+$ |
| DP5 | 478.2298 | $C_{28}H_{30}F_2N_3O_2^+$ | 478.2301 | 14.5 | -0.03 | 326.1709 | 326.1715 | $C_{21}H_{22}F_2N^+$ |
| | | | | | | 230.1276 | 230.1288 | $C_{13}H_{16}N_3O^+$ |
| | | | | | | 201.1009 | 201.0902 | $C_{11}H_{11}N_3O$ |
| | | | | | | 149.0754 | 149.0709 | $C_8H_9N_2O^+$ |
| | | | | | | 109.0438 | 109.0448 | $C_7H_6F^+$ |
| PIMO | 462.2380 | $C_{28}H_{30}F_2N_3O^+$ | 462.2351 | 14.5 | 0.29 | 328.1889 | 328.1871 | $C_{21}H_{24}F_2N^+$ |
| | | | | | | 201.1028 | 201.0902 | $C_{11}H_{11}N_3O$ |
| | | | | | | 109.0452 | 109.0448 | $C_7H_6F^+$ |

## 4.3.6. *In-silico* ADMET studies of PIMO and its DPs

The *in-silico* absorption, distribution, metabolism, excretion and toxicity profile (ADMET) of the drug and its DPs was investigated by using various opensource tools like the pkCSM[68-69] webserver and software packages like ToxTree[70] and OSIRIS property explorer[71].

pKCSM constructs its prediction based on compounds general properties viz. molecular, toxophores and pharmacophores. Its prediction algorithms employ a distance-based graph signature approach to arrive at a prediction. pKCSM predicts properties like intestinal absorption, P-glycoprotein (PgP) inhibition, blood-brain barrier permeability, inhibition of various isoforms of cytochrome P-450 enzyme system, ames toxicity and hepatotoxicity. The output obtained from pkCSM provides values for certain parameters e.g. intestinal absorption, which can be interpreted based on the literature available for pkCSM while output for certain parameters is categorical in the form of yes/No.

ToxTree is an offline utility that uses a decision-based approach to predict a selected endpoint (in-vitro mutagenicity (Ames test) alerts by I.S.S.). Depending upon the structural features, it classifies compounds into low risk, intermediate risk, and high risk[72-73].

OSIRIS depends upon a set of precomputed set of structural fragments. The fragment sets were prepared by shredding compounds from RTECS (Registry of Toxic Effects of Chemical Substances) database known to have toxicity.

Since all the tools mentioned above use different approaches, databases to compute results, two levels of screening were done to avoid missing of any structural alert for mutagenicity. For this purpose, Primary screening was done by pKCSM while ToxTree and OSRIS was used for secondary screening.

**pKCSM**

PIMO, DP2, and DP3 had absorption (% absorbed) above 85%. While. DP1, DP4, and DP5 above 90%. All the compounds were predicted to act as PgP substrates. DP3, DP4, and DP5 had log BB value > 0.3, indicating that they readily cross the blood-brain barrier.

Regarding metabolism, PIMO, and its DPs inhibited specific isoforms of the cytochrome P540 enzyme system. The details are expressed categorically in table 4.3.6.1. PIMO, DP1,

DP3, and DP5 turned out positive for Ames toxicity and PIMO, DP3 and DP5 for hepatotoxicity.

**Toxtree and OSIRIS property explorer**

ToxTree scans molecules for fragments known to have toxic potential. However, it did not raise any warning for the compounds mutagenicity. This was also reiterated by OSIRIS property explorer, which further cleared them for tumorigenic, irritant, or reproductive risk

**Table 4.3.6.1:** Summary of pKCSM predictions

| Compound | Intestinal absorption (%absorbed) | PgP Substrate | B.B.B. Permeability (log BB) | CYP1A2 inhibitor | CYP2C19 inhibitor | CYP2C9 Inhibitor | CYP2D6 Inhibitor | CYP3A4 Inhibitor | AMES toxicity | Hepato toxicity |
|---|---|---|---|---|---|---|---|---|---|---|
| Pimozide | 88.38 | yes | 0.095 | Yes | No | Yes | Yes | Yes | Yes | Yes |
| DP1 | 90.13 | yes | 0.035 | Yes | No | No | Yes | No | Yes | No |
| DP2 | 86.22 | Yes | 0.536 | Yes | Yes | Yes | Yes | Yes | No | No |
| DP3 | 88.31 | Yes | 0.115 | Yes | No | Yes | Yes | Yes | Yes | Yes |
| DP4 | 92.44 | Yes | 1.302 | Yes | Yes | Yes | Yes | No | No | No |
| DP5 | 90.98 | Yes | 1.079 | Yes | Yes | Yes | Yes | Yes | Yes | Yes |

# 4.4 Experimental work

## 4.4.1. Instrumentation

**Table 4.4.1.1:** List of instruments

| Sr.no. | Instrument | Make and specification |
|---|---|---|
| **1** | **HPLC** | LC-4000, Jasco, Japan. Made up of a model CO-4061 temperature controlled column compartment, a model PU 4180 quaternary pump system with inline degasser, a model AS-4050 autosampler, Chromenav (version, 2.01.06) data acquisition software, LC-NET II interface box, Acer workstation computer running Microsoft windows 7 professional operating system. |
| **2** | **Column** | Phenomenex C18 (150mm ×4.6mm, 5µm). |
| **3** | **Sonicator** | Citizon, Vadodra, India. |
| **4** | **pH meter** | Digital pH meter, Elico, India. |
| **5** | **Precision balance** | Wensar digital, Chennai, India. |
| **6** | **Double distillation assembly** | Bhanu scientific instruments, Bangalore, Karnataka. |
| **7** | **Hot air oven** | Universal, Ambala, India. |
| **8** | **Constant temperature water bath** | Generic. |
| **9** | **Photostability chamber** | Newtronics lifecare Pvt.Ltd, Mumbai,India. |
| **10** | **MS system** | Agilent 1200 series HPLC system, 6200 series QTOF. |
| **11** | **Workstation for *in-silico* studies** | Intel i7 5820k based workstation computer running windows 10 professional operating system with 32 GB of ram, ToxTree (version, 3.1.0-1851-1525442531402), OSIRIS property explorer. |

## 4.4.2. Chemicals and reagents

1. **Acetonitrile (HPLC grade):** Qualigen, Mumbai, Maharashtra
2. **Hydrochloric acid:** Molychem, Thane, Mumbai.
3. **Hydrogen peroxide:** Molychem, Thane, Mumbai.
4. **Ammonium acetate:** Molychem, Thane, Mumbai.
5. **Water (HPLC grade):** Finar, Ahmedabad, Gujarat.

6. **Sodium Hydroxide:** Finar, Ahmedabad, Gujarat.

## 4.4.3. Chemicals and reagents

Pimozide was obtained as a gift sample from Intas pharmaceutical Ltd, Ahmedabad, Gujarat, India.

## 4.4.4. Solution preparation

### 4.4.4.1. Preparation of stock solution of PIMO

PIMO (50 mg) was weighed on a precision balance and transferred into a calibrated 50 mL volumetric flask. To it, 20 mL of acetonitrile was added and the contents were sonicated for 5 min. The volume was made to mark with acetonitrile (HPLC grade) to get a solution having a concentration of 1000 µg/mL.

### 4.4.4.2. Preparation of ammonium acetate buffer (pH 3.7)

Ammonium acetate (770.8 mg) was weighed and transferred into 1000 mL HPLC grade water and mixed thoroughly. Solution was then filtered through a 0.45 µ membrane filter under vacuum and the pH was adjusted to 3.7 with glacial acetic acid.

### 4.4.4.3. Preparation of diluent

Ammonium acetate buffer and acetonitrile were mixed in a ratio of 50:50 (v/v) and sonicated for five minutes to prepare the diluent.

### 4.4.4.4. Preparation of 0.1 N hydrochloric acid

Concentrated hydrochloric acid (0.85 mL) was slowly diluted to 100 mL mark using HPLC grade water in volumetric flask to get 0.1 N hydrochloric acid.

### 4.4.4.5. Preparation of 1 N hydrochloric acid

Concentrated hydrochloric acid (8.5 mL) was slowly diluted to 100 mL mark using HPLC grade water in volumetric flask to get 0.1 N hydrochloric acid.

### 4.4.4.6. Preparation of 0.1 N sodium hydroxide

Sodium hydroxide flakes (400 mg) was dissolved with the aid of sonication in 50 mL of HPLC grade water using 100 mL volumetric flask. The volume was made up to mark with HPLC grade water to get 0.1 N sodium hydroxide solution.

#### 4.4.4.7. Preparation of 1 N sodium hydroxide

Sodium hydroxide flakes (4000 mg) was dissolved with the aid of sonication in 50 mL of HPLC grade water using 100 mL volumetric flask. The volume was made up to mark with HPLC grade water to get 0.1 N sodium hydroxide solution.

#### 4.4.4.8. Preparation of 15% hydrogen peroxide

Hydrogen peroxide (15%) was prepared by diluting 5 mL of 30% hydrogen peroxide to 10 mL with HPLC grade water using 10 mL volumetric flask.

### 4.4.5. Forced degradation studies

The forced degradation studies were performed to get substantial degradation of drug. The drug was stressed under conditions viz. acidic, basic, neutral, oxidative, thermal, and photolytic. To get an accurate representation, four samples were prepared under each condition excluding thermal and photolytic; blank under normal condition (blank untreated), blank under stress condition (blank treated), drug solution under normal condition (standard), and drug under the stress condition. For thermal and photolytic conditions, the chromatogram obtained were compared with the chromatogram of drug stored under normal conditions.

#### 4.4.5.1. Hydrolytic degradation

The hydrolytic degradation was conducted under acidic, basic, and neutral condition. The stock solution of drug (1 mL) was mixed with 0.1 mL of 0.1 N / 1 N HCl in 10 mL volumetric flask and the solution was kept under stress for 48 h. In order to accelerate the degradation the study was caried out at 70 ℃ for 7 h using 1 N HCl. After the stress period the samples were neutralized by using equal strength of sodium hydroxide and the volume was made to mark with diluent to get a concentration of 100 µg/mL of PIMO. For base and neutral hydrolysis, a similar methodology was used. The samples treated with base were neutralized

using corresponding strength of hydrochloric acid. All the samples were analysed using HPLC under optimized chromatographic conditions.

#### 4.4.5.2. Oxidative degradation

Stock solution PIMO (1 mL) was allowed to mix with 0.1 mL of oxidant (15% hydrogen peroxide) for 48 h in 10 mL volumetric flask. The volume was made up to mark with diluent to get a concentration of 100 µg/mL and samples were analysed using HPLC under optimized chromatographic conditions.

#### 4.4.5.3. Thermal degradation

PIMO (100 mg) was sealed in a glass ampoule and heated in an oven at 70 ℃ for 7 hours. After the stress period, the contents of the ampoules were diluted with diluent to get a concentration of 100 µg/mL. In similar fashion, one sample of PIMO was kept at room temperature as control. The samples were analysed using HPLC under optimized chromatographic conditions.

#### 4.4.5.4. Photolytic degradation

Photolytic degradation was carried out in solid and liquid state. Two samples were prepared for solid state degradation study. In first case, the drug was spread as a thin layer inside a petri dish and kept in a photostability chamber along with control sample covered with aluminium foil. In the second case, 10 mg of drug was taken into 10 mL volumetric flask and exposed to sunlight for 7 days along with control sample in aluminium foil.

Photolytic degradation in liquid state was carried out by keeping 1 mL stock solution of PIMO in volumetric flask inside a photostability chamber along with a control sample covered using aluminium foil.

The samples that were kept in the photostability chamber were exposed to ICH-mandated dose of light (1.2 million lux h of overall illumination and 200 wh/$m^2$ of integrated near U.V. energy). After the exposure period, the samples were diluted up to the mark to get 100 µg/mL concentration of drug using diluent and analysed using HPLC under optimized chromatographic conditions.

## 4.4.6. Validation studies

The developed and optimized HPLC method was validated as per the relevant ICH guideline.

### 4.4.6.1. Specificity and selectivity

The specificity of the HPLC method was ascertained by the resolution values obtained between the nearest eluting peaks of degradation product and peak of drug and degradation product. The method's selectivity for the individual component was done through the % peak purity value obtained through the data acquisition software. The degradation samples were mixed in equal proportion and injected into HPLC.

### 4.4.6.2. Linearity and range

A series of dilutions (5 levels) were prepared in range of 10-100 µg/mL. At each level the sample was injected in triplicate, and the average area was obtained. The average area was plotted against the concentration to obtain a simple linear regression equation and the correlation coefficient. Five incremental concentration ( 10, 30, 50, 80 and 100 µg/mL) were prepared by accurately withdrawing 0.1, 0.3, 0.5, 0.8 and 1 mL of stock solution of PIMO (1000 µg/mL) and diluting it to 10 mL using diluent in a volumetric flask.

### 4.4.6.3. Accuracy

The accuracy of the HPLC method was determined by the standard addition method. The degraded sample was spiked at 80%, 100%, and 120% of the target assay concentration (50 µg/mL) with standard drug solution. At each level, the sample was injected in triplicate, and the average % recovery was computed. Spiked samples were prepared by accurately transferring 0.4, 0.5 and 0.6 mL of stock solution of PIMO to degraded sample and making the volume to 10 mL.

### 4.4.6.4. Precision

Precision (intra and inter) of the HPLC method was done at 30, 50, and 100 µg/mL. At each level, the sample was injected in triplicate, and the % relative standard deviation was determined (% RSD). Three incremental concentration (30, 50, and 100 µg/mL) were prepared by accurately withdrawing 0.3, 0.5, and 1 mL of stock solution of PIMO (1000 µg/mL) and diluting it to 10 mL using diluent in a volumetric flask.

### 4.4.7. *In-silico* studies

The *in-silico* studies were done using open-source options like the pKCSM webserver, ToxTree and OSIRIS property explorer.

The structures of the degradation products were sketched using Marvin by ChemAxon. The structures were copied as smiles and fed into the pKCSM webserver. ADMET prediction mode was selected which uploads the task for processing.

Toxtree accepts the structure in the form of SMILES which were generated similarly as discussed above. The decision tree (In vitro mutagenicity (Ames test) alerts by ISS) was selected from the method tab, and the estimate button was clicked.

OSIRIS property explorer accepts SMILES or CAS no as input and runs predictions.

# Chapter 5

# Characterization and *in-silico* toxicity prediction of degradation products of felbamate

## 5.0. Introduction

Felbamate is an official drug in the United States Pharmacopeia and National Formulary (USP-NF). Its profile is also available in Clark's Analysis of Drugs and Poisons.

Felbamate is a second-generation antiepileptic agent[74]. It is used in treatment of partial seizures in adults, and in children with generalized seizures caused because of Lennox-Gast taut syndrome[75-76].

The work presented herein focuses on the following objectives:

1. Conduct of forced degradation studies on felbamate as per the ICH-mandated stress conditions.
2. Development of a stability-indicating assay method (SIAM) for felbamate.
3. Validation of the SIAM as per the ICH guidelines.
4. Structural characterization of the degradation products by liquid chromatography coupled with mass and tandem mass spectrometry.
5. Prediction of absorption, distribution, metabolism, excretion, and toxicity (ADMET) profile using *in-silico* studies.

# 5.1. Drug profile[52]

## 5.1.1 Felbamate (FMTE)

**Chemical structure:**

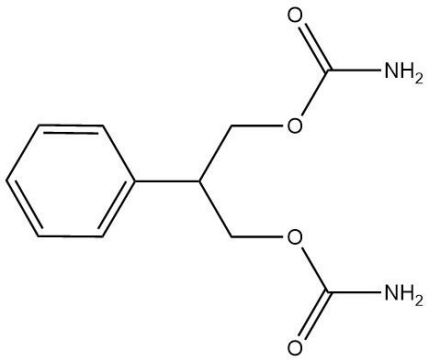


**IUPAC name:** 2-phenyl-1,3-propanediol dicarbamate.

**Molecular formula:** $C_{11}H_{14}N_2O_4$.

**Melting point:** 151-152°C

**pKa:** 14.98 (predicted by Marvin, Chemaxon)

**LogP:** 0.76

**Description:** White, odourless powder.

**Solubility:** Sparingly soluble in methanol, acetone, ethanol and chloroform. Freely soluble in dimethyl sulfoxide, dimethylformamide, and 1-methyl-2-pyrrolidinone.

**Drug category:** Anti-convulsant.

**Listed impurities of FMTE in monograph:** USP-NF

A. 3-hydroxy-2-phenylpropyl carbamate.

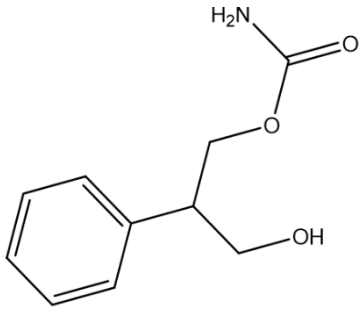


B. Phenylethyl carbamate.

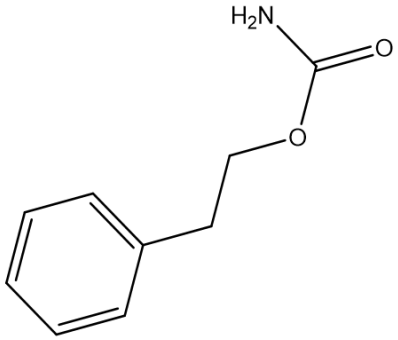


**Clinical pharmacology:**

Studies have established that the anti-convulsant activity of FMTE is primarily through inhibitory effect on $GABA_A$ receptor. Its secondary action involves inhibition of glycine facilitated activation of the NMDA receptor.

The $GABA_A$ receptor controls the passage of chloride ions through the ion channel. Whereas, the calcium and the sodium passage are controlled by the NMDA receptor. Extracellular magnesium binds to NMDA receptor blocking the transport of cations across the membrane. These voltage -dependent channels manage neuronal excitability and stabilization[77-80].

**Pharmacokinetics:**

Studies have shown that FMTE is metabolised by the cytochrome P-450 enzymes in liver. Subsequently it undergoes glucuronidation. Roughly fifty percent of the absorbed FMTE is

excreted in urine. There are 3 main metabolites of FMTE: 3-carbamoyloxy-2-phenylpropanoic acid, 2-(4-hydoxyphenol)-1,3-propanediol dicarbamate and 3-carbamoyloxy-2-phenylpropanoic acid. The secondary metabolite is 2-hydroxy-2-phenyl-1,3-propanediol monocarbamate. However, no therapeutic activity is reported for any of these metabolites.

**Toxicity:**

Anorexia, headache, nausea, insomnia, and GIT disturbances are common adverse effects of felbamate therapy however, they are reversible post discontinuation or dose reduction. Two rare but severe idiosyncratic harmful effects of felbamate seen during phase four clinical trials were aplastic anaemia and hepatic toxicity[76].

## 5.2. Literature survey

A literature survey was carried out to find out the different physiochemical properties and analytical methods available for the drug. The various physiochemical properties for it are listed under section 5.1 (drug profile). FMTE is official in USP-NF[51] and its monograph mentions two process impurities.

There are only some bioanalytical and analytical methods for estimation and quantification of FMTE in plasma[81-85] and formulations[86]; these methods mainly use high-performance liquid chromatography (HPLC), hyphenated techniques (LC-MS), capillary electrophoresis and gas chromatography.

A single UHPLC method for felbamate and related impurities is available [87]. However, it lacks in stress studies, identification of DPs and *in-silico* ADMET prediction.

A summary of the various HPLC method is shown in the table 5.2.1.

**Table 5.2.1:** Summary of HPLC methods available for determination of FMTE by HPLC

| | Type of method | Column Type | Mobile Phase composition | Flow rate | Detector used | References |
|---|---|---|---|---|---|---|
| 1 | | | **USP method.** | | | |
| | HPLC | L1, 150mmX4.6mm, 5µm | Acetonitrile: methanol: water (126:84:790, v/v/v) | 1.8ml/min | UV,210nm | 51 |
| 2 | **Title: An automated analytical method for the determination of felbamate in human plasma by robotic sample preparation and reversed-phase high performance liquid chromatography.** | | | | | |
| | HPLC | Hypersil C18, 150mmX4.6mm, 5µm | Phosphate buffer (0.015M, pH 6.5 adjusted using 85% phosphoric acid): Acetonitrile (79:21, v/v) | 1ml/min | - | 81 |
| 3 | **Title: Rapid and sensitive LC–MS/MS method for determination of felbamate in mouse plasma and tissues and human plasma.** | | | | | |
| | LC-MS | Xbridge Phenyl, 50mmX4.6mm, 2.5µm | Ammonium acetate (10 mM) [A]: Acetonitrile [B], ($T_{min}$/A:B (v/v) -$T_0$/90:10; $T_{1.5}$/15:85;$T_3$/15:85;$T_{3.25}$/90:10;$T_4$90:10) | 1ml/min | MS | 82 |
| 4 | **Title: Validation of a liquid chromatographic method for the determination of felbamate in tablets.** | | | | | |
| | HPLC | Nova-Pack C18, 150mmX3.9mm, 4µm. | Acetonitrile: Water (1:4, v/v) | 1.2ml/min | UV,210nm | |
| 5 | **Title: Drug Monitoring and Toxicology: A simple procedure for the monitoring of felbamate by HPLC-UV detection.** | | | | | |
| | HPLC | Microsorb-MV C18, 250mmX4.6mm, 5µm. | Phosphate buffer (50 mM, pH 6.9 adjusted using phosphoric acid): Methanol: Acetonitrile (64:18:18,v/v/v) | 1.0ml/min | UV,210nm | 83 |

**Table 5.2.1:** Summary of HPLC methods available for determination of FMTE by HPLC (*Conti…*)

| | Type of method | Column Type | Mobile Phase composition | Flow rate | Detector used | References |
|---|---|---|---|---|---|---|
| 6 | **Title: Chromatographic procedures for the determination of felbamate in serum.** | | | | | |
| | HPLC | Zorbax C18, 250mmX4.6mm, 5µm. | Acetonitrile: Methanol: Tetrahydrofuran: Phosphate buffer (210:410:500:280, v/v/v/v) | 1.5ml/min | UV,254nm | 84 |
| 7 | **Title: Felbamate measured in serum by two methods: HPLC and capillary electrophoresis.** | | | | | |
| | HPLC | Merck C8, 125mmX4mm, 5µm. | Phosphate buffer (20mM, pH 6.1): Acetonitrile | 1.8ml/min | UV,205nm | 85 |

# 5.3. Present work and discussion

## 5.3.1. Development of HPLC method to monitor the drug degradation behaviour of FMTE

### 5.3.1.1. Selection of chromatographic methods

Most of the published methods have use RPC for identification and quantification of FMTE. Due to this, it was decided to develop the HPLC method using RPC approach.

### 5.3.1.2. Selection of stationary phase

The compendial method depicted under monograph and other reported methods for FMTE were developed using C18 column as stationary phase. Hence, preference was shown towards Agilent XDB C18 column (150mm × 4.6mm, 5 µm) due to availability.

### 5.3.1.3. Selection of wavelength of analysis

During the initial scouting runs, the diode array detector (DAD) was set to scan the entire UV range (200-400 nm) to determine the wavelength of maximum absorbance ($\lambda_{max}$) of FMTE. The UV spectrum obtained is depicted in figure 5.3.1.3.1. The UV spectrum showed a wavelength maximum at 206 nm. Hence, 206 nm was selected for further analysis.

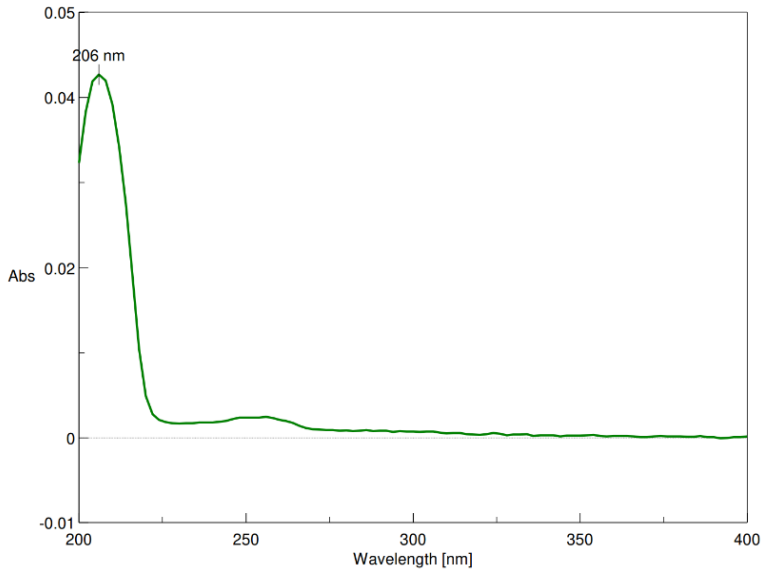


**Figure 5.3.1.3.1:** UV spectrum of FMTE having concentration (10 µg/mL in acetonitrile)

### 5.3.1.4. Selection and optimization of mobile phase for monitoring degradation of felbamate

The objectives of the HPLC method development were to develop a simple, robust, isocratic, and mass friendly method with *k'* in-between 5 to 10. The reported methods for FMTE mainly consisted of phosphate (pH 6-7) and ammonium acetate buffers as the aqueous portion of the mobile phase and acetonitrile was the preferred organic component.

The pKa of FMTE was determined by using mavin sketch[88]. The software has shown pKa = 14.98. The high pKa value for FMTE is due to the two amine groups which gets ionized in acidic pH. Initial runs were carried out using ammonium formate buffer solution (10 mM, pH 3.7, adjusted using formic acid) to obtain retention of ionized form of FMTE. Ammonium formate provides buffer capacity at pKa value of 3.7 and 9.2 due to the pKa values of formic acid and ammonium ion respectively.

The first trial was conducted on Agilent XDB C18 column (150mm × 4.6mm, 5 µm) using acetonitrile and ammonium formate (10mM, pH adjusted to 3.7 with formic acid) in ratio of 80:20 (v/v). However, the drug lacked the desired retention and eluted close to the void volume. To enhance the retention of the drug, the percentage of organic phase was successively decreased to 20%. The decrease in organic phase improved $t_R$ of the drug to 6.1 min. Though, the retention behaviour of the drug improved, NTP (< 2000) was not in acceptable range. The chromatogram of the trial is depicted in figure 5.3.1.4.1.

It was decided to change the chromatographic column from Agilent XDB C18 column (150mm × 4.6mm, 5 µm) to a Phenomenex C8 column (250 × 4.6mm, 5 µm) to increase the polarity of the stationary phase. This modification brought all the system suitability parameters within the acceptable range (NTP > 3000, peak asymmetry = 0.8, and a *k'* = 4.3). The chromatogram obtained is shown in figure 5.3.1.4.2.

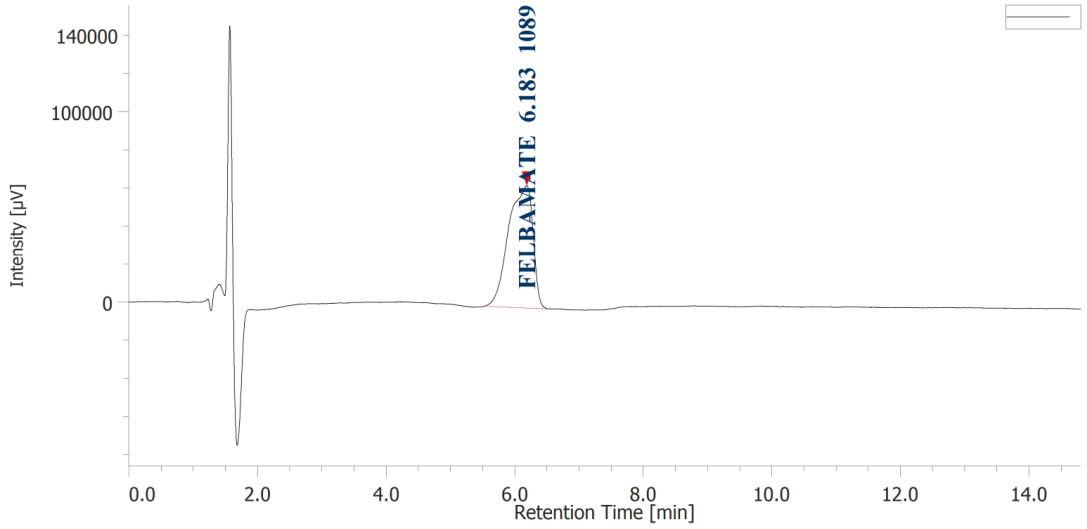


**Figure 5.3.1.4.1: Chromatogram of felbamate (10 µg/mL)** (Mobile phase, acetonitrile: ammonium formate buffer (pH 3.7, adjusted with formic acid), 80:20 (v/v); flow rate: 1 mL/min; wavelength: 206 nm; Column: Agilent XDB C18 (150mm ×4.6mm, 5µm))

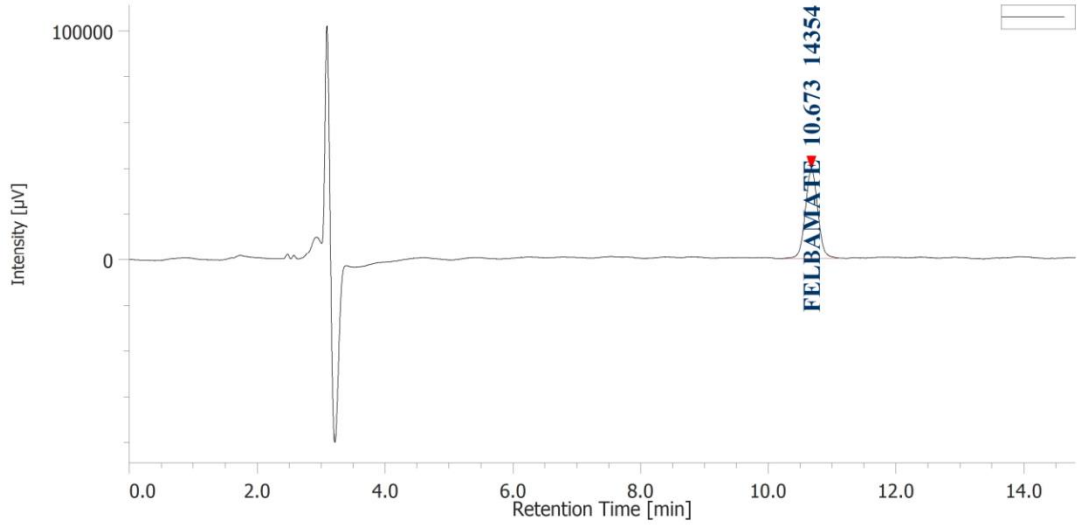


**Figure 5.3.1.4.2: Chromatogram of felbamate (10 µg/mL)** (Mobile phase, acetonitrile: ammonium formate buffer (pH 3.7, adjusted with formic acid), 20:80 (v/v); flow rate: 1mL/min; wavelength: 206nm; Column: Phenomenex C8 column (150 × 4.6mm, 5 µm))

The optimized chromatographic condition to monitor the drug degradation behaviour was as follows.

**Mobile phase:** Acetonitrile: ammonium formate buffer (pH 3.7, adjusted with formic acid), 20:80 (v/v).

**Column:** Phenomenex C8 (250mm ×4.6mm, 5µm).

**Wavelength:** 206 nm.

**Flow rate:** 1 mL/min.

## 5.3.2. Forced degradation studies

The stability of the drug was probed as per the guidance provided in the ICH Q1A(R2) guideline. The drug was tested under hydrolytic (acidic, basic, and neutral), oxidative, thermal, and photolytic conditions. The stressed samples were subjected to HPLC analysis using optimized chromatographic conditions, and the chromatogram obtained was compared with blank stored under normal condition (blank untreated), blank subjected to stress conditions like the drug (blank treated), and the drug solution stored under normal condition (standard untreated)

### 5.3.2.1. Hydrolytic degradation

Hydrolytic degradation was performed using acidic, basic, and neutral conditions. The degradation studies were carried out at room temperature in order to get desired degradation of the drug. The degradation studies were also carried out at higher temperature (70 ℃, 7 h), in case, no degradation was observed at room temperature. The concentration of the stressors was also optimized from low to high depending upon the degradation behaviour of the drug. Periodically, samples were withdrawn, neutralized, and diluted to the desired concentration and injected into HPLC using optimized chromatographic conditions.

**Acid degradation**

Acid degradation was carried out at room temperature by exposing drug solution to 0.1 N HCl for 48 hours in a volumetric flask to get desired degradation of the drug. The studies were repeated using 0.1 N HCl at 70℃ for 7 hours since no degradation was observed at room temperature. After applying the stress conditions, the samples were neutralized by using equal strength of base (NaOH). The neutralized samples were diluted to get the desired concentration and injected into HPLC using optimized chromatographic conditions.

The drug showed resilience to degradation under acidic conditions, and no degradation was observed.

**Base degradation**

Base degradation was carried out at room temperature by exposing drug solution to 0.1 N NaOH for 48 hours in a volumetric flask to get desired degradation of the drug. After applying the stress conditions, the samples were neutralized by using equal strength of acid (HCl). The neutralized samples were diluted to get the desired concentration and injected into HPLC using optimized chromatographic conditions.

The drug was highly susceptible to degradation under basic conditions with ~ 52 % of degradation. Two unknown degradation products were observed (DP1 and DP2) having $t_R$ of 5.4 and 7.4 min respectively. On heating it was observed that after 2 h drug degrades entirely with DP1 being the prominent degradation product. The chromatogram obtained under the basic condition is seen in figure 5.3.2.1.

The unknown peaks and FMTE was well resolved in the developed HPLC method with good system suitability parameters indicating no further requirement of HPLC method optimization.

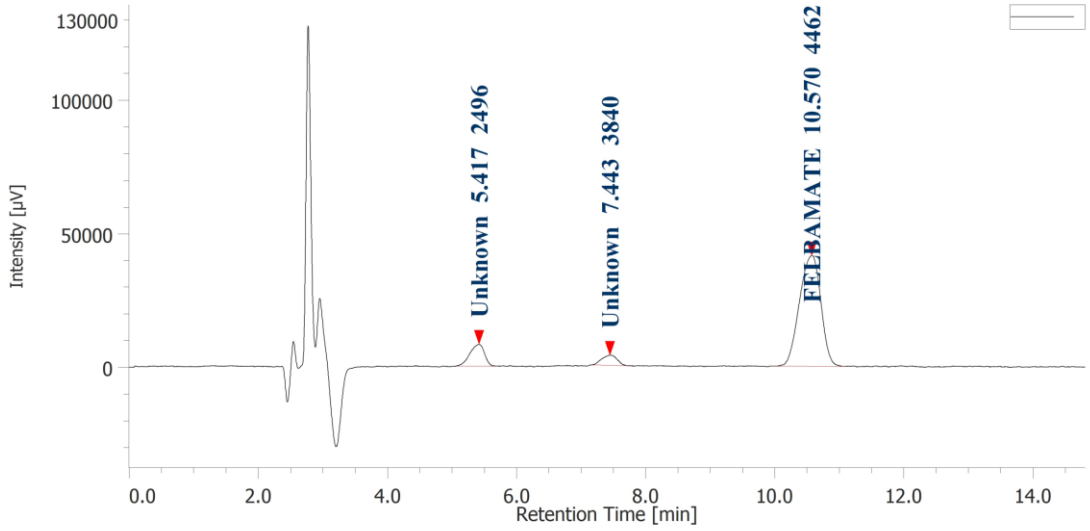


**Figure 5.3.2.1: Chromatogram of FMTE (100 µg/mL) treated with 0.1 N NaOH at room temperature for 48 h. (**Mobile phase, acetonitrile: ammonium formate buffer (pH 3.7, adjusted with formic acid), 20:80 (v/v); flow rate: 1mL/min; wavelength: 206nm; Column: Phenomenex C8 column (150 × 4.6mm, 5 µm))

To ascertain the identity of the degradation products their UV spectra acquired using DAD detector were overlain with that of the drug. The UV spectra of Drug and DP2 were

displaying similarity indicating both have similar structure. Spectra of DP1 showed subtle difference to that of drug. The overlain spectra can be seen in figure 5.3.2.2.

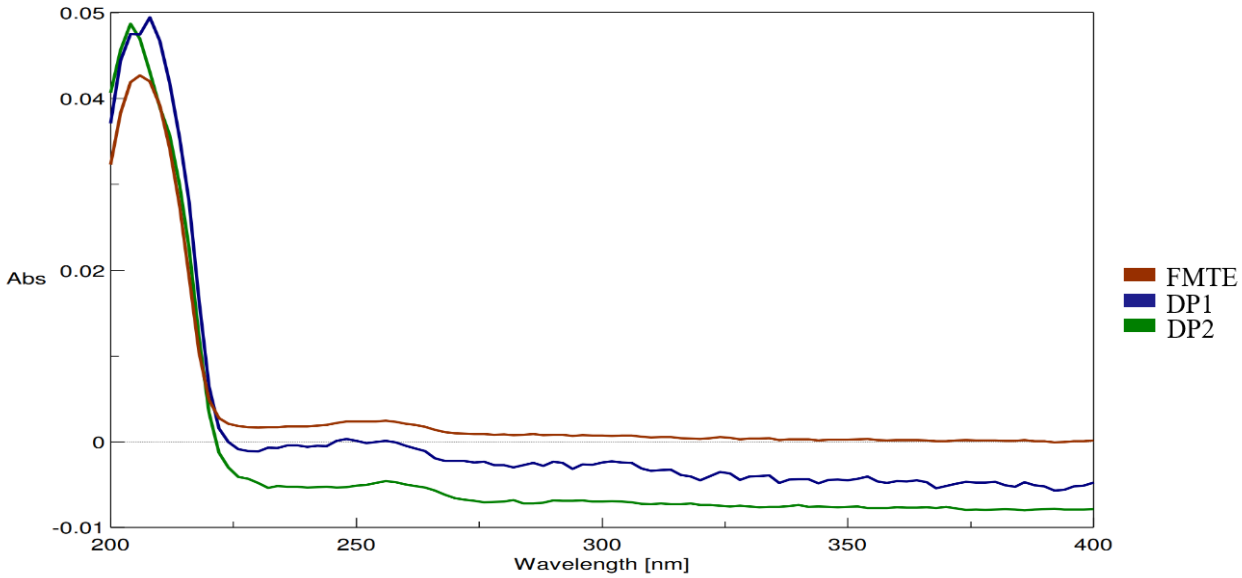


**Figure 5.3.2.2:** Overlain of UV spectra of FMTE with its DPs

**Neutral degradation**

Neutral degradation was carried out at room temperature by exposing drug solution to water for 48 hours in a volumetric flask to get desired degradation of the drug. The studies were repeated by heating the drug solution with water at 70℃ for 7 h since no degradation was observed at room temperature. Samples were diluted to get the desired concentration and injected into HPLC using optimized chromatographic conditions.

The drug showed resilience to degradation under neutral basic condition, and no degradation was observed.

**5.3.2.3. Thermal degradation**

Thermal degradation was carried out by exposing the drug in sealed ampoule to dry heat at 70 ℃ for 7 days using hot air oven. A control sample was maintained by placing drug into a separate glass ampoule stored at room temperature. After the stress period, the sample was diluted with diluent to get the desired concentration and injected into HPLC using optimized chromatographic conditions.

The drug did not show degradation under thermal conditions.

### 5.3.2.2. Oxidative degradation

Oxidative degradation was carried out by stressing FMTE in presence of 15% $H_2O_2$ at room temperature for 48 h. The drug was also heated with 15% $H_2O_2$ for 7 h at 70 ℃ to promote degradation. After the stress period, diluent was added to get the required concentration and the sample analysed by HPLC.

FMTE was resilient to oxidative degradation, and no unknown peaks were observed in the chromatogram of the stressed samples.

### 5.3.2.4. Photolytic degradation

Photolytic degradation studies were carried out in the solid and liquid states using photostability chamber. Solid state stress studies were carried out by spreading the drug as a thin layer inside a petri dish while, liquid state stress studies were carried out by placing drug solution inside a volumetric flask. Both the samples were exposed to ICH Q1B mandated dose of light. In addition, solid-state studies were also carried out by exposing the drug placed inside a volumetric flask to sunlight for 7 days.

The chromatogram obtained from photolytic stressed samples did not show degradation.

## 5.3.3. Validation of developed Stability indicating assay method (SIAM)

HPLC method validation is required to ensure that the method achieves an adequate standard of specificity, accuracy, and precision. The developed SIAM was validated as per the guidance of the ICH Q2 guideline. The parameters considered during the validation process is summarized in table 5.3.3.1.

### 5.3.3.1. Specificity and selectivity

The specificity of the HPLC method was expressed in terms of resolution between the closely eluting peaks. It is evident from figure 6.3.2.2.1. that the peaks were well resolved with a resolution value greater than one which confirms the specificity of the method. The method's selectivity was determined by measuring % peak purity value acquired using data acquisition software. The peak purity(%) was > 99% which indicates that the method is selective.

**Table 5.3.3.1:** Validation parameters and acceptance criteria

| Sr.No. | Validation Parameters | Acceptance Criteria |
|---|---|---|
| **1** | **Specificity** | Resolution > 1 |
| **2** | **Selectivity** | Peak purity (%) > 99 |
| **3** | **Linearity** | Correlation coefficient not less than 0.999 |
| **4** | **Accuracy (across the specified range)** | Recovery (%) between 98.0 to 102% |
| **5** | **Precision (intraday & interday )** | RSD (%) of replicate injections not more than 2.0 |
| **6** | **Robustness** | 1) Resolution between adjacent peak should not be less than 1.0<br>2) Numbers of theoretical plates of analyte peak should not be less than 2000.<br>3) Asymmetry of peak should not be more than 2.0 |

### 5.3.3.2. Linearity and range

The linearity was established in triplicate by taking seven incremental concentrations in a range of 20-120 µg/mL. The graph plotted between the average area under peak v/s concentration. The data obtained was subjected to regression analysis. The calculated value of the corelation coefficient ($r^2$) was 0.999. The linearity plot and the data pertaining to linearity is given in figure 5.3.3.2.1 and table 5.3.3.2.1. The representative chromatogram at each concentration level is seen in figure 5.3.3.2.2.

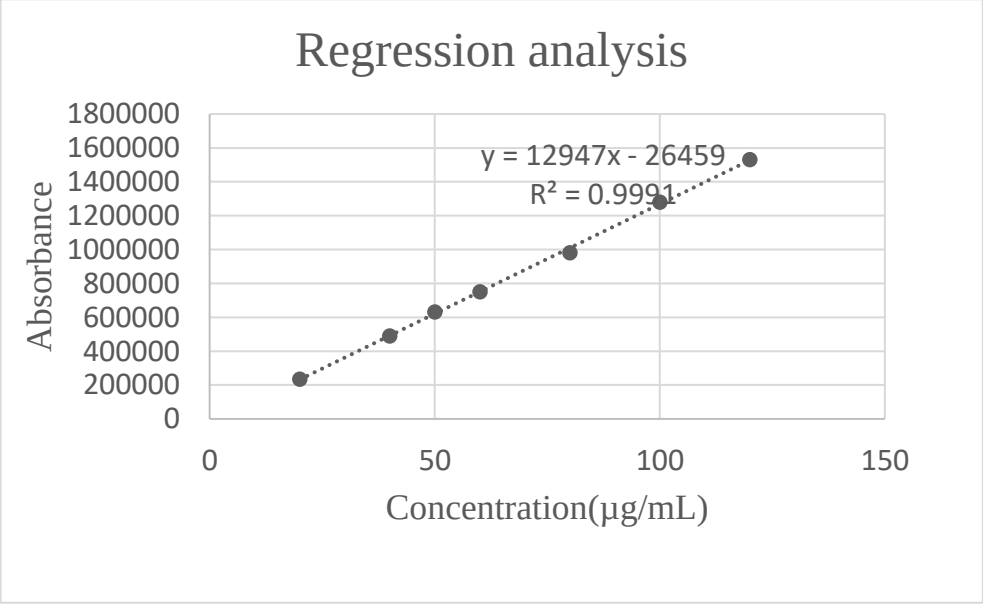


**Figure 5.3.3.2.1:** Linearity graph of FMTE

**Table 5.3.3.2.1:** Linearity data for FMTE

| Sr. No. | Concentration (µg/mL) | Peak area | | | | RSD(%) |
|---|---|---|---|---|---|---|
| | | Injection 1 | Injection 2 | Injection 3 | Average | |
| 1 | 20 | 236029 | 231317 | 237425 | 234924 | 1.4 |
| 2 | 40 | 489423 | 488537 | 491739 | 489900 | 0.3 |
| 3 | 50 | 638398 | 632948 | 622891 | 631412 | 1.2 |
| 4 | 60 | 742047 | 748355 | 762420 | 750941 | 1.4 |
| 5 | 80 | 977779 | 979726 | 985593 | 981033 | 0.4 |
| 6 | 100 | 1269315 | 1283746 | 1286440 | 1279834 | 0.7 |
| 7 | 120 | 1521497 | 1542356 | 1531239 | 1531697 | 0.7 |

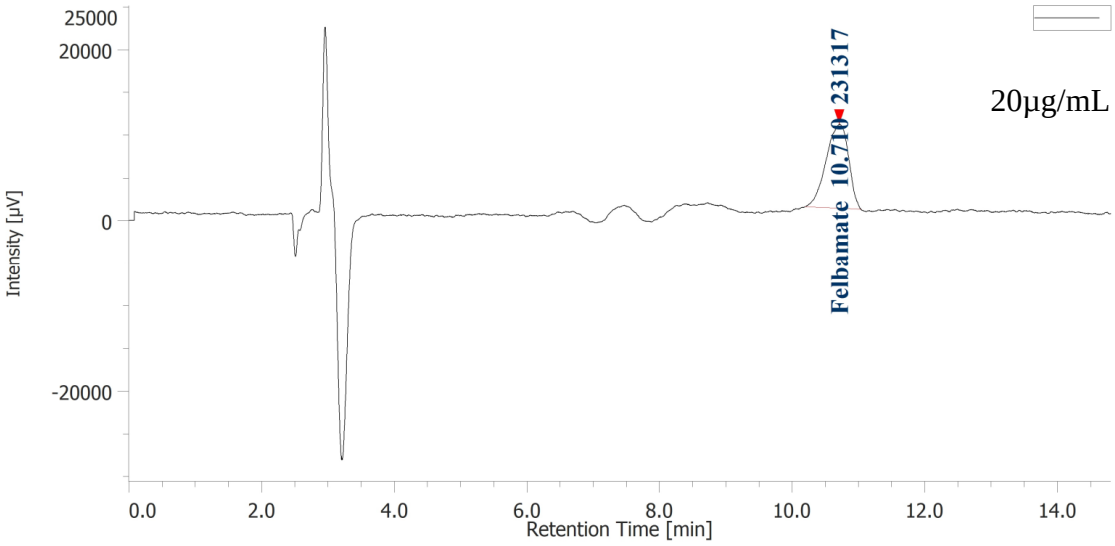


**Chromatogram no 1**

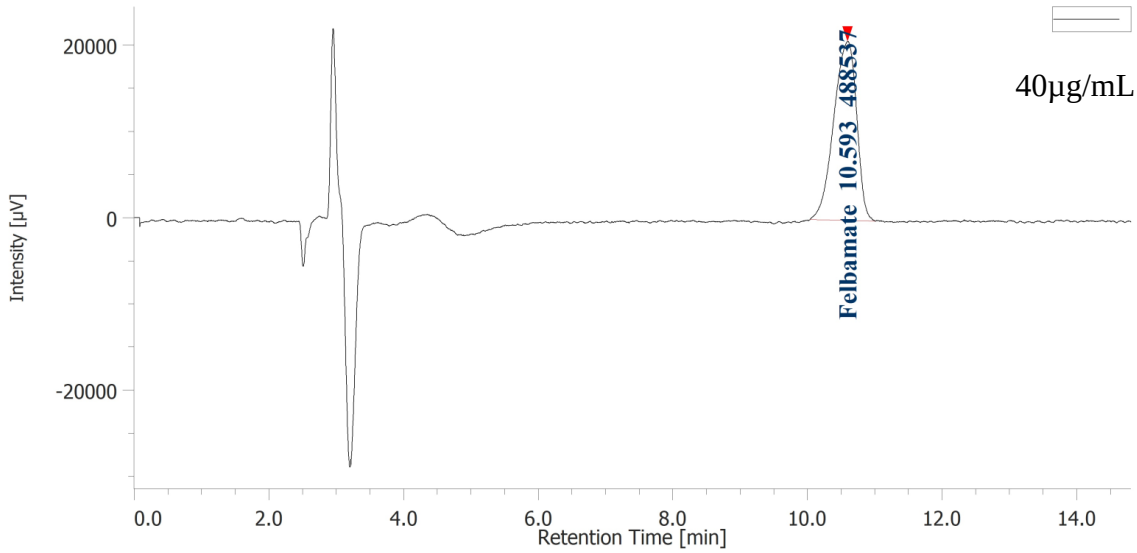


**Chromatogram no 2**

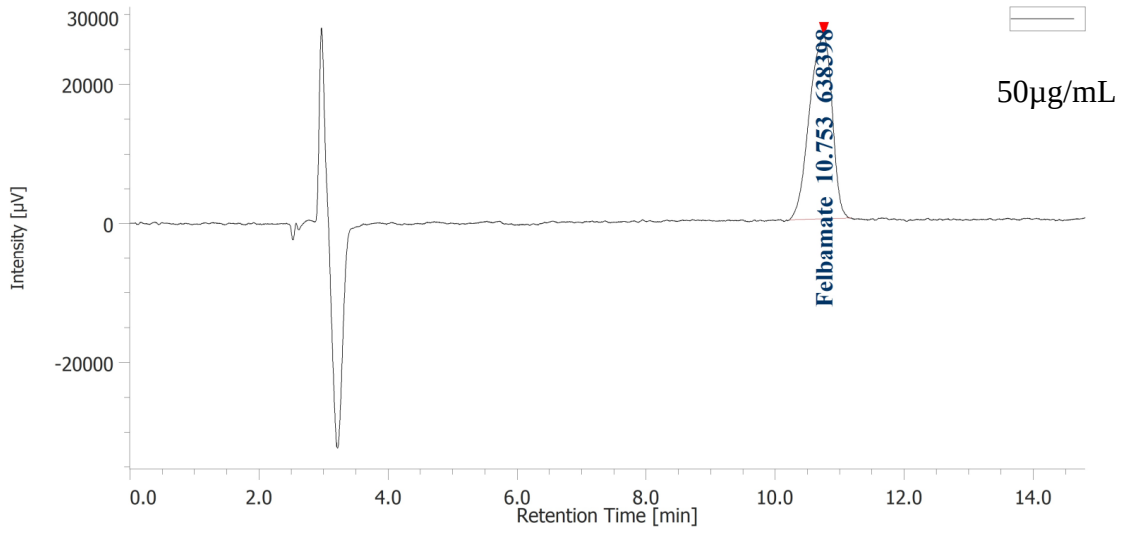


**Chromatogram no 3**

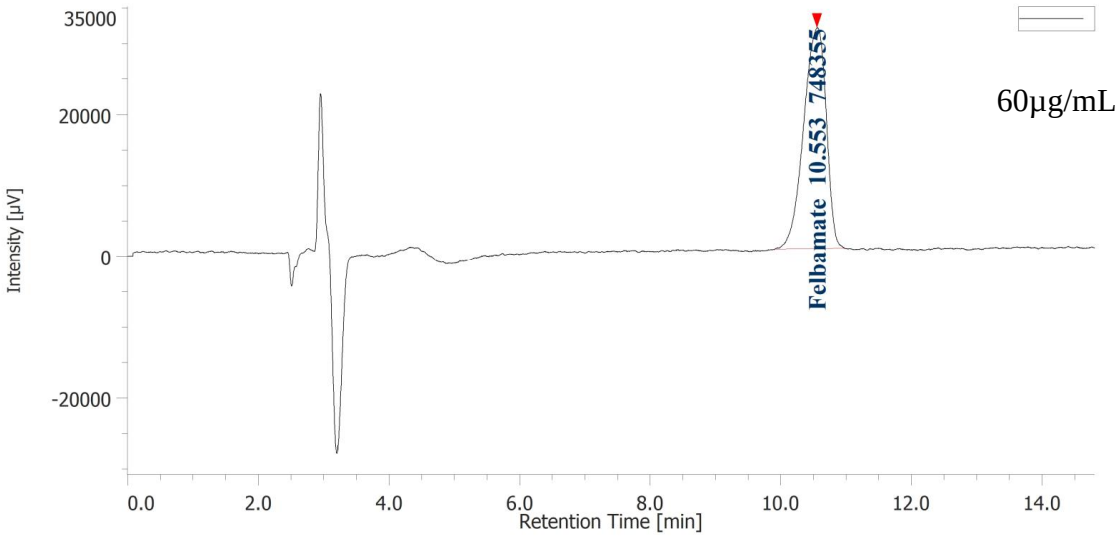


**Chromatogram no 4**

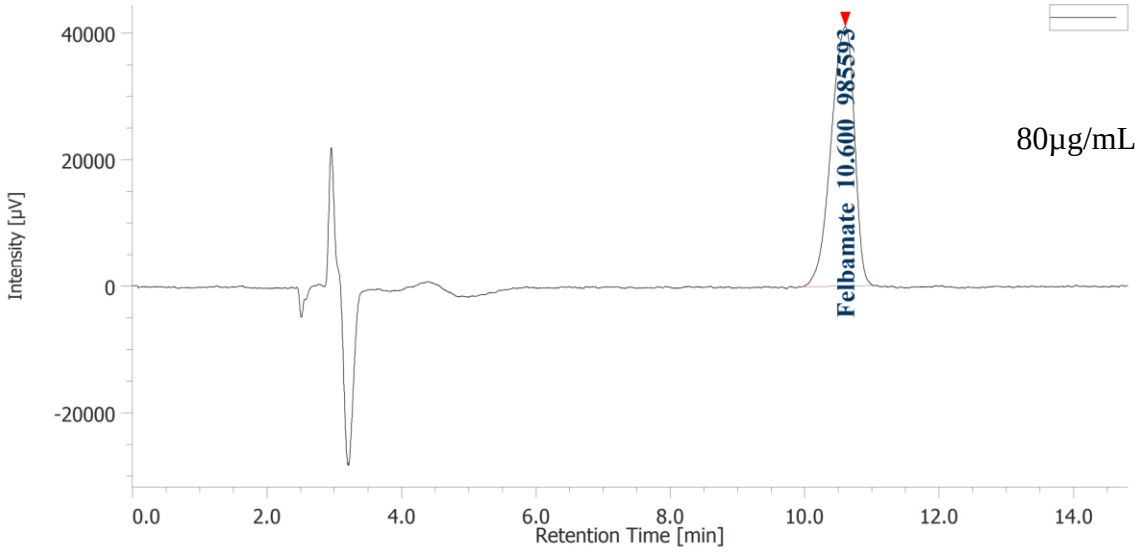


**Chromatogram no 5**

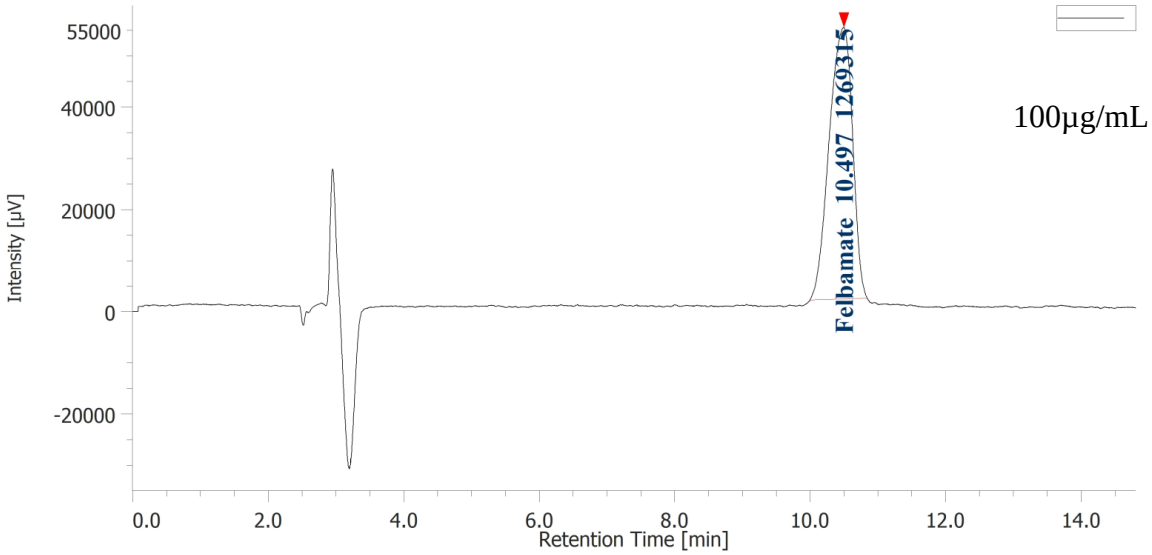


**Chromatogram no 6**

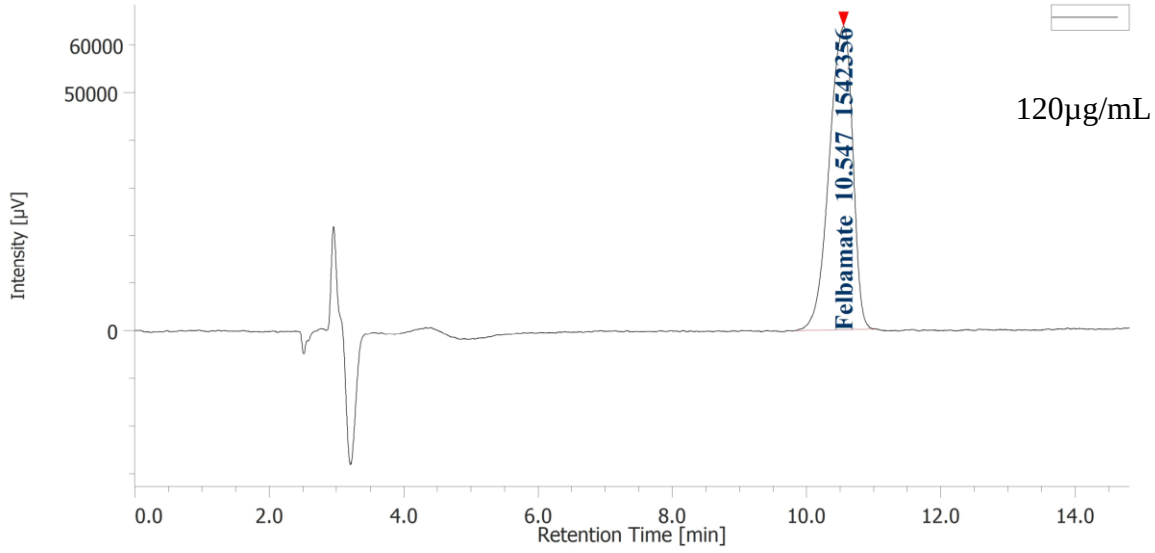


**Chromatogram no 7**

**Figure 5.3.3.2.2:** Representative chromatograms at concentration level 20, 40, 50, 60, 80, 100 and 120 µg/mL.

### 5.3.3.3. Accuracy

The accuracy was expressed in terms of recovery (%) of the spiked standard drug and was done by the standard addition method. The stressed sample were separately spiked with standard drug with concentrations 40 µg/mL (80%), 50 µg/mL (100%) and 60 µg/mL (120%) of the target assay concentration (50 µg/mL) and injected in triplicate. The average recovery at each level was between 98 to 102 %, with the mean recovery of 100.2 %. The data and representative chromatogram of recovery studies is seen in table 5.3.3.3.1 and figure 5.3.3.3.1.

**Table 5.3.3.3.1:** Recovery studies for FMTE (n=3)

| Spiked drug concentration (µg/mL) | Recovered concentration (µg/mL) ± S. D, % R.S.D. | Recovery (%) |
|---|---|---|
| 40 | 40.4 ± 0.4, 1.0 | 100.9 |
| 50 | 49.4 ± 0.6,1.3 | 98.9 |
| 60 | 60.4 ± 0.5,0.9 | 100.8 |

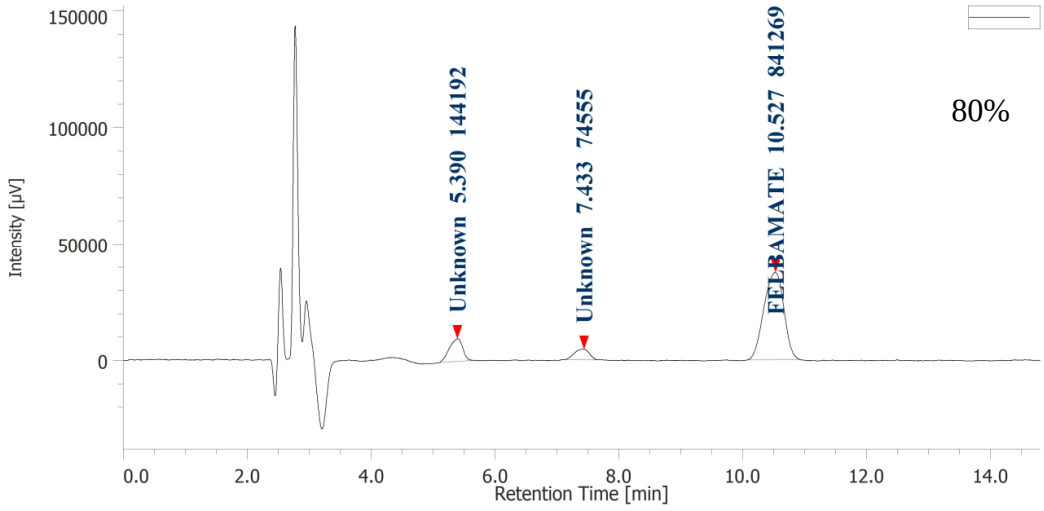


**Chromatogram no 8**

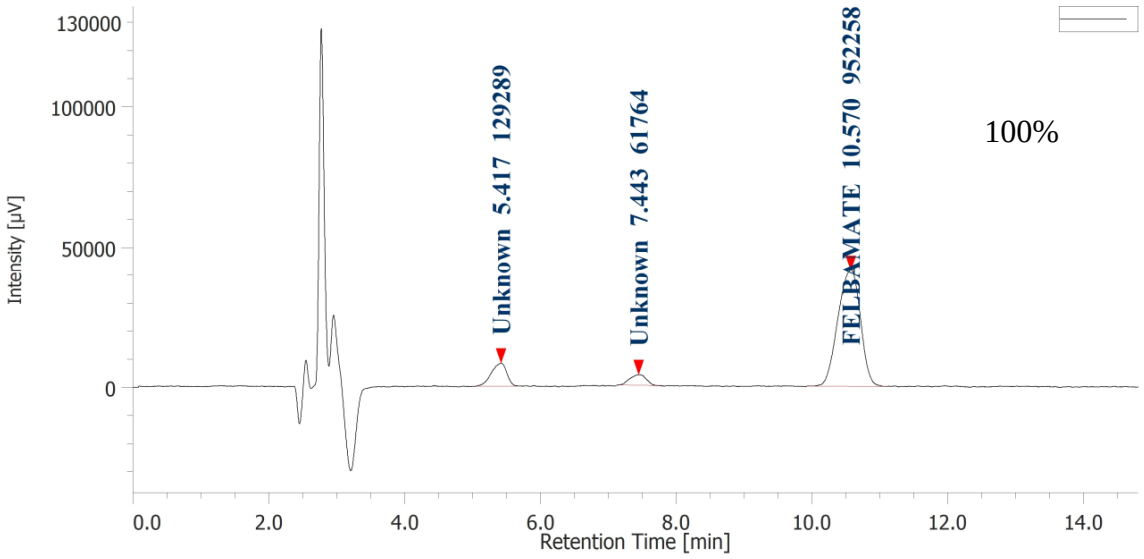


**Chromatogram no 9**

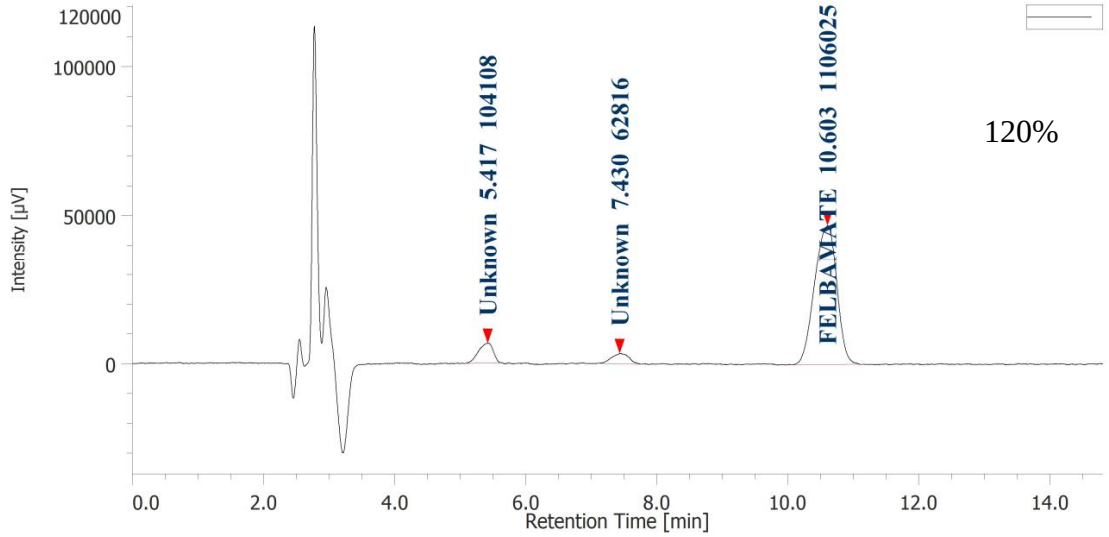


**Chromatogram no 10**

**Figure 5.3.3.3.1.** Representative chromatograms of recovery studies at 80%,100% and 120%

### 5.3.3.4. Precision

Intraday and inter-day precision studies were carried out at 3 concentration levels. 40, 80, and 120 µg/mL in triplicate. The % RSD at each level was found to be < 2% inferring that the method was precise.

**Table 5.3.3.4.1:** Precision data obtained during intra-day and inter-day studies

| Concentration (µg/mL) | Intraday Mean peak area± SD; %RSD | Inter-day Mean peak area ± SD; %RSD |
|---|---|---|
| 40 | 489900 ± 1353, 0.3 | 491919 ± 10430, 0.3 |
| 80 | 631412 ± 4068, 0.4 | 633906 ± 9433, 1.5 |
| 120 | 750941 ± 10430, 1.4 | 743905 ± 4482, 0.6 |

### 5.3.3.5. Robustness

The robustness of the HPLC method was established to understand the HPLC methods tolerance to deliberate change in the chromatographic parameters. For this purpose, the following changes were carried out to observe its effect on the developed method.

1) The pH of the mobile phase (±0.5 of the optimized value.)
2) Flow rate (±0.2ml of the optimized flow rate)
3) Mobile phase composition (±2% of the optimized ratio)
4) Wavelength (±3 units of the optimized wavelength)

The results of the robustness studies are depicted in the tables below.

**Table 5.3.3.5.1:** Data pertaining to robustness studies.

| Peak | Theoretical plates | Peak asymmetry | Resolution |
|---|---|---|---|
| | **pH 3.2** | | |
| DP1 | 4136 | 1.0 | 5.6 |
| DP2 | 6085 | 1.0 | 7.2 |
| FMTE | 7859 | 1.0 | -- |
| | **pH 4.2** | | |
| DP1 | 4448 | 0.9 | 5.7 |
| DP2 | 6235 | 1.0 | 7.2 |
| FMTE | 8037 | 1.0 | -- |

| Peak | Theoretical plates | Peak asymmetry | Resolution |
|---|---|---|---|
| **0.8mL/min** | | | |
| DP1 | 3608 | 0.9 | 5.3 |
| DP2 | 5194 | 0.9 | 6.7 |
| FMTE | 6681 | 0.9 | -- |
| **1.2mL/min** | | | |
| DP1 | 3798 | 1.0 | 5.6 |
| DP2 | 5560 | 1.0 | 7.1 |
| FMTE | 7230 | 1.0 | -- |

| Peak | Theoretical plates | Peak asymmetry | Resolution |
|---|---|---|---|
| **Organic phase +2% of the optimized ratio** | | | |
| DP1 | 4003 | 1.0 | 4.6 |
| DP2 | 5173 | 1.0 | 5.7 |
| FMTE | 6464 | 1.0 | - |
| **Organic phase -2% of the optimized ratio** | | | |
| DP1 | 3751 | 0.9 | 6.6 |
| DP2 | 5941 | 0.9 | 8.7 |
| FMTE | 8176 | 1.0 | - |

| Peak | Theoretical plates | Peak asymmetry | Resolution |
|---|---|---|---|
| **Wavelength (203 nm)** | | | |
| DP1 | 4120 | 1.0 | 5.6 |
| DP2 | 5944 | 1.0 | 7.0 |
| FMTE | 7468 | 1.0 | -- |
| **Wavelength (209 nm)** | | | |
| DP1 | 4081 | 1.0 | 5.5 |
| DP2 | 5886 | 1.0 | 7.0 |
| FMTE | 7552 | 1.0 | -- |

## 5.3.4. Characterization of the degradation products by mass and tandem mass spectrometry

The structural characterization of the oxidative degradation products of FMTE wad done by LC-MS and LC-MS/MS studies. The LC-MS and LC-MS/MS spectra were captured in positive electro spray ionization mode(+ESI). The optimized parameters of LC-MS/MS studies are depicted in table 5.3.5.1

**Table 5.3.5.1:** The optimized parameters of LC-MS/MS studies

| Parameter | Value |
|---|---|
| **Dying, sheath, and nebulizing gas** | Nitrogen |
| **Vcap** | 3100 V |
| **Fragmentor** | 150 V |
| **Skimmer** | 45 V |
| **Octopol RF peak** | 750 V |
| **Drying gas flow** | 11 L/min |
| **Sheath gas flow** | 10 L/min |
| **Nebulizing gas** | 25 psi |
| **Sheath gas temp** | 295℃ |

### 5.3.4.1. FMTE

FMTE has molecular weight of 238.0953 g/mole. The LC-MS spectra captured in + ESI showed a peak at *m/z* 239.1029. The formation of a sodium adduct $(M+Na)^+$ peak at *m/z* 261.0855 confirmed the presence of the molecular ion. The MS/MS spectra of FMTE showed two major fragment ions at *m/z* 178.0857 and 117.0697. The fragment with *m/z* 178.0857 is formed due to the loss of the carbamic acid fragment having exact mass 61.0163. This Fragment furthers losses another carbamic acid moiety to form fragment with *m/z* 117.0697. The MS, MS/MS spectra and the fragmentation pathway for FMTE is seen in figures 5.3.4.1.1 to 5.3.4.1.3.

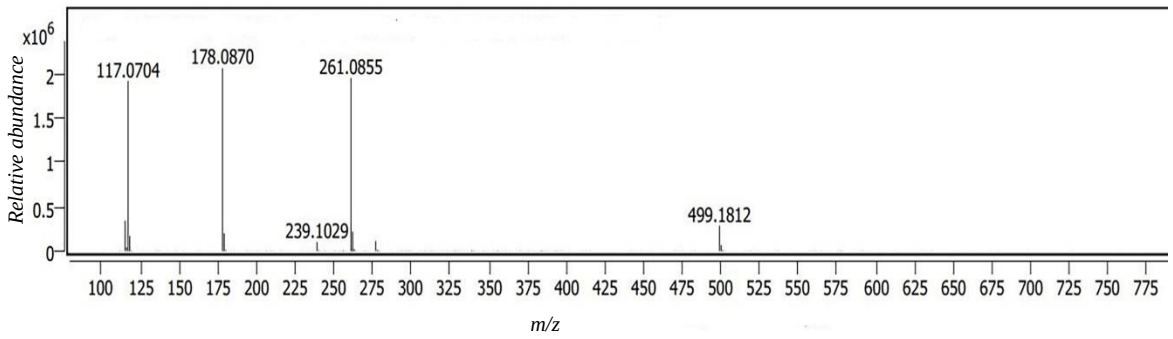


**Figure 5.3.4.1.1:** MS spectra of FMTE

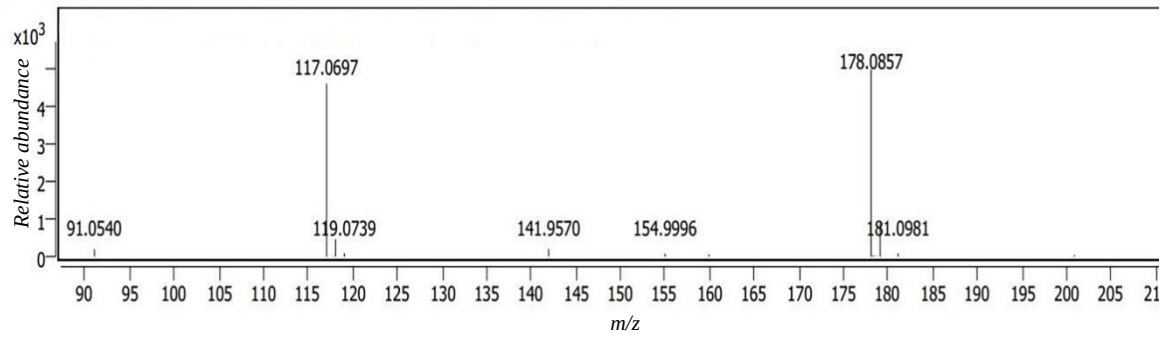


**Figure 5.3.4.1.2:** MS/MS spectra of FMTE.

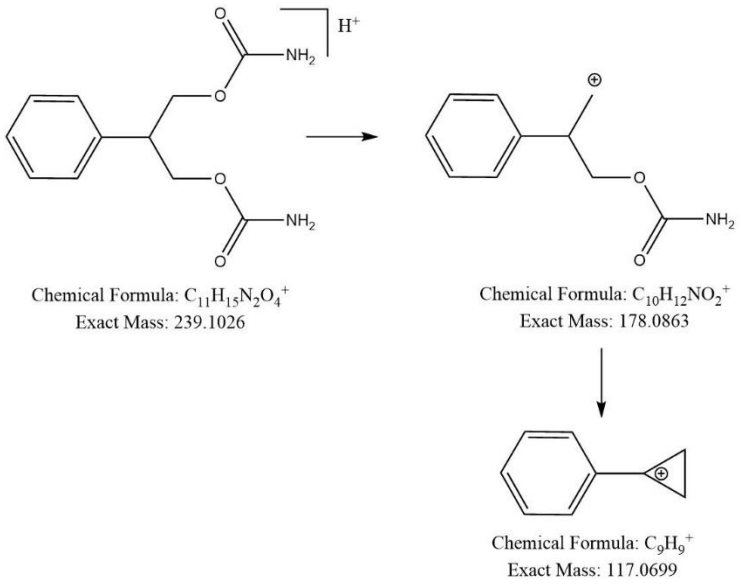


**Figure 5.3.4.1.3:** MS/MS fragmentation pathway of FMTE.

### 5.3.4.2. DP2

The protonated peak for DP2 was seen at *m/z* 218.0794. Partial hydrolysis of carbamate moieties in presence of a strong nucleophile followed with cyclization leads to the formation of DP2. The MS/MS of DP2 showed peaks with *m/z* 202.8967, 159.9556, 118.9924 and 96.9581. DP2 loses an oxygen atom to form fragment with *m/z* 202. 8967.This fragment in the subsequent step loses $CO_2$ to yield a fragment with *m/z* 159.9556. Further loss of 1,2-oxazirene from the preceding fragment forms fragment with *m/z* 118.9924. In the last step, the fragment with *m/z* 96.9581 is formed due to conversion of phenyl cyclopropane ring to cycloheptane.

DP2 of FMTE was identified as 6-(1,2-oxaziren-3-yl)-5-phenyl-4H-1,3-dioxin-2-one. RDB for it was found to be 8.5 and error in mmu -3.46. The MS, MS/MS spectra and the fragmentation pathway for DP2 of FMTE is seen in figures 5.3.4.2.1 to 5.3.4.2.3.

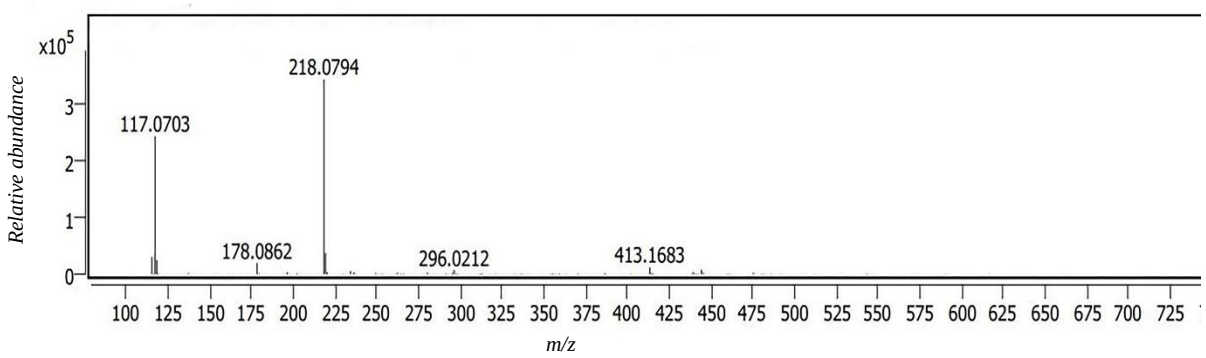


**Figure 5.3.4.2.1:** MS spectra of DP2.

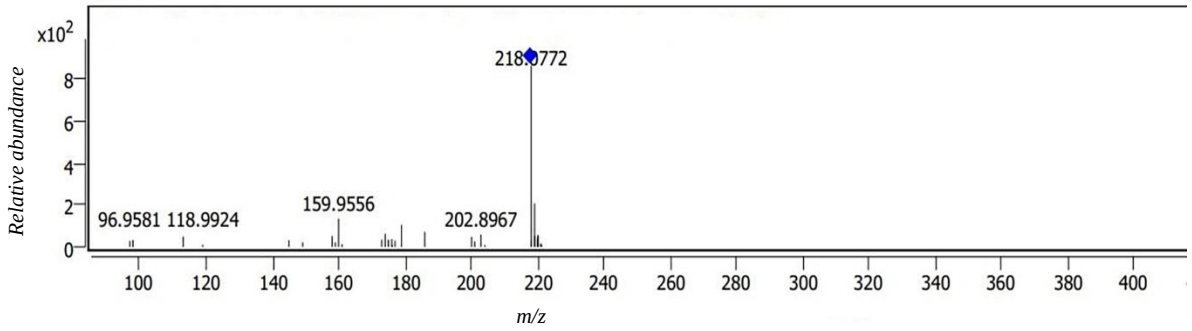


**Figure 5.3.4.2.2:** MS/MS spectra of DP2.

### 5.3.4.3. DP1

The MS spectra for DP1 showed a peak at *m/z* 117.0701. This was like the fragment formed from the drug. So, it was proposed that DP1 share a similar structure to fragment with *m/z* 117.0701. DP1 is formed to due to total hydrolysis of the carbamate moieties followed by cyclization.

DP1 of FMTE was identified as cyclopropyl benzene. The mass spectra for DP1 is seen in figure 5.3.4.3.1. The RDB and error in mmu for the structure was 5.5 and -0.02 respectively.

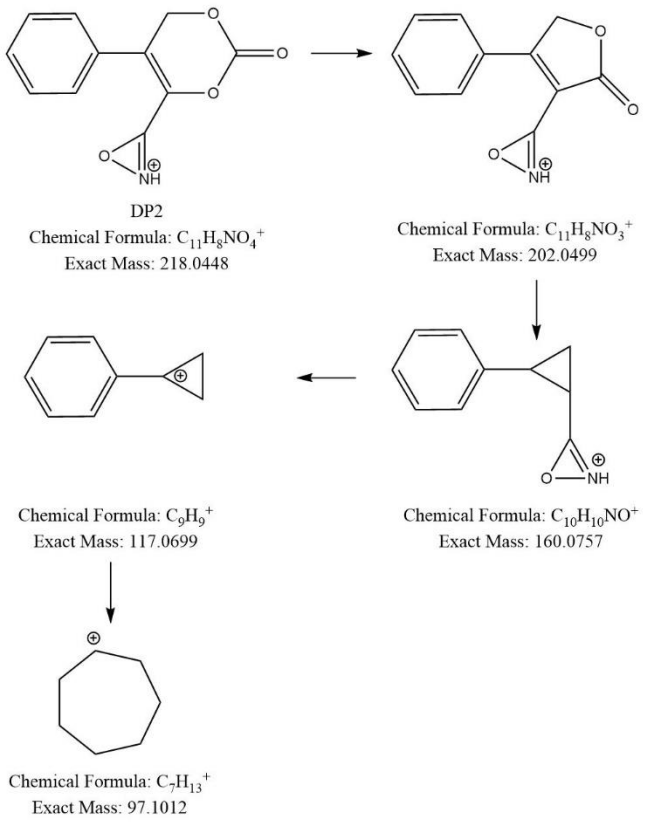


**Figure 5.3.4.2.3:** MS/MS fragmentation pathway of DP2.

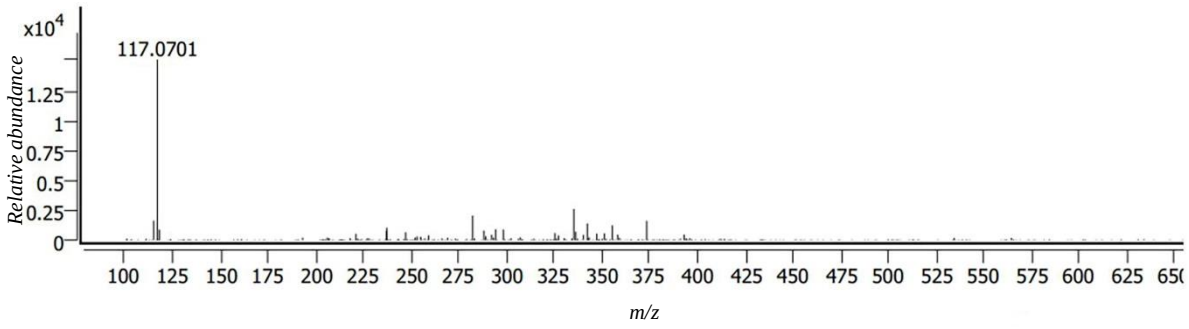


**Figure 5.3.4.3.1:** MS spectra of DP1.

The Summary of the mass data is seen in table 5.3.4.1.

**Table 5.3.4.1:** Summary of mass data of FMTE and its degradation products

| **Compound** | **Experimental mass** | **Most likely molecular formulae** | **Theoretical mass** | **RDB** | **Error in mmu** | **Major fragments** | | **Most likely molecular formulae for fragments** |
|---|---|---|---|---|---|---|---|---|
| | | | | | | Experimental mass | Theoretical mass | |
| Felbamate | 239.1029 | $C_{11}H_{15}N_2O_4^+$ | 239.1026 | 5.5 | -0.03 | 178.0857 | 178.0863 | $C_{10}H_{12}NO_2^+$ |
| | | | | | | 117.0697 | 117.0699 | $C_9H_9^+$ |
| DP-2 | 218.0794 | $C_{11}H_8NO_4^+$ | 218.0448 | 8.5 | -3.46 | 202.8967 | 202.0499 | $C_{11}H_8NO_3^+$ |
| | | | | | | 159.9556 | 160.0757 | $C_{10}H_{10}NO^+$ |
| | | | | | | 118.9924 | 117.0699 | $C_9H_9^+$ |
| | | | | | | 96.9581 | 97.1012 | $C_7H_{13}$+ |
| DP-1 | 117.0701 | $C_9H_9^+$ | 117.0699 | 5.5 | -0.02 | -- | -- | -- |

### 5.3.5. *In-silico* ADMET studies of FMTE and its DPs.

The *In-silico* ADMET predictions were performed by using opensource tools like the pkCSM webserver, ToxTree and OSIRIS property explorer.

**pkCSM**

FMTE was predicted to have intestinal absorption of 68% while both the degradation products were above 95%. None of them possessed the ability to bind to p-glycoprotein and cause its inhibition. DP1 had log BB value of > 0.3 indicating that it would readily cross the brain blood barrier. FMTE and DP2 had value > -1 showing that they do not readily pass through the blood brain barrier.

CYP1A2 was inhibited by DP1 and DP2 while CYP3A4 is inhibited only by DP2. Other isoforms of the cytochrome P450 enzyme system does not seem to be affected by FMTE and its degradation products. DP2 was predicted to possess genotoxic potential and FMTE hepatotoxicity. The Summary of the pkCSM is shown in the table 5.3.5.1.

**ToxTree and OSIRIS property explorer**

ToxTree could not detect any genotoxic fragments in the drug structure thus freeing them of toxic potential. A similar inference pertaining to genotoxicity was drawn by OSIRIS property explorer. Further it cleared them for tumorigenic, irritant, and reproductive risks.

**Table 5.3.5.1:** Summary of pkCSM predictions

| Compound | Intestinal absorption (%absorbed) | PgP Substrate | BBB Permeability (log BB) | CYP1A2 inhibitor | CYP2C19 inhibitor | CYP2C9 Inhibitor | CYP2D6 Inhibitor | CYP3A4 Inhibitor | AMES toxicity | Hepato toxicity |
|---|---|---|---|---|---|---|---|---|---|---|
| **Felbamate** | 67.85 | No | -0.206 | No | No | No | No | No | No | Yes |
| **DP1** | 96.10 | No | 0.516 | Yes | No | No | No | No | No | No |
| **DP2** | 95.16 | No | 0.125 | Yes | No | No | No | Yes | Yes | No |

# 5.4 Experimental work

## 5.4.1. Instrumentation

**Table 5.4.1.1:** List of instruments

| Sr.no. | Instrument | Make and specification |
|---|---|---|
| **1** | **HPLC** | LC-4000, Jasco, Japan. Made up of a model CO-4061 temperature-controlled column compartment, a model PU 4180 quaternary pump system with inline degasser, a model AS-4050 autosampler, Chromenav (version, 2.01.06) data acquisition software, LC-NET II interface box, Acer workstation computer running Microsoft windows 7 professional operating system. |
| **2** | **Column** | Phenomenex C18 (150mm ×4.6mm, 5µm). |
| **3** | **Sonicator** | Citizon, Vadodra, India. |
| **4** | **pH meter** | Digital pH meter, Elico, India. |
| **5** | **Precision balance** | Wensar digital, Chennai, India. |
| **6** | **Double distillation assembly** | Bhanu scientific instruments, Bangalore, Karnataka. |
| **7** | **Hot air oven** | Universal, Ambala, India. |
| **8** | **Constant temperature water bath** | Generic. |
| **9** | **Photostability chamber** | Newtronics lifecare Pvt.Ltd, Mumbai,India. |
| **10** | **MS system** | Agilent 1200 series HPLC system, 6200 series QTOF. |
| **11** | **Workstation for *in-silico* studies** | Intel i7 5820k based workstation computer running windows 10 professional operating system with 32 GB of ram, ToxTree (version, 3.1.0-1851-1525442531402), OSIRIS property explorer. |

## 5.4.2. Chemicals and reagents

1. **Acetonitrile (HPLC grade):** Qualigen, Mumbai, Maharashtra
2. **Hydrochloric acid:** Molychem, Thane, Mumbai.
3. **Hydrogen peroxide:** Molychem, Thane, Mumbai.
4. **Ammonium formate:** Molychem, Thane, Mumbai.
5. **Water (HPLC grade):** Finar, Ahmedabad, Gujarat.
6. **Sodium Hydroxide:** Finar, Ahmedabad, Gujarat.

## 5.4.3. Chemicals and reagents

Felbamate was obtained as a gift sample from Cadila healthcare limited, Ahmedabad, Gujarat, India.

## 5.4.4. Solution preparation

### 5.4.4.1. Preparation of stock solution of FMTE

FMTE (50 mg) was weighed on a precision balance and transferred into a calibrated 50 mL volumetric flask. To it, 20 mL of acetonitrile was added, and the contents were sonicated for 5 min. The volume was made to mark with acetonitrile (HPLC grade) to get a solution having a concentration of 1000 µg/mL.

### 5.4.4.2. Preparation of ammonium Formate buffer (pH=3.7)

Ammonium formate (630 mg) was weighed and transferred into 1000 mL HPLC grade water and mixed thoroughly. Solution was then filtered through a 0.45µ membrane filter under vacuum and the pH was adjusted to 3.7 with formic acid.

### 5.4.4.3. Preparation of diluent

Ammonium formate buffer and acetonitrile were mixed in a ratio of 50:50 (v/v) and sonicated for five minutes to prepare the diluent.

### 5.4.4.4. Preparation of 0.1 N hydrochloric acid

Concentrated hydrochloric acid (0.85 mL) was slowly diluted to 100 mL mark using HPLC grade water in volumetric flask to get 0.1 N hydrochloric acid.

### 5.4.4.5. Preparation of 0.1 N sodium hydroxide

Sodium hydroxide flakes (400 mg) was dissolved with the aid of sonication in 50 mL of HPLC grade water using 100 mL volumetric flask. The volume was made up to mark with HPLC grade water to get 0.1 N sodium hydroxide solution.

### 5.4.4.8. Preparation of 15% hydrogen peroxide

Hydrogen peroxide (15%) was prepared by diluting 5 mL of 30% hydrogen peroxide to 10 mL with water in 10 mL volumetric flask.

## 5.4.5. Forced degradation studies

The forced degradation studies were performed to get substantial degradation of drug. The drug was stressed under conditions viz. acidic, basic, neutral, oxidative, thermal, and photolytic. To get an accurate representation, four samples were prepared under each condition excluding thermal and photolytic; blank under normal condition (blank untreated), blank under stress condition (blank treated), drug solution under normal condition (standard), and drug under the stress condition. For thermal and photolytic conditions, the chromatogram obtained were compared with the chromatogram of drug stored under normal conditions.

### 5.4.5.1. Hydrolytic degradation

The hydrolytic degradation was conducted under acidic, basic, and neutral condition. The stock solution of drug (1 mL) was mixed with 0.1 mL 0.1 N HCl in 10 mL volumetric flask and the solution was kept under stress for 48 h. In order to accelerate the degradation, the study was caried out at 70 ℃ for 7 h using 0.1 N HCl. After the stress period the samples were neutralized by using equal strength of sodium hydroxide and the volume was made to mark with diluent to get a concentration of 100 µg/mL of FMTE. For base and neutral hydrolysis, a similar methodology was used. The samples treated with base were neutralized using corresponding strength of hydrochloric acid. All the samples were analysed using HPLC under optimized chromatographic conditions.

### 5.4.5.2. Oxidative degradation

Stock solution FMTE ( 1 mL) was allowed to mix with 0.1 mL of oxidant (15% hydrogen peroxide) for 48 h in 10 mL volumetric flask. The volume was made up to mark with diluent to get a concentration of 100 µg/mL and samples were analysed using HPLC under optimized chromatographic conditions.

### 5.4.5.3. Thermal degradation

FMTE (100 mg) was sealed in a glass ampoule and heated in an oven at 70 ℃ for 7 hours. After the stress period, the contents of the ampoules were diluted with diluent to get a concentration of 100 µg/mL. In similar fashion, one sample of FMTE was kept at room temperature as control and samples were analysed using HPLC under optimized chromatographic conditions.

#### 5.4.5.4. Photolytic degradation

Photolytic degradation was carried out in solid and liquid state. Two samples were prepared for solid state degradation study. In first case, the drug was spread as a thin layer inside a petri dish and kept in a photostability chamber along with control sample covered with aluminium foil. In the second case, 10 mg of drug was taken into 10 mL volumetric flask and exposed to sunlight for 7 days along with control sample in aluminium foil.

Photolytic degradation in liquid state was carried out by keeping 1 mL stock solution of FMTE in volumetric flask inside a photostability chamber along with a control sample covered using aluminium foil.

The samples that were kept in the photostability chamber were exposed to ICH-mandated dose of light (1.2 million lux H of overall illumination and 200 wh/$m^2$ of integrated near U.V. energy). After the exposure period, the samples were diluted up to the mark to get 100 µg/mL concentration of drug using diluent and analysed using HPLC under optimized chromatographic conditions.

### 5.4.6. Validation studies

The developed and optimized HPLC method was validated as per the relevant ICH guideline.

#### 5.4.6.1. Specificity and selectivity

The specificity of the HPLC method was ascertained by the resolution values obtained between the nearest eluting peaks of degradation product and peak of drug and degradation product. The method's selectivity for the individual component was done through the % peak purity value obtained through the data acquisition software. The degradation samples were mixed in equal proportion and injected into HPLC.

#### 5.4.6.2. Linearity and range

A series of dilutions (7 levels) were prepared in range of 20-120 µg/mL. At each level the sample was injected in triplicate, and the average area was obtained. The average area was plotted against the concentration to obtain a simple linear regression equation and the correlation coefficient. Five incremental concentrations (20, 40, 50, 60, 80, 100 and 120 µg/mL) were prepared by accurately withdrawing 0.2, 0.4, 0.5, 0.6, 0.8, 1.0 and 1.2 mL of

stock solution of FMTE (1000 µg/mL) and diluting it to 10 mL using diluent in a volumetric flask.

#### 5.4.6.3. Accuracy

The accuracy of the HPLC method was determined by the standard addition method. The degraded sample was spiked at 80%, 100%, and 120% of the target assay concentration (50 µg/mL) with standard drug solution. At each level, the sample was injected in triplicate, and the average % recovery was computed. Spiked samples were prepared by accurately transferring 0.4, 0.5 and 0.6 mL of stock solution of FMTE to degraded sample and making the volume to 10 mL.

#### 5.4.6.4. Precision

Precision (intra and inter) of the HPLC method was done at 40, 80, and 120 µg/mL. At each level, the sample was injected in triplicate, and the % relative standard deviation was determined (% RSD). Three incremental concentrations (40, 80, and 120 µg/mL) were prepared by accurately withdrawing 0.4, 0.8, and 1.2 mL of stock solution of FMTE (1000 µg/mL) and diluting it to 10 mL using diluent in a volumetric flask.

### 5.4.7. *In-silico* studies

The *in-silico* studies were done using open-source options like the pkCSM webserver, ToxTree and OSIRIS property explorer.

The structures of the degradation products were sketched using Marvin by ChemAxon. The structures were copied as smiles and fed into the pkCSM webserver. ADMET prediction mode was selected which uploads the task for processing.

Toxtree accepts the structure in the form of SMILES which were generated similarly as discussed above. The decision tree (In vitro mutagenicity (Ames test) alerts by ISS) was selected from the method tab, and the estimate button was clicked.

OSIRIS property explorer accepts SMILES or CAS no as input and runs predictions.

# Chapter 6

# Characterization and *in-silico* toxicity prediction of degradation products of haloperidol

## 6.0. Introduction

Haloperidol is an official in the USP-NF, British, European, and Indian pharmacopoeia (IP) [89-90]. Its drug Profile is also available in Clark's analysis of drugs and poisons.

Haloperidol is a neuroleptic drug that is used to treat psychotic disorders, prophylaxis of nausea and vomiting, and postoperative recovery[91-92].

The work presented herein focuses on the following objectives:

1. Conduct of forced degradation studies on haloperidol as per the ICH-mandated stress conditions.
2. Development of a stability-indicating assay method (SIAM) for haloperidol.
3. Validation of the SIAM as per the ICH guidelines.
4. Structural characterization of the degradation products by liquid chromatography coupled with mass and tandem mass spectrometry.
5. Prediction of absorption, distribution, metabolism, excretion, and toxicity (ADMET) profile using *in-silico* studies.

# 6.1. Drug profile[52]

## 6.1.1 Haloperidol (HALO)

**Chemical structure:**

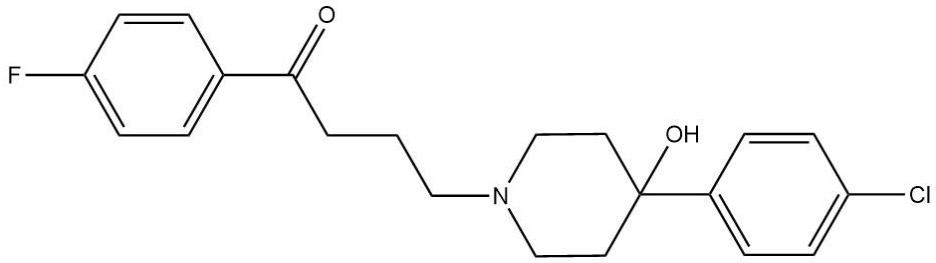


**IUPAC name:** 4-[4-(4-Chlorophenyl)-4-hydroxypiperidin-1-yl]-1-(4-fluorophenyl) butan-1-one

**Molecular formula:** $C_{21}H_{23}CIFNO_2$

**Melting point:** 148-149℃

**pKa:** 8.3

**LogP:** 3.23

**Description:** White or almost white powder

**Solubility:** Water solubility (1.4mg/100mL); freely soluble in methanol, chloroform, benzene, acetone, and dilute acids

**Drug category:** Neuroleptic

**Listed impurities of HALO in monograph:** USP-NF, BP

A. 1-(4-flurophenyl)-4-(4-hydroxy-4-phenylpiperidin-1yl)butan-1-one.

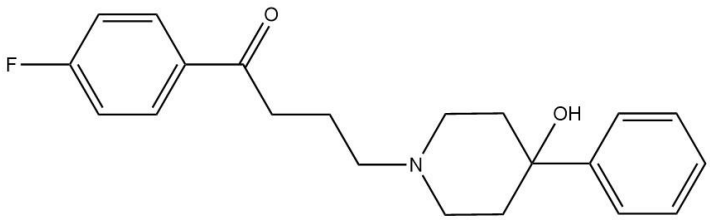


B. 4-[4-(4-chlorophenyl)-4-hydroxypiperidin-1-yl]-1-(2-flurophenyl)butane-1-one.

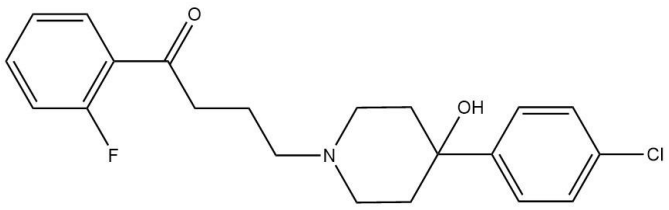


C. 4-[4-(4-chlorophenyl)-4-hydroxypiperidin-1-yl]-1-(3-ethyl-4-flurophenyl)butane-1-one.

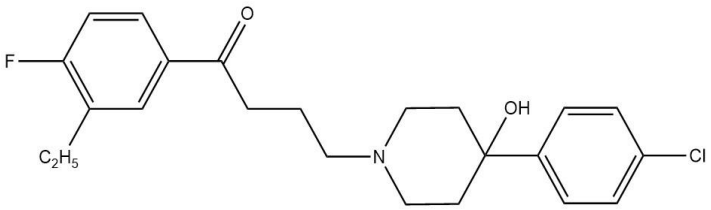


D. 4-[4-(4-chlorphenyl)-4-hydroxypiperidin-1yl]-1-[4-{4-(4-chlorophenyl)-4-hydroxypiperidin-1-yl} phenyl]butan-1-one.

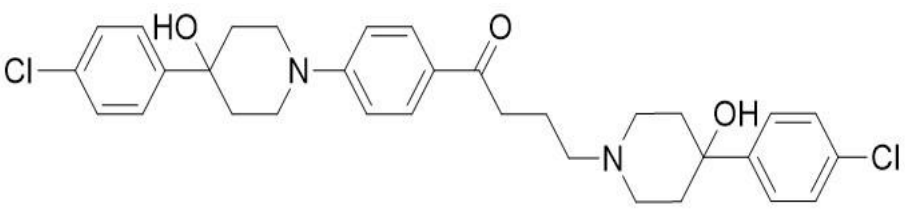

E. 4-[4-(4'-chlorophenyl)-4-hydroxypiperidin-1-yl]-1-(4-flurophenyl)butane-1-one.

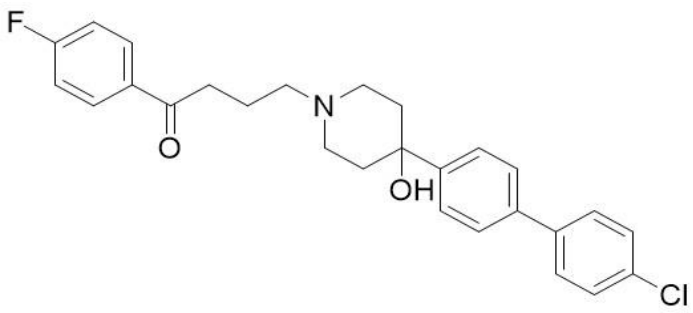


F. 4-[4-(3'-chlorobiphenyl-4-yl)-4-hydroxypiperidin-1-yl]-1-(4-flurophenyl)butan-1-one.

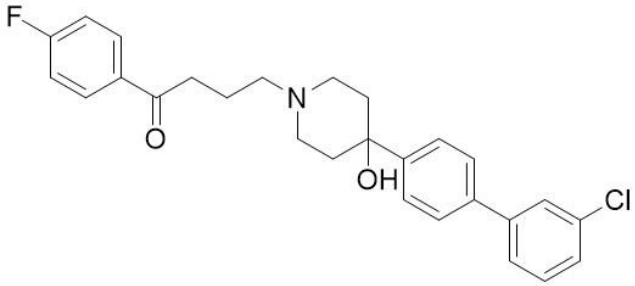


**Clinical pharmacology:**

HALO shows antipsychotic activity by antagonizing the D2 receptor in the mesolimbic and the mesocortical areas of the brain.

Schizophrenia is a mental disorder caused due to imbalance of neurotransmitter in the brain (hyper-dopaminergic state) in the limbic system of the brain. HALO improves the psychotic symptoms (delusions and hallucination) by thwarting the production of dopamine and restoring balance. HALO is also known for anti-emetic activity which is due to the blockage of the D2 receptor in the chemoreceptive trigger zone[93-94].

**Pharmacokinetics:**

HALO undergoes transformation *in-vivo* to form various metabolites like; 4-(4-chlorophenyl)-4-hydroxypiperidine, p-fluorobenzoylpropionic acid, reduced haloperidol (major metabolite), haloperidol glucuronide and pyridinium metabolites.

CYP3A4, CYP2D6, uridine di-phosphoglucose glucuronosyltransferase are involved in the biotransformation of HALO. Its clearance is by glucuronidation and formation of reduced HALO which is devoid of any biological activity[95-96].

**Toxicity:**

Sparse incidents of QT interval extension, sudden death and torsades de pointes (TdP) have been reported for HALO. More commonly observed contraindications of HALO is hypersensitivity, Parkinson disease, severe central nervous system depression and coma. HALO can also cause dysphoria which is a condition characterized by a sense of dissatisfaction, distress and general uneasiness[92-93, 97].

## 6.2. Literature survey

A detailed literature survey was carried out to find out the various physiochemical properties and the analytical method available for HALO. The physiochemical properties have been discussed under the preceding section 6.1. HALO is an official drug in USP-NF, British pharmacopoeia (BP), EP, and the Indian pharmacopoeia (IP). They all used a similar method for the identification of related substances comprising of 50mM solution of tetrabutylammonium hydrogen sulphate and acetonitrile in gradient elution on a C18 column.

Literature also revealed a few HPLC method for estimation of HALO in dosage forms as a single entity or in combination with other active pharmaceutical ingredients and biological fluids.

All the reported methods used a C18 column for separation. The buffer used varied depending upon the purpose of the analytical method. The bioanalytical methods, especially those conjugated with mass spectrometry used volatile buffer like ammonium formate with pH mostly adjusted between 3 to 7.

However, none of the methods have systematically carried out stability testing of HALO under ICH-mandated stress conditions, structural characterization of DPs by mass and tandem mass spectrometry, and *in-silico* ADMET studies of DPs.

A summary of the available methods is seen in the table 6.2.1.

**Table 6.2.1:** Summary of the HPLC methods available for determination of HALO by HPLC

| Sr.No | Type of method | Column type | Mobile Phase composition | Flow rate | Detector used | References |
|---|---|---|---|---|---|---|
| **1** | **USP-NF, British and European Pharmacopoeia (related substance method)** | | | | | |
| | HPLC | Base deactivated (BDS) endcapped C18, 150×4.6mm, 3µm | Tetrabutylammonium hydrogen sulfate (50mM) [A]: Acetonitrile[B], $T_{(min)}$/A:B= $T_0$/90:10; $T_2$/90:10; $T_{17}$/50:50; $T_{22}$/50:50 | 1.5 mL/min | UV,230 | 50,51,90 |
| **2** | **Indian Pharmacopoeia (related substance method)** | | | | | |
| | HPLC | Base deactivated (BDS) endcapped C18, 150×4.6mm, 3µm | Tetrabutylammonium hydrogen sulfate (50mM) [A]: Acetonitrile[B], $T_{(min)}$/A:B= $T_0$/90:10; $T_{15}$/50:50; $T_{20}$/50:50; $T_{25}$/90:10 | 1.5 mL/min | UV,230 | 89 |
| 3 | **Title: Development and validation of stability indicating assay method of Haloperidol in Oral Solution** | | | | | |
| | HPLC | Restek Pinnacle II C18, 250 ×4.6mm, 5µ | Methanol: Tetrabutyl aamonium hydrogen sulphate (55:45, v/v) | 1ml/min | UV, 254nm | 98 |
| 4 | **Title: Stability indicating method development and validation for the determination of haloperidol and benzhexol by RP-HPLC** | | | | | |
| | HPLC | Kromasil C18, 250×4.6mm, 5µ | OPA: Acetonitrile (48:52, v/v) | 1.0ml/min | UV, 210nm | 99 |

**Table 6.2.1:** Summary of the HPLC methods available for determination of HALO by HPLC (*Conti…*)

| Sr.No | Type of method | Column type | Mobile Phase composition | Flow rate | Detector use | References |
|---|---|---|---|---|---|---|
| | **Title: Determination of haloperidol and its reduced metabolite in human plasma by liquid chromatography-mass spectrometry with electrospray ionization** | | | | | |
| | LC-MS | Nucleosil C18, 150×1mm | 2mM Ammonium formate(pH 3.0): Acetonitrile(55:45,v/v) | -- | MS | 91 |
| 5 | **Title: Development and validation of a new HPLC method for in-vitro studies of Haloperidol in solid lipid nanoparticles** | | | | | |
| | HPLC | Cosmosil C18 , 250×4.6mm, 5µ | Potassium dihydrogen phosphate:Acetonitrile:TEA(10:90:0.1, v/v/v) | 2ml/min | UV,230nm | 100 |
| 5 | **Title: Rapid determination of haloperidol and its metabolites in human plasma by HPLC using monolithic silica column and solid-phase extraction** | | | | | |
| | HPLC | Chromolith Performance C18, 100 ×4.6mm, 5µ | 100 mM Sodium phosphate(pH 3.5): Acetonitrile(80:20, v/v) | 2mL/min | UV,230nm | 101 |
| 6 | **Title: High-performance liquid chromatographic method with diode array detection for quantification of haloperidol levels in schizophrenic patients during routine clinical practice** | | | | | |
| | HPLC | Thermo C18 column | Water(pH 2.5 with 0.1% acetic acid): Acetonitrile(50:50,v/v) | 1.6mL/min | UV, 240nm | 102 |
| 7 | **Title: Determination of haloperidol in biological samples with the aid of ultrasound-assisted emulsification microextraction followed by HPLC-DAD** | | | | | |
| | HPLC | Capital C18 column,250×4.6mm, 5µ | 20 mM monobasic potassium phosphate(pH 4):methanol(60:40,v/v) | -- | UV,264nm | 103 |

# 6.3. Present work and discussion

## 6.3.1. Development of HPLC method to monitor the drug degradation behaviour of HALO

### 6.3.1.1. Selection of chromatographic methods

All the published HPLC methods for HALO use RPC approach for detection and quantification of HALO. Due to this, it was decided to develop the HPLC method using RPC approach.

### 6.3.1.2. Selection of stationary phase

The compendial method depicted under monograph and other reported methods for HALO were developed using C18 column as stationary phase. Hence, preference was shown towards HiQsil C18 column (250 × 4.6mm, 5µm) due to availability.

### 6.3.1.3. Selection of wavelength of analysis

During the initial scouting runs, the diode array detector (DAD) was set to scan the entire UV range (200-400nm) to determine the wavelength of maximum absorbance ($\lambda_{max}$) of HALO. The UV spectrum obtained is depicted in figure 6.3.1.3.1. The UV spectrum showed a wavelength maximum at 246nm. Hence, 246nm was selected for further analysis.

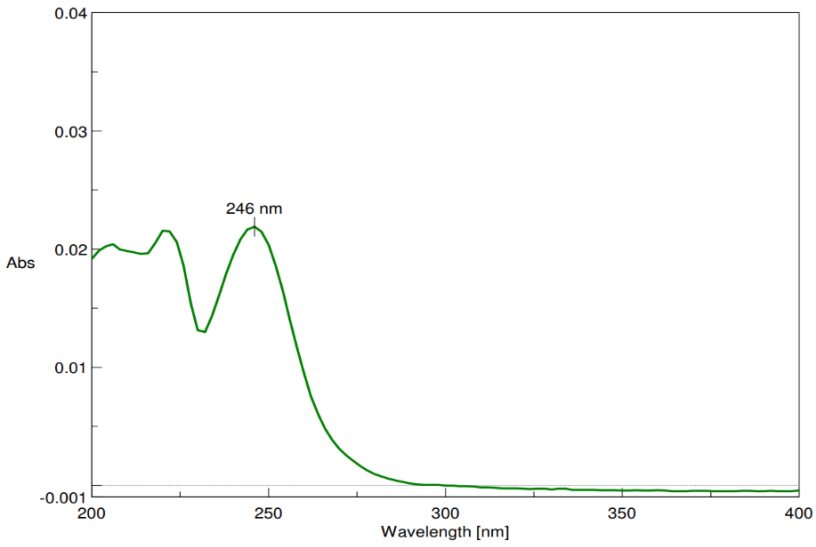


**Figure 6.3.1.3.1:** UV spectrum of HALO having concentration (10 µg/mL in acetonitrile)

### 6.3.1.4. Selection and optimization of mobile phase for monitoring degradation of HALO

The objectives of the HPLC method development were to develop a simple, robust, isocratic, mass friendly HPLC method with capacity factor (*k'*) value in-between 4-10. The compendial methods used gradient elution mode comprising of 50mM tetra butyl ammonium hydrogen sulfate (TBAHS) with acetonitrile as mobile phase. Other reported methods mostly used phosphate buffer (3.5-4 range) for estimation of HALO in formulation while the volatile buffers like acetic acid (pH 2.5) and ammonium formate (pH 3) were used for bioanalytical methods.

The pKa of HALO is 8.3. The acidic pH converts HALO into ionized form. Hence, it was decided to carry out trials with the buffer maintained in acidic pH. Ammonium formate (10mM, pH adjusted to 3.7 with formic acid) was used along with acetonitrile in isoractic elution mode.

The preliminary trial was taken on HiQsil C18 column (250 × 4.6mm, 5µm) using the ammonium formate buffer (10mM, pH adjusted to 3.7 with formic acid) and acetonitrile in ratio of 40:60 (v/v). This trial yielded a chromatogram seen in figure 6.3.1.4.1.

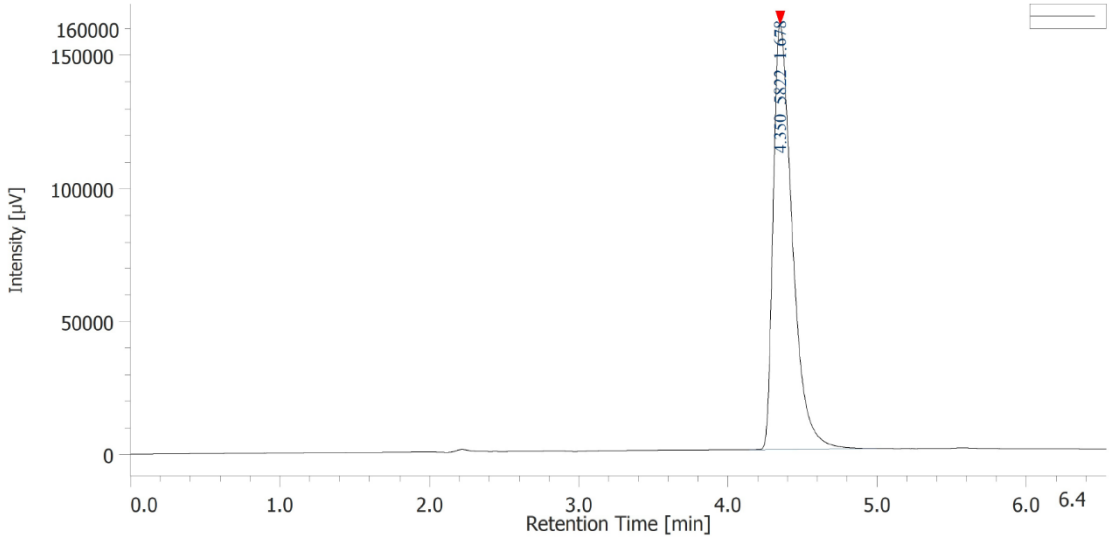


**Figure 6.3.1.4.1: Chromatogram of HALO (10µg/mL)** (Mobile phase, acetonitrile: ammonium formate buffer (pH 3.7, adjusted with formic acid), 60:40 v/v; flow rate: 1mL/min; wavelength: 246nm; Column: HiQsil C18 column (250 × 4.6mm, 5µm))

The $t_R$ for HALO was 4.3 min with NTP>2000, symmetry < 2.0 and $k'$ = 1.0. Hence, further trials were taken by systematically decreasing the strength of the organic phase to obtain the desired retention of the drug.

Decreasing the composition of acetonitrile to 40 % resulted in the retention time for HALO of 10.4 min, NTP > 2000, $k'$ = 3.7. This trial resulted in increasing peak symmetry > 2. The chromatogram obtained is seen in figure 6.3.1.4.2.

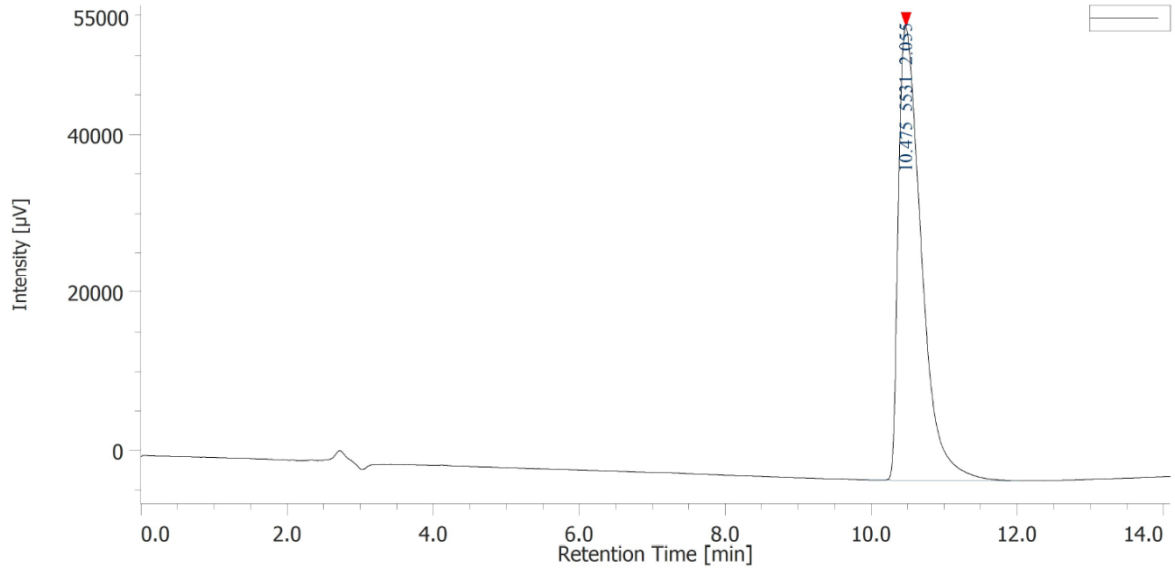


**Figure 6.3.1.4.2: Chromatogram of HALO (10µg/mL)** (Mobile phase, acetonitrile: ammonium formate buffer (pH 3.7, adjusted with formic acid), 40:60 v/v; flow rate: 1mL/min; wavelength: 246nm; Column: HiQsil C18 column (250 × 4.6mm, 5µm))

It's often observed that HPLC columns use stationary phases with significant silanol activity. Silanol activity can be reduced by using the columns designed for basic samples (base deactivated columns [BDS]) or by using higher buffer concentration ( >10mM). Band tailing can also be controlled by addition of an organic modifies like triethylamine (TEA). TEA behaves like a competing base reducing the availability of free silanols to interact with analyte of interest. However, the TEA concentration should be kept as low as possible because higher concentration significantly increases the equilibration time and is difficult to wash off from the columns[42,104-106].

Before procuring a BDS column other approaches to reduce tailing were deliberated like increasing buffer concentration and using organic modifier. Increasing the concentration of buffer was ruled out as recommended buffer concentration for mass spectrometry is 1-10

mM[44]. Hence, use of organic modifier was considered. Trial was taken by using ammonium formate buffer (pH 3.7), acetonitrile and TEA in the ratio of 60:40:0.1 (v/v/v). The chromatogram obtained is seen in figure 6.3.1.4.3.

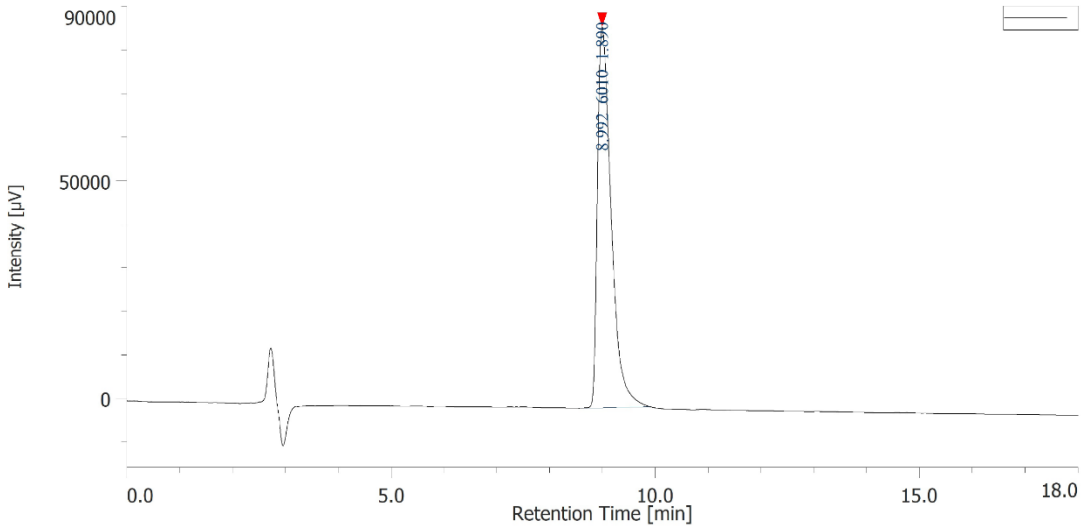


**Figure 6.3.1.4.2: Chromatogram of HALO (10µg/mL)** (Mobile phase, acetonitrile: ammonium formate buffer (pH 3.7, adjusted with formic acid), TEA 40:60:0.1(v/v/v); flow rate: 1mL/min; wavelength: 246nm; Column: HiQsil C18 column (250 × 4.6mm, 5µm))

The above trial resulted in retention time of 8.9 min for HALO, NTP > 2000 and peak symmetry value < 2. It was observed that addition of TEA was effective in curtailing band tailing. This method was adopted to monitor the drug degradation behaviour.

The summary of the chromatographic conditions to monitor the drug degradation behaviour was.

**Mobile phase:** acetonitrile: ammonium formate buffer (pH=3.7, adjusted with formic acid), TEA 40:60:0.1(v/v/v).

**Column:** HiQsil C18 column (150 × 4.6mm, 5µm).

**Wavelength:** 246 nm.

**Flow rate:** 1mL/min.

## 6.3.2. Forced degradation studies

The stability of the drug was probed as per the guidance provided in the ICH Q1A(R2) guideline. The drug was tested under hydrolytic (acidic, basic, and neutral), oxidative, thermal, and photolytic conditions. The stressed samples were subjected to HPLC analysis using optimized chromatographic conditions, and the chromatogram obtained was compared with blank stored under normal condition (blank untreated), blank subjected to stress conditions like the drug (blank treated), and the drug solution stored under normal condition (standard untreated)

### 6.3.2.1. Hydrolytic degradation

Hydrolytic degradation was performed using acidic, basic, and neutral conditions. The degradation studies were carried out at room temperature in order to get desired degradation of the drug. The degradation studies were also carried out at higher temperature ( 70 ℃, 7 h), in case, no degradation was observed at room temperature. The concentration of the stressors was also optimized from low to high depending upon the degradation behaviour of the drug. Periodically, samples were withdrawn, neutralized, and diluted to the desired concentration and injected into HPLC using optimized chromatographic conditions.

**Acid degradation**

Acid degradation was carried out at room temperature by exposing drug solution to 0.1 N /1 N HCl for 48 hours in a volumetric flask to get desired degradation of the drug. The studies were repeated using 1 N HCl at 70℃ for 7 hours since no degradation was observed at room temperature. After applying the stress conditions, the samples were neutralized by using equal strength of base (NaOH). The neutralized samples were diluted to get the desired concentration and injected into HPLC using optimized chromatographic conditions.

The drug showed resilience to degradation under acidic conditions and hence, no degradation was observed.

**Base degradation**

Base degradation was carried out at room temperature by exposing drug solution to 0.1 N /1 N NaOH for 48 hours in a volumetric flask to get desired degradation of the drug. The studies were repeated using 1 N NaOH at 70℃ for 7 hours since no degradation was observed at room temperature. After applying the stress conditions, the samples were neutralized by

using equal strength of acid (HCl). The neutralized samples were diluted to get the desired concentration and injected into HPLC using optimized chromatographic conditions.

The drug showed resilience to degradation under basic conditions and hence, no degradation was observed.

**Neutral degradation**

Neutral degradation was carried out at room temperature by exposing drug solution to water for 48 hours in a volumetric flask to get desired degradation of the drug. The studies were repeated by heating the drug solution with water at 70℃ for 7 h since no degradation was observed at room temperature. Samples were diluted to get the desired concentration and injected into HPLC using optimized chromatographic conditions.

The drug showed resilience to degradation under neutral basic condition and hence, no degradation was observed.

**6.3.2.2. Oxidative degradation**

Oxidative degradation was carried out by stressing HALO in presence of 15% $H_2O_2$ at room temperature for 48 h. After the stress period, diluent was added to get the required concentration and the sample analysed by HPLC. HALO degraded (~ 38%) to form a single degradation product (DP1) with $t_R$ of 11.1 min. The drug was further stressed by heating with 15% $H_2O_2$ at 70℃. In 2 h, there was formation of another degradation product (DP2) with $t_R$ of 13.3 along with DP1. The peak area for DP1 was significantly higher than DP2 indicating that DP1 is easier to form. The chromatogram obtained of the oxidative stress sample (15% $H_2O_2$ , 70℃ for 2 h) is seen in figure 6.3.2.2.1. All the peaks were well separated in the developed HPLC method with resolution $R_s$ > 1, hence, no further modification was required in the developed HPLC method.

To ascertain the identity of the degradation products the UV spectra of the degradation products acquired using the DAD detector were overlain with that of the drug. The UV spectra of the degradation product were found to be identical to the drug indicating close resemblance among the drug and DPs. The overlain spectra is seen in figure 6.3.2.2.2.

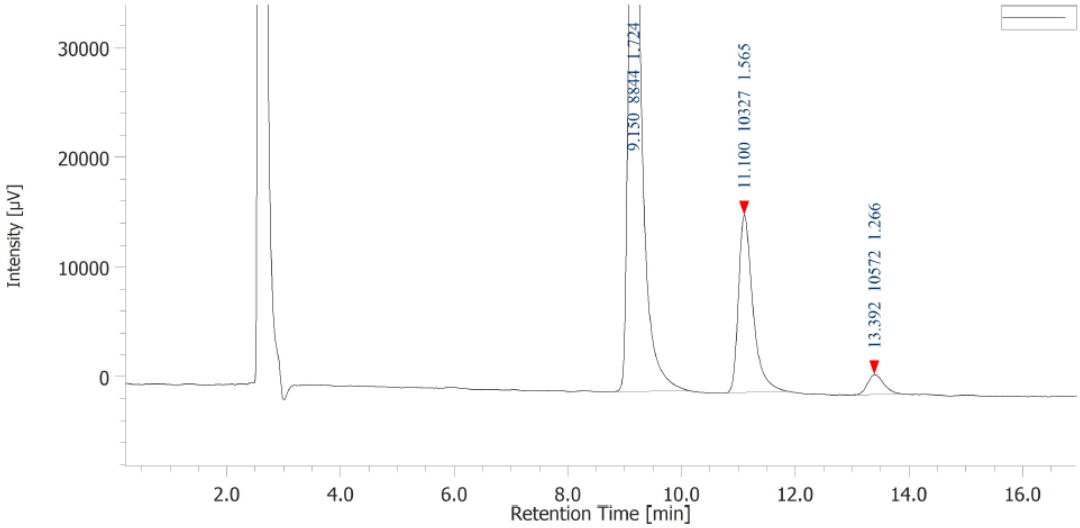


**Figure 6.3.2.2.1: Chromatogram of HALO (100 µg/mL) treated with 15% $H_2O_2$ at 70°C for 2h. (**Mobile phase, acetonitrile: ammonium formate buffer (pH 3.7, adjusted with formic acid), TEA 40:60:0.1(v/v/v); flow rate: 1mL/min; wavelength: 246nm; Column: HiQsil C18 column (250 × 4.6mm, 5µm))

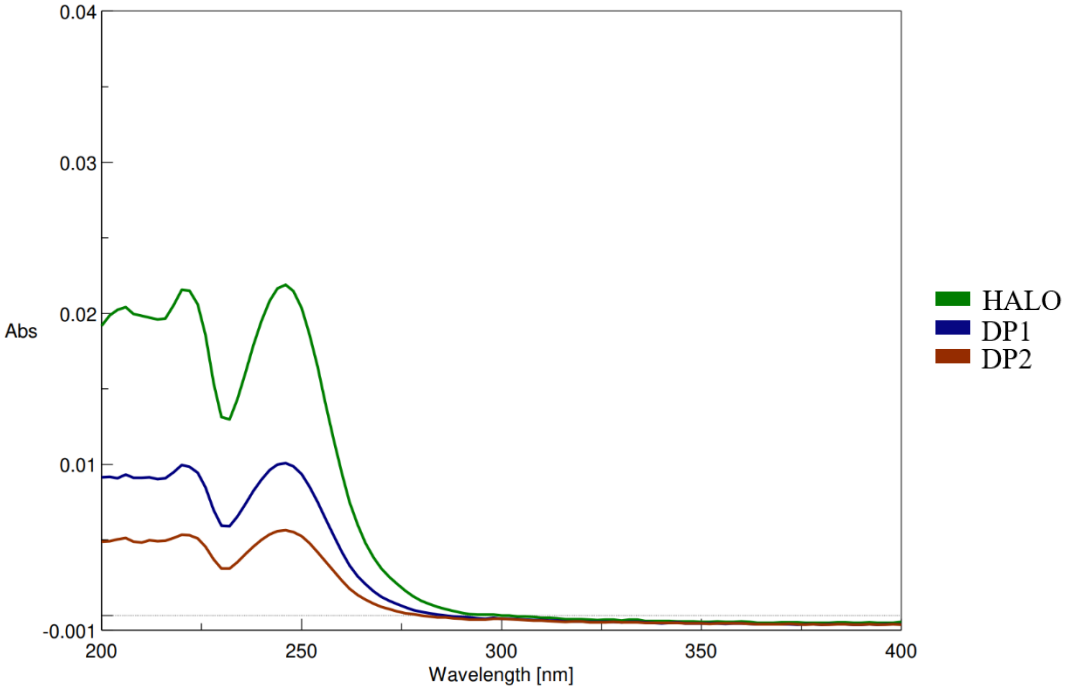


**Figure 6.3.2.2.2:** Overlain of UV spectra of HALO with its DPs

#### 6.3.2.3. Thermal degradation

Thermal degradation was carried out by exposing the drug stock solution in sealed ampoule to dry heat at 70 ℃ for 7 days using hot air oven. A control sample was maintained by placing drug into a separate glass ampoule stored at room temperature. After the stress period, the sample was diluted with diluent to get the desired concentration and injected into HPLC using optimized chromatographic conditions.

The drug did not show degradation under thermal conditions.

#### 6.3.2.4. Photolytic degradation

Photolytic degradation studies were carried out in the liquid state using photostability chamber. Stress studies were carried out by placing drug solution inside a volumetric flask. Samples were exposed to ICH Q1B mandated dose of light. In addition, photolytic stress studies were also carried out by exposing the drug solution placed inside a volumetric flask to sunlight for 7 days.

The chromatogram obtained from photolytic stressed samples did not show degradation.

### 6.3.3. Validation of developed Stability indicating assay method (SIAM)

HPLC method validation is required to ensure that the method achieves an adequate standard of specificity, accuracy, and precision. The developed SIAM was validated as per the guidance of the ICH Q2 guideline. The parameters considered during the validation process is summarized in table 6.3.3.1.

#### 6.3.3.1. Specificity and selectivity

The specificity of the HPLC method was expressed in terms of resolution between the closely eluting peaks. It is evident from figure 6.3.2.2.1. that the peaks were well resolved with a resolution value greater than one which confirms the specificity of the method. The method's selectivity was determined by measuring % peak purity value acquired using data acquisition software. The peak purity(%) was > 99% which indicates that the method is selective.

**Table 6.3.3.1:** Validation parameters and acceptance criteria

| Sr.No. | Validation Parameters | Acceptance Criteria |
|---|---|---|
| **1** | **Specificity** | Resolution > 1 |
| **2** | **Selectivity** | Peak purity (%) > 99 |
| **3** | **Linearity** | Correlation coefficient not less than 0.999 |
| **4** | **Accuracy (across the specified range)** | Recovery (%) between 98.0 to 102% |
| **5** | **Precision (intra day & inter day)** | RSD (%) of replicate injections not more than 2.0 |
| **6** | **Robustness** | 1) Resolution between adjacent peak should not be less than 1.0<br>2) Numbers of theoretical plates of analyte peak should not be less than 2000.<br>3) Asymmetry of peak should not be more than 2.0 |

### 6.3.3.2. Linearity and range

The linearity was established in triplicate by taking five incremental concentrations in a range of 10-110 µg/mL. The graph plotted between the average area under peak v/s concentration. The data obtained was subjected to regression analysis. The calculated value of the corelation coefficient ($r^2$) was 0.999. The linearity plot and the data pertaining to linearity is given in figure 6.3.4.2.1 and table 6.3.1.2.1. The representative chromatogram at each concentration level is seen in figure 6.3.4.2.2.

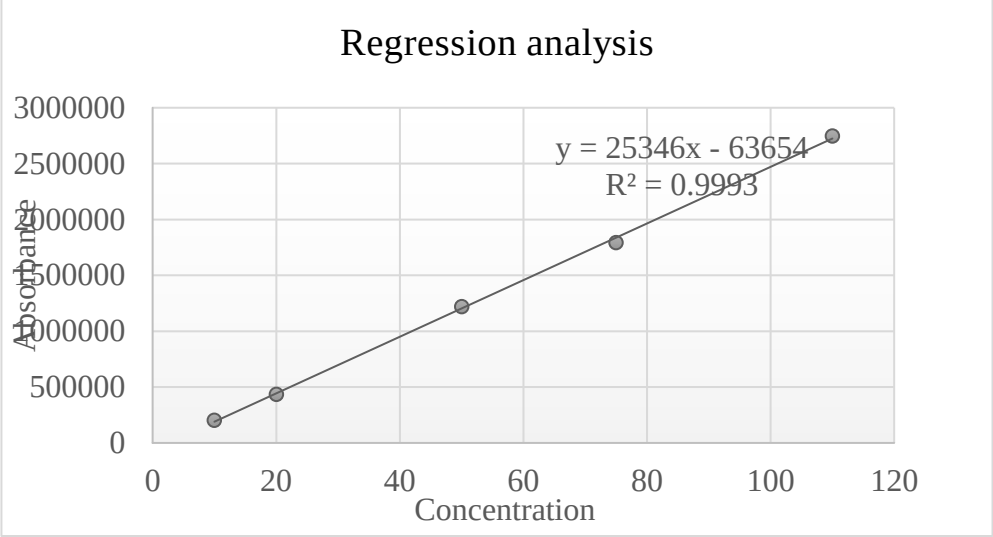


**Figure 6.3.4.2.1:** Linearity graph of HALO

**Table 6.3.3.2.1:** Linearity data for HALO

| Sr. No. | Concentration (µg/mL) | Peak area | | | | RSD(%) |
|---|---|---|---|---|---|---|
| | | Injection 1 | Injection 2 | Injection 3 | Average | |
| 1 | 10 | 204853 | 201693 | 202412 | 202986 | 0.8 |
| 2 | 20 | 430231 | 441796 | 433413 | 435147 | 1.3 |
| 3 | 50 | 1241625 | 1215076 | 1204771 | 1220491 | 1.5 |
| 4 | 75 | 1793498 | 1787507 | 1791607 | 1791607 | 0.1 |
| 5 | 110 | 2788007 | 2721324 | 2735129 | 2748153 | 1.2 |

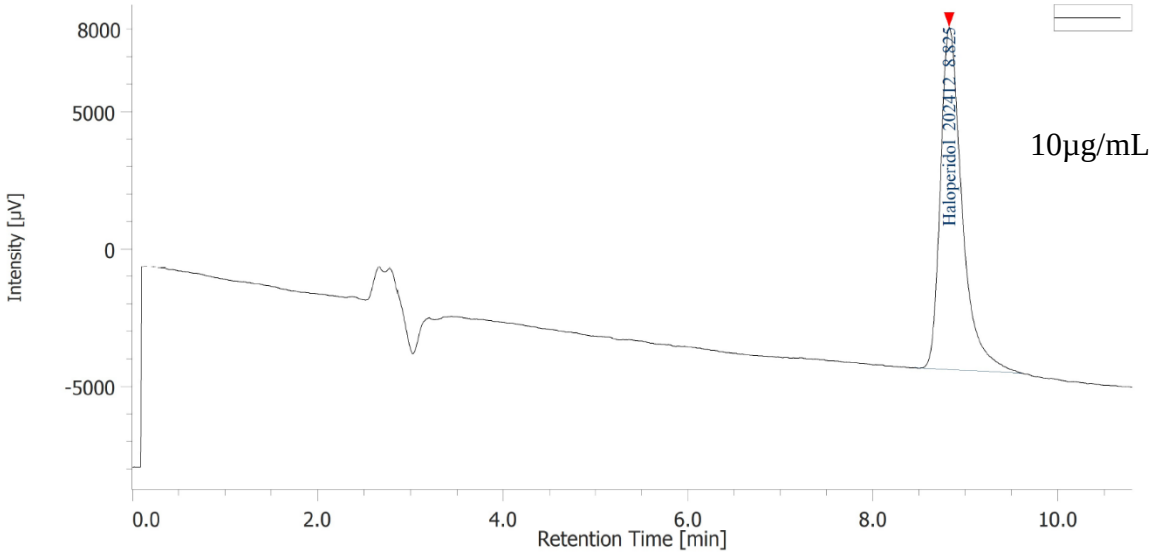


**Chromatogram no 1**

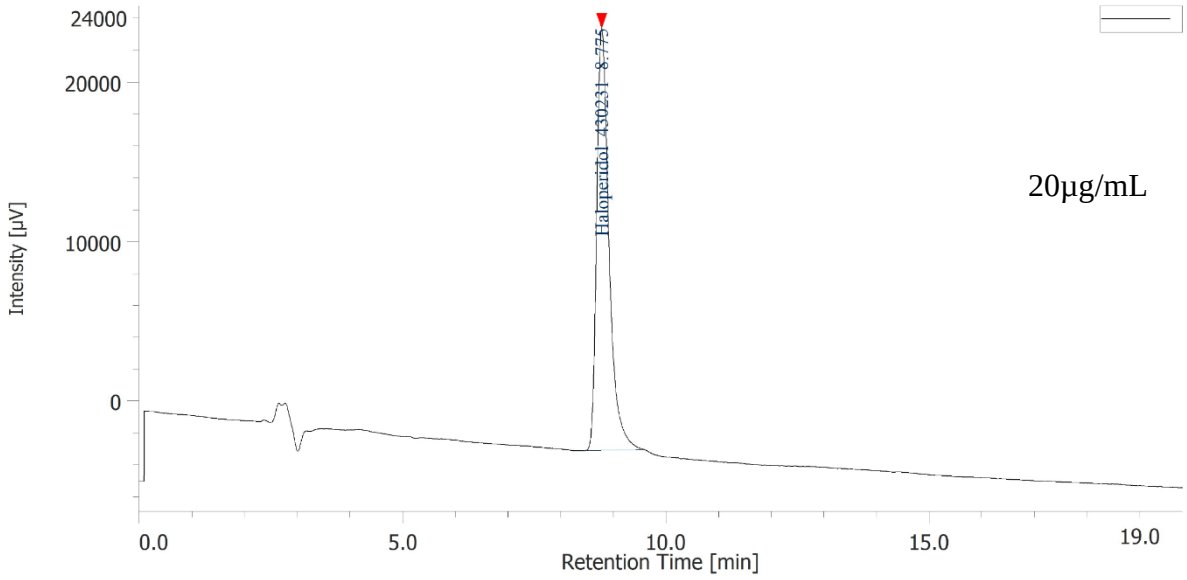


**Chromatogram no 2**

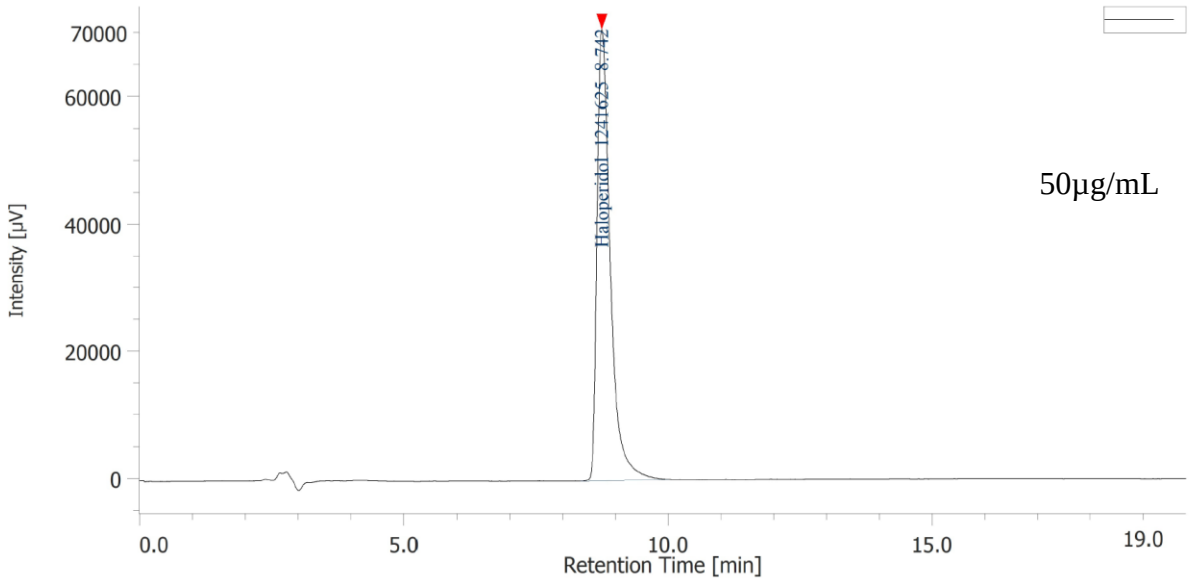


**Chromatogram no 3**

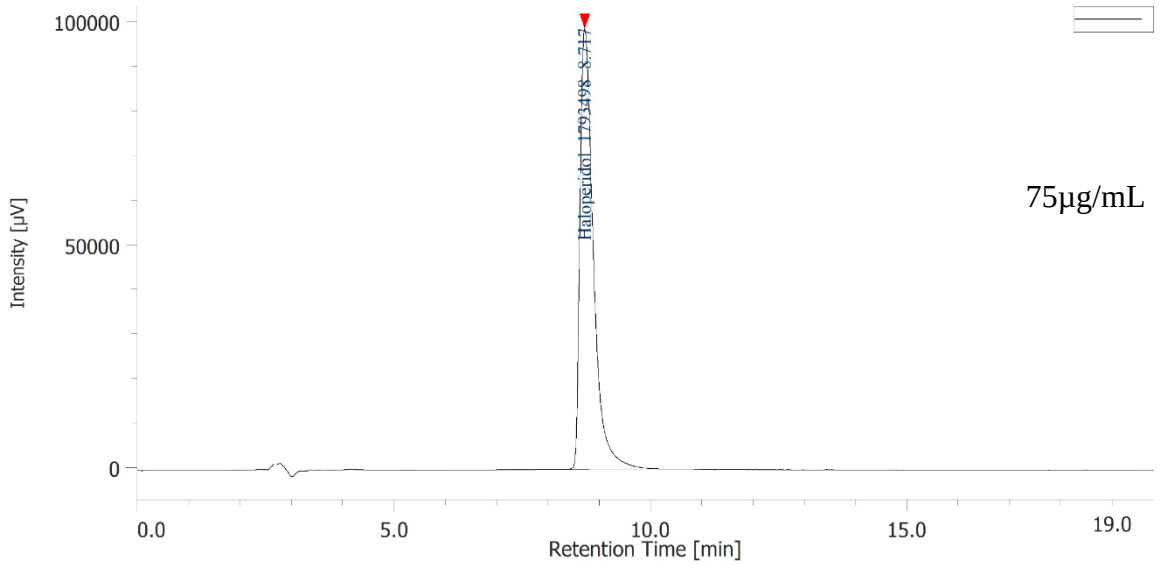


**Chromatogram no 4**

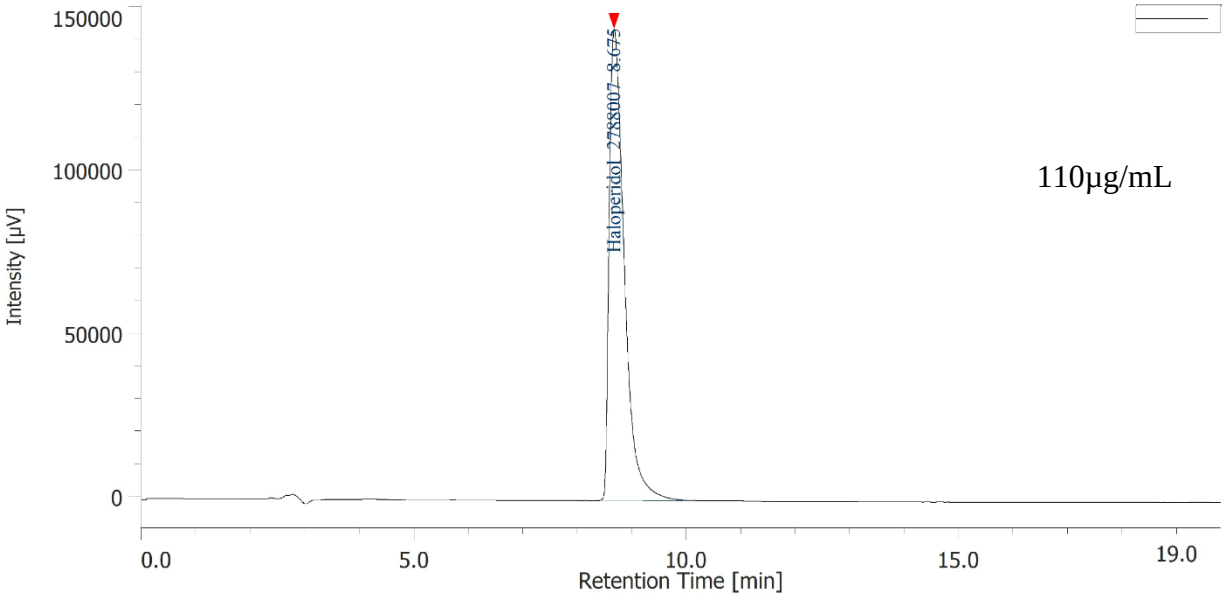


**Chromatogram no 5**

**Figure 6.3.3.2.2:** Representative chromatograms at concentration level 10, 20, 50, 75 and 110 µg/mL

### 6.3.3.3. Accuracy

The accuracy was expressed in terms of recovery (%) of the spiked standard drug and was done by the standard addition method. The stressed sample were separately spiked with standard drug with concentrations 40 µg/mL (80%), 50 µg/mL (100%) and 60 µg/mL (120%) of the target assay concentration (50 µg/mL) and injected in triplicate. The average recovery at each level was between 98 to 102 %, with the mean recovery of 100.1 %. The data of recovery studies is shown in table 6.3.3.3.1.

**Table 6.3.3.3.1:** Recovery studies for HALO (n=3)

| Spiked drug concentration (µg/mL) | Recovered concentration (µg/mL) ±S. D, %RSD, n=3 | Recovery (%) |
|---|---|---|
| 40 | 40.4 ± 0.26, 0.6 | 101 |
| 50 | 49.7 ±0 .34,0.6 | 99.5 |
| 60 | 59.9 ± 0.91,1.52 | 99.9 |

The representative chromatogram obtained at each level of accuracy study is shown in figure 6.3.4.3.1.

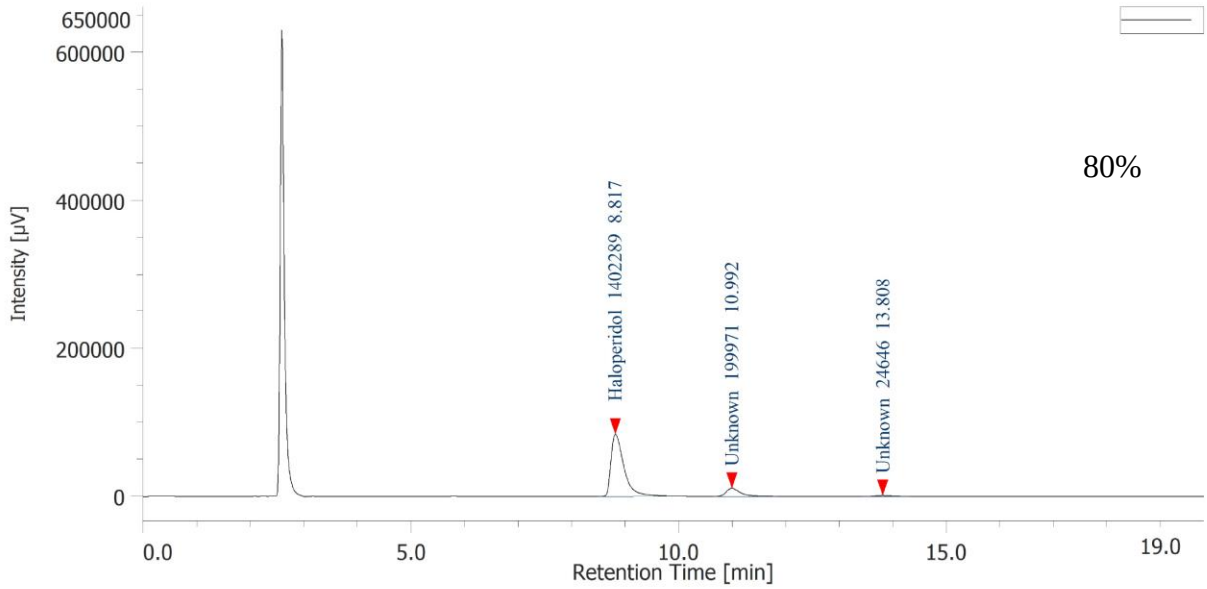


**Chromatogram no 6**

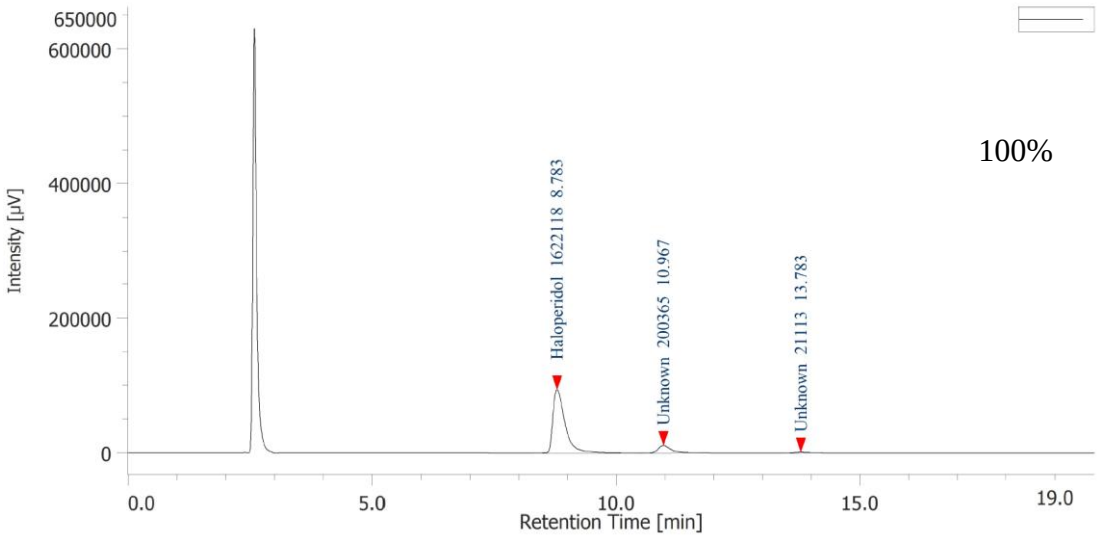


**Chromatogram no 7**

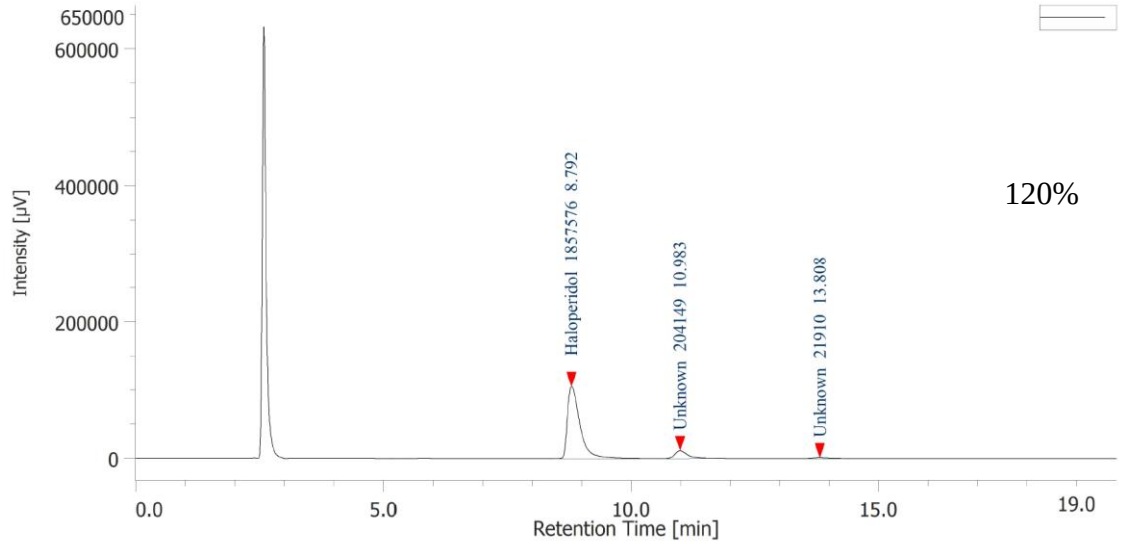


**Chromatogram no 8**

**Figure 6.3.3.3.1:** Representative chromatograms obtained at each level of accuracy studies at 80%, 100% and 120%

### 6.3.3.4. Precision

Intraday and inter-day precision studies were carried out at 3 concentration levels. 10,50, and 75 µg/mL in triplicate. The % RSD at each level was found to be < 2% inferring that the method was precise.

**Table 6.3.3.4.1:** Precision data obtained during intra-day and inter-day studies

| Concentration (µg/mL) | Intraday (n=3) Mean peak area ± SD; %RSD | Inter-day (n =3) Mean peak area ± SD; %RSD |
|---|---|---|
| 10 | 202986 ± 1656, 0.8 | 203815 ± 2310,1.1 |
| 50 | 1220491 ± 19014, 1.6 | 1223161 ± 20765, 1.7 |
| 75 | 1791607 ± 3555, 0.2 | 1782827 ± 8952, 0.5 |

### 6.3.3.5. Robustness.

The robustness of the HPLC method was established to understand the HPLC methods tolerance to deliberate change in the chromatographic parameters. For this purpose, the following changes were carried out to observe its effect on the developed method.

1) The pH of the mobile phase (±0.5 of the optimized value.)
2) Flow rate (±0.2ml of the optimized flow rate)
3) Mobile phase composition (±2% of the optimized ratio)
4) Wavelength (±3 units of the optimized wavelength)

The results of the robustness studies are depicted in the tables below.

**Table 6.3.3.5.1:** Data pertaining to robustness studies

| Peak | Theoretical plates | Peak asymmetry | Resolution |
|---|---|---|---|
| **pH 3.2** | | | |
| HALO | 7606 | 1.8 | 5.0 |
| DP1 | 9700 | 1.5 | 5.4 |
| DP2 | 9005 | 1.1 | -- |
| **pH 4.2** | | | |
| HALO | 7557 | 1.7 | 5.1 |
| DP1 | 9755 | 1.3 | 5.3 |
| DP2 | 7873 | 1.4 | -- |

| Peak | Theoretical plates | Peak asymmetry | Resolution |
|---|---|---|---|
| **0.8mL/min** | | | |
| HALO | 7997 | 1.8 | 5.7 |
| DP1 | 10671 | 1.3 | 6.8 |
| DP2 | 13839 | 1.1 | -- |
| **1.2mL/min** | | | |
| HALO | 7236 | 1.8 | 4.7 |
| DP1 | 9719 | 1.3 | 5.1 |
| DP2 | 9593 | 1.0 | -- |

| Peak | Theoretical plates | Peak asymmetry | Resolution |
|---|---|---|---|
| **Organic phase +2% above the optimized ratio** | | | |
| HALO | 7237 | 1.7 | 4.7 |
| DP1 | 9825 | 1.2 | 5.2 |
| DP2 | 9893 | 1.0 | -- |
| **Organic phase -2% above the optimized ratio** | | | |
| HALO | 7734 | 1.8 | 5.7 |
| DP1 | 10793 | 1.2 | 5.9 |
| DP2 | 8398 | 1.1 | -- |

| Peak | Theoretical plates | Peak asymmetry | Resolution |
|---|---|---|---|
| **Wavelength (243 nm)** | | | |
| HALO | 9391 | 1.5 | 5.3 |
| DP1 | 10668 | 1.2 | 6.0 |
| DP2 | 11082 | 1.0 | -- |
| **Wavelength (249 nm)** | | | |
| HALO | 9246 | 1.6 | 5.2 |
| DP1 | 9789 | 1.5 | 5.7 |
| DP2 | 10202 | 1.1 | -- |

## 6.3.4. Characterization of the degradation products by mass and tandem mass spectrometry

The structural characterization of the oxidative degradation products of HALO was done by LC-MS and LC-MS/MS studies. The LC-MS and LC-MS/MS spectra were captured in positive electro spray ionization mode(+ESI). The optimized parameters of LC-MS/MS studies are depicted in table 6.3.5.1

**Table 6.3.5.1:** The optimized parameters of LC-MS/MS

| Parameter | Value |
|---|---|
| **Dying, sheath, and nebulizing gas** | Nitrogen |
| **Vcap** | 3100 V |
| **Fragmentor** | 150 V |
| **Skimmer** | 45 V |
| **Octopol RF peak** | 750 V |
| **Drying gas flow** | 11 L/min |
| **Sheath gas flow** | 10 L/min |
| **Nebulizing gas** | 25 psi |
| **Sheath gas temp** | 295°C |

Based on the MS and the MS/MS data the most probable structure for degradation products was postulated along with fragmentation pathway.

### 6.3.4.1. HALO

HALO has molecular mass of 375.9 g/mol. Its molecular ion peak was seen at *m/z* = 376.1. The MS/MS spectra showed fragment ion peaks at *m/z* value of 165, 122.9, and 95.1. The fragment with *m/z*=165 was formed due to ionization of the piperidine nitrogen followed by inductive cleavage. Further of loss of propyl side chain and carbon monoxide (CO) leads to the formation of fragment with *m/z* 122.9 (secondary cation) and 95.1.

The MS, MS/MS spectra and the fragmentation pathway for HALO is seen in figure 6.3.4.1.1 to 6.3.4.1.3.

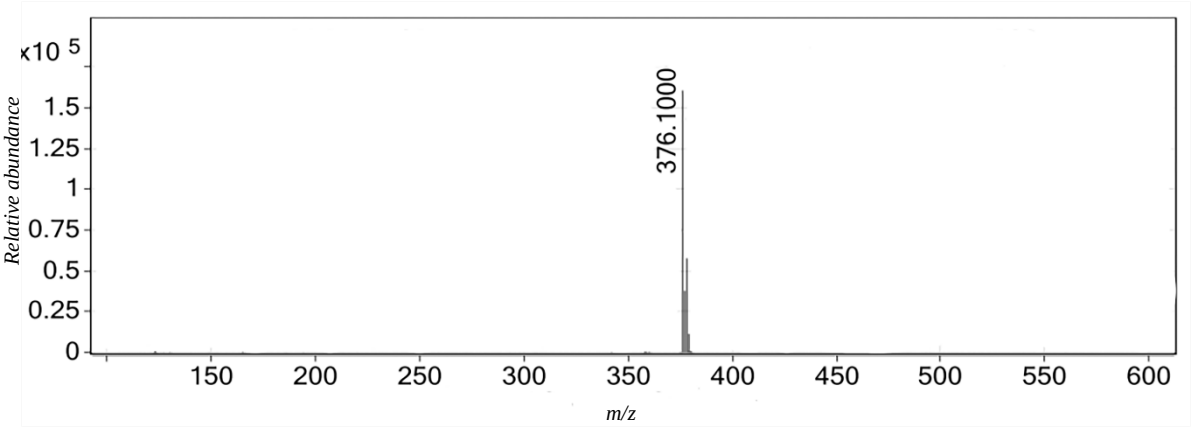


**Figure 6.3.4.1.1:** MS spectra of HALO

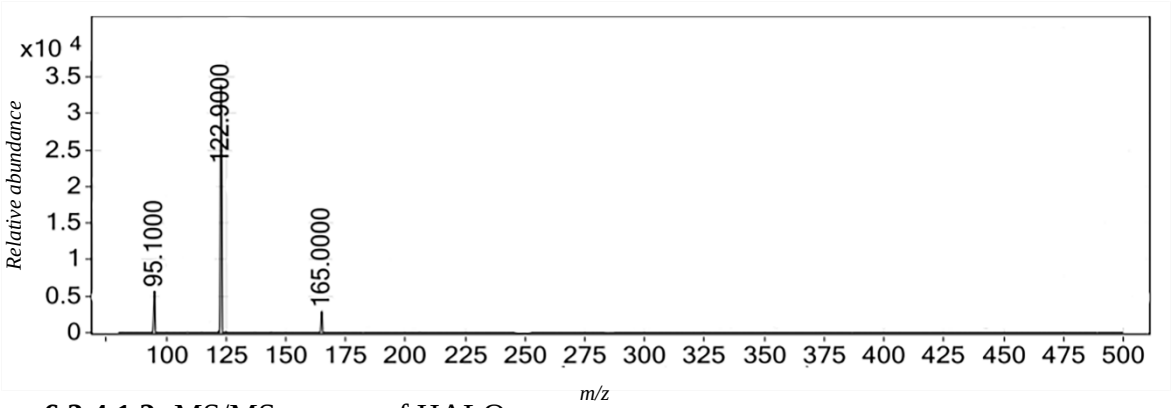


**Figure 6.3.4.1.2:** MS/MS spectra of HALO

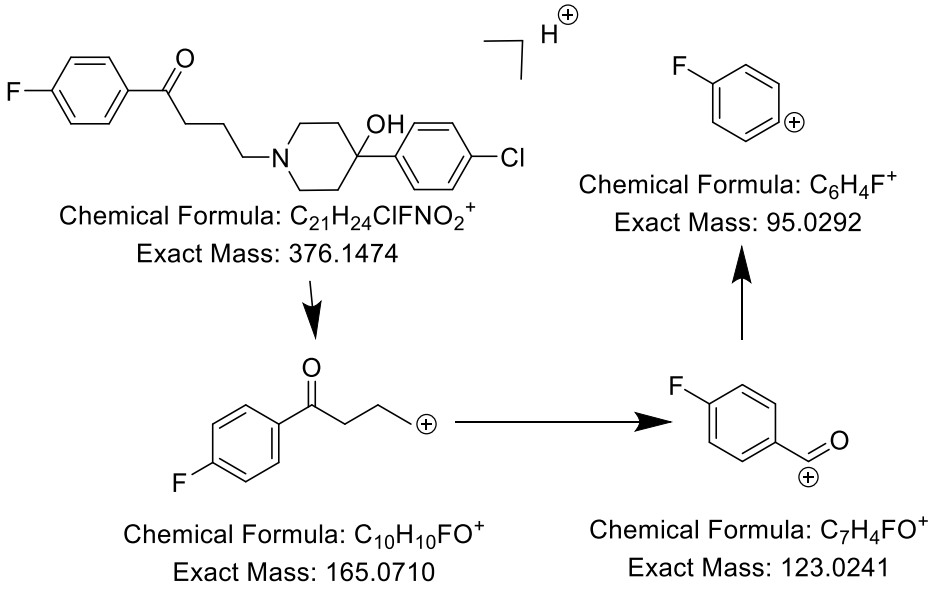


**Figure 6.3.4.1.3:** MS/MS fragmentation pathway of HALO

### 6.3.4.2. DP1 and DP2

The protonated peaks for DP1 and DP2 were seen at *m/z* 392.0891 and 392.0879 respectively, which were 16 amu higher than the *m/z* of HALO. The MS/MS fragmentation patterns for both the DPs were like the drug except the fragment with *m/z* 95. This indicated formation of a pair of N-oxide geometric isomers (*cis* and *trans*-N-oxides). Tertiary nitrogens are known to have propensity to form N-oxides and in the case of HALO, the piperidine nitrogen gets oxidised.

From the stress studies it was known that DP1 is more easily formed then DP2. Generally, the trans isomer is easier to form than its *cis* counterpart as the substituents are located on the opposite side of the rings. Based on this reasoning, DP1 was identified as *Trans*-Haloperidol-N-Oxide and DP2 as *Cis*-Haloperidol-N-Oxide.

The MS, MS/MS spectra and the fragmentation pattern for DP1 and DP2 is seen in figures 6.3.4.2.1 to 6.3.4.2.5 and summary of mass data is seen in table 6.3.4.2.1.

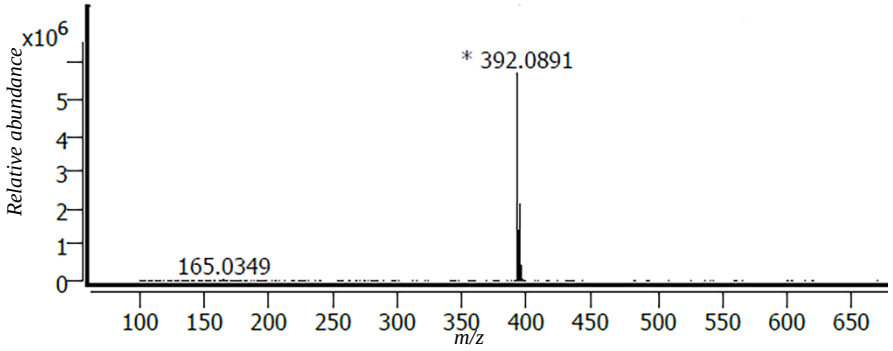


**Figure 6.3.4.2.1:** MS spectra of DP1

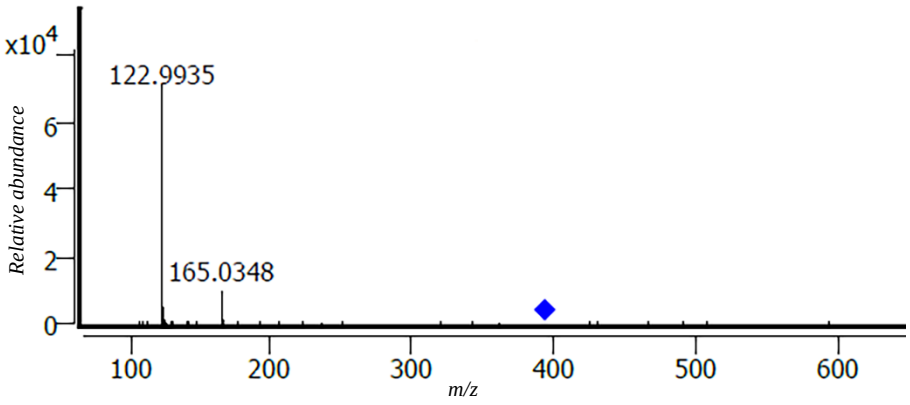


**Figure 6.3.4.2.2:** MS/MS spectra of DP1

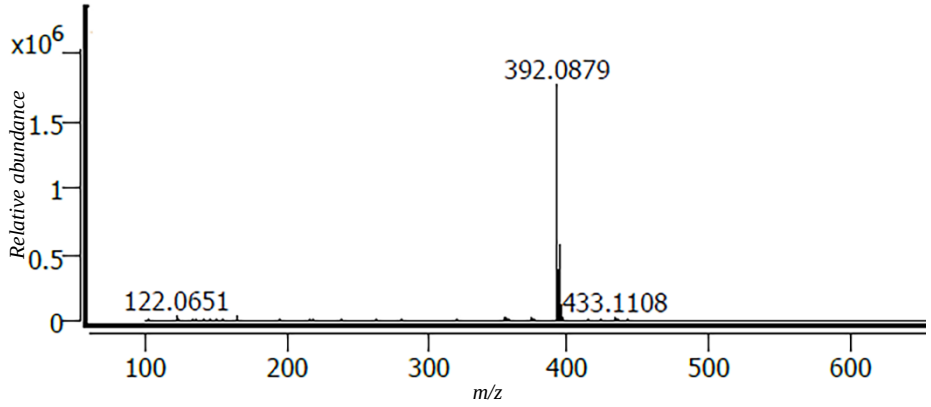


**Figure 6.3.4.2.3:** MS spectra of DP2

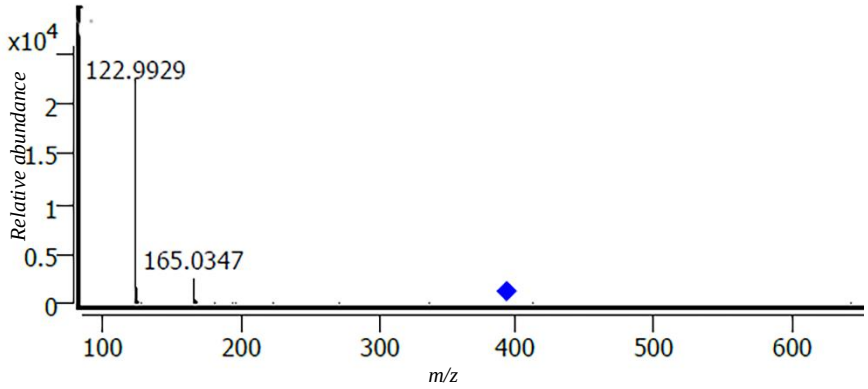


**Figure 6.3.4.2.4:** MS/MS spectra of DP2

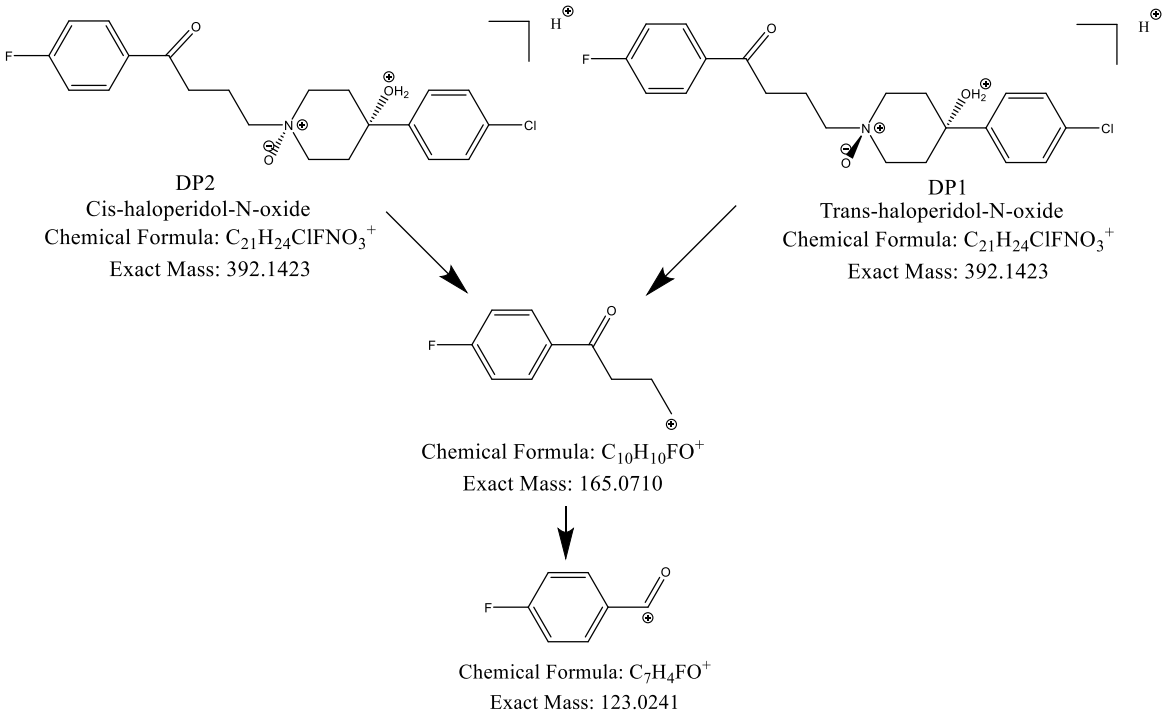


**Figure 6.3.4.2.5:** MS/MS fragmentation pathway of DP1 and DP2

**Table 6.3.4.2.1:** Summary of mass data of HALO and its DPs

| Compound | Experimental mass | Most likely molecular formulae | Theoretical mass | RDB | Error in mmu | Fragments | | Most probable molecular formulae for fragments. |
|---|---|---|---|---|---|---|---|---|
| | | | | | | Experimental mass | Theoretical mass | |
| **HALO* (TQMS)** | 376.1 | $C_{21}H_{23}ClFNO_2^+$ | 376.1 | 10 | -- | 165.0 | 165.1 | $C_{10}H_{10}FO^+$ |
| | | | | | | 122.9 | 123.0 | $C_7H_4FO^+$ |
| | | | | | | 95.1 | 95.0 | $C_6H_4F^+$ |
| **DP1(QTOF)** | 392.0891 | $C_{21}H_{23}ClFNO_3^+$ | 392.1423 | 10 | -5.32 | 165.0348 | 165.0710 | $C_{10}H_{10}FO^+$ |
| | | | | | | 122.9935 | 123.0241 | $C_7H_4FO^+$ |
| **DP2(QTOF)** | 392.0879 | $C_{21}H_{23}ClFNO_3^+$ | 392.1423 | 10 | -5.44 | 165.0347 | 165.0710 | $C_{10}H_{10}FO^+$ |
| | | | | | | 122.9929 | 123.0241 | $C_7H_4FO^+$ |

**MS and MS/MS analysis for HALO was done using Triple quad (TQMS). TQMS is not high-resolution mass (HRMS) hence, error in mmu could not be computed.*

### 6.3.5. *In-silico* ADMET studies of HALO and its DPs

The *In-silico* ADMET studies were conducted by using pkCSM webserver, ToxTree and the OSIRIS property explorer.

**pkCSM**

HALO and its degradation products were predicted to possess intestinal absorption of > 89%. None of them had affinity to bind to P-glycoprotein and based on the log BB value it was determined that they can pass through the blood brain barrier but not readily. DP1 and DP2 inhibited CYP1A2, CYP2C9 and CYP3A4 while HALO inhibited CYP2D6 and CYP3A4. With regards to toxicity, HALO was flagged for Hepatotoxic potential whereas, none were positive for AMES toxicity (Mutagenicity). The Summary of the pkCSM predictions is shown in table 6.3.5.1.

**ToxTree and OSIRIS property explorer**

Second level of screening using ToxTree and OSIRIS did not reveal any new information about mutagenic potential of the degradation products. OSIRIS further stated that none of them possess any tumorigenic, irritant, and reproductive risks.

**Table 6.3.5.1:** Summary of pkCSM predictions

| Compounds | Intestinal absorption (% absorbed) | PgP Substrate | BBB Permeability (log BB) | CYP1A2 inhibitor | CYP2C19 inhibitor | CYP2C9 Inhibitor | CYP2D6 Inhibitor | CYP3A4 Inhibitor | Hepatotoxicity | Ames toxicity |
|---|---|---|---|---|---|---|---|---|---|---|
| **HALO** | 89.5 | yes | 0.112 | No | No | No | Yes | Yes | Yes | No |
| **DP1** | 91.1 | yes | -0.144 | No | Yes | Yes | No | Yes | No | No |
| **DP2** | 91.1 | yes | -0.144 | No | Yes | Yes | No | Yes | No | No |

# 6.4 Experimental work

## 6.4.1. Instrumentation

**Table 6.4.1.1:** List of instruments

| Sr.no. | Instrument | Make and specification |
|---|---|---|
| **1** | **HPLC** | LC-4000, Jasco, Japan. Made up of a model CO-4061 temperature controlled column compartment, a model PU 4180 quaternary pump system with inline degasser, a model AS-4050 autosampler, Chromenav (version, 2.01.06) data acquisition software, LC-NET II interface box, Acer workstation computer running Microsoft windows 7 professional operating system. |
| **2** | **Column** | Phenomenex C18 (150mm ×4.6mm, 5µm). |
| **3** | **Sonicator** | Citizon, Vadodra, India. |
| **4** | **pH meter** | Digital pH meter, Elico, India. |
| **5** | **Precision balance** | Wensar digital, Chennai, India. |
| **6** | **Double distillation assembly** | Bhanu scientific instruments, Bangalore, Karnataka. |
| **7** | **Hot air oven** | Universal, Ambala, India. |
| **8** | **Constant temperature water bath** | Generic. |
| **9** | **Photostability chamber** | Newtronics lifecare Pvt.Ltd, Mumbai,India. |
| **10** | **MS system** | Agilent 1200 series HPLC system, 6200 series QTOF. Intel i7 5820k based workstation computer running windows 10 professional operating system with 32 GB of ram, ToxTree (version, 3.1.0-1851-1525442531402), OSIRIS property explorer. |
| **11** | **Workstation for *in-silico* studies** | |

## 6.4.2. Chemicals and reagents

1. **Acetonitrile (HPLC grade):** Qualigen, Mumbai, Maharashtra
2. **Hydrochloric acid:** Molychem, Thane, Mumbai.
3. **Hydrogen peroxide:** Molychem, Thane, Mumbai.
4. **Ammonium formate:** Molychem, Thane, Mumbai.
5. **Water (HPLC grade):** Finar, Ahmedabad, Gujarat.
6. **Sodium Hydroxide:** Finar, Ahmedabad, Gujarat.

## 6.4.3. Working standard

Haloperidol injections (Serenace®) were purchased from a local pharmacy.

## 6.4.4. Solution preparation

### 6.4.4.1. Preparation of stock solution of HALO

HALO stock solution was prepared by taking the drug formulation(injection) equivalent to 25 mg of HALO in 25 ml volumetric flask. To it, 10 mL of acetonitrile was added, and the contents were sonicated for 5 minutes. The volume was made to mark with acetonitrile (HPLC grade) to get a solution with a concentration of 1000µg/mL.

### 6.4.4.2. Preparation of ammonium Formate buffer (pH=3.7)

Ammonium formate (630 mg) was weighed and transferred into 1000 mL HPLC grade water and mixed thoroughly. Solution was then filtered through a 0.45µ membrane filter under vacuum and the pH was adjusted to 3.7 with formic acid.

### 6.4.4.3. Preparation of diluent

Ammonium formate buffer and acetonitrile were mixed in a ratio of 50:50 (v/v) and sonicated for five minutes to prepare the diluent.

### 6.4.4.4. Preparation of 0.1 N hydrochloric acid

Concentrated hydrochloric acid (0.85 mL) was slowly diluted to 100 mL mark using HPLC grade water in volumetric flask to get 0.1 N hydrochloric acid.

### 6.4.4.5. Preparation of 1 N hydrochloric acid

Concentrated hydrochloric acid (8.5 mL) was slowly diluted to 100 mL mark using HPLC grade water in volumetric flask to get 0.1 N hydrochloric acid.

### 6.4.4.6. Preparation of 0.1 N sodium hydroxide

Sodium hydroxide flakes (400 mg) was dissolved with the aid of sonication in 50 mL of HPLC grade water using 100 mL volumetric flask. The volume was made up to mark with HPLC grade water to get 0.1 N sodium hydroxide solution.

#### 6.4.4.7. Preparation of 1 N sodium hydroxide

Sodium hydroxide flakes (4000 mg) was dissolved with the aid of sonication in 50 mL of HPLC grade water using 100 mL volumetric flask. The volume was made up to mark with HPLC grade water to get 0.1 N sodium hydroxide solution.

#### 6.4.4.8. Preparation of 15% hydrogen peroxide

Hydrogen peroxide (15%) was prepared by diluting 5 mL of 30% hydrogen peroxide to 10 mL with water in 10 mL volumetric flask.

### 6.4.5. Forced degradation studies

The forced degradation studies were performed to get substantial degradation of drug. The drug was stressed under conditions viz. acidic, basic, neutral, oxidative, thermal, and photolytic. To get an accurate representation, four samples were prepared under each condition excluding thermal and photolytic; blank under normal condition (blank untreated), blank under stress condition (blank treated), drug solution under normal condition (standard), and drug under the stress condition. For thermal and photolytic conditions, the chromatogram obtained were compared with the chromatogram of drug stored under normal conditions.

#### 6.4.5.1. Hydrolytic degradation

The hydrolytic degradation was conducted under acidic, basic, and neutral condition. The stock solution of drug (1 mL) was mixed with 0.1 N / 1 N HCl in 10 mL volumetric flask and the solution was kept under stress for 48 h. In order to accelerate the degradation, the study was caried out at 70 ℃ for 7 h using 1 N HCl. After the stress period the samples were neutralized by using equal strength of sodium hydroxide and the volume was made to mark with diluent to get a concentration of 100 µg/mL of HALO. For base and neutral hydrolysis, a similar methodology was used. The samples treated with base were neutralized using corresponding strength of hydrochloric acid. All the samples were analysed using HPLC under optimized chromatographic conditions.

#### 6.4.5.2. Oxidative degradation

stock solution HALO ( 1 mL) was allowed to mix with 0.1 mL of oxidant (15% hydrogen peroxide) for 48 h in 10 mL volumetric flask. The volume was made up to mark with diluent

to get a concentration of 100 µg/mL and samples were analysed using HPLC under optimized chromatographic conditions.

#### 6.4.5.3. Thermal degradation

HALO stock solution was sealed in a glass ampoule and heated in an oven at 70 ℃ for 7 hours. After the stress period, the contents of the ampoules were diluted with diluent to get a concentration of 100 µg/mL. In similar fashion, one sample of HALO was kept at room temperature as control and samples were analysed using HPLC under optimized chromatographic conditions.

#### 6.4.5.4. Photolytic degradation

Photolytic degradation was carried out liquid state. Photolytic degradation was carried out by keeping 1 mL stock solution of HALO in volumetric flask inside a photostability chamber along with a control sample covered using aluminium foil.

The samples that were kept in the photostability chamber were exposed to ICH-mandated dose of light (1.2 million lux H of overall illumination and 200 wh/$m^2$ of integrated near U.V. energy). After the exposure period, the samples were diluted up to the mark to get 100 µg/mL concentration of drug using diluent and analysed using HPLC under optimized chromatographic conditions.

### 6.4.6. Validation studies

The developed and optimized HPLC method was validated as per the relevant ICH guideline.

#### 6.4.6.1. Specificity and selectivity

The specificity of the HPLC method was ascertained by the resolution values obtained between the nearest eluting peaks of degradation product and peak of drug and degradation product. The method's selectivity for the individual component was done through the % peak purity value obtained through the data acquisition software. The degradation samples were mixed in equal proportion and injected into HPLC.

### 6.4.6.2. Linearity and range

A series of dilutions (5 levels) were prepared in range of 10-110 µg/mL. At each level the sample was injected in triplicate, and the average area was obtained. The average area was plotted against the concentration to obtain a simple linear regression equation and the correlation coefficient. Five incremental concentration ( 10, 20, 50, 75 and 110 µg/mL) were prepared by accurately withdrawing 0.1, 0.2, 0.5, 0.75 and 1.1 mL of stock solution of HALO (1000 µg/mL) and diluting it to 10 mL using diluent in a volumetric flask.

### 6.4.6.3. Accuracy

The accuracy of the HPLC method was determined by the standard addition method. The degraded sample was spiked at 80%, 100%, and 120% of the target assay concentration (50 µg/mL) with standard drug solution. At each level, the sample was injected in triplicate, and the average % recovery was computed. Spiked samples were prepared by accurately transferring 0.4, 0.5 and 0.6 mL of stock solution of HALO to degraded sample and making the volume to 10 mL.

### 6.4.6.4. Precision

Precision (intra and inter) of the HPLC method was done at 10, 50, and 75 µg/mL. At each level, the sample was injected in triplicate, and the % relative standard deviation was determined (% RSD). Three incremental concentrations (10, 50, and 75 µg/mL) were prepared by accurately withdrawing 0.1, 0.5, and 0.75 mL of stock solution of HALO (1000 µg/mL) and diluting it to 10 mL using diluent in a volumetric flask.

### 6.4.7. *In-silico* studies

The *in-silico* studies were done using open-source options like the pkCSM webserver, ToxTree and OSIRIS property explorer.

The structures of the degradation products were sketched using Marvin by ChemAxon. The structures were copied as smiles and fed into the pkCSM webserver. ADMET prediction mode was selected which uploads the task for processing.

Toxtree accepts the structure in the form of SMILES which were generated similarly as discussed above. The decision tree (In vitro mutagenicity (Ames test) alerts by ISS) was selected from the method tab, and the estimate button was clicked.

OSIRIS property explorer accepts SMILES or CAS no as input and runs predictions.

`

# Chapter 7

# Characterization and *in-silico* toxicity prediction of degradation products of riociguat.

## 7.0. Introduction

Riociguat is mostly used in the treatment of persistent/ chronic thromboembolic pulmonary hypertension. It is a stimulator of soluble guanylate cyclase (sGC). It is not yet official in any compendia. The new drug application (NDA) for riociguat was filed with US-FDA on 8$^{th}$ October 2013 by Bayer Healthcare Pharmaceuticals Inc[107-109].

The work presented herein focuses on the following objectives:

1. Conduct of forced degradation studies on riociguat as per the ICH-mandated stress conditions.
2. Development of a stability-indicating assay method (SIAM) for riociguat.
3. Validation of the SIAM as per the ICH guidelines.
4. Structural characterization of the degradation products by liquid chromatography coupled with mass and tandem mass spectrometry.
5. Prediction of absorption, distribution, metabolism, excretion, and toxicity (ADMET) profile using *in-silico* studies.

# 7.1. Drug profile[108]

## 7.1.1 Riociguat (RIO)

**Chemical structure:**

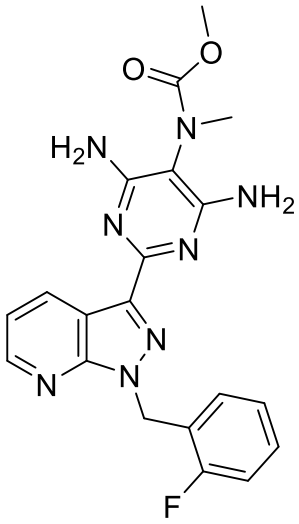


**IUPAC name:** Methyl N- [4,6-Diamino-2- [1-[(2- fluorophenyl)methyl]-1H-pyrazolo[3,4-b]pyridin-3-yl]-5-pyrimidinyl]-N-methylcarbamate

**Molecular formula:** $C_{20}H_{19}FN_8O_2$

**Melting point:** 247-251℃

**pKa:** 4.34

**LogP:** 2.37

**Description:** Yellowish to white crystalline solid

**Solubility:** Water solubility (1.4mg/100mL); freely soluble in methanol, chloroform, benzene, acetone, and dilute acids

**Drug category:** soluble guanylate cyclase (sGC) stimulators

**Clinical pharmacology:**

Soluble guanylate cyclase is a receptor for nitric oxide (NO). The binding of NO to sGC stimulates the synthesis of cyclic guanosine monophosphate, which plays a vital role in regulating the vascular tone.

Pulmonary hypertension is characterized by endothelial dysfunction, irregularities in the synthesis of nitric oxide, and inadequate stimulation of sGC.

Riociguat shows its activity by stimulating sGC to the internal NO. It also directly activates sGC by binding at an alternate binding site independent of NO[110].

**Pharmacokinetics:**

RIO has high bioavailability through the oral route because of unrestrained absorption and little pre-systematic first pass extraction. RIO undergoes N-demethylation catalysed by the various isoforms of the cytochrome P-450 enzyme family. CYP1A1 is responsible for formation of the active metabolite M1 which possesses 33 % of the biological activity of RIO. Metabolite M1, through action of uridine diphosphate glucuronosyltransferase (UGT) produces the inactive metabolite M4. RIO and its metabolites is excreted by both renal and bilary / fecal route. Overall, majority of the administered dose is excreted by oxidative biotransformation whereas, 9-44 % is excreted unchanged in feces and 4-19 % is excreted unchanged in urine by glomerular filtration[110].

**Toxicity:**

RIO in rare circumstances, can cause severe adverse reactions like pulmonary hemorrhage and fetal toxicity. Other side effects of riociguat includes, hypotension, syncope, dizziness, headache, gastrointestinal upset, nausea, vomiting and constipation[111].

## 7.2. Literature survey

A thorough survey of literature was done to collect information about the various physiochemical properties and the analytical methods available for RIO. The various physiochemical properties of riociguat is discussed in the section 7.1. RIO is not official in any of the pharmacopeia. Therefore, no compendial methods are available.

Literature shows some bioanalytical methods for estimation of RIO in plasma[113,115], few HPLC methods for estimation of RIO in formulation[112,114] and a couple of methods for estimation of riociguat by UV[117,118].

Literature also revealed a single stability indicating assay method for RIO. However, it lacks in toxicity studies and a comparative binding study with target receptor. The only similarity between research worked described in the ensuing chapter and the reported method is formation of a base degradation product with *m/z* 391[116].

The summary of the chromatographic conditions used by the various HPLC methods is described in the following table.

**Table 7.2.1:** Summary of the HPLC methods available for determination of RIO by HPLC

| Sr.No | Type of method | Column type | Mobile Phase composition | Flow rate | Detector used | References |
|---|---|---|---|---|---|---|
| **1** | Title: Development and validation of reverse-phase high-performance liquid chromatography method for quantitative estimation of riociguat in tablet dosage | | | | | |
| | HPLC | Interstil ODS-3 C18 (250mm ×4.6mm, 5µm) | 0.2% v/v trifluoracetic acid: acetonitrile (60:40 v/v) | 1.0 mL/min | UV, 245 | 112 |
| **2** | Title: Determination of riociguat and its major human metabolite M-1 in human plasma by stable-isotope dilution LC-MS/MS | | | | | |
| | HPLC | Purosphere RP-18 (125 × 4mm, 5µm) | Ammonium formate [A] (2 mM, pH 6.8): acetonitrile [B] ($T_{min}$/A:B (v/v) - $T_0$/95:5;$T_1$/95:5;$T_{1.5}$/45:55;$T_{3.5}$/45:55;$T_{3.6}$/10:90 $T_5$/10:90, $T_6$/95:5 ) | 1.0 mL/min | MS | 113 |
| **3** | Title: Analytical method development and validation for the determination of riociguat in their formulations by LC-MS/MS | | | | | |
| | HPLC | Zorbax C18 (50 ×4.6mm, 5µm) | 0.1% formic acid: acetonitrile (15: 85 v/v) | 0.5mL/min | MS | 114 |
| **4** | Title: In vitro and in vivo investigation of metabolic fate of riociguat by HPLC-Q-TOF/MS/MS and in silico evaluation of the metabolites by ADMET predictor ™ | | | | | |
| | HPLC | Sunfire C-18 column (250 mm× 4.1mm, 5µm) | 0.1% formic acid [A]: ACN [B], ($T_{min}$/A:B (v/v) - $T_0$/95:5;$T_4$/95:5;$T_{22}$/55:45;$T_{30}$/10:90;$T_{40}$/80:20 $T_{45}$/95:5) | 0.8 mL/min | MS | 115 |

**Table 7.2.1:** Summary of the HPLC methods available for determination of RIO by HPLC (*Conti…*)

| Sr.No | Type of method | Column type | Mobile Phase composition | Flow rate | Detector used | References |
|---|---|---|---|---|---|---|
| 5 | Title: Stress degradation studies of riociguat, development of validated stability indicating method, identification, isolation and characterization of degradation products by LC-HR-MS/MS and NMR studies. | | | | | |
| | HPLC | Waters Symmetry C18 Column (150mm X 4.6 mm, 5µm) | Ammonium acetate (10 mM, pH 5.7 adjusted with acetic acid): acetonitrile (70:30 v/v) | 1 mL/min | UV, 254 nm | 116 |

# 7.3. Present work and discussion

## 7.3.1. Development of HPLC method to monitor the drug degradation behaviour of RIO

### 7.3.1.1. Selection of chromatographic methods

All the reported HPLC methods for RIO use RPC approach for detection and quantification of RIO. Due to this, it was decided to develop the HPLC method using RPC approach.

### 7.3.1.2. Selection of stationary phase

All the reported method used C18 column as a stationary phase for estimation of RIO. So, considering the majority of the references Agilent Eclipse Zorbax XDB C18 column (150mm × 4.6 mm, 5µm) column was selected as a stationary phase due to availability.

### 7.3.1.3. Selection of wavelength of analysis

During the initial HPLC runs, the diode array detector (DAD) was set to scan the entire UV range (200-400nm) to determine the wavelength of maximum absorbance ($\lambda_{max}$) of RIO. The UV spectrum obtained is depicted in figure 7.3.1.3.1. The UV spectrum showed two wavelength maxima, one at 220 nm and other at 322 nm. The wavelength maxima at 322 nm was selected for further analysis. The preference was given to the higher wavelength to obtain stable baseline during the HPLC analysis.

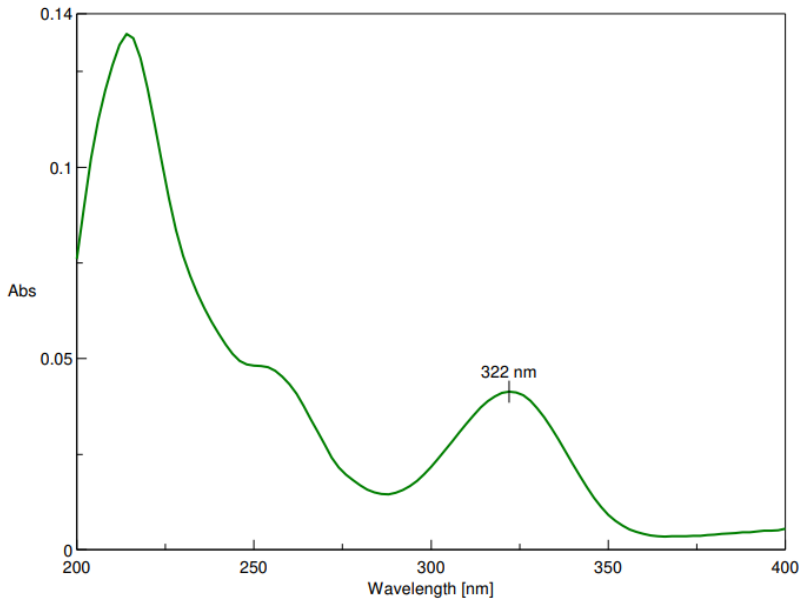


**Figure 7.3.1.3.1:** UV spectrum of RIO having concentration (10 µg/ mL in acetonitrile)

### 7.3.1.4. Selection and optimization of mobile phase for monitoring degradation of RIO

The main objectives of the HPLC method development were to develop a simple, robust, isocratic, mass friendly HPLC method with capacity factor(*K'*) value in-between 4-10. The reported HPLC methods for estimation of RIO in formulations uses various aqueous phases consisting of potassium dihydrogen phosphate (50 mM, pH 5), 0.2% acetic acid and ammonium formate (2 mM, pH 6.8) while the bioanalytical methods used ammonium formate (2 mM, pH 6.8) and 0.1% formic acid. The most preferred organic phase for all the reported methods was acetonitrile.

The pKa of RIO is 4.3, so in acidic pH it is present in the non-ionized form. For initial HPLC trials, the pH of the mobile phase was maintained acidic to enhance the robustness of the method. HPLC trials were conducted using ammonium formate (10mM, pH adjusted to 3.7 with formic acid) as the aqueous, and acetonitrile as the organic components of the mobile phase.

The preliminary trial was taken by using a mobile phase ratio (50:50, v/v) of acetonitrile and ammonium formate buffer (10 mM, pH 3.7). The chromatogram obtained is shown in figure 7.3.1.4.1

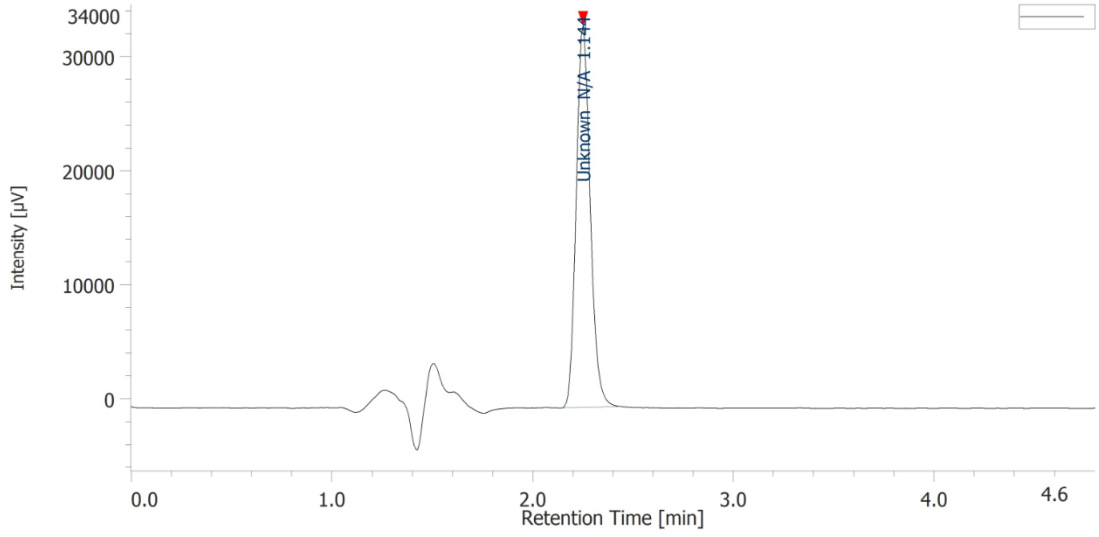


**Figure 7.3.1.4.1: Chromatogram of RIO (10µg/mL)** (Mobile phase, acetonitrile: ammonium formate buffer (pH 3.7, adjusted with formic acid), 50:50, v/v; flow rate: 1mL/min; wavelength: 322nm, Column: Agilent Eclipse Zorbax XDB C18 column (150mm × 4.6 mm, 5µm))

In the above trial, RIO had a retention time of 2.2 min, NTP > 3000, peak asymmetry < 2, and *k'* value was 1.2. Hence, to increase the separation of the drug peak from the void volume subsequent trials were conducted by systematically reducing the percentage of organic phase.

When organic phase was reduced to 30 % , retention time for RIO was 8.1 min. This modification also resulted in favourable system suitability with *k'* value of 7.1, NTP > 3000 and a peak asymmetry < 2.0. The chromatogram for this trial is depicted in figure 7.3.1.4.2.

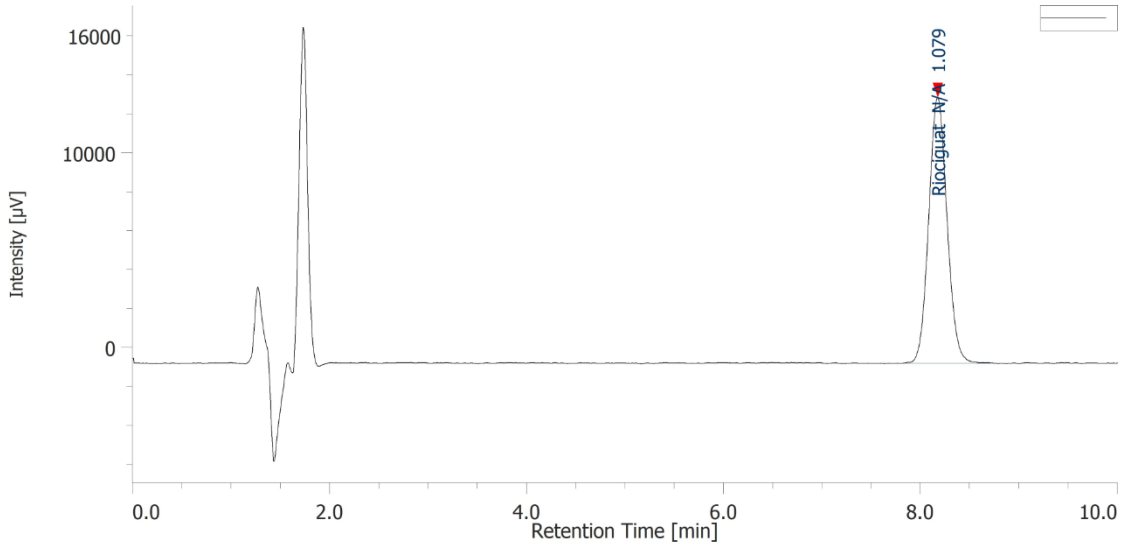


**Figure 7.3.1.4.2: Chromatogram of RIO (10µg/mL)** (Mobile phase, acetonitrile: ammonium formate buffer (pH 3.7, adjusted with formic acid), 30:70, v/v; flow rate: 1mL/min; wavelength: 322nm, Column: Agilent Eclipse Zorbax XDB C18 column (150mm × 4.6 mm, 5µm))

The Summary of the chromatographic conditions used to monitor the drug degradation behaviour was as follows;

**Mobile phase:** Acetonitrile: ammonium formate buffer (pH 3.7, adjusted with formic acid), 30:70 (v/v).

**Column:** Agilent Eclipse Zorbax XDB C18 column (150mm × 4.6 mm, 5µm).

**Wavelength:** 322 nm.

**Flow rate:** 1 mL/min.

## 7.3.2. Forced degradation studies

The stability of the drug was probed as per the guidance provided in the ICH Q1A(R2) guideline. The drug was tested under hydrolytic (acidic, basic, and neutral), oxidative, thermal, and photolytic conditions. The stressed samples were subjected to HPLC analysis using optimized chromatographic conditions, and the chromatogram obtained was compared with blank stored under normal condition (blank untreated), blank subjected to stress conditions like the drug (blank treated), and the drug solution stored under normal condition (standard untreated)

### 7.3.2.1. Hydrolytic degradation

Hydrolytic degradation was performed using acidic, basic, and neutral conditions. The degradation studies were carried out at room temperature in order to get desired degradation of the drug. The degradation studies were also carried out at higher temperature (70 ℃, 7 h), in case, no degradation was observed at room temperature. The concentration of the stressors was also optimized from low to high depending upon the degradation behaviour of the drug. Periodically, samples were withdrawn, neutralized, and diluted to the desired concentration and injected into HPLC using optimized chromatographic conditions.

**Acid degradation**

Acid degradation was carried out at room temperature by exposing drug solution to 1 N /2 N HCl for 48 hours in a volumetric flask to get desired degradation of the drug. The studies were repeated using 2 N HCl at 70℃ for 7 hours since no degradation was observed at room temperature. After applying the stress conditions, the samples were neutralized by using equal strength of base (NaOH). The neutralized samples were diluted to get the desired concentration and injected into HPLC using optimized chromatographic conditions.

The drug showed resilience to degradation under acidic conditions, and no degradation was observed.

**Base degradation**

Base degradation was carried out at room temperature by exposing drug solution to 1 N NaOH for 48 hours in a volumetric flask to get desired degradation of the drug. The studies were repeated using 1 N NaOH at 70℃ for 7 hours to enhance the concentration of DPs. After applying the stress conditions, the samples were neutralized by using equal strength

of acid (HCl). The neutralized samples were diluted to get the desired concentration and injected into HPLC using optimized chromatographic conditions.

The drug was susceptible towards degradation under basic conditions. The drug degraded ~ 37% at room temperature for 48 h and led to formation two degradation products with $t_R$ of 7.3 and 8.1 mins respectively. The representative chromatogram is shown in figure 7.3.2.1.1.

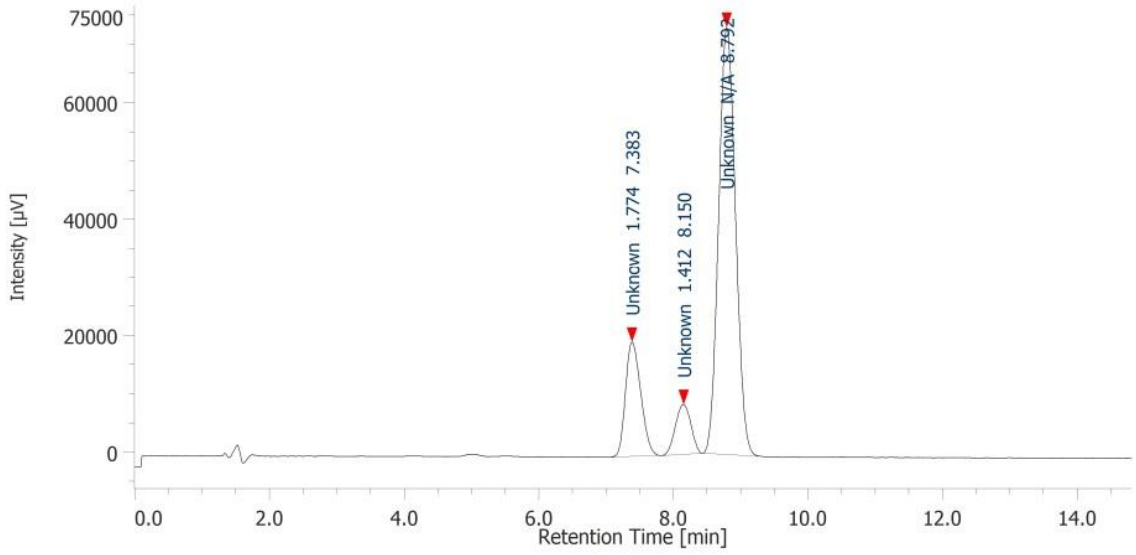


**Figure 7.3.2.1.1: Chromatogram of RIO (100µg/mL) treated with 1 N NaOH at room temperature for 48 h** (Mobile phase, acetonitrile: ammonium formate buffer (pH 3.7, adjusted with formic acid), 30:70, v/v; flow rate: 1mL/min; wavelength: 322nm, Column: Agilent Eclipse Zorbax XDB C18 column (150mm × 4.6 mm, 5µm))

**Neutral degradation**

Neutral degradation was carried out at room temperature by exposing drug solution to water for 48 hours in a volumetric flask to get desired degradation of the drug. The studies were repeated by heating the drug solution with water at 70°C for 7 h since no degradation was observed at room temperature. Samples were diluted to get the desired concentration and injected into HPLC using optimized chromatographic conditions.

The drug showed resilience to degradation under neutral basic condition, and no degradation was observed.

### 7.3.2.2. Oxidative degradation

Oxidative degradation was carried out at room temperature by exposing drug solution to 15% $H_2O_2$ for 48 hours in a volumetric flask to get desired degradation of the drug. Samples were diluted to get the desired concentration and injected into HPLC using optimized chromatographic conditions.

The drug was susceptible towards degradation under oxidative stress. The drug degraded ~ 38. 2 % at room temperature for 48 h and led to formation 2 degradation products with $t_R$ of 3.4 and 5.3 mins respectively. The representative chromatogram is shown in figure 7.3.2.2.1.

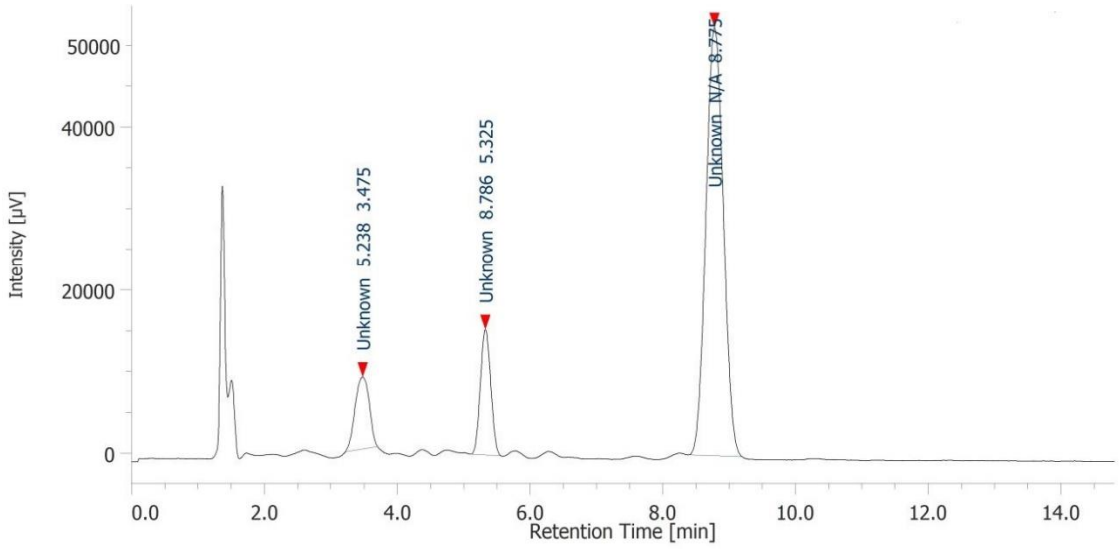


**Figure 7.3.2.2.1: Chromatogram of RIO (100µg/mL) treated with 15 % $H_2O_2$ at room temperature for 48 h** (Mobile phase, acetonitrile: ammonium formate buffer (pH 3.7, adjusted with formic acid), 30:70, v/v; flow rate: 1mL/min; wavelength: 322nm, Column: Agilent Eclipse Zorbax XDB C18 column (150mm × 4.6 mm, 5µm))

### 7.3.2.3. Thermal degradation

Thermal degradation was carried out by exposing the drug in sealed ampoule to dry heat at 70 ℃ for 7 days using hot air oven. A control sample was maintained by placing drug into a separate glass ampoule stored at room temperature. After the stress period, the sample was diluted with diluent to get the desired concentration and injected into HPLC using optimized chromatographic conditions.

The drug did not show degradation under thermal conditions**.**

### 7.3.2.4. Photolytic degradation

Photolytic degradation studies were carried out in the solid and liquid states using photostability chamber. Solid state stress studies were carried out by spreading the drug as a thin layer inside a petri dish while, liquid state stress studies were carried out by placing drug solution inside a volumetric flask. Both the samples were exposed to ICH Q1B mandated dose of light. In addition, solid-state studies were also carried out by exposing the drug placed inside a volumetric flask to sunlight for 7 days.

The chromatogram obtained from photolytic stressed samples did not show degradation.

## 7.3.3. Development and optimization of the stability-indicating assay method

During the base degradation studies, it was observed that there was formation of a peak group comprising of the drug peak (Rt 8.7) and the base degradation products with $R_t$ of 7.3 and 8.1 respectively with $\boldsymbol{R_s} < 2$ among them. The chromatogram of the mixture of base and oxidative samples of RIO is shown in figure 7.3.3.1.

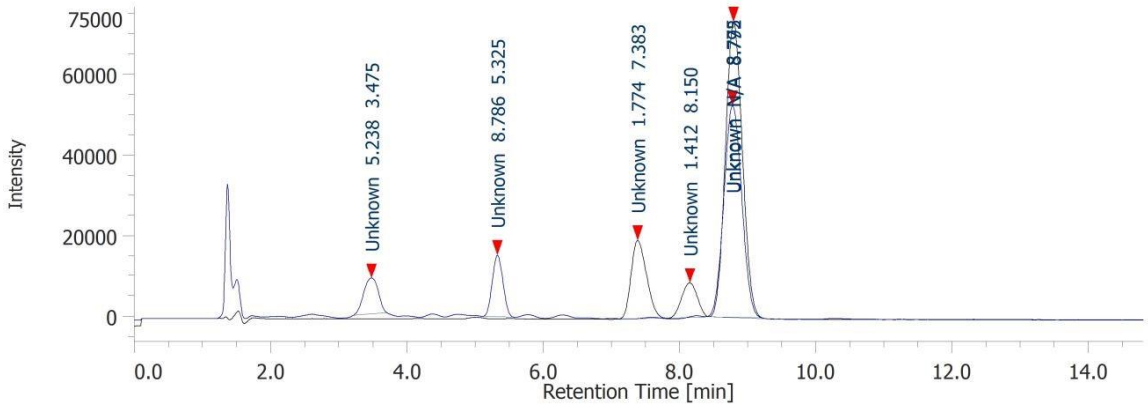


**Figure 7.3.3.1: Chromatogram of mixture of base and oxidative degraded RIO (100µg/mL) at room temperature for 48 h** (Mobile phase, acetonitrile: ammonium formate buffer (pH 3.7, adjusted with formic acid), 30:70, v/v; flow rate: 1mL/min; wavelength: 322nm, Column: Agilent Eclipse Zorbax XDB C18 column (150mm × 4.6 mm, 5µm))

The separation among the peaks of this group was enhanced by reducing the organic phase to 28%. This modification resulted in $R_s$ > 2 among the peaks. The chromatogram obtained is depicted in figure 7.3.2.2.2.

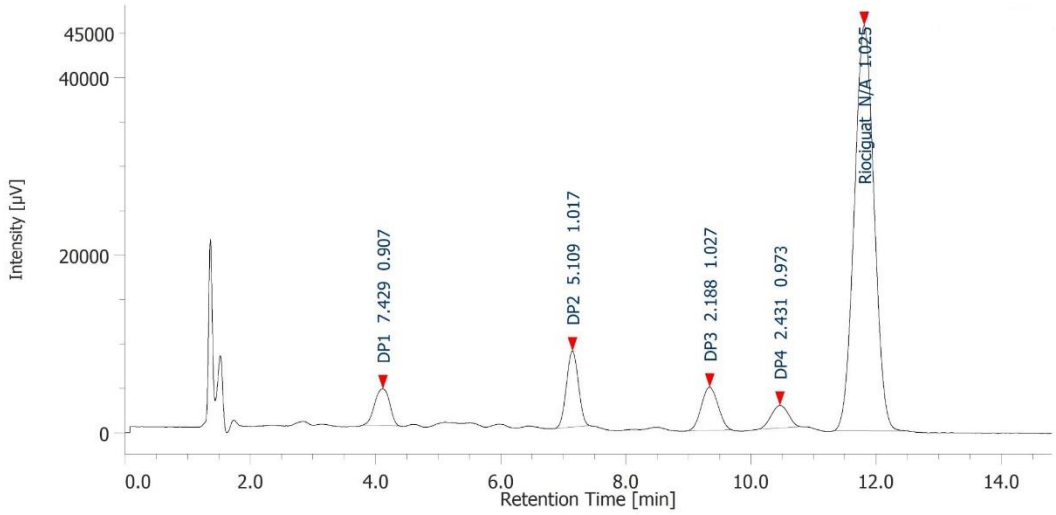


**Figure 7.3.3.2: Chromatogram of mixture of base and oxidative degraded RIO (100µg/mL) at room temperature for 48 h** (Mobile phase, acetonitrile: ammonium formate buffer (pH 3.7, adjusted with formic acid), 28:72, v/v; flow rate: 1mL/min; wavelength: 322nm, Column: Agilent Eclipse Zorbax XDB C18 column (150mm × 4.6 mm, 5µm))

The UV spectra of the individual degradation products was recorded using the diode array detector and overlain with the UV spectra of the drug as shown in 7.3.3.3.

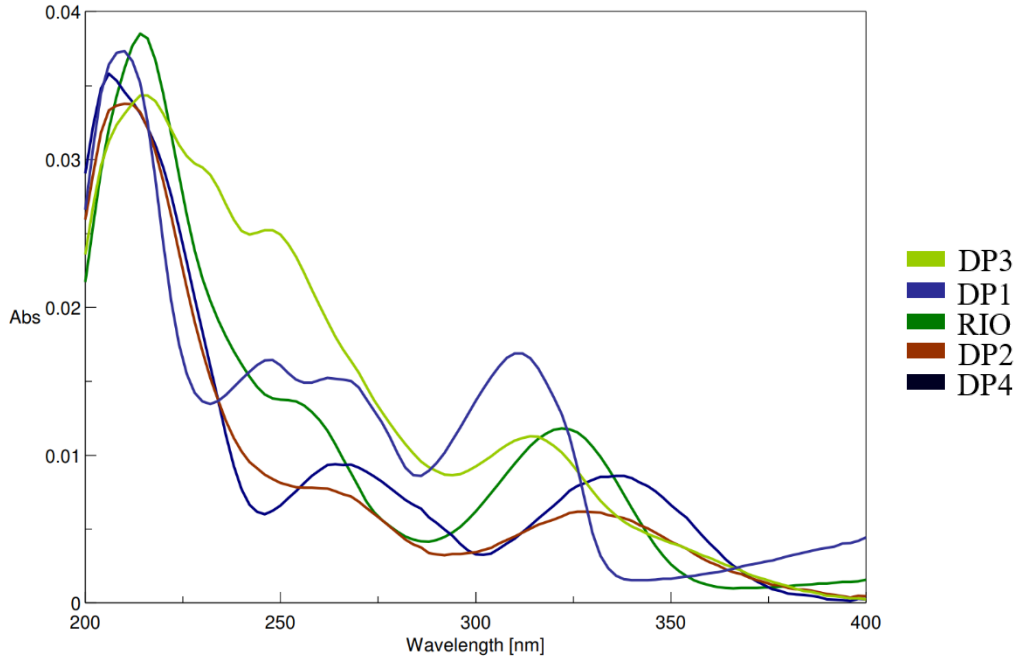


**Figure 7.3.3.3:** Overlain of UV spectra of RIO with its degradation products

## 7.3.4. Validation of the developed stability-indicating assay method (SIAM)

HPLC method validation is required to ensure that the method achieves an adequate standard of specificity, accuracy, and precision. The developed SIAM was validated as per the guidance of the ICH Q2 guideline. The parameters considered during the validation process is summarized in table 7.3.4.1.

**Table 7.3.4.1:** Validation parameters and acceptance criteria

| Sr.No | Validation Parameters | Acceptance Criteria |
|---|---|---|
| **1** | **Specificity** | Resolution > 1 |
| **2** | **Selectivity** | Peak purity (%) > 99 |
| **3** | **Linearity** | Correlation coefficient not less than 0.999 |
| **4** | **Accuracy (across the specified range)** | Recovery (%) between 98.0 to 102% |
| **5** | **Precision (intra day & inter day)** | RSD (%) of replicate injections not more than 2.0 |
| **6** | **Robustness** | 1) Resolution between adjacent peak should not be less than 1.0<br>2) Numbers of theoretical plates of analyte peak should not be less than 2000.<br>3) Asymmetry of peak should not be more than 2.0 |

### 7.3.4.1. Specificity and selectivity

The specificity of the HPLC method was expressed in terms of resolution between the closely eluting peaks. It is evident from figure 7.3.3.2 that the peaks were well resolved with a resolution value greater than one which confirms the specificity of the method. The method's selectivity was determined by measuring % peak purity value acquired using data acquisition software. The peak purity(%) was > 99% which indicates that the method is selective.

### 7.3.4.2. Linearity and range

The linearity was established in triplicate by taking five incremental concentrations in a range of 20-120 µg/mL. The graph plotted between the average area under peak v/s concentration. The data obtained was subjected to regression analysis. The calculated value of the corelation coefficient ($r^2$) was 0.999. The linearity plot and the data pertaining to

linearity is given in figure 7.3.4.2.1 and table 7.3.1.2.1. The representative chromatogram at each concentration level is seen in figure 7.3.4.2.2.

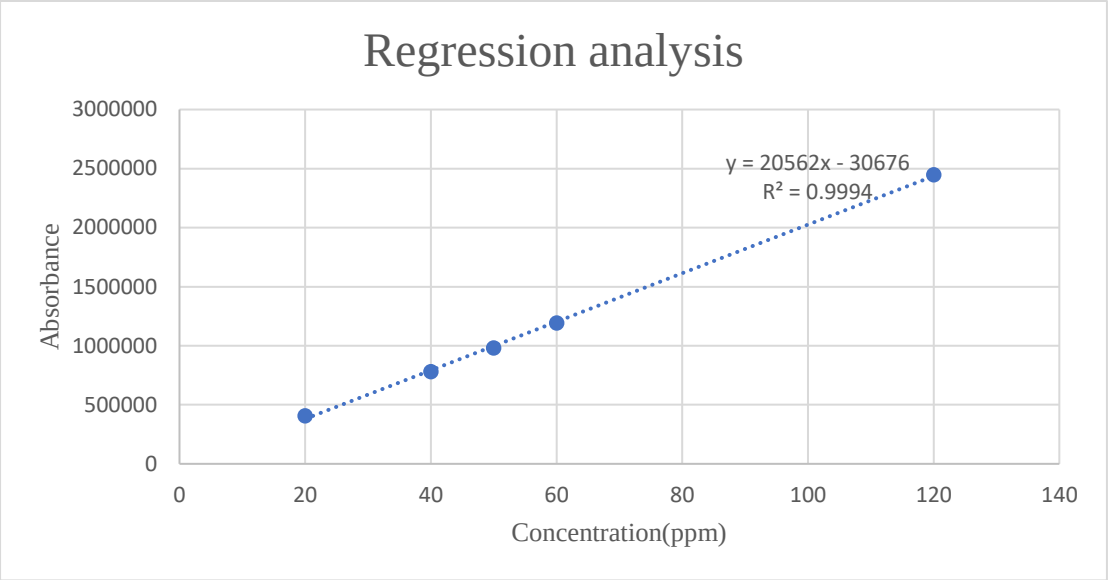


**Figure 7.3.4.2.1.** Linearity graph of RIO

**Table 7.3.1.2.1:** Linearity data for RIO

| Sr. No. | Concentration (µg/mL) | Peak area | | | | RSD(%) |
|---|---|---|---|---|---|---|
| | | Injection 1 | Injection 2 | Injection 3 | Average | |
| 1 | 20 | 404330 | 409145 | 409081 | 407519 | 0.7 |
| 2 | 40 | 778177 | 782435 | 780597 | 780403 | 0.3 |
| 3 | 50 | 982860 | 978796 | 978175 | 979944 | 0.3 |
| 4 | 60 | 1197815 | 1202105 | 1181149 | 1193690 | 0.9 |
| 5 | 120 | 2444889 | 2442261 | 2456882 | 2448011 | 0.3 |

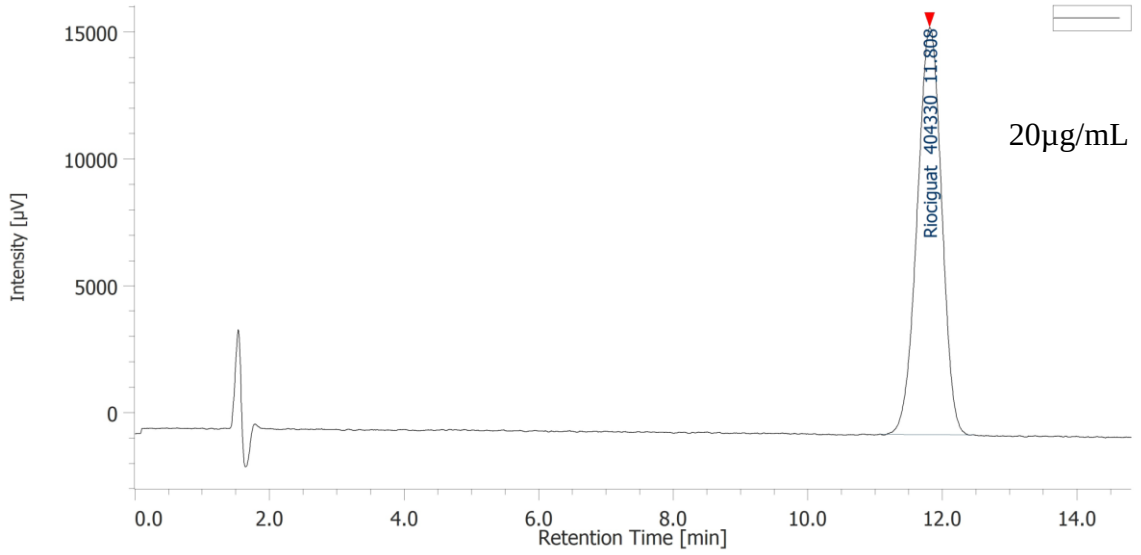


**Chromatogram 1**

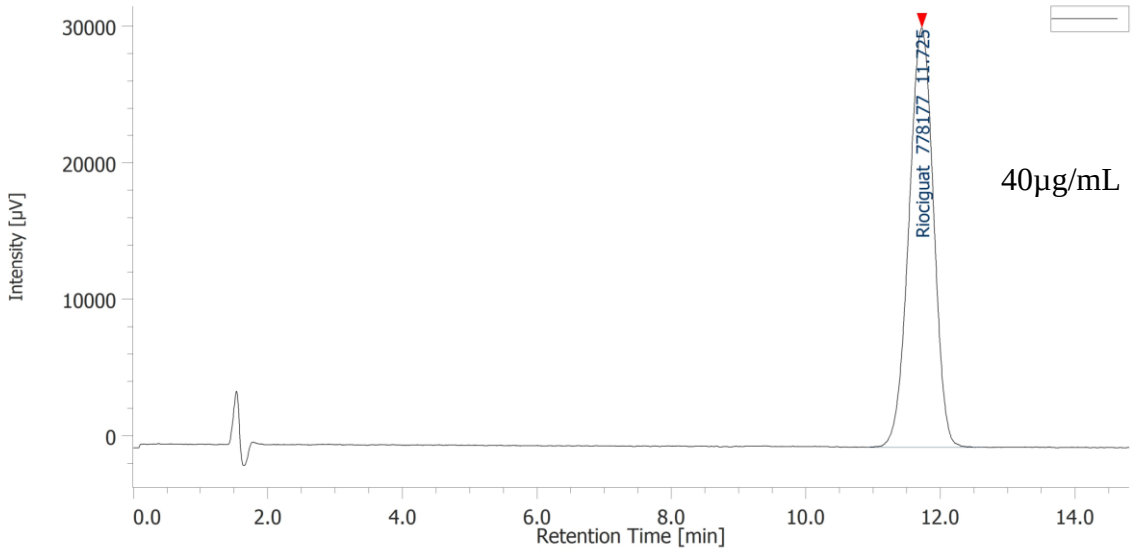


**Chromatogram 2**

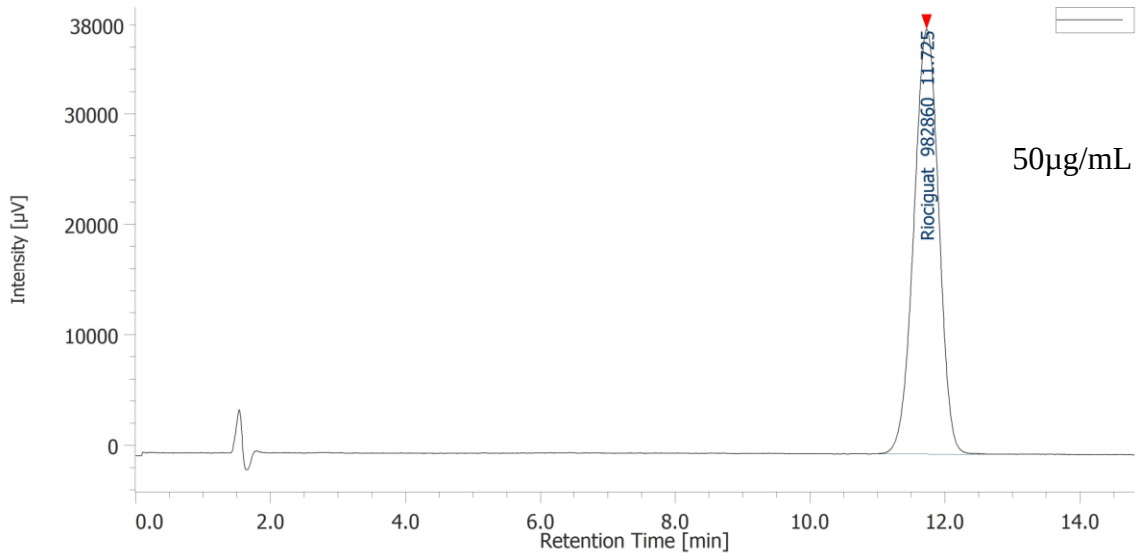


**Chromatogram 3**

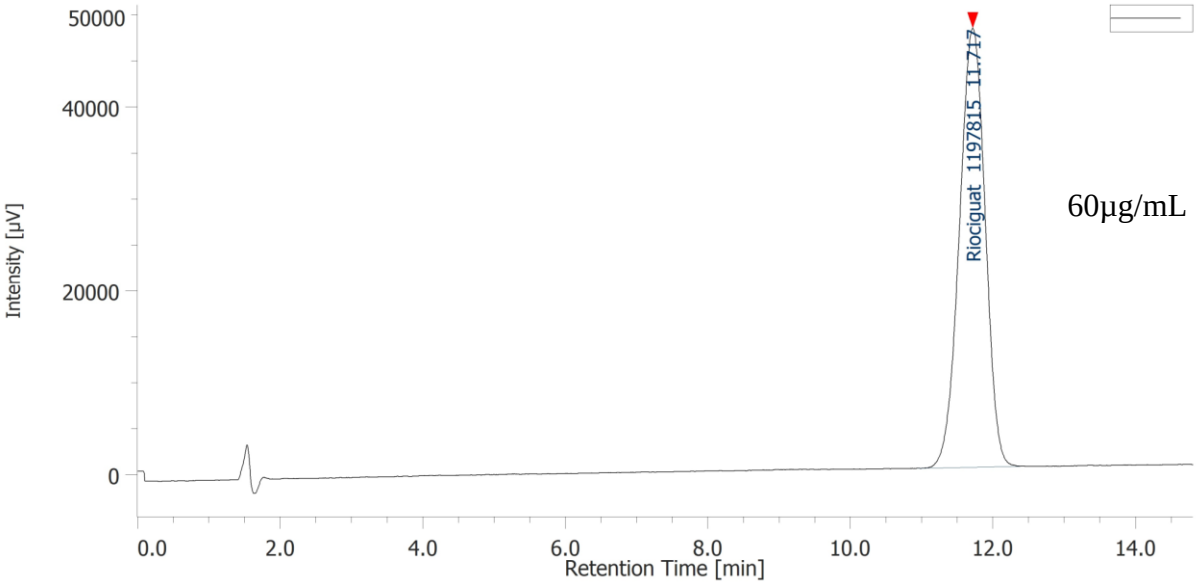


**Chromatogram 4**

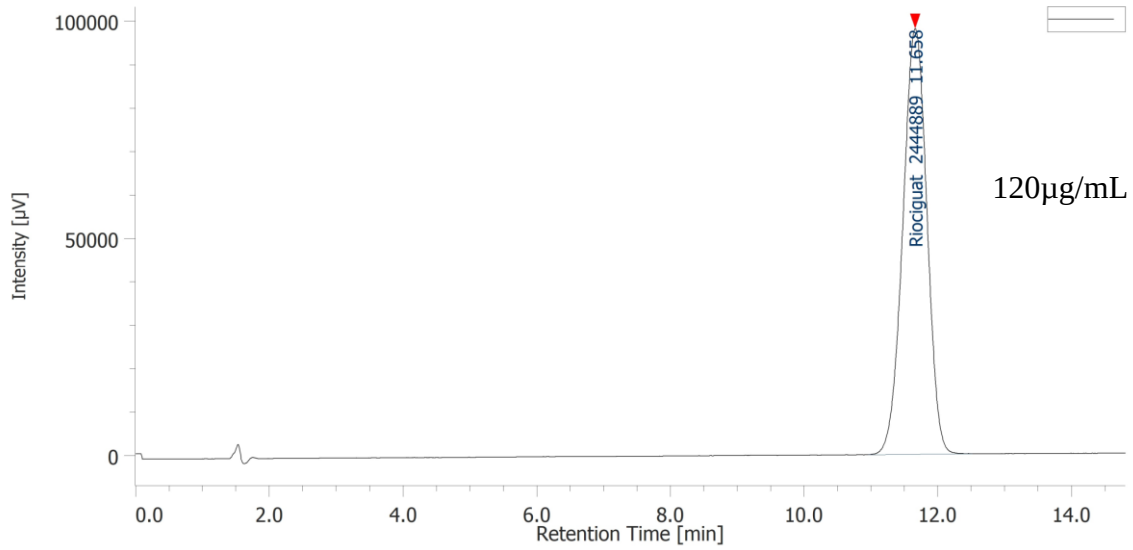


**Chromatogram 5**

**Figure 7.3.4.2.2:** Representative chromatograms at concentration level 20, 40, 50, 60 and 120 µg/mL

### 7.3.4.3. Accuracy

The accuracy was expressed in terms of recovery (%) of the spiked standard drug and was done by the standard addition method. The stressed sample were separately spiked with standard drug with concentrations 40 µg/mL (80%), 50 µg/mL (100%) and 60 µg/mL (120%) of the target assay concentration (50 µg/mL) and injected in triplicate. The average recovery at each level was between 98 to 102 %, with the mean recovery of 100.1 %. The data of recovery studies is shown in table 7.3.4.3.1.

**Table 7.3.4.3.1:** Recovery studies for RIO (n=3)

| Spiked drug concentration (µg/mL) | Recovered concentration (µg/mL) ± S. D, % R.S.D. | Recovery (%) |
|---|---|---|
| 40 | 40.1 ± 0.53,1.32 | 100.3 |
| 50 | 49.8 ± 0.31,0.62 | 99.5 |
| 60 | 60.1 ± 0.72,1.21 | 100.2 |

The representative chromatogram obtained at each level of accuracy study is shown in figure 7.3.4.3.1.

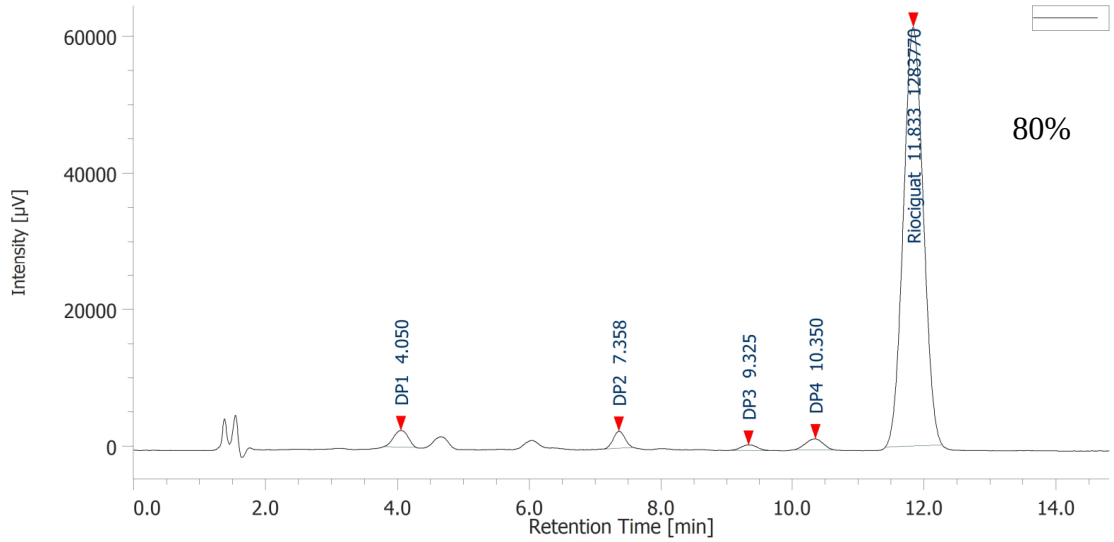


**Chromatogram 6**

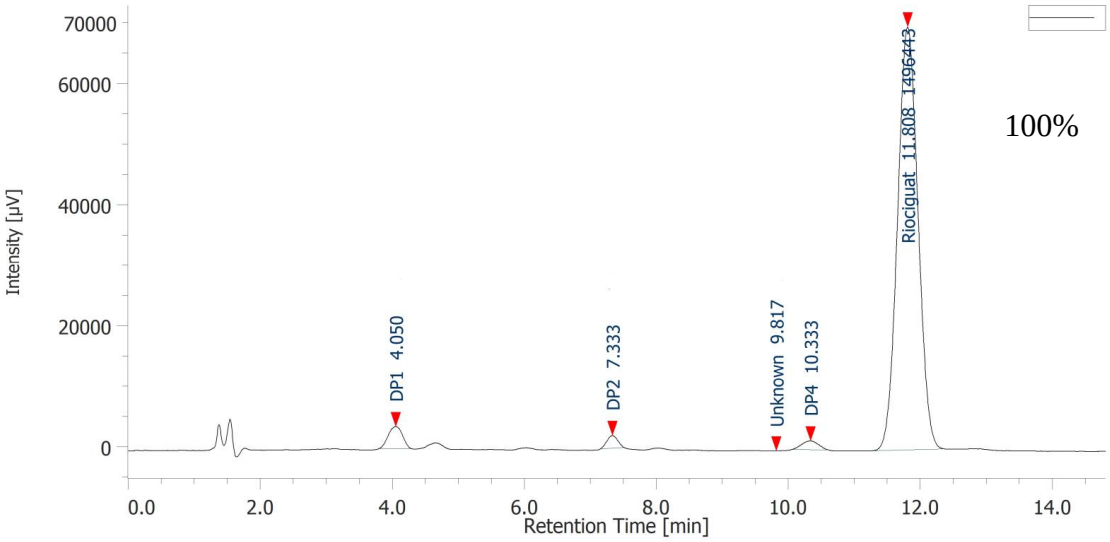


**Chromatogram 7**

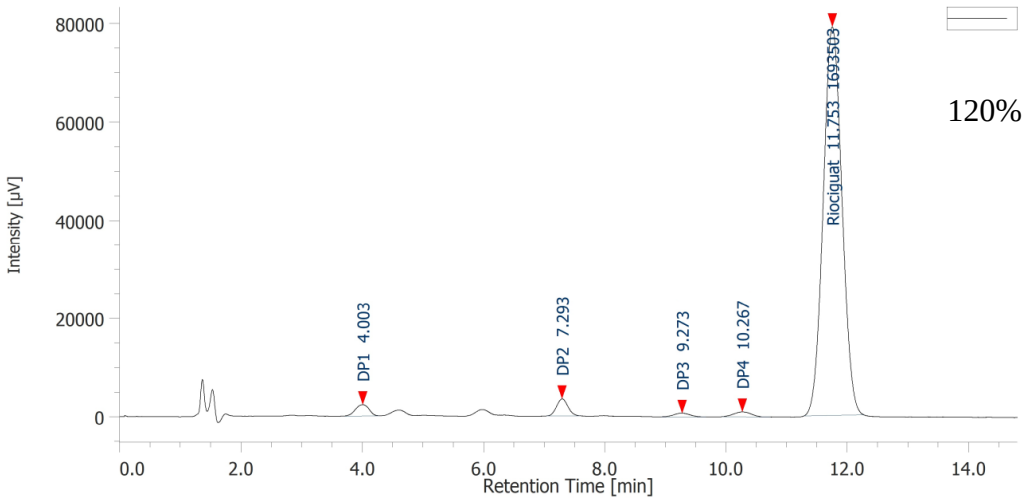


**Chromatogram 7**

**Figure 7.3.4.3.1:** Representative chromatograms obtained at each level of accuracy studies at 80, 100, and 120%.

### 7.3.4.4. Precision

Intra and inter-day precision studies were performed at three concentration levels: 40, 50, and 60 µg/mL in triplicate. The % RSD at each level was found to be < 2% inferring that the method was precise.

**Table 7.3.4.4.1:** Precision data obtained during intra-day and inter-day studies.

| Concentration (µg/mL) | Intraday (n=3) Mean peak area ± SD; %RSD | Inter-day (n =3) Mean peak area ± SD; %RSD |
|---|---|---|
| 40 | 780403 ± 2136,0.3 | 779370 ± 7088,0.9 |
| 50 | 979944 ± 2545,0.3 | 979421 ± 9435,1.0 |
| 60 | 1193690 ± 11070,0.9 | 1208794 ± 4358,0.4 |

### 7.3.4.5. Robustness

The robustness of the HPLC method was established to understand the HPLC methods tolerance to deliberate change in the chromatographic parameters. For this purpose, the following changes were carried out to observe its effect on the developed method.

1) The pH of the mobile phase (± 0.5 of the optimized value.)
2) Flow rate (± 0.2 mL of the optimized flow rate)
3) Mobile phase composition (± 2% strength of the optimized ratio)
4) Wavelength (± 3 units of the optimized wavelength)

The results of the robustness studies are depicted in the tables below.

**Table 7.3.4.5.1:** Data pertaining to robustness studies

| Peak | Theoretical plates | Peak asymmetry | Resolution |
|---|---|---|---|
| **pH 3.2** | | | |
| DP1 | 2538 | 0.9 | 7.4 |
| DP2 | 6718 | 0.9 | 5.1 |
| DP3 | 5374 | 1.0 | 2.1 |
| DP4 | 6029 | 0.9 | 2.3 |
| RIO | 6451 | 1.0 | -- |
| **pH 4.2** | | | |
| DP1 | **2368** | 1.0 | 7.4 |
| DP2 | 6034 | 1.0 | 5.1 |
| DP3 | 5881 | 1.1 | 2..2 |
| DP4 | 6522 | 0.9 | 2.4 |
| RIO | 6464 | 1.0 | -- |

| Peak | Theoretical plates | Peak asymmetry | Resolution |
|---|---|---|---|
| **Flow rate 0.8 mL/min** | | | |
| DP1 | 2300 | 0.9 | 8.9 |
| DP2 | 8673 | 1.1 | 407 |
| DP3 | 5585 | 1.1 | 2.0 |
| DP4 | 6425 | 0.9 | 2.7 |
| RIO | 7025 | 1.0 | -- |
| **Flow rate 1.2 mL/min** | | | |
| DP1 | 2425 | 0.9 | 8.6 |
| DP2 | 6781 | 1.0 | 4.9 |
| DP3 | 6452 | 0.7 | 1.9 |
| DP4 | 5804 | 0.9 | 2.6 |
| RIO | 6634 | 1.0 | -- |

| Peak | Theoretical plates | Asymmetry | Resolution |
|---|---|---|---|
| **Organic phase +2 % above the optimized ratio** | | | |
| DP1 | 2762 | 0.9 | 7.6 |
| DP2 | 6215 | 1.0 | 3.0 |
| DP3 | 4712 | 1.0 | 1.6 |
| DP4 | 4801 | 0.9 | 2.4 |
| RIO | 5566 | 1.0 | -- |
| **Organic phase -2 % below the optimized ratio** | | | |
| DP1 | 2413 | 0.8 | 7.2 |
| DP2 | 7307 | 0.9 | 7.9 |
| DP3 | 6349 | 0.9 | 2.6 |
| DP4 | 6863 | 1.0 | 2.1 |
| RIO | 7220 | 1.0 | -- |
| **Peak** | **Theoretical plates** | **Asymmetry** | **Resolution** |
| **Wavelength (319 nm)** | | | |
| DP1 | **2482** | **0.9** | **7.4** |
| DP2 | 6466 | 1.0 | 5.1 |
| DP3 | 5457 | 1.0 | 2.1 |
| DP4 | 6373 | 0.9 | 2.4 |
| RIO | 6475 | 1.0 | -- |
| **Wavelength (325 nm)** | | | |
| DP1 | **2575** | **0.8** | **7.3** |
| DP2 | 6467 | 0.9 | 5.0 |
| DP3 | 5261 | 1.0 | 2.1 |
| DP4 | 5870 | 0.9 | 2.3 |
| RIO | 6441 | 1.0 | -- |

## 7.3.5. Characterization of the degradation products by mass and tandem mass spectrometry

The structural characterization of the degradation products was carried out using LC-MS and LC-MS/MS. The LC-MS and LC-MS/MS spectra were recorded in positive electro spray ionization mode(+ESI). The optimized parameters of LC-MS/MS studies are depicted in table 7.3.5.1

Based on the MS and the MS/MS data the most probable structure for degradation products was postulated along with fragmentation pathway.

**Table 7.3.5.1:** The optimized parameters of LC-MS/MS studies.

| Parameter | Value |
|---|---|
| **Dying, sheath, and nebulizing gas** | Nitrogen |
| **Vcap** | 3100 V |
| **Fragmentor** | 150 V |
| **Skimmer** | 45 V |
| **Octopol RF peak** | 750 V |
| **Drying gas flow** | 11 L/min |
| **Sheath gas flow** | 10 L/min |
| **Nebulizing gas** | 25 psi |
| **Sheath gas temp** | 295°C |

### 7.3.5.1. RIO

The molecular weight of RIO is 422.1645 g/mole. The LC-MS spectra recorded in the +ESI mode showed molecular peak ion at *m/z* 423.1147, and its MS/MS spectra showed two distinct peaks at *m/z* values of 253.0476 and 109.0163. The cleavage of the pyrimidine ring forms the fragment with *m/z* 253.0476, which further loses the pyrazolo pyridine ring to form a fragment with *m/z* 109.0163.

The MS, MS/MS spectra, and the fragmentation pattern for RIO is shown in the following figures.

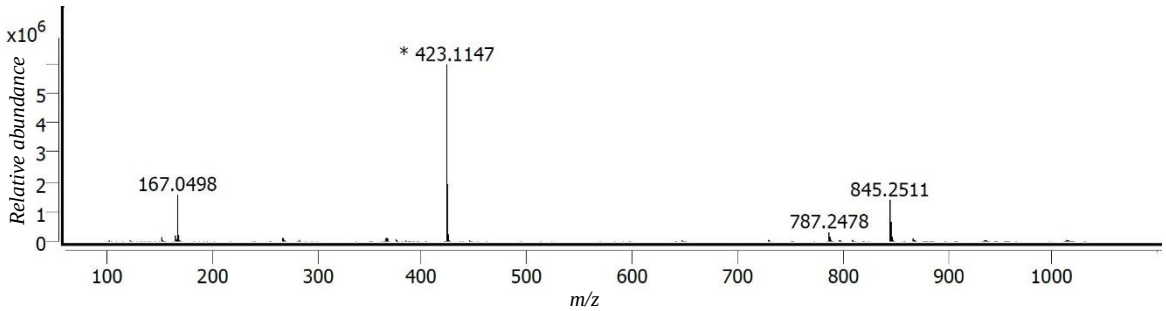


**Figure 7.3.5.1.1:** MS spectra of RIO

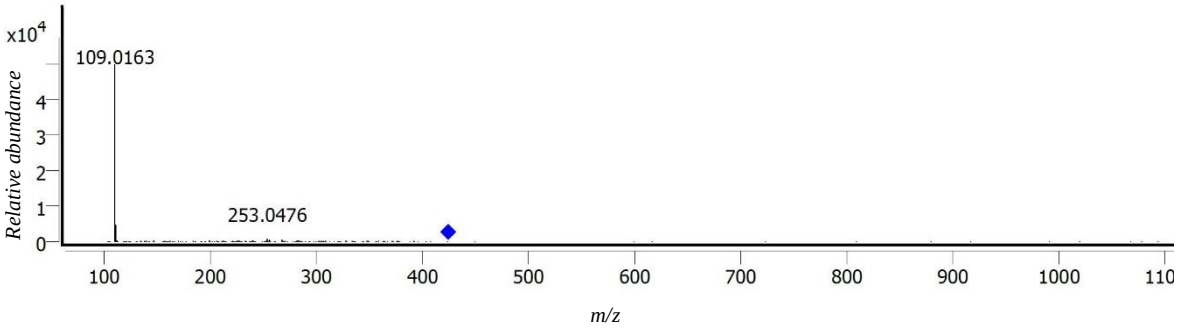


**Figure 7.3.5.1.2:** MS/MS spectra of RIO

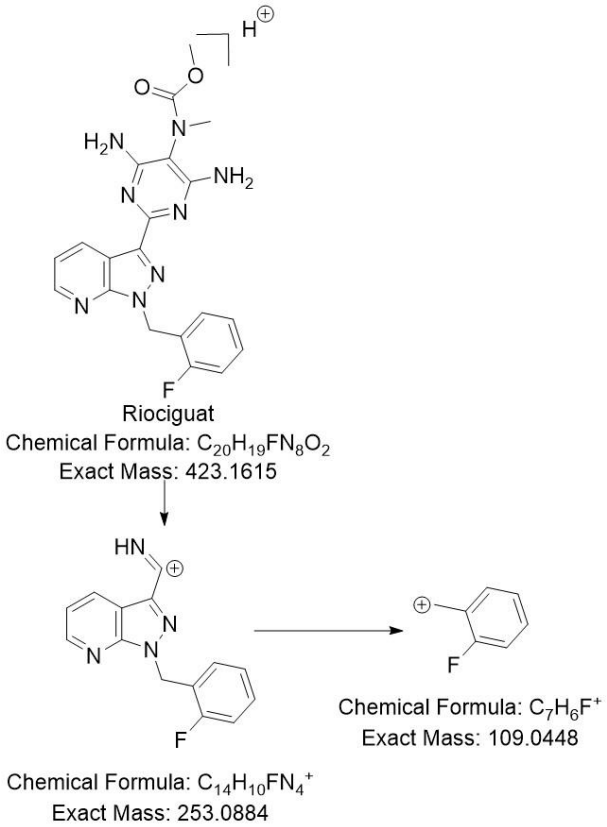


**Figure 7.3.5.1.3:** MS/MS fragmentation pattern of RIO

### 7.3.5.2. DP1

DP1 showed molecular ion peak at *m/z* 270.0699 and its MS/MS spectra showed peaks at *m/z* values of 109.0157 and 102.0056. The fragment ion (*m/z* 109.0157) was formed due to the ionization of the tertiary nitrogen bridging with fluorobenzene followed by an inductive

cleavage, while the fragment ion with *m/z* 102.0056 was formed due to the breakdown of the core pyrazolo pyridine structure.

DP1 of RIO was identified as 3-(diaziridin-3-yl)-1-(2-fluorobenzyl)-1H-pyrazolo[3,4-b] pyridine. The RDB value for the proposed structure was 10.5, and the error in mmu was –4.51. The MS, MS/MS spectra, and the fragmentation pattern for DP1 is shown in the following figures.

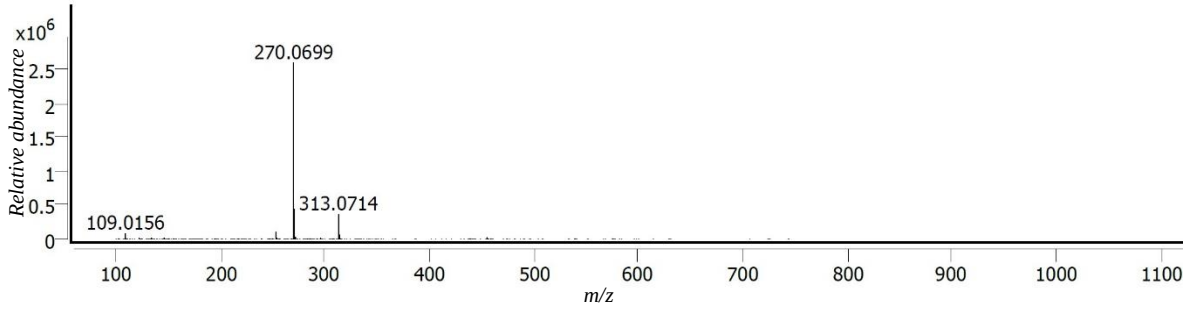


**Figure 7.3.5.2.1:** MS spectra of DP1

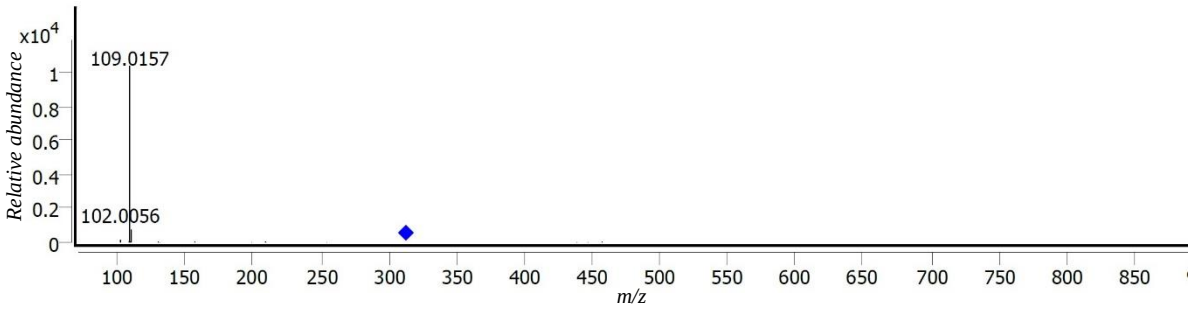


**Figure 7.3.5.2.2:** MS/MS spectra of DP1

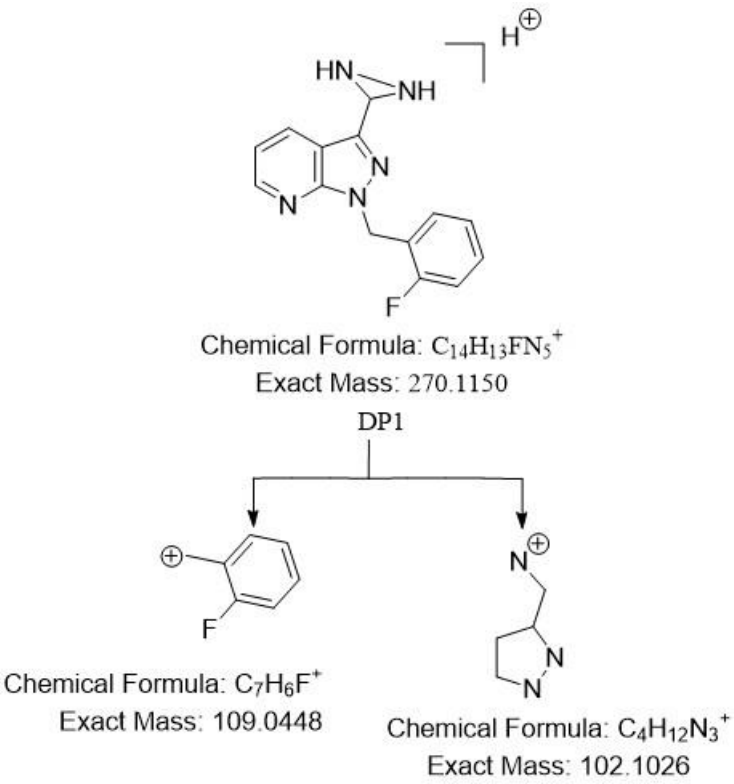


**Figure 7.3.5.2.3:** MS/MS fragmentation pathway of DP1

### 7.3.5.3. DP2

DP2 showed protonated ion peak at *m/z* 315.0581. Its MS/MS spectra showed peaks at *m/z* values of 132.0242, 103.0006, and 109.0159. The fragment with *m/z* 132.0242 was formed due to the cleavage of the pyridine ring. Further loss of $CH_3N$ from this fragment results in the formation of the fragment with *m/z* 103.0006. The fragment with *m/z* 109.0159 was due to the formation of diaminopyrimidine cation.

DP2 was identified as methyl (4,6-diamino-2-(3H-pyrazolo[3,4-b]pyridin-3-yl)pyrimidin-5-yl)(methyl)carbamate. The RDB value for the proposed structure was 10.5, and the error in mmu was –7.31. The MS, MS/MS spectra, and the fragmentation pattern for DP1 is shown in the following figures.

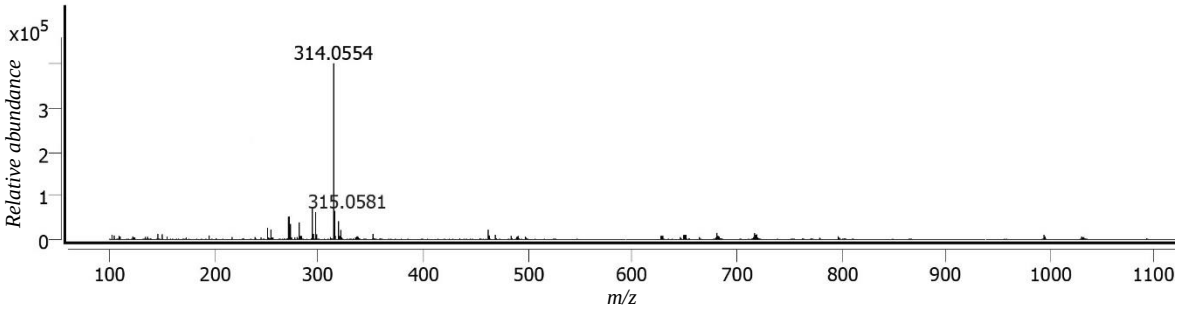


**Figure 7.3.5.3.1:** MS spectra of DP2

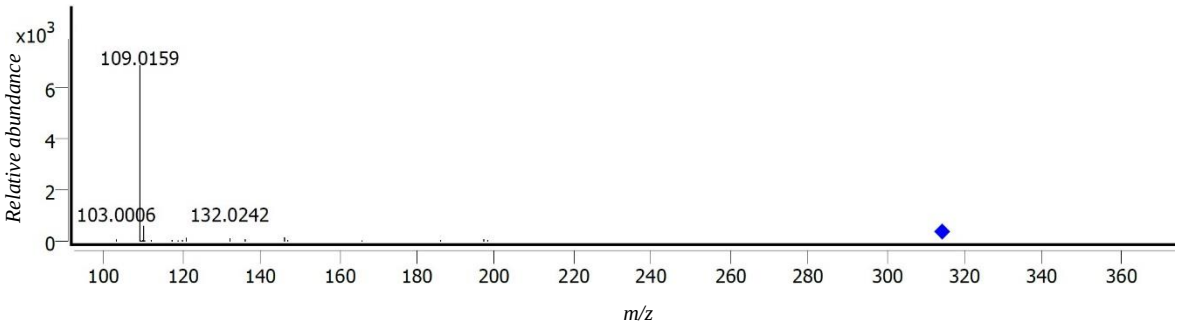


**Figure 7.3.5.3.2:** MS/MS spectra of DP2

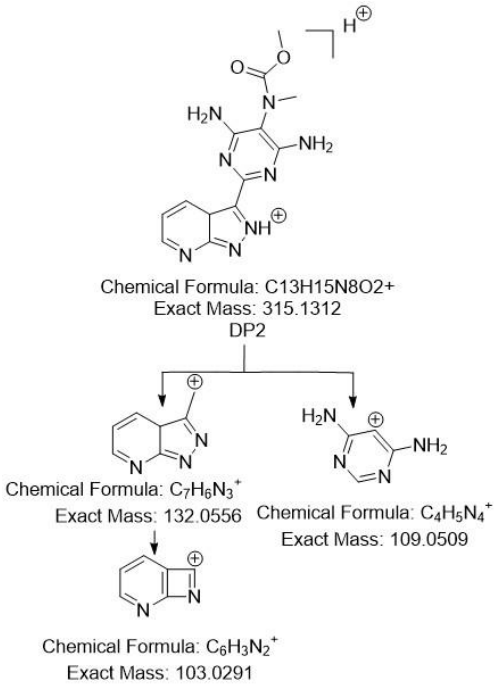


**Figure 7.3.5.3.2:** MS/MS fragmentation pathway of DP2

### 7.3.5.4. DP3

The molecular ion peak of DP3 was seen at *m/z* 351.0962. The MS/MS spectra for DP3 showed peaks at *m/z* 109.0829 (diaminopyrimidine cation), 242.0594 (formed due to cleavage of the pyrimidine ring) and 109.0156 (loss of pyrazolo pyridine moiety from fragment with *m/z* 242.0594).

DP3 was identified as 2-(1-(2-fluorobenzyl)-1H-pyrazolo [3,4-b]pyridin-3-yl)pyrimidine 4,5,6-triamine. The RDB value for the proposed structure was 13.5, and the error in mmu was –5.14. The MS, MS/MS spectra, and the fragmentation pattern for DP1 is shown in the following figures.

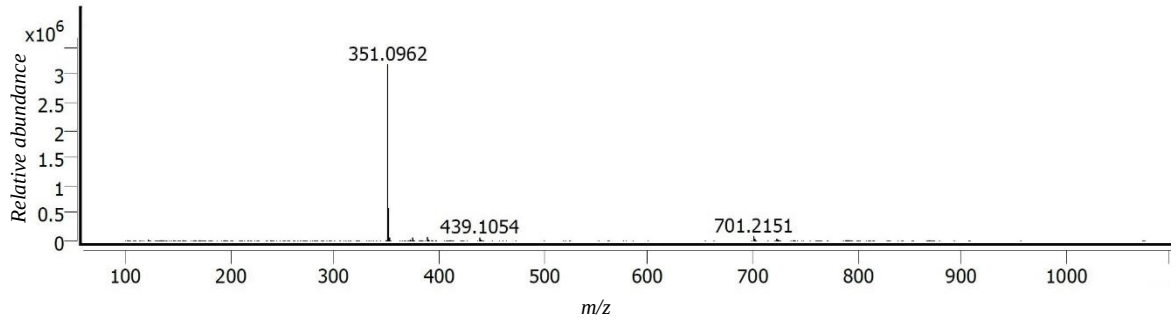


**Figure 7.3.5.4.1:** MS spectra of DP3

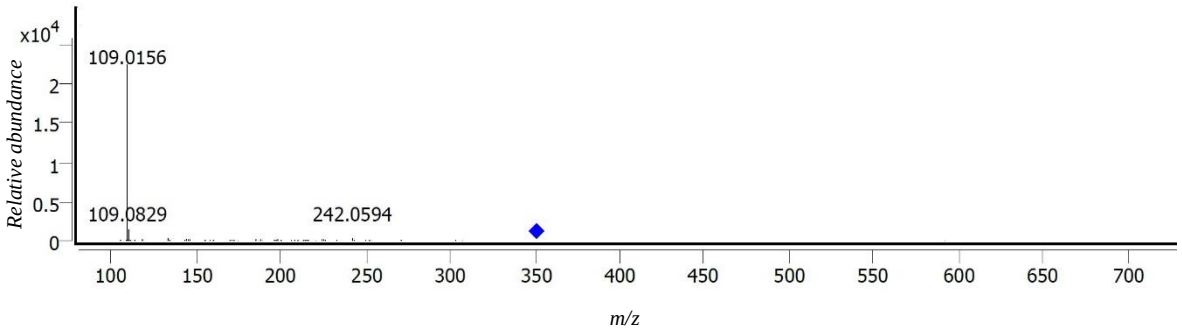


**Figure 7.3.5.4.2:** MS/MS spectra of DP3

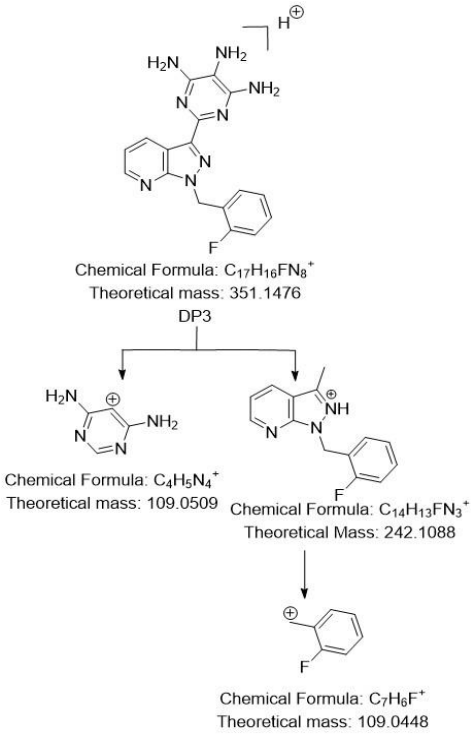


**Figure 7.3.5.4.2:** MS/MS fragmentation pathway of DP3

### 7.3.5.5. DP4

The molecular ion peak for DP4 appeared at *m/z* value of 391.0876. Its fragment ion peaks were seen at *m/z* values of 109.0156 and 118.0204 due to the formation of (4-flurophenyl) methylium and pyrazolo pyridine cations respectively.

DP4 was identified as 6-amino-2-(1-(2-fluorobenzyl)-1H-pyrazolo[3,4-b]pyridin-3-yl)-7-methyl-7,9-dihydro-8H-purin-8-one. The RDB value for the proposed structure was 15.5, and the error in mmu was –5.5. The MS, MS/MS spectra, and the fragmentation pattern for DP1 is shown in the following figures.

The Summary of the MS and MS/MS data along with other attributes is summarized in table 7.3.5.1.

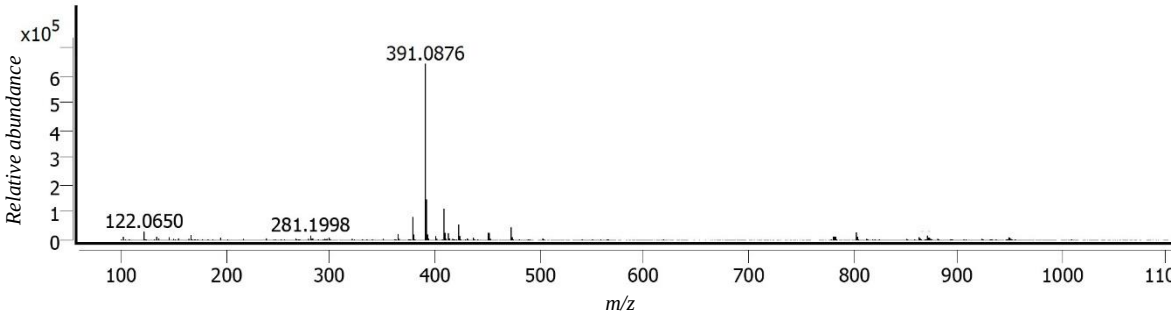


**Figure 7.3.5.5.1:** MS spectra of DP4

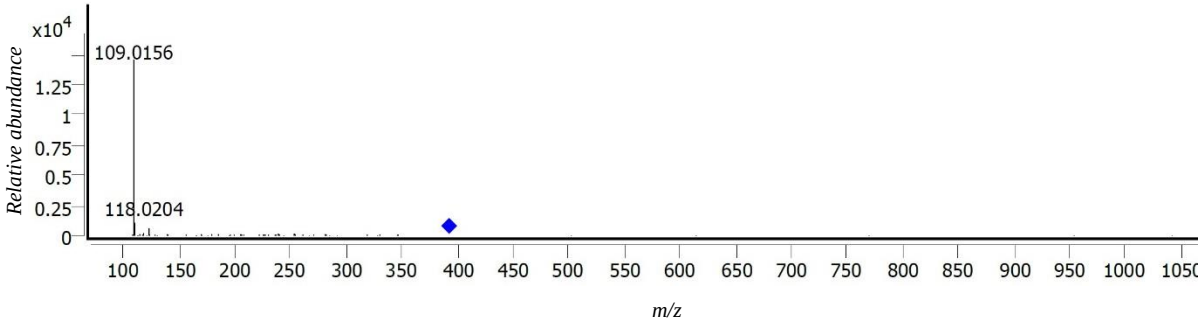


**Figure 7.3.5.5.2:** MS/MS spectra of DP4

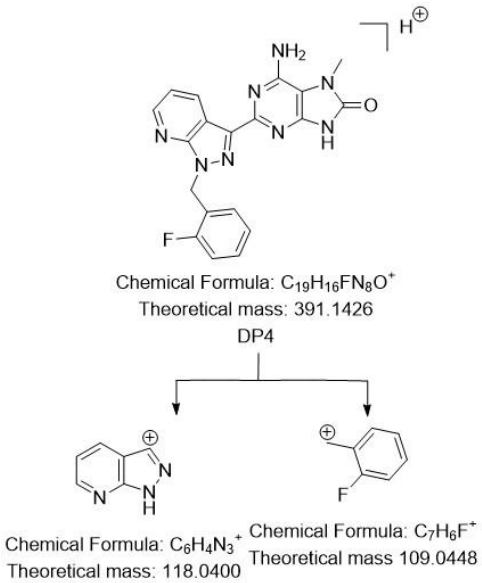


**Figure 7.3.5.5.3:** MS/MS fragmentation pathway of DP4

**Table 7.3.5.1:** Summary of mass data of RIO and its DPs

| Compound | Experimental mass | Most likely molecular formulae | Theoretical mass | RDB | Error in mmu | Fragments | | Most probable molecular formulae for fragments. |
|---|---|---|---|---|---|---|---|---|
| | | | | | | Experimental mass | Theoretical mass | |
| DP1 | 270.0699 | $C_{14}H_{13}FN_5^+$ | 270.1150 | 10.5 | -4.51 | 109.0157 | 109.0448 | $C_7H_6F^+$ |
| | | | | | | 102.0056 | 102.1026 | $C_4H_{12}N_3^+$ |
| DP2 | 315.0581 | $C_{13}H_{15}N_8O_2^+$ | 315.1312 | 10.5 | -7.31 | 132.0242 | 132.0556 | $C_7H_6N_3^+$ |
| | | | | | | 103.0006 | 103.0291 | $C_6H_3N_2^+$ |
| | | | | | | 109.0159 | 109.0509 | $C_4H_5N_4^+$ |
| DP3 | 351.0962 | $C_{17}H_{16}FN_8^+$ | 351.1476 | 13.5 | -5.14 | 109.0829 | 109.0509 | $C_4H_5N_4^+$ |
| | | | | | | 242.0594 | 242.1088 | $C_{14}H_{13}FN_3^+$ |
| DP4 | 391.0876 | $C_{19}H_{16}FN_8O^+$ | 391.1426 | 15.5 | -5.5 | 109.0156 | 109.0448 | $C_7H_6F^+$ |
| | | | | | | 118.0204 | 118.0400 | $C_6H_4N_3^+$ |
| RIO | 423.1147 | $C_{20}H_{19}FN_8O_{2+}$ | 423.1615 | 15 | -4.68 | 109.0156 | 109.0448 | $C_7H_6F^+$ |
| | | | | | | 253.0476 | 253.0884 | $C_{14}H_{10}FN_4^+$ |
| | | | | | | 109.0163 | 109.0448 | $C_7H_6F^+$ |

## 7.3.6. *In-silico* ADMET studies of RIO and its DPs

### Molecular modelling studies

Molecular modelling studies were performed to assess binding affinities of RIO and its DPs with sGC receptor. The following docking protocol was used.

Using Marvin Sketch[88], the structure of RIO and its DPs were sketched and cleaned. The soluble guanylate cyclase structure (PDB code:7LGK) was retrieved from the protein data bank. Utilizing Discovery studio visualizer[119] and Swiss PDB viewer[120], respectively, it was prepared and minimized. Using a grid receptor generation tool. The native ligand downloaded with the protein (Runcaciguat) was used to determine the binding site through a grid receptor generation tool. The investigated compounds were optimized and docked with the aid of the PyRx virtual screening tool[121] and evaluated with the aid of the discovery studio visualizer.

The overall binding affinity for RIO was 9.2 kcal/mole and the binding affinities of DPs (1–4) were 8.3, 7.5, 8.9, and 10.2 kcal/mole, indicating that DP4 has a marginally higher binding affinity than the intact drug.

The summary of the binding interactions of the compounds with the receptor is seen in figure 7.3.6.1 and table 7.3.6.1.

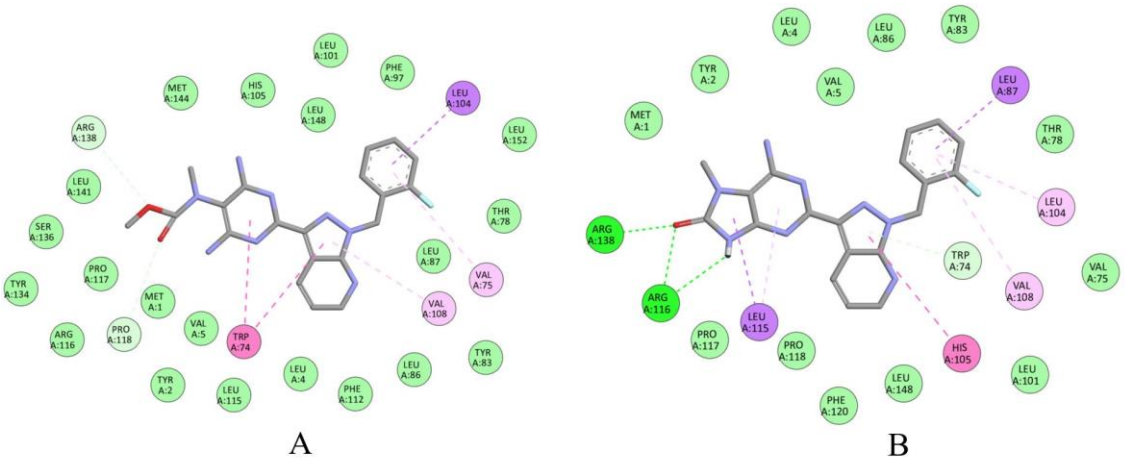


**Figure 7.3.6.1:** Interaction of RIO(A) and DP4(B) with receptor(7LGK).

**Table 7.3.6.1:** Summary of interactions with the receptor

| Name | Interactions. | | | | | | |
|---|---|---|---|---|---|---|---|
| | **Van der waals** | **Carbon hydrogen bond** | **Conventional hydrogen bond** | **Pi-Hydrogen bond** | **Pi-sigma** | **Pi-Pi T shaped** | **Pi-alkyl** |
| **RIO** | Met 144, His 105, LEU 148, Leu 101, PHE 97LEU 152 THR 78, LEU 87, TYR 83, LEU 86, PHE 112, LEU 4, LEU 115, VAL 5, TYR 2, MET 1, ARG 116, PRO 117, TYR 134,SER 136, LEU 141 | PRO 118, ARG 138. | -- | -- | LEU 104 | TRP 74 | VAL 108, VAL 75 |
| **DP4** | MET 1, TYR 2, LEU 4, VAL 5, LEU 86, TYR 83, THR 78, VAL 75, LEU 101, LEU 158, PHE120, PRO 118, PRO 117 | -- | ARG 138, ARG 116 | TRP 74 | LEU 87, LEU 115 | HIS 105 | LEU 104, VAL 108. |

**pkCSM**

RIO and its DPs were predicted to have intestinal absorption of > 80 %. Except DP2 all acted as PgP substrate. All had log BB value of > -0.3 indicating that they have poor blood brain permeability. RIO, DP2, DP3, and DP4 were predicted to possess hepatotoxicity, while DP4 was flagged for mutagenic potential. Besides, Riociguat also inhibited CYP2C9 and CYP3A4, while DP1 inhibited CYP1A2. The summary of the various predictions of pkCSM is shown in table 7.3.6.2.

**ToxTree and OSIRIS property explorer**

Screening through ToxTree indicated that RIO, DP2, DP3, and DP4 are mutagenic to the presence of the primary aromatic amine in their structure; however, the final screening through OSIRIS property explorer returned a negative mutagenic result for all and revealed that they do not possess any, irritant, tumorigenic or reproductive risks.

**Table no 7.3.6.2:** Summary of pKCSM predictions

| Compound | Intestinal absorption (%absorbed) | PgP Substrate | BBB Permeability (log BB) | CYP1A2 inhibitor | CYP2C19 inhibitor | CYP2C9 Inhibitor | CYP2D6 Inhibitor | CYP3A4 Inhibitor | AMES toxicity | Hepato toxicity |
|---|---|---|---|---|---|---|---|---|---|---|
| Riociguat | 93.8% | Yes | -0.79 | No | No | Yes | No | Yes | No | Yes |
| DP1 | 96% | Yes | -0.55 | Yes | No | No | No | No | No | No |
| DP2 | 81% | No | -1.087 | No | No | No | No | No | No | Yes |
| DP3 | 81.6% | Yes | -1.547 | No | No | No | No | No | No | Yes |
| DP4 | 81.4% | Yes | -2.134 | No | No | No | No | No | Yes | Yes |

# 7.4 Experimental work

## 7.4.1. Instrumentation

**Table 7.4.1.1:** List of instruments.

| Sr.no. | Instrument | Make and specification |
|---|---|---|
| **1** | **HPLC** | LC-4000, Jasco, Japan. Made up of a model CO-4061 temperature controlled column compartment, a model PU 4180 quaternary pump system with inline degasser, a model AS-4050 autosampler, Chromenav (version, 2.01.06) data acquisition software, LC-NET II interface box, Acer workstation computer running Microsoft windows 7 professional operating system. |
| **2** | **Column** | Phenomenex C18 (150mm ×4.6mm, 5µm). |
| **3** | **Sonicator** | Citizon, Vadodra, India. |
| **4** | **pH meter** | Digital pH meter, Elico, India. |
| **5** | **Precision balance** | Wensar digital, Chennai, India. |
| **6** | **Double distillation assembly** | Bhanu scientific instruments, Bangalore, Karnataka. |
| **7** | **Hot air oven** | Universal, Ambala, India. |
| **8** | **Constant temperature water bath** | Generic. |
| **9** | **Photostability chamber** | Newtronics lifecare Pvt.Ltd, Mumbai,India. |
| **10** | **MS system** | Agilent 1200 series HPLC system, 6200 series QTOF. Intel i7 5820k based workstation computer running windows 10 professional operating system with 32 GB of ram, ToxTree (version, 3.1.0-1851-1525442531402), OSIRIS property explorer. |
| **11** | **Workstation for *in-silico* studies** | |

## 7.4.2. Chemicals and reagents

1. **Acetonitrile (HPLC grade):** Qualigen, Mumbai, Maharashtra
2. **Hydrochloric acid:** Molychem, Thane, Mumbai.
3. **Hydrogen peroxide:** Molychem, Thane, Mumbai.
4. **Ammonium formate:** Molychem, Thane, Mumbai.
5. **Water (HPLC grade):** Finar, Ahmedabad, Gujarat.
6. **Sodium Hydroxide:** Finar, Ahmedabad, Gujarat.

## 7.4.3. Working standard

RIO was obtained as a gift sample from MSN laboratories, Hyderabad, India

## 7.4.4. Solution preparation

### 7.4.4.1. Preparation of stock solution of RIO

RIO (50 mg) was weighed on a precision balance and transferred into a calibrated 50 mL volumetric flask. To it, 20 mL of acetonitrile was added and the contents were sonicated for 5 min. The volume was made to mark with acetonitrile (HPLC grade) to get a solution having a concentration of 1000µg/mL.

### 7.4.4.2. Preparation of ammonium formate buffer (pH=3.7)

Ammonium formate (630 mg) was weighed and transferred into 1000 mL HPLC grade water and mixed thoroughly. Solution was then filtered through a 0.45µ membrane filter under vacuum and the pH was adjusted to 3.7 with glacial acetic acid.

### 7.4.4.3. Preparation of diluent

Ammonium formate buffer and acetonitrile were mixed in a ratio of 50:50 (v/v) and sonicated for five minutes to prepare the diluent.

### 7.4.4.4. Preparation of 1 N hydrochloric acid

Concentrated hydrochloric acid (8.5 mL) was slowly diluted to 100 mL mark using HPLC grade water in volumetric flask to get 0.1 N hydrochloric acid.

### 7.4.4.5. Preparation of 2 N hydrochloric acid

Concentrated hydrochloric acid (17 mL) was slowly diluted to 100 mL mark using HPLC grade water in volumetric flask to get 2 N hydrochloric acid

### 7.4.4.6. Preparation of 1 N sodium hydroxide

Sodium hydroxide flakes (4000 mg) was dissolved with the aid of sonication in 50 mL of HPLC grade water using 100 mL volumetric flask. The volume was made up to mark with HPLC grade water to get 0.1 N sodium hydroxide solution.

#### 7.4.4.8. Preparation of 15% hydrogen peroxide

Hydrogen peroxide (15%) was prepared by diluting 5 mL of 30% hydrogen peroxide to 10 mL with HPLC grade water using 10 mL volumetric flask.

### 7.4.5. Forced degradation studies

The forced degradation studies were performed to get substantial degradation of drug. The drug was stressed under conditions viz. acidic, basic, neutral, oxidative, thermal, and photolytic. To get an accurate representation, four samples were prepared under each condition excluding thermal and photolytic; blank under normal condition (blank untreated), blank under stress condition (blank treated), drug solution under normal condition (standard), and drug under the stress condition. For thermal and photolytic conditions, the chromatogram obtained were compared with the chromatogram of drug stored under normal conditions.

#### 7.4.5.1. Hydrolytic degradation

The hydrolytic degradation was conducted under acidic, basic, and neutral condition. The stock solution of drug (1 mL) was mixed with 0.1 mL 1 N / 2 N HCl in 10 mL volumetric flask and the solution was kept under stress for 48 h. In order to accelerate the degradation the study was caried out at 70 ℃ for 7 h using 2 N HCl. After the stress period the samples were neutralized by using equal strength of sodium hydroxide and the volume was made to mark with diluent to get a concentration of 100 µg/mL of RIO. For base and neutral hydrolysis, a similar methodology was used. The samples treated with base were neutralized using corresponding strength of hydrochloric acid. All the samples were analysed using HPLC under optimized chromatographic conditions.

#### 7.4.5.2. Oxidative degradation

Stock solution RIO ( 1 mL) was allowed to mix with 0.1 mL of oxidant (15% hydrogen peroxide) for 48 h in 10 mL volumetric flask. The volume was made up to mark with diluent to get a concentration of 100 µg/mL and samples were analysed using HPLC under optimized chromatographic conditions.

#### 7.4.5.3. Thermal degradation

RIO (100 mg) was sealed in a glass ampoule and heated in an oven at 70 ℃ for 7 hours. After the stress period, the contents of the ampoules were diluted with diluent to get a

concentration of 100 µg/mL. In similar fashion, one sample of RIO was kept at room temperature as control and samples were analysed using HPLC under optimized chromatographic conditions.

#### 7.4.5.4. Photolytic degradation

Photolytic degradation was carried out in solid and liquid state. Two samples were prepared for solid state degradation study. In first case, the drug was spread as a thin layer inside a petri dish and kept in a photostability chamber along with control sample covered with aluminium foil. In the second case, 10 mg of drug was taken into 10 mL volumetric flask and exposed to sunlight for 7 days along with control sample in aluminium foil.

Photolytic degradation in liquid state was carried out by keeping 1 mL stock solution of RIO in volumetric flask inside a photostability chamber along with a control sample covered using aluminium foil.

The samples that were kept in the photostability chamber were exposed to ICH-mandated dose of light (1.2 million lux H of overall illumination and 200 wh/$m^2$ of integrated near U.V. energy). After the exposure period, the samples were diluted up to the mark to get 100 µg/mL concentration of drug using diluent and analysed using HPLC under optimized chromatographic conditions.

## 7.4.6. Validation studies

The developed and optimized HPLC method was validated as per the relevant ICH guideline.

#### 7.4.6.1. Specificity and selectivity

The specificity of the HPLC method was ascertained by the resolution values obtained between the nearest eluting peaks of degradation product and peak of drug and degradation product. The method's selectivity for the individual component was done through the % peak purity value obtained through the data acquisition software. The degradation samples were mixed in equal proportion and injected into HPLC.

#### 7.4.6.2. Linearity and range

A series of dilutions (5 levels) were prepared in range of 20-120 µg/mL. At each level the sample was injected in triplicate, and the average area was obtained. The average area was plotted against the concentration to obtain a simple linear regression equation and the correlation coefficient. Five incremental concentrations (20, 40, 50, 60 and 120 µg/mL) were prepared by accurately withdrawing 0.1, 0.2, 0.5, 0.6 and 1.2 mL of stock solution of RIO (100 µg/mL) and diluting it to 10 mL using diluent in a volumetric flask.

#### 7.4.6.3. Accuracy

The accuracy of the HPLC method was determined by the standard addition method. The degraded sample was spiked at 80%, 100%, and 120% of the target assay concentration (50 µg/mL) with standard drug solution. At each level, the sample was injected in triplicate, and the average % recovery was computed. Spiked samples were prepared by accurately transferring 0.4, 0.5 and 0.6 mL of stock solution of RIO to degraded sample and making the volume to 10 mL.

#### 7.4.6.4. Precision

Precision (intra and inter) of the HPLC method was done at 40, 50, and 60 µg/mL. At each level, the sample was injected in triplicate, and the % relative standard deviation was determined (% RSD). Three incremental concentration (40, 50, and 60 µg/mL) were prepared by accurately withdrawing 0.4, 0.5, and 0.6 mL of stock solution of RIO (1000 µg/mL) and diluting it to 10 mL using diluent in a volumetric flask.

### 7.4.7. *In-silico* studies

The *in-silico* studies were done using open-source options like the pkCSM webserver, ToxTree and OSIRIS property explorer.

The structures of the degradation products were sketched using Marvin by ChemAxon. The structures were copied as smiles and fed into the pkCSM webserver. ADMET prediction mode was selected which uploads the task for processing.

Toxtree accepts the structure in the form of SMILES which were generated similarly as discussed above. The decision tree (In vitro mutagenicity (Ames test) alerts by ISS) was selected from the method tab, and the estimate button was clicked.

OSIRIS property explorer accepts SMILES or CAS no as input and runs predictions.

The comparative receptor binding studies was done by using PyRx virtual screen tool. The sGC structure (PDB id: 7LGK) was downloaded from protein data bank. The protein was prepared for docking using standard protocol by using discovery studio visualizer and Swiss PDB viewer. The sketched compounds structure were imported in SDF format in PyRx virtual screening tool. They were then prepared for docking by converting them to PDBQT format and minimized using the inbuilt module. Receptor grid box was generated by using the native ligand (Runcaciguat) and docking was carried out. The binding interactions were analyzed using discovery studio visualizer.

# Chapter 8

# Summary and conclusion

## 8.0. Introduction

Based on the literature review, FMTE, PIMO, RIO and HALO (APIs) were selected as drug candidates for the stability testing. RP-HPLC methods were developed for the selected drugs to monitor drug degradation behavior. Individual drugs were then subjected to various stress conditions mentioned in the ICH Q1A (R2) guideline, and the samples were analyzed by the RP-HPLC method. Whenever required HPLC method was optimized by changing the chromatographic parameters like; elution mode, the composition of mobile phase, pH, and column to get the desired resolution between the drug and the DPs and among the DPs. Following the method optimization, the RP-HPLC methods were validated in accordance with the ICH Q2 (R1) guideline.

The developed RP-HPLC method was adopted for the mass spectrometry studies, which were used to determine the molecular mass (MS), chemical structure and the fragmentation pattern (MS/MS) of the individual DPs. The data thus obtained was used to construct the fragmentation pattern of the DPs.

The structure of the DPs were then scanned through the opensource ADMET prediction tools like the pKCSM webserver. Secondary screening for the mutagenic potential was performed using freely available offline utilities like ToxTree and the OSIRIS property explorer. For the drug riociguat, docking studies were carried out by using PyRx virtual screening tool to access the binding affinities between the drug and DPs with the soluble guanylate cyclase receptor (PDB code: 7LGK).

# 8.1 Pimozide (PIMO)

## 8.1.1. Drug profile

PIMO is a neuroleptic drug used to treat schizophrenia and relieve the symptoms associated with Tourette's disorder. A recent study has also revealed that PIMO therapy can be used to treat the intracellular bacterial infection.

PIMO is colourless, microcrystalline powder, insoluble in water but exhibits varying solubility in ethanol, ether, and methanol. Its IUPAC name is 3-[1-[4,4-bis(4-fluorophenyl)butyl] piperidin-4-yl]- 1H-benzimidazole-2-one.

PIMO is an official drug in the USP-NF and the EP. The EP lists five process impurities of PIMO (A-E).

## 8.1.2. Mechanism of action

PIMO's ability to suppress the motor and the phonic tics associated with Tourette's syndrome is due to its dopaminergic blocking activity. The tics are believed to be caused by the oversensitivity of the dopamine receptors. PIMO binds to the D2 receptor and causes its inhibition in the central nervous system.

## 8.1.3. Development of a RP-HPLC method for monitoring the drug degradation behavior of PIMO

Authentic literature sources were referred to get an idea about published HPLC methods developed for the determination of PIMO. Initially, preference was given to compendial methods. The related substances (RS) method in the USP-NF and EP used gradient mode (flow rate 2.0 ml/min, $\lambda_{max}$ 280 nm) of elution with mobile phase made of ammonium acetate (32 mM) and tetrabutylammonium hydrogen sulfate (32 mM) as aqueous, and acetonitrile as an organic component. Bioanalytical HPLC methods used isocratic mode of elution using buffers like ammonium acetate (5 mM, pH 3.5, adjusted using acetic acid, flow rate 0.22 ml/min, $\lambda_{max}$ 280 nm) and sodium dihydrogen phosphate (50 mM, pH 3.0, adjusted using 1% phosphoric acid). HPLC method for estimation of PIMO from bulk drug used disodium hydrogen phosphate (50 mM, pH 6.2, adjusted using orthophosphoric acid, flow rate 1.0

mL/min, $\lambda_{max}$ 285 nm) as aqueous component. Common factors among the reported HPLC methods were the use of acetonitrile and C18 column for better retention and effective separation of the components. Moreover, the wavelength of detection was 280 nm. Based on these facts, a HPLC method was designed using ammonium acetate (10 mM, pH adjusted to 3.7 with glacial acetic acid, $\lambda_{max}$ 280 nm) as the aqueous phase and acetonitrile as the organic phase. Gradient elution mode was applied for effective separation of polar impurities on Phenomenex C18 (150 mm X 4.6 mm, 5µm) column. The pH of buffer was maintained at 3.7 to get drug into completely ionized form. Moreover, ammonium acetate is a volatile buffer compatible with mass detector. It is a salt of weak acid and weak base, its solution has pH 7. The buffer does not have significant buffer capacity at pH 7 but it exhibit buffer capacity near pH 4.75 ± 1 (pKa of acetic acid) and pH 9.25 ± 1 (pKa of ammonia).

The summary of the optimized stability indicating assay method (SIAM) parameters for PIMO is provided table 8.1.3.1.

**Table 8.1.3.1:** Optimized chromatographic conditions for monitoring the drug degradation pattern for PIMO.

| | |
|---|---|
| **Mobile phase** | Acetonitrile: Ammonium acetate (10 mM, pH adjusted to 3.7 with glacial acetic acid) in gradient elution mode ($T_{min}$/A:B v/v-$T_0$/15:85;$T_{30}$/45:55;$T_{35}$/15:85;$T_{40}$/15:85) |
| **Column** | Phenomenex C18 (150 mm X 4.6 mm, 5µm) |
| **Flow rate** | 1 mL/min |
| **Wavelength** | 280 nm. |

## 8.1.4. Forced degradation studies

PIMO was stressed under the conditions specified in the ICH guideline Q1A (R2) *viz* hydrolytic (acidic, basic, neutral), oxidative, thermal, and photolytic. The drug exhibited stability under hydrolytic, thermal, and photolytic conditions, while it degraded (~ 26 %) under oxidative stress condition (15% $H_2O_2$ at room temperature for 48 h). Oxidative stress condition led to the formation of five DPs named DP 1 to 5 from left to right as per their elution order.

Among all DPs generated, DP-3, and major degradation product DP-5 were later identified as impurity B and impurity E respectively as per USP monograph**.** DP1, DP2, and DP4 were unknown degradation products of PIMO.

A summary of the applied stress conditions is tabularized in table no 8.1.4.1.

**Table 8.1.4.1:** Summary of the stress conditions applied to PIMO.

| **Conditions** | **Stressor** | | **Duration and nature of exposure.** | **Observation.** |
|---|---|---|---|---|
| **Hydrolysis** | Acid | 0.1,1N HCl | RT (2 days), Heat at 70℃ on constant temperature water bath for 7 h. | No degradation. |
| | Base | 0.1,1N NaOH | RT (2 days), Heat at 70℃ on constant temperature water bath for 7 h. | No degradation. . |
| | Neutral | water | RT (2 days), Heat at 70℃ on constant temperature water bath for 7 h. | No degradation. |
| **Oxidation** | 15% $H_2O_2$ | | RT (2days). | Formation of DPs (1-5) |
| **Photolysis** | Sunlight | | 7 days | No degradation |
| | Photo-stability chamber | | Fluorescence light 1.2 million lux hours and UV light 200 $Whm^{-2}$ | No degradation |
| **Thermal** | 70℃ | | 7 days. | No degradation. |

*RT= room temperature.*

## 8.1.5. Validation of the HPLC method

The HPLC methods was validated as per the ICH guideline. The method was found to be specific (resolution > 1 among all the peaks) and selective (peak purity > 99%). The linearity, range, precision, accuracy, and robustness results are as summarized in table no 8.1.5.1.

**Table 8.1.5.1:** Summary of validation parameters for PIMO.

| Validation parameters | | | Results. |
|---|---|---|---|
| **Specificity and selectivity** | | | Resolution >1, peak purity> 99% |
| **Linearity** | Equation of the regression line | | y=6936.9x-20506 |
| | $r^2$ | | 0.999 |
| | Range (µg/mL) | | 10-100 |
| **Precision** | | µg/mL | Mean peak area ± SD; %CV |
| | Intra-day | 40 | 178008 ±1906; 1.1 |
| | | 50 | 336338 ±4650; 1.4 |
| | | 60 | 672615 ± 1844; 0.3 |
| | Inter-day | 40 | 168221 ±3111; 1.8 |
| | | 50 | 343607 ±1021; 0.3 |
| | | 60 | 676497 ± 4107; 0.6 |
| **Accuracy** | Spiked concentration (Target concentration=50 µg/mL) | µg/mL | % recovery mean ± SD, %CV |
| | | 40 (80%) | 40.6 ± 0.26,0.64 |
| | | 50 (100%) | 50.8 ± 0.10,0.19 |
| | | 60 (120%) | 61.1 ± 0.19,0.31 |
| **Robustness** | | pH (±0.5), flow rate(±0.1 mL), mobile phase composition(±1%), wavelength (± 3nm) of optimized value. | Theoretical plates >2000<br>Resolution >1<br>Asymmetry <2 |

## 8.1.6. Mass studies.

The structural characterization of the degradation products was carried out using LC-MS and LC-MS/MS. The LC-MS and LC-MS/MS spectra were recorded in positive electro spray ionization mode (+ESI).

The molecular weight of PIMO is 461.2351 g/mole. The LC-MS spectra recorded in the +ESI mode showed molecular peak ion at *m/z* 462.2380. The MS/MS spectra of PIMO showed peaks at *m/z* 328.1889 and 201.1028. PIMO loses $C_7H_6N_2O$ fragment with theoretical mass 134.0480 (1,3-dihydro-*2H*-benzo[*d*]imidazol-2-one) to yield fragment with *m/z* 328.1889. Further cleavage of this fragment forms the fragment with *m/z* 109.0452 ((4-fluorophenyl) methylium). This fragment forms a tropylium carbocation which confers stability due to the conjugation of positive charge with pi electrons. The radical cation with *m/z* 201.1028 is formed due to loss of bis-4-flurophenyl-butyl moiety from the drug and subsequent collapse of the piperidine ring.

The protonated ion peak for DP1 was seen at *m/z* 428.1978. The MS/MS spectra showed three fragment ion peaks at *m/z* 276.1383, 230.1279, and 201.1008. The fragment with *m/z* 276.1383 is created due to the loss of the benzimidazole fragment and the formation of the 5-membered heterocyclic pyrrolidine from piperidine. The loss of $C_{15}H_{18}$ from DP1 forms the fragment with *m/z* 230.1279. The fragment with *m/z* 201.1008 is seen in the fragmentation of the drug and is formed via a similar mechanism. This fragment loses the pyrrole ring to form a fragment with *m/z* 149.0754. DP1 was identified as 1-(1-(4,4-diphenylbutyl) piperidin-4-yl)-2,3-dihydro-1H-benzo[d]imidazole-2-ol.

The molecular ion peak for DP2 was seen at *m/z* 404.2140. DP2 showed fragment ion peaks at *m/z* 326.1704 and 387.1868. The fragment with *m/z* 326.1704 is formed due to the loss of $C_6H_6$ (theoretical mass = 78.0470). The fragment with *m/z* 387.1868 is formed due to conversion of five membered ring to four membered ring along with loss of a nitrogen. The Loss of $C_2H_2$ from this fragment creates a secondary fragment with *m/z* 361.2073. Based on the deduced structure DP2 was assigned the name as 1-(1-(4,4-diphenylbut-1-en-1-yl)-1,4-dihydropyridin-4-yl)-1H-benzo[d]imidazole.

The molecular ion peak for DP3 was seen at *m/z* 444.2088. The formation of DP3 was attributed to the dehalogenation of a single fluorophenyl moiety. The MS/MS spectra showed peaks at *m/z* 427.2042, 326.1699, 149.0750, and 109.0444,. The formation of the tropylium cation (*m/z* 109.0444) is like that of the drug. The fragment with *m/z* 427.2042 was formed due to cleavage of imidazole ring. Loss of a fluorophenyl moiety from DP3 forms the fragment with *m/z* 326.1699. This fragment further loses but-3-en-1-ylbenzene ($C_{10}H_{10}$) to form a secondary fragment with *m/z* 196.1072. At the same time, the fragment with *m/z* 149.0750 is formed due to the cleavage of the bond connecting benzimidazole

moiety to piperidine. DP3 was identified as 1-(1-(4-(4-flurophenyl)-4-phenylbutyl) piperidie-4-yl)-1,3-dihydro-2H-benzo[d]imidazole-2-one.

The molecular ion peak for DP4 was observed at *m/z* 324.1552. The CID-MS/MS spectra showed three major fragments with *m/z* 203.0658, 135.0596, and 109.0442. The fragment with *m/z* 203.0658 is formed due to the loss of a fragment with a theoretical mass of 121.0892 and molecular formulae $C_8H_{11}N$. This fragment further loses a fluorobenzene moiety to create a fragment with *m/z* 109.0442. The radical cation with *m/z* 135.0596 has formed due to the loss of bis(4-fluorophenyl) methane moiety. DP4 was designated IUPAC name as 1-(4,4-bis(4-fluorophenyl) but-1-en-1-yl)-1,2-dihydropyridine.

The molecular ion peak for DP5 was seen at *m/z* 478.2298. It had a molecular weight of sixteen amu higher than PIMO, indicating the formation of N-oxide. Tertiary amines are known for their propensity to form N-oxides. The MS/MS spectra showed two major fragments at *m/z* 326.1709 and 230.1276. The fragment with *m/z* 326.1709 is formed due to loss of benzimidazole moiety from PIMO. This fragment further breaks down to give fragment with *m/z* 109.0438. The loss of 4,4′-Bis(fluorophenyl) propyl moiety fragment creates the fragment with *m/z* 230.1276. This fragment undergoes cleavage to form a radical cation with *m/z* 201.1009 which, further fragments to produce another fragment with *m/z* 149.0754. DP5 was identified as; 1-(4,4-bis(4-fluorophenyl) butyl)-4-(2-oxo-2,3-dihydro-1H-benzo[d]imidazol-1-yl) piperidine-1-oxide.

### 8.1.7. *In-silico* ADMET studies.

The *in-silico* studies were done to access the ADMET profile of the drug and the degradation products. The pkCSM webserver was used to predict the ADMET properties like intestinal absorption, the extent of binding with p-glycoprotein (PgP), blood-brain permeability, inhibition of the various isoforms of the cytochrome P450, AMES toxicity, and hepatotoxicity. The secondary screening of the compounds for mutagenicity was carried out using ToxTree and OSIRIS property explorer.

There were a few alerts regarding the inhibition of specific CYP450 enzyme subfamilies. PIMO, DP3 and DP5 were flagged to possess hepatotoxicity whereas, PIMO, DP1, DP3, and DP5 were positive for genotoxicity.

Secondary screening for genotoxicity was done with ToxTree and OSIRIS property explorer. However, screening results were negative for the drug and its degradation products. OSIRIS property explorer also showed that they did not possess tumorigenic, irritant, or reproductive risks.

## 8.2. Felbamate (FMTE)

### 8.2.1 Drug Profile

FMTE is an anticonvulsant drug used to treat partial seizures, and generalized seizures in children due to Lennox-Gas taut syndrome. The IUPAC name for FMTE is 2-phenyl-1, 3-propanediol.

It is a white crystalline powder with a very slight solubility in water, slightly soluble in alcohol, and freely soluble in organic solvents.

### 8.2.2 Mechanism of action

FMTE has anticonvulsant activity due to the inhibitory effect on the $GABA_A$ receptor. It also inhibits the glycine-mediated triggering of the N-methyl-D-aspartate (NMDA) receptor. $GABA_A$ receptor controls the transmission of the chloride anion, which is associated with inhibitory activities while, the NMDA receptor controls the sodium and the calcium passage.

These voltage-dependent ion channels functions by controlling the excitability and stabilizing the neuronal membrane.

### 8.2.3. Development of an RP-HPLC method for monitoring the drug degradation behavior of FMTE

A detailed literature search was conducted to find out the available analytical methods for FMTE. FMTE is official in the USP-NF. Its compendial method uses octadecylsilane column (C18) and isocratic mode of elution (flow rate 1.8 mL/min, $\lambda_{max}$ 210nm) with mobile phase comprising of acetonitrile, methanol, and water (126:84:790, v/v/v). The reported bioanalytical HPLC methods use mobile phase consisting of phosphate buffer (15-50mM,

pH (6.1-7.4), adjusted by using phosphoric acid) and ammonium acetate (10 mM), as aqueous phase and acetonitrile as an organic constituent. There was a report on HPLC method for determination of FMTE in tablets which uses mobile phase made up of acetonitrile and water. Literature also revealed a single stability-indicating UHPLC method that was developed using mobile phase comprised of potassium dihydrogen orthophosphate (pH 3.5) and methanol. Based on the information gathered HPLC trials were devised, which led to the development of an isocratic HPLC method consisting of ammonium formate (10 mM, pH 3.7, adjusted with formic acid) and acetonitrile in a ratio of 40: 60 (v/v). The pH selected maintains the drug in completely ionized form. Ammonium formate is a volatile buffer compatible with mass spectrometry having buffering capacity in pH of 3.77 ± 1 (pKa of formic acid 3.77) and pH of 9.25 ± 1(pKa of ammonia 9.25). The optimized stability indicating assay method (SIAM) parameters for FMTE and the chromatogram showing FMTE and its hydrolytic (basic) degradation products is shown in table 8.2.3.1.

**Table 8.2.3.1:** Optimized chromatographic conditions for monitoring the drug degradation pattern for FMTE

| | |
|---|---|
| **Mobile phase** | Acetonitrile: Ammonium formate (10 mM, pH adjusted to 3.7 with formic acid), 40:60 (v/v) |
| **Column** | Phenomenex C8 (250mmX4.6mm, 5µm) |
| **Flow rate** | 1 mL/min |
| **Wavelength** | 206nm. |

## 8.2.4. Forced degradation studies

The forced degradation studies were carried out under the conditions summarized in table 8.2.4.1. The drug exhibited degradation (~ 52 %) in the presence of 0.1 N NaOH at room temperature for 48 hours and formed two degradation products. Both the degradation products were polar and eluted before the drug. At room temperature, DP2 emerged as the major degradation product. On heating at 70 ℃ with 0.1 N NaOH, it was observed that after 2 h, the drug degraded completely, with DP1 being the prominent degradation product.

FMTE was stable under acidic, neutral, oxidative, photolytic, and thermal conditions.

**Table 8.2.4.1:** Summary of the stress conditions applied to FMTE

| Conditions | Stressor | | Duration and nature of exposure. | Observation. |
|---|---|---|---|---|
| **Hydrolysis** | Acid | 0.1 HCl | RT (2 days), Heat at 70℃ on constant temperature water bath for 7 hours. | No degradation. |
| | Base | 0.1 NaOH | RT (2 days), Heat at 70℃ on constant temperature water bath for 7 hours | Formation of DP1 and DP2. |
| | Neutral | water | RT (2 days), Heat at 70℃ on constant temperature water bath for 7 hours | No degradation. |
| **Oxidation** | 15% $H_2O_2$ | | RT (2 days), Heat at 70℃ on a constant temperature water bath for 7 hours | No degradation. |
| **Photolysis** | Sunlight | | 7 days | No degradation |
| | Photo-stability chamber | | Fluorescence light 1.2 million lux hours and UV light 200 $Whm^{-2}$ | No degradation |
| **Thermal** | 70℃ | | 7 days. | No degradation. |

*RT= room temperature*

## 8.2.5. Validation of the HPLC method

The HPLC methods was validated as per the ICH guideline. The method was found to be specific (resolution > 1 among all the peaks) and selective (peak purity >99%). The linearity, range, precision, accuracy, and robustness results are as summarized in table no 8.2.5.1.

**Table 8.2.5.1 :** Summary of validation parameters for FMTE

| Validation parameters | | | Results. |
|---|---|---|---|
| **Specificity and selectivity** | | | Resolution >1, peak purity> 99% |
| **Linearity** | Equation of the regression line | | y=12947x-26459 |
| | $r^2$ | | 0.9991 |
| | Range (µg $mL^{-1}$) | | 20-120 |
| **Precision** | | µg/mL | Mean peak area ± SD; %CV |
| | Intra-day | 40 | 489900 ± 1353, 0.3 |
| | | 50 | 631412 ± 4068, 0.4 |
| | | 60 | 750941 ± 10430, 1.4 |
| | Inter-day | 40 | 491919 ± 10430, 0.3 |
| | | 50 | 633906 ± 9433, 1.5 |
| | | 60 | 743905 ± 4482, 0.6 |
| **Accuracy** | Spiked concentration (Target concentration=50 µg/mL) | µg/mL | % recovery mean ± SD, %CV |
| | | 40 (80%) | 40.4 ± 0.4, 1.0 |
| | | 50 (100%) | 49.4 ± 0.6,1.3 |
| | | 60 (120%) | 60.4 ± 0.5,0.9 |
| **Robustness** | | pH (±0.5), flow rate (±0.2 mL), mobile phase composition(±2%), wavelength (± 3) of optimized value. | Theoretical plates >2000<br>Resolution >1<br>Asymmetry < 2 |

## 8.2.6. Mass studies

The drug FMTE, and its DPs were subjected for mass spectral analysis. The protonated ion peak for FMTE was observed at *m/z* of 239.1029 in the MS studies carried out in positive electrospray ionization (+ESI) mode, which exactly corresponds to its molecular weight

(238.0953 gm/mole). The drug fragmented during MS/MS to form two ions having *m/z* value of 178.0857 and 117.0697 via successive cleavage of carbamic acid moieties.

DP1 showed molecular ion peak at *m/z* 117.0701. This value was a closely matching with fragment having *m/z* 117.0697 in the MS/MS fragmentation of the drug, indicating both share a similar structure. DP1 of FMTE was identified as cyclopropyl benzene.

DP2 showed molecular ion peak at *m/z* 218.0794 and fragment ions at *m/z* 202.8967, 159.9556, 118.9924, and 96.9581. The structure of DP2 and its fragmentation pattern were proposed based on this information. It was observed that DP2 followed a different route of fragmentation than the drug because of cyclization of carbamic acid side chain under alkaline stress condition leading to formation of a different structure than the drug scaffold**.** DP2 of FMTE was identified as 6-(1,2-oxaziren-3-yl)-5-phenyl-4H-1,3-dioxin-2-one.

### 8.2.7. *In-silico* ADMET studies

*In-silico* screenings were carried out for the drug FMTE and its two newly discovered degradants. Webserver pkCSM was used to study ADMET properties, whereas Toxtree and OSIRIS property explorer were used for secondary screening of mutagenic alerts.

The predictions using pkCSM indicated intestinal absorption of 67.85% for the drug and, for its DPs it was > 90%. Both the drug and the DPs were negative for PgP substrate. DP1 could cross the blood-brain barrier due to a log BB value > 0.3.

On the metabolism front, DP1 inhibited CYP1A2, and DP2 inhibited CYP1A2 and CYP3A4.

The prediction also showed the drugs hepatotoxic potential, and DP2 possessed a structural alert for mutagenicity.

The predictions of ToxTree showed no mutagenic alert for the drug and its DPs, whereas OSIRIS property explorer cleared them from the threat of having tumorigenic, irritant, or reproductive hazards.

# 8.3. Haloperidol (HALO)

## 8.3.1. Drug profile

HALO chemically is a butyrophenone derivative with IUPAC name 4-[4-(4-Chlorophenyl)-4-hydroxypiperidin-1-yl]-1-(4-fluorophenyl) butane-1-one. It is a neuroleptic drug frequently used to treat psychotic disorders and also widely used to treat nausea and vomiting after administering general anaesthesia.

HALO has a solubility of 1.4mg/100ml in water. It is freely soluble in chloroform, methanol, acetone, benzene, and dilute acids.

HALO is official in the United States pharmacopeia and the national formulary (USP-NF), EP, BP, and IP.

## 8.3.2. Mechanism of action

HALO antagonizes the postsynaptic (D2) receptor in the brain's mesolimbic system. This action contributes to the anti-delusionary and anti-hallucinogenic effects. The antiemetic effect is mediated through the antidopaminergic effect in the chemoreceptive trigger zone (CTZ).

## 8.3.3. Development of RP-HPLC method to monitor the drug degradation behavior

A search of literature was done to study the various methods available for the estimation of HALO using an HPLC system. HALO is an official USP-NF, EP, BP, and IP drug. The compendial methods used a mixture of tetrabutylammonium hydrogen sulfate (TBAHS) (50 mM) and acetonitrile as mobile phase in gradient elution mode (1.5 mL/min, $\lambda_{max}$ = 230nm). There were a few bioanalytical methods that used ammonium formate (2 mM, pH 3.0, adjusted with formic acid), Sodium phosphate (100 mM, pH 3.5, adjusted with orthophosphoric acid), water (pH 2.5, adjusted with 0.1% acetic acid) and monobasic potassium phosphate (20 mM, pH 4) as an aqueous component of the mobile phase, while the preferred organic component was acetonitrile. There were also a few methods for estimating HALO in formulations. All the reported methods used C18 column to carry out

separation. Based on the information gathered, trials were taken to get the required separation using ammonium formate (10mM, pH adjusted to 3.7 with formic acid) and acetonitrile on a C18 column. Ammonium formate is a volatile buffer compatible with mass spectrometry having buffering capacity in pH of 3.77 ± 1(pKa of formic acid 3.77) and pH of 9.25 ± 1(pKa of ammonia 9.25)**.** At the selected pH, the drug is present in the ionized form. An ideal separation was achieved using a ratio of 40: 60(v/v) of acetonitrile and buffer, but a tailing factor > 2 was observed. The tailing was curtailed by using a 0.1% of organic modifier (triethylamine).

The summary of optimized stability indicating assay method (SIAM) parameters for HALO is seen in table 8.3.3.1.

**Table 8.3.3.1:** Optimized chromatographic conditions for monitoring the drug degradation pattern for HALO

| | |
|---|---|
| **Mobile phase** | Acetonitrile: Ammonium formate buffer (10mM, pH 3.7) in the ratio (40:60, v/v) + Triethylamine (0.1%) |
| **Column** | HiQ sil C18 column (250mm×4.6mm, 5µ) |
| **Flow rate** | 1ml/min |
| **Wavelength** | 246nm |

## 8.3.4. Forced degradation studies

HALO was stressed under hydrolytic conditions (acidic, basic, and neutral), thermal, photolytic, and oxidative stress conditions. The drug showed degradation (~ 38%) in the presence of 15% hydrogen peroxide at room temperature for 48 h to form a single degradation product (DP1). A further study was carried out by heating the drug with 15% $H_2O_2$ at 70℃. In 2 h, another degradation product (DP2) appeared along with DP1. The peak area for DP1 was significantly higher than DP2 indicating that DP1 is easier to form.

HALO was stabled under other stress conditions. The summary of the stress conditions applied on HALO is seen in table 8.3.4.1.

**Table 8.3.4.1:** Summary of the stress conditions applied to HALO

| Conditions | Stressor | | Duration and nature of exposure. | Observation. |
|---|---|---|---|---|
| **Hydrolysis** | Acid | 0.1,1N HCl | RT (2 days), Heat at 70℃ on constant temperature water bath for 7 hours. | No degradation. |
| | Base | 0.1,1N NaOH | RT (2 days), Heat at 70℃ on constant temperature water bath for 7 hours | No degradation. |
| | Neutral | water | RT (2 days), Heat at 70℃ on constant temperature water bath for 7 hours | No degradation. |
| **Oxidation** | 15% $H_2O_2$ | | RT(2days). | 1)Formation of DP1 at RT(2days) 2)Formation of DP1 and DP2 at 70℃ in 2 hours. |
| **Photolysis** | Sunlight | | 7 days | No degradation |
| | Photo-stability chamber | | Fluorescence light 1.2 million lux hours and UV light 200 $Whm^{-2}$ | No degradation |
| **Thermal** | 70℃ | | 7 days. | No degradation. |

*RT= room temperature*

## 8.3.5. HPLC method validation

HPLC method validation was performed as per the ICH guidelines. The developed method was found to be specific and selective towards the drug and the degradation products with

resolution > 1 among the peaks and the peak purity for individual peaks > 99%. The linearity, precision, accuracy, and robustness data are summarized in table no 8.3.5.1.

**Table 8.3.5.1:** Summary of validation parameters for HALO

| Validation parameters | | | Results. |
|---|---|---|---|
| **Specificity and selectivity** | | | Resolution >1, peak purity> 99% |
| **Linearity** | Equation of the regression line | | y=25346x-63654 |
| | $r^2$ | | 0.9991 |
| | Range (µg/mL) | | 10-110 |
| **Precision** | | µg/mL | Mean peak area ± SD; %CV |
| | Intra-day | 10 | 202986 ± 1656, 0.8 |
| | | 50 | 1220491 ± 19014, 1.6 |
| | | 75 | 1791607 ± 3555, 0.2 |
| | Inter-day | 10 | 203815 ± 2310,1.1 |
| | | 50 | 1223161 ± 20765, 1.7 |
| | | 75 | 1782827 ± 8952, 0.5 |
| **Accuracy** | Spiked concentration (Target concentration=50 µg/mL) | µg/mL | % recovery mean ± SD, %CV |
| | | 40 (80%) | 40.4 ± 0.26, 0.6 |
| | | 50 (100%) | 49.7 ± 0.34,0.6 |
| | | 60 (120%) | 59.9 ± 0.91,1.52 |
| **Robustness** | | pH (±0.5) , flow rate (±0.2mL), mobile phase composition(±2%), wavelength (± 3nm) of optimized value. | Theoretical plates >2000<br>Resolution >1<br>Asymmetry <1 |

## 8.3.6. Mass studies

HALO has a molecular weight of 375.1 gm/mole. The molecular ion peak for the same was observed at *m/z* value of 376.1. The MS/MS spectra of HALO showed three peaks, one at *m/z* value of 165.0 (loss of 4-(Chlorophenyl)-4-hydroxypiperidin moiety, $C_{11}H_{13}ClNO$).

second at *m/z* value of 122.9 (loss of propyl group) and third at *m/z* value of 95.1(due to loss of carbon monoxide). The protonated peaks for DP1 and DP2 were seen at *m/z* 392.0891, and 392.0879 respectively and both showed fragmentation patterns similar to the drug.

The molecular mass of DP1 and DP2 were at an *m/z* value > 16 than the drug indicating the formation of a pair of N-oxide geometrical isomers (*cis* and *trans*)

Generally, the trans isomer is easier to form than its *cis* counterpart as the substituents are located on the opposite side of the rings. Since, DP1 was more easily formed, as revealed in the stress studies, it was identified as *trans*- haloperidol-N-oxide and DP2 as *cis*-haloperidol-N-oxide. Both oxidative degradation products of HALO were known and reported.

### 8.3.7. In-silico ADMET studies

HALO and its oxidative degradation products were predicted to possess intestinal absorption > 89% and acted as the substrate for P-glycoprotein (PgP). Based on the log BB value it was clear that all would pass through the blood brain barrier but not readily.

HALO inhibited CYP2D6 and CYP3A4, while its degradation products inhibited CYP2C19, CYP2C9, and CYP3A4. HALO was predicted to possess hepatotoxic potential, while its degradation products were safe. None of them were predicted to possess Ames's toxicity.

The mutagenic potential of the drug and degradation products were further screened through ToxTree and the OSIRIS property explorer. Their predictions were unanimous on the negative mutagenic potential of the drug and its degradation products. Also, OSIRIS further stated that none possess tumorigenic, irritant, or reproductive risks.

## 8.4. Riociguat (RIO)

### 8.4.1. Drug profile.

RIO is white to yellowish crystalline powder. It is freely soluble in dimethyl sulfoxide, N,N-dimethyl formamide; slightly soluble in tetrahydrofuran, and insoluble in water. IUPAC name assigned to RIO is Methyl N-[4,6-Diamino-2-[1-[(2-fluorophenyl) methyl]-1H-pyrazolo[3,4-b] pyridin-3-yl]-5-pyrimidinyl]-N-methylcarbamate.

RIO is a soluble guanylate cyclase stimulator (sGC) and is primarily used in treating pulmonary hypertension.

## 8.4.2. Mechanism of action.

Soluble guanylate cyclase is a receptor for nitric oxide(NO). The binding of NO to sGC stimulates the synthesis of cyclic guanosine monophosphate, which plays a vital role in regulating the vascular tone,

Pulmonary hypertension is characterized by; endothelial dysfunction, irregularities in the synthesis of nitric oxide, and inadequate stimulation of sGC.

RIO shows its activity by stimulating sGC to the internal NO. It also directly activates sGC by binding at an alternate binding site independent of NO.

## 8.4.3. Development and optimization of HPLC method to monitor the drug degradation behavior

RIO is not official in any of the pharmacopoeias hence, no official methods were available. A couple of bioanalytical methods were available for estimating RIO in plasma. These methods reported use of ammonium formate (2 mM, pH 6.8) and 0.1% formic acid as the aqueous component of the mobile phase, while non-bioanalytical methods used; 0.2% trifluoracetic acid and ammonium acetate (10mM, pH 5.7, adjusted with acetic acid). The most preferred organic phase and the reverse phase column used were acetonitrile and C18. Based on the information gathered, HPLC trials were conducted. Desired separation was achieved on C18 column using acetonitrile and ammonium formate (10 mM, pH 3.7, adjusted with formic acid) in a ratio of 28:72 (v/v). Ammonium formate is a volatile buffer compatible with mass spectrometry having buffering capacity in pH of 3.77 ± 1(pKa of formic acid 3.77) and pH of 9.25 ± 1(pKa of ammonia 9.25). The drug (pKa=4.3) is present in an ionized state at the selected pH. The summary of the optimized stability indicating assay method (SIAM) parameters for RIO is seen in tables 8.4.3.1.

**Table 8.4.3.1:** Optimized chromatographic conditions for monitoring the drug degradation pattern for RIO

| | |
|---|---|
| **Mobile phase** | Acetonitrile : Ammonium formate ( 28:72, **v/v**)<br>(Concentration 10mM, pH of the buffer was adjusted to 3.7 with formic acid) |
| **Column** | Agilent Eclipse Zorbax XDB C18 column (150mmX4.6mm, 5µm) |
| **Flow rate** | 1ml/min |
| **Wavelength** | 322nm |

## 8.4.4. Forced degradation studies

RIO degraded under hydrolytic (~ 37%) and oxidative (~ 38.2%) conditions in the presence of 1 N NaOH and 15% $H_2O_2$ for 48 h at room temperature. There was formation of two degradation products under each stress condition. DP1 and DP2 were formed under oxidative conditions, while DP3 and DP4 were under basic conditions. The oxidative DPs of RIO were more polar than the basic DPs. RIO was found to be stable under other hydrolytic stress conditions (acid & neutral), thermal and photolytic.

The summary of the forced degradation conditions applied to RIO is seen in table no 8.4.4.1.

## 8.4.5. Validation of HPLC method

The developed HPLC method was found to be specific and selective towards the drug and the degradation products. The method was also found to be linear in specified concentration range, precise, accurate, and robust. The summary of the validation parameters is seen in table 8.4.5.1.

## 4.4.6. Mass studies

RIO showed protonated ion peak at 423.1147, and its MS/MS spectra showed two distinct peaks at *m/z* values of 253.0476 and 109.0163. The cleavage of the pyrimidine ring forms the fragment with *m/z* 253.0476, which further loses the pyrazolo pyridine ring to form a fragment with *m/z* 109.0163.

**Table 8.4.4.1:** Summary of the stress conditions applied to RIO.

| Conditions | Stressor | | Duration and nature of exposure. | Observation. |
|---|---|---|---|---|
| **Hydrolysis** | Acid | 1N,2N HCl | RT (2 days), Heat at 70℃ on constant temperature water bath for 7 hours. | No degradation. |
| | Base | 1N NaOH | RT (2 days). | Formation of DP3 and DP4. |
| | Neutral | water | RT (2 days), Heat at 70℃ on constant temperature water bath for 7 hours. | No degradation. |
| **Oxidation** | 15% $H_2O_2$ | | RT(2days). | Formation of DP1 and DP2. |
| **Photolysis** | Sunlight | | 7 days | No degradation |
| | Photo-stability chamber | | Fluorescence light 1.2 million lux hours and UV light 200 $Whm^{-2}$ | No degradation |
| **Thermal** | 70℃. | | 7 days. | No degradation. |

*RT= room temperature*

MS spectra for DP1 showed the quasi-molecular ion peak at *m/z* 270.0699 and, on fragmentation, produced daughter ions peaks at *m/z* values of 109.0157 and 102.0056. The fragment ion (*m/z* 109.0157) is formed due to the ionization of the tertiary nitrogen bridging with fluorobenzene followed by an inductive cleavage, while the fragment ion with *m/z* 102.0056 is formed due to the breakdown of the core pyrazolo pyridine structure. DP1 of RIO was identified as 3-(diaziridin-3-yl)-1-(2-fluorobenzyl)-1H-pyrazolo[3,4-b] pyridine.

DP2 showed protonated ion peak at *m/z* value of 315.0581. its MS/MS spectra showed peaks at *m/z* values of 132.0242, 103.0006, and 109.0159. The fragment with *m/z* 132.0242 is formed due to the cleavage of the pyridine ring. Further loss of $CH_3N$ from this fragment

results in the formation of the fragment with *m/z* 103.0006. The fragment with *m/z* 109.0159 is due to the formation of diaminopyrimidine cation. DP2 was identified as methyl(4,6-diamino-2-(3H-pyrazolo[3,4-b] pyridin-3-yl) pyrimidin-5-yl)(methyl)carbamate.

DP3 showed a molecular ion peak at *m/z* value of 351.0962 and, on its fragmentation, produced peaks at *m/z* value of 109.0829 (diaminopyrimidine cation), 242.0594 ( formed due to cleavage of the pyrimidine ring) and 109.0156 (loss of pyrazolo pyridine moiety from fragment with *m/z* 242.0594). DP3 was identified as 2-(1-(2-fluorobenzyl)-1H-pyrazolo [3,4-b] pyridin-3-yl) pyrimidine 4,5,6-triamine.

Lastly, DP4 appeared at *m/z* value of 391.0876. Its fragment ion peaks were seen at *m/z* values of 109.0156 and 118.0204 due to the formation of (4-flurophenyl) methylium and pyrazolo pyridine cations. DP4 was identified as 6-amino-2-(1-(2-fluorobenzyl)-1H-pyrazolo[3,4-b] pyridin-3-yl)-7-methyl-7,9-dihydro-8H-purin-8-one.

DP1, DP2 and DP3 were unknown degradation products of RIO and not reported, while DP4 was a known degradation product.

### 8.4.7. *In-silico* ADMET studies.

Molecular docking studies were performed to do a comparative study of the binding affinities of the drug and the degradation products with the sGC receptor (PDB code: 7LGK). This study indicated that DP4 has a slightly better binding affinity towards the receptor than the intact drug.

pkCSM predictions revealed that RIO and DP1 has intestinal absorption greater than 90% and DP2, DP3 and DP4 greater than 80%. RIO and its degradation products had poor blood-brain permeability, and except DP2 all behaved as PgP substrates. RIO, DP2, DP3, and DP4 were predicted to possess hepatotoxicity, while DP4 was flagged for mutagenic potential. Besides, RIO also inhibited CYP2C9 and CYP3A4, while DP1 inhibited CYP1A2.

Screening through ToxTree indicated that RIO, DP2, DP3, and DP4 are mutagenic to the presence of the primary aromatic amine in their structure; however, the final screening through OSIRIS property explorer returned a negative mutagenic result for all and also revealed that they do not possess any, irritant, tumorigenic or reproductive risks.

**Table 8.4.5.1:** Summary of validation parameters for RIO.

| Validation parameters | | | Results. |
|---|---|---|---|
| **Specificity and selectivity** | | | Resolution >1, peak purity> 99% |
| **Linearity** | Equation of the regression line | | y=20562x-30676 |
| | $r^2$ | | 0.9994 |
| | Range (µg $mL^{-1}$) | | 20-120 |
| **Precision** | Intra-day | µg $mL^{-1}$ | Mean peak area ± SD; %CV |
| | | 40 | 78043 ± 2136 0.3 |
| | | 50 | 979944 ± 4068, 0.3 |
| | | 60 | 1193960 ± 11070 0.9 |
| | Inter-day | 40 | 779370 ± 7088, 0.9 |
| | | 50 | 979421 ± 9435, 1.0 |
| | | 60 | 1208794 ± 4358, 0.4 |
| **Accuracy** | Spiked concentration (Target concentration=50 µg/mL) | µg $mL^{-1}$ | % recovery mean ± SD, %CV |
| | | 40 (80%) | 40.1 ± 0.5, 1.3 |
| | | 50 (100%) | 49.8 ± 0.3,0.6 |
| | | 60 (120%) | 60.1 ± 0.7,1.2 |
| **Robustness** | | pH (± 0.5) , flow rate (± 0.2mL), mobile phase composition(±2%), wavelength (± 3nm) of optimized value. | Theoretical plates >2000<br>Resolution >1<br>Asymmetry <1 |

# References


1. Rahman N, Azmi SNH, Wu HF. The importance of impurity analysis in pharmaceutical products: An integrated approach. Accredit Qual Assur. 2006;11(1–2):69–74.
2. Linda Ng, George Lunn and PF. Organic impurities in drug substance:origin, control and measurement. In: Analysis of Drug impurties. Blackwell Publishing; 2007. p. 1–19.
3. Takeuchi T. Identification and Determination of Impurities in Drugs. Vol. 18, Analytical Sciences. 2002. 379 p.
4. Bari S, Kadam B, Jaiswal Y, Shirkhedkar A. Impurity profile: Significance in Active Pharmaceutical Ingredient. Eurasian J Anal Chem. 2017;2(1):32–53.
5. Jacobson-Kram D, McGovern T. Toxicological overview of impurities in pharmaceutical products. Adv Drug Deliv Rev. 2007;59(1):38–42.
6. Cok I, Emerce E. Overview of impurities in pharmaceuticals : Toxicological aspects. Asian Chem Lett. 2012;16(1):87–97.
7. Custer LL, Sweder KS. The role of genetic toxicology in drug discovery and optimization. Curr Drug Metab [Internet]. 2008;9(9):978–85. Available from: http://www.ncbi.nlm.nih.gov/pubmed/18991595.
8. Dobo KL, Greene N, Cyr MO, Caron S, Ku WW. The application of structure-based assessment to support safety and chemistry diligence to manage genotoxic impurities in active pharmaceutical ingredients during drug development. Regul Toxicol Pharmacol. 2006;44(3):282–93.
9. L. Müller, R.J. Mauthe, C.M. Riley, M.M. Andino, D. De Antonis, C. Beels, J. DeGeorge, A.G.M. De Knaep, D. Ellison, J.A. Fagerland, et al., A rationale for determining, testing, and controlling specific impurities in pharmaceuticals that possess potential for genotoxicity. Regul. Toxicol. and Pharmacol. 44 (2006) 198–211.

10. P.M.J. Bos, B. Baars, T.M. Marcel, M.T.M. van Raaij, Risk assessment of peak exposure to genotoxic carcinogens: a pragmatic approach, Toxicology Letters 151 (2004) 43–50.
11. International Conference on Harmonisation of Technical Requirements for Registration of Pharmaceuticals for Human Use Quality guideline Q3A(R2), impurities in new drug Substance, 2006.
12. International Conference on Harmonisation of Technical Requirements for Registration of Pharmaceuticals for Human Use Quality guideline Q3B(R2), impurities in new drug Products, 2006.
13. International Conference on Harmonisation of Technical Requirements for Registration of Pharmaceuticals for Human Use Quality guideline Q3C(R7), Impurities:Guidelines for residual solvents, 2018.
14. International Council for Harmonisation of Technical Requirements for Pharmaceuticals for Human Use guideline M7(R1), Assessment and control of dna reactive (mutagenic) impurities in pharmaceuticals to limit potential carcinogenic risk,2017.
15. European Medicines Evaluation Agency, Committee for Medicinal Products for Human Use (CHMP). Guideline on the limits of genotoxic impurities. CPMP/SWP/5199/02, June 28, 2006 London.
16. Guidance for industry, ANDAs: Impurities in drug substances, U.S. department of health and human services, Food and Drug administration, center for drug evaluation and research, January 2005.
17. Baertschi S, Alsante K, Reed R. Pharmaceutical stress testing, predicting drug degrdation. Second edi. Informa healthcare; 2011.
18. Görög S. The importance and the challenges of impurity profiling in modern pharmaceutical analysis. TrAC - Trends Anal Chem. 2006;25(8):755–7.
19. Bari S, Kadam B, Jaiswal Y, Shirkhedkar A. Impurity profile: Significance in Active Pharmaceutical Ingredient. Eurasian J Anal Chem. 2017;2(1):32–53.
20. International Conference on Harmonisation of Technical Requirements for Registration of Pharmaceuticals for Human Use Quality guideline Q1A(R2), Stability testing of new drug substance and products, 2003.
21. Guidance for industry, ANDAs: stability testing of drug substances and products, Food and Drug administration, center for drug evaluation and research, may 2014.

22. Nicolette J, Müller L, Vock E, Dobo KL, Brigo A, Amberg A, et al. Use of in silico systems and expert knowledge for structure-based assessment of potentially mutagenic impurities. Regul Toxicol Pharmacol [Internet]. 2013;67(1):39–52. Available from: http://dx.doi.org/10.1016/j.yrtph.2013.05.001
23. Pires DEV, Blundell TL, Ascher DB. pkCSM: Predicting small-molecule pharmacokinetic and toxicity properties using graph-based signatures. J Med Chem. 2015;58(9):4066–72.
24. Daina A, Michielin O, Zoete V. SwissADME: A free web tool to evaluate pharmacokinetics, drug-likeness and medicinal chemistry friendliness of small molecules. Sci Rep. 2017;7(March):1–13.
25. S.Gorog (Ed.), Identification and Determination of Impurities in Drugs, Elsevier Science B.V, Amsterdam 2000.
26. S. Ahuja, Impurities Evaluation of Pharmaceuticals, Marcel Dekker, New York, NY, 1998.
27. S.W. Hovorka, C. Schoneich, Oxidative degradation of pharmaceuticals: theory, mechanisms and inhibition, J. Pharm. Sci. 90 (2001) 253–269.
28. Ahuja S., Alsante K.M., Handbook of isolation and Characterization of Impurities in Pharmaceuticals, academic press.
29. Satinder Ahuja, Assuring Quality of Drugs by Monitoring Impurities, Advanced Drug Delivery Review, 59, 2007, 3-11.
30. Blessy M, Patel RD, Prajapati PN, Agrawal YK. Development of forced degradation and stability indicating studies of drugs - A review. J Pharm Anal [Internet]. 2014;4(3):159–65. Available from: http://dx.doi.org/10.1016/j.jpha.2013.09.003
31. Bakshi M, Singh S. Development of validated stability-indicating assay methods - Critical review. J Pharm Biomed Anal. 2002;28(6):1011–40.
32. Venkataraman S, Manasa M. Re view Article Forced degradation studies : Regulatory guidance , characterization of drugs , and their degradation products - a review. 2018;10(2).
33. Alsante K.M., Ando A., Brown R., Ensing J., Hatajik T.D., Kong W., Tsuda Y., The Role of Degradant Profiling in Active Pharmaceutical Ingredients and Drug Products, Advanced Drug Delivery Reviews, 59, 2007, 29 – 37.
34. Ruan J., Tattersall P., Lozano R., Shah P., The role of forced degradation studies instability indicating HPLC method development, Am Pharm Rev, 2004, 9:46–53.

35. Srivastava M. High-performance thin-layer chromatography (HPTLC). High-Performance Thin-Layer Chromatography (HPTLC). 2011. 1–397 p.

36. Kulkarni SP, Amin PD. Stability indicating HPTLC determination of timolol maleate as bulk drug and in pharmaceutical preparations. J Pharm Biomed Anal. 2000 Nov;23(6):983–7.

37. Puthli SP, Vavia PR. Stability indicating HPTLC determination of piroxicam. J Pharm Biomed Anal [Internet]. 2000 May;22(4):673—677. Available from: https://doi.org/10.1016/s0731-7085(99)00300-3.

38. Stavchansky S, Wu P, Wallace JE. Gas Liquid Chromatographic Determination of Promethazine Hydrochloride in Cocoa Butter-White Wax Suppositories. Drug Dev Ind Pharm [Internet]. 1983;9(6):989–98. Available from: https://doi.org/10.3109/03639048309042837

39. Bergh JJ, Lötter AP. A Stability-Indicating Gas-Liquid Chromatographic Method for the Determination of Acetaminophen and Aspirin in Suppositories. Drug Dev Ind Pharm [Internet]. 1984;10(1):127–36. Available from: https://doi.org/10.3109/03639048409038297

40. Kazakevich Y., Lobrutto R., HPLC for Pharmaceutical Scientists, John Wiley & Sons, 2007.

41. Dong M.W., Modern HPLC for Practicing Scientist, John Wiley & Sons, 2006.

42. Snyder L.R., Kirkland J.J., Dolan J.W., Introduction to Modern Liquid Chromatography, Third edition, John Wiley & Sons, 2010.

43. Silverstein RM, Webster FX, Kiemle DJ, Byrce DL. Spectrometric identification of organic compounds. eight. Wiley-Interscience. 2014.

44. McMASTER M. LC / MS A Practical User ’ s Guide. WILEY-INTERSCIENCE; 2005.

45. Benfenati E. In Silico Methods for Predicting Drug Toxicity Methods in Molecular Biology. 2016. 1–87 p.

46. Stroud R, Moore J finer. Computational and structural approaches to drug discovery. RSC publishing; 2008.

47. Kruhlak NL, Contrera JF, Benz RD, Matthews EJ. Progress in QSAR toxicity screening of pharmaceutical impurities and other FDA regulated products. Adv Drug Deliv Rev. 2007;59(1):43–55.

48. van Lier RBL, Bercu JP, Morton SM, Callis CM, Deahl JT, Gombar VK. In silico approaches to predicting cancer potency for risk assessment of genotoxic impurities in drug substances. Regul Toxicol Pharmacol [Internet]. 2010;57(2–3):300–6. Available from: http://dx.doi.org/10.1016/j.yrtph.2010.03.010

49. Matveieva M, Polishchuk P. Benchmarks for interpretation of QSAR models. J Cheminform [Internet]. 2021;13(1):1–20. Available from: https://doi.org/10.1186/s13321-021-00519-x.

50. European Directorate for the quaity of medicine, European Pharmacopeia. 7th ed. strasbourg, France: Council of europe; 2011.

51. The united states pharmacopeial convention. The united states pharmacopeia 34 national formulary. Rockville, MD: United States Pharmacopeial Convention; 2010.

52. Moffat, Anthony C, M David Osselton B widdop. Clarke's Analysis of Drugs and Poisons. Pharmaceutical press. Pharmaceutical press; 2011. 1928–1929 p.

53. Rathbone J, McMonagle T. Pimozide for schizophrenia or related psychoses. Cochrane Database Syst Rev. 2007;Jul 18(18(3)):CD001949.

54. Shapiro A, Shapiro E, Fulop G. Pimozide treatment of tic and Tourette disorders. Pediatrics. 1987;Jun(79(6)):1032–9.

55. Pringsheim T, Marras C. Pimozide for tics in Tourette's syndrome. Cochrane Database Syst Rev. 2009;Apr 15(2009(2)):CD006996.

56. Liberman L, Higgins D. A small-molecule screen identifies the antipsychotic drug pimozide as an inhibitor of Listeria monocytogenes infection. Antimicrob Agents Chemother. 2009;53(2):756–64.

57. Rampino A, Marakhovskaia A, Soares-Silva T, Torretta S, Veneziani F, Beaulieu JM. Antipsychotic drug responsiveness and dopamine receptor signaling; old players and new prospects. Front Psychiatry. 2019;10(JAN):1–13.

58. National Center for Biotechnology Information (2022). PubChem Compound Summary for CID 16362, Pimozide. Retrieved November 15, 2022 from https://pubchem.ncbi.nlm.nih.gov/compound/Pimozide.

59. Michiels L, Heykants J, Knaeps A, Janssen P. Radioimmunoassay of the neuroleptic drug pimozide. Life Sci. 1975;Mar 15(16(6)).

60. Yan M, Li H De, Chen BM, Liu XL, Xu P, Zhu YG. Quantitative determination of pimozide in human plasma by liquid chromatography-mass spectrometry and its application in a bioequivalence study. J Pharm Biomed Anal. 2010;51(5):1161–4.

61. Kerbusch T, Desta Z, Soukhova N V., Thacker D, Flockhart DA. Sensitive assay for pimozide in human plasma using high-performance liquid chromatography with fluorescence detection: Application to pharmacokinetic studies. J Chromatogr B Biomed Appl. 1997;694(1):163–8

62. Kabra P, Nargund LVG, Srinivasa Murthy M. RP-HPLC method for estimation of an antipsychotic drug - Pimozide. Asian J Pharm Clin Res. 2014;7(SUPPL. 2):49–51.

63. Manjula Devi AS, Ravi TK. Stability indicating HPTLC determination of pimozide in bulk and pharmaceutical dosage form. Der Pharm Lett. 2013;5(1):182–7.

64. Alamein AMA Al, Hussien LAEA, Mohamed EH. Univariate spectrophotometry and multivariate calibration: Stability-indicating analytical tools for the quantification of pimozide in bulk and pharmaceutical dosage form. Bull Fac Pharmacy, Cairo Univ [Internet]. 2015;53(2):173–83. Available from: http://dx.doi.org/10.1016/j.bfopcu.2015.10.003.

65. Shabir GA. Validation of high-performance liquid chromatography methods for pharmaceutical analysis. J Chromatogr A. 2003;987(1–2):57–66.

66. Konermann L. Addressing a Common Misconception: Ammonium Acetate as Neutral pH "Buffer" for Native Electrospray Mass Spectrometry. J Am Soc Mass Spectrom. 2017 Sep;28(9):1827-1835. doi: 10.1007/s13361-017-1739-3. Epub 2017 Jul 14. PMID: 28710594.

67. Pavia D, Lampman G, Kriz G, Vyvyan J. Spectroscopy. In: Indian edition., editor. BROOKS/COLE CENAGE learning; 2007.

68. Yeni Y, Supandi S, Merdekawati F. In silico toxicity prediction of 1-phenyl-1-(quinazolin-4-yl) ethanol compounds by using Toxtree, pkCSM and preADMET. Pharmaciana. 2018;8(2):216.

69. Pires DEV, Blundell TL, Ascher DB. pkCSM: Predicting small-molecule pharmacokinetic and toxicity properties using graph-based signatures. J Med Chem. 2015;58(9):4066–72.

70. Patlewicz G, Jeliazkova N, Safford RJ, Worth AP, Aleksiev B. An evaluation of the implementation of the Cramer classification scheme in the Toxtree softwareo Title. SAR QSAR Env Res. 2008;19(5–6):495–524.

71. Thomas S, Freyss J, Korff M. OSIRIS, an entirely in-house developed drug discovery informatics systemtle. J Chem Inf Model. 2009;Feb;49(2):232–46.

72. Benigni R, Bossa C. Mechanisms of Chemical Carcinogenicity and Mutagenicity: A Review with Implications for Predictive Toxicology. Chem Rev [Internet]. 2011 Apr 13;111(4):2507–36. Available from: https://doi.org/10.1021/cr100222q

73. Benigni R, Bossa C, Tcheremenskaia O. In vitro cell transformation assays for an integrated, alternative assessment of carcinogenicity: a data-based analysis. Mutagenesis. 2013 Jan;28(1):107–16.

74. Jensen P. Felbamate in the treatment of refractory partial-onset seizures. Epilepsia. 1993;34 suppl 7(S25-9).

75. Snodgrass S. Felbamate therapy in the Lennox-Gastaut syndrome. N Engl J Med . 1993;328(22)(1641).

76. Palmer KJ, McTavish D. Felbamate. A review of its pharmacodynamic and pharmacokinetic properties, and therapeutic efficacy in epilepsy. Drugs. 1993;Jun;45(6):1041-1065.

77. Martinez AH, Mohiuddin SS. Biochemistry, Chloride Channels. [Updated 2022 Jul 18]. In: StatPearls [Internet]. Treasure Island (FL): StatPearls Publishing; 2023 Jan-. Available from: https://www.ncbi.nlm.nih.gov/books/NBK545138/

78. Adusmalli VE, Wong K, Kucharczyk N, Sofia. Felbamate in vitro metabolism by rat liver microsomes. Drug Metab Dipos. 1991;19(6):1135–8.

79. Yang J, Adusumalli V, Wong K, Kucharczyk N, Sofia R. Felbamate metabolism in the rat, rabbit, and dog. Drug Metab Dipos. 1991;19(6):1126–34.

80. National Center for Biotechnology Information (2022). PubChem Compound Summary for CID 3331, Felbamate. Retrieved November 15, 2022 from https://pubchem.ncbi.nlm.nih.gov/compound/Felbamate.

81. Hempenius J, Hendriks G, Hingstman J, Mensink CK, Jonkman JHG, Lin CC. An automated analytical method for the determination of felbamate in human plasma by robotic sample preparation and reversed-phase high performance liquid chromatography. J Pharm Biomed Anal. 1994;12(11):1443–51.

82. Hansen RJ, Samber BJ, Gustafson DL. Rapid and sensitive LC-MS/MS method for determination of felbamate in mouse plasma and tissues and human plasma. J Chromatogr B Anal Technol Biomed Life Sci [Internet]. 2010;878(32):3432–6. Available from: http://dx.doi.org/10.1016/j.jchromb.2010.10.006.

83. Tang PH. Drug monitoring and toxicology: A simple procedure for the monitoring of felbamate by HPLC-UV detection. J Anal Toxicol. 2008;32(5):373–8.

84. Gur P, Poklis A, Saady J, Costantino A. Chromatographic Procedures for the Determination of Felbamate in Serum [Internet]. Vol. 19, Journal of Analytical Toxicology. 1995 [cited 2021 Mar 7]. Available from: https://academic.oup.com/jat/article/19/6/499/774262.

85. Shihabi ZK, Oles KS. Felbamate measured in serum by two methods: HPLC and capillary electrophoresis. Clin Chem. 1994;40(10):1904–8.

86. Paw B, Misztal G, Tajer A. Validation of a liquid chromatographic method for the determination of felbamate in tablets. J Liq Chromatogr Relat Technol. 2002;25(10–11):1643–9.

87. Shetty S, Surendranath K, Kaja R, Satish J, Jogul J, Manitripathi U. Development and validation of a stability-indicating UHPLC method for assay of felbamate and related substances. Acta Chromatogr. 2010;22(2):161–72.

88. Marvin sketch (ver 19.9.0, 2019, www.chemaxon.com).

89. The Indian pharmacopoeia commission, Indian pharmacopoeia laboratory, Govt. of India, Ministry of health and family welfare, sector 23, Raj Nagar, ghaziabad-201002.

90. British Pharmacopoeia, Medicines and Healthcare Products Regulatory Agency (MHRA), London, 2010.

91. Hoja H, Marquet P, Verneuil B, Lotfi H, Dupuy JL, Pénicaut B, et al. Determination of haloperidol and its reduced metabolite in human plasma by liquid chromatography-

mass.

92. National Center for Biotechnology Information (2023). PubChem Compound Summary for CID 3559, Haloperidol. Retrieved May 3, 2023 from https://pubchem.ncbi.nlm.nih.gov/compound/Haloperidol.

93. Seeman P, Kapur S. Schizophrenia: more dopamine, more D2 receptors. Proc Natl Acad Sci U S A. 2000 Jul 5;97(14):7673-5. doi: 10.1073/pnas.97.14.7673. PMID: 10884398; PMCID: PMC33999.

94. Seeman P. Atypical antipsychotics: mechanism of action. Can J Psychiatry. 2002 Feb;47(1):27-38. PMID: 11873706.

95. Froemming JS, Lam YWF, Jann MW, Davis CM. Pharmacokinetics of Haloperidol. Clin Pharmacokinet. 1989;17(6):396–423.

96. Shin J-G, Kane K, Flockhart D. Potent inhibition of CYP2D6 by haloperidol metabolites: stereoselective inhibition by reduced haloperidol. Br J Clin Pharmacol. 2001;Jan(51(1)):45–52.

97. Tyler MW, Zaldivar-Diez J, Haggarty SJ. Classics in Chemical Neuroscience: Haloperidol. ACS Chem Neurosci. 2017;8(3):444–53.

98. Gadhavi R, Patel J. Development and Validation of Stability Indicating Assay Method of Haloperidol in Oral Solution. 2014;4(5):319–29.

99. Syamala M, Angalaparameswari S, Vimalakannan T, Sumanjali C, Jyotshna T. Pharmaceutical Chemistry and Analysis Stability indicating method development and validation for the determination of haloperidol and benzhexol by RP-HPLC. 2019;1:52–8.

100. Yasir M, Singh Sara UV, Som I, Singh L. Development and Validation of a New HPLC Method for In-vitro Studies of Haloperidol in Solid Lipid Nanoparticles. J Anal Bioanal Tech. 2016;07(06):6–11.

101. Aboul-Enein H, Ali I, Hoenen H. Rapid determination of haloperidol and its metabolites in human plasma by HPLC using monolithic silica column and solid-phase extraction. Biomed Chromatogr. 2006;20(8):760–4.

102. Jain T, Bhandari A, Ram V, Sharma S, Chaudhary RK, Parakh M. High-performance liquid chromatographic method with diode array detection for quantification of haloperidol levels in schizophrenic patients during routine clinical practice. J Bioanal Biomed. 2011;3(1):8–12.

103. Ebrahimzadeh H, Dehghani Z, Asgharinezhad AA, Shekari N, Molaei K. Determination of haloperidol in biological samples with the aid of ultrasound-assisted

emulsification microextraction followed by HPLC-DAD. J Sep Sci. 2013;36(9–10):1597–603.

104. Chuang C-Z, Jr. FAR, Prasad C. Use of Triethylamine as an Ion-Pairing Reagent. J Liq Chromatogr [Internet]. 1994;17(11):2383–94. Available from: https://doi.org/10.1080/10826079408013487

105. Roos RW, Lau-Cam CA. General reversed-phase high-performance liquid chromatographic method for the separation of drugs using triethylamine as a competing base. J Chromatogr. 1986 Dec;370(3):403–18.

106. Kalariya PD, Namdev D, Srinivas R, Gananadhamu S. Application of experimental design and response surface technique for selecting the optimum RP-HPLC conditions for the determination of moxifloxacin HCl and ketorolac tromethamine in eye drops.

107. Toxvig A, Wehland M, Grimm D. A focus on riociguat in the treatment of pulmonary arterial hypertension. Basic Clin Pharmacol Toxicol. 2019;Sep(125(3)):202–14.

108. National Center for Biotechnology Information (2022). PubChem Compound Summary for CID 11304743, Riociguat. Retrieved November 17, 2022 from https://pubchem.ncbi.nlm.nih.gov/compound/Riociguat.

109. https://www.accessdata.fda.gov/drugsatfda_docs/nda/2013/204819orig1s000toc.cfm.

110. Frey R, Becker C, Saleh S, Unger S, van der Mey D, Mück W. Clinical Pharmacokinetic and Pharmacodynamic Profile of Riociguat. Clin Pharmacokinet. 2018;57(6):647–61.

111. LiverTox: Clinical and Research Information on Drug-Induced Liver Injury [Internet]. Bethesda (MD): National Institute of Diabetes and Digestive and Kidney Diseases; 2012-. Riociguat. [Updated 2018 Jun 4]. Available from: https://www.ncbi.nlm.nih.gov/books/NBK548167/.

112. RA P, NS G, R M. Development and Validation of New Rp-Hplc Method for Quantitative Estimation of Riociguat in Tablet Dosage Form. Bull Pharm Res. 2019;9(1–3):1–5.

113. Gnoth MJ, Hopfe PM, Czembor W. Determination of riociguat and its major human metabolite M-1 in human plasma by stable-isotope dilution LCMS/MS. Bioanalysis. 2015;7(2):193–205.

114. Nayak R, Narenderan ST, Krishna LVS, Meyyanathan SN, Babu B, Kalaivani M. Analytical method development and validation for the determination of riociguat in their formulations by LC-MS/MS. J Glob Pharma Technol. 2018;10(12):19–23.

115. Tiwari S, Chavan B. In vitroand in vivo investigation of metabolic fate of riociguat by HPLC-Q-TOF/MS/MS and in silico evaluation of the metabolites by ADMET predictor ™. J Pharm Biomed Anal . 2019;Feb 5(164):326–36.

116. Pandya CP, Rajput SJ. Stress degradation studies of riociguat, development of validated stability indicating method, identification, isolation and characterization of degradation products by LC-HR-MS/MS and NMR studies. Indian J Pharm Educ Res. 2019;53(4):s630–41.

117. Ashok Chakravarthy V, Sailaja BBV, Praveen Kumar A. Method development and validation of ultraviolet-visible spectroscopic method for the estimation of assay of sugammadex sodium, apremilast, riociguat, and vorapaxa sulfate drugs in active pharmaceutical ingredient form. Asian J Pharm Clin Res. 2017;10(2):241–50.

118. Gorumutchu GP, Ratnakaram VN, Malladi S. Determination of Riociguat by Oxidative Coupling Using Visible Spectrophotometry. Orient J Chem. 2019;35(Special Issue 1):48–53.

119. BIOVIA, Dassault Systèmes, Discovery Studio Visualizer, 21.1.0.20298, San Diego: Dassault Systèmes, 2020.

120. Kaplan W, Littlejohn T. Swiss-PDB Viewer (Deep View). Br Bioinform. 2001;May(2(2)):195–7.

121. Dallakyan S, Olson AJ. Small-molecule library screening by docking with PyRx. Methods Mol Biol. 2015;1263(January):243–50.

*Page intentionally left blank.*

# Appendix

## Publications

1. Chodankar RS, Mahajan AA. Characterization and In-silico toxicity prediction of degradation products of felbamate. Futur J Pharm Sci. 2021;7(1):1–10.
2. Chodankar R. Characterization and in-silico toxicity prediction of the oxidative degradation products of Pimozide. 2022;(April):275–84.
3. Chodankar RS, Mahajan AA. Identification and toxicity profiling of degradation impurities of riociguat using tandem mass spectrometry and in-silico studies. J Chromatogr Open [Internet]. 2022;100058.

## Presentations

1. Presented poster at Applied pharmaceutical analysis (APA) India having title “development of a stability indicating assay method for determination of pimozide in bulk drug”.
2. Presented poster at $6^{th}$ annual international conference on IPR having title “development of a stability indicating assay method for determination of pimozide in bulk drug”.

Future Journal of Pharmaceutical Sciences

RESEARCH

Open Access

# Characterization and *In-silico* toxicity prediction of degradation products of felbamate

Rahul S. Chodankar* and Anand A. Mahajan

## Abstract

**Background:** The objective of the work carried out was to assess the toxicity of the degradation products (DPs) for the drug felbamate. Stress studies were performed in the condition specified in the international council of harmonization (ICH) guideline Q1A (R2).

**Results:** The drug degraded under the alkaline stress conditions to generate two degradation products (DPs). They were separated on a Phenomenex C8 column (250 mm × 4.6 mm, 5 µm); mobile phase composition was 10 mM ammonium formate (pH adjusted to 3.7 with formic acid) and acetonitrile (80:20, v/v); flow rate and wavelength for recording absorbance were 1.0 ml/min and 206 nm, respectively. The structures of the degradation products were characterized by LC–MS/MS analysis.

**Conclusion:** The drug was prone to hydrolysis in the presence of alkali. It was found to be stable under other stress conditions, viz., acidic, neutral, thermal, photolytic and oxidative. The structures of the impurities were characterized by LC–MS/MS. The drug and the DPs were screened through ADME and toxicity prediction software's like pkCSM, Toxtree and OSIRIS property explorer. Felbamate was flagged for possible hepatotoxicity.

**Keywords:** Felbamate, Stress studies, *In-silico* toxicity, Mass spectrometry

## Background

Felbamate is an antiepileptic drug. It is one of the first in its class belonging to the second generation. In adults, it is used in the treatment of partial seizures [1], while in children for generalized seizures due to Lennox-Gas taut syndrome [2, 3].

Felbamate is official in the US Pharmacopeia and National Formulary (USP-NF) [4]. It is also mentioned in Clarke's Analysis of Drugs and Poisons [5]. Chemically felbamate is 2-phenyl-1,3-propanediol (Fig. 1). It is a white lipophilic powder, very slightly soluble in water, slightly soluble in alcohol, but freely soluble in organic solvents [6].

*Correspondence: Chodankar.rahul@gmail.com
Department of Pharmaceutical Chemistry, Goa College of Pharmacy, 18th June road, Panaji, Goa 403001, India

Studies have shown that the antiepileptic activity of felbamate is attributed primarily due to the inhibitory effect on $GABA_A$ receptor. Secondly, it is also known to inhibit the glycine-mediated activation of the NMDA receptor. The $GABA_A$ receptor is known to modulate the chloride channel, whereas the NMDA receptor control sodium and calcium passage. Extracellular magnesium can bind to NMDA receptors blocking the movement of cations across the membrane. These voltage-dependent ion channels control neuronal excitability and membrane stabilization [7, 8]. After administration, felbamate is metabolized in the liver by cytochrome P-450, followed by glucuronidation. Approximately half of the absorbed felbamate is excreted in the urine. There are three major metabolites of felbamate: 2-(4-hydoxyphenol)-1,3-propanediol dicarbamate, 3-carbamoyloxy-2-phenylpropanoic acid and 2-hydroxy-2-phenylpropanoic acid. The minor metabolite is 2-hydroxy-2-phenyl-1,3-propanediol

# Journal Details

| | |
|---|---|
| **Journal Title (in English Language)** | Future Journal of Pharmaceutical Sciences |
| **Publication Language** | English |
| **Publisher** | Future University in Egypt |
| **ISSN** | 2314-7245 |
| **E-ISSN** | 2314-7253 |
| **Discipline** | Science |
| **Subject** | Pharmacology, Toxicology and Pharmaceutics (all) |
| **Focus Subject** | Pharmaceutical Science |
| **UGC-CARE coverage year** | from June-2019 to Present |

Received: 12 December 2021 | Revised: 12 April 2022 | Accepted: 12 April 2022

DOI: 10.1002/sscp.202100065

RESEARCH ARTICLE

# Characterization and in-silico toxicity prediction of the oxidative degradation products of Pimozide

**Rahul Chodankar**[1] | **Anand Mahajan**[2]

[1]Department of Pharmaceutical Chemistry, Goa College of Pharmacy, Panaji, India

[2]Department of Pharmaceutical Analysis, Goa College of Pharmacy, Panaji, India

**Correspondence**
Rahul S. Chodankar, Department of Pharmaceutical Chemistry, Goa College of Pharmacy, 18th June road, Panaji, Goa, 403001, India.
Email: Chodankar.rahul@gmail.com

The investigation's objective was to access the stability of the drug substance Pimozide under the stress conditions specified in the International Conference on Harmonization Q1A(R2) guideline and to separate, identify, and characterize the degradation products by using liquid chromatography-tandem mass spectrometry studies without isolating them from the reaction mixture. It was observed that the drug was susceptible to oxidative degradation (15% hydrogen peroxide, 48 h, room temperature) forming four novel degradation products while being stable under hydrolytic, Photolytic, and thermal conditions. The separation of the drug and the degradation products was achieved with good resolution on a Phenomenex C18 column (150 mm × 4.6 mm, 5 μm) using gradient elution. The fragmentation pattern constructed from the liquid chromatography-quadrupole-time of flight mass spectrometry data was used for structural characterization of the degradation products. Lastly, the in-silico absorption, distribution, metabolism, excretion, and toxicity properties prediction was performed by using in-silico tools like the pKCSM webserver, ToxTree, and OSIRIS property explorer. The primary screening through the pKCSM webserver exposed the hepatoxic and the mutagenic potential of Pimozide, 1-(1-(4-(4-fluorophenyl)-4-phenylbutyl) piperidin-4-yl)-1,3-dihydro-2H-benzo[d]imidazol-2-one (degradation product 3) and 1-(4,4-bis(4-fluorophenyl)butyl)-4-(2-oxo-2,3-dihydro-1H-benzo[d]imidazol-1-yl)piperidine 1-oxide (degradation product 5) whereas, 1-(1-(4,4-diphenylbutyl) piperidin-4-yl)-2,3-dihydro-1H-benzo[d]imidazol-2-ol (degradation product 1) was predicted to only possess mutagenic potential. Secondary screening for mutagenicity was done by using ToxTree and OSIRIS property explorer.

**KEYWORDS**
impurity profiling, in-silico toxicity, mass spectrometry, Pimozide, stress study

## 1 | INTRODUCTION

Pimozide is a potent, long-acting neuroleptic drug. Its chemical name is 3-[1-[4,4-bis(4-fluorophenyl)butyl]piperidin-4-yl]- 1H-benzimidazole-2-one (Figure 1). TEVA Pharma filed a new drug application

**Article Related Abbreviations:** ADMET, absorption, distribution, metabolism, excretion, and toxicity; CID, collisions induced dissociation; DP, degradation product; EP, European Pharmacopoeia; USP, US Pharmacopeia

  

Journal of Chromatography Open 2 (2022) 100058

Contents lists available at ScienceDirect

Journal of Chromatography Open

journal homepage: www.elsevier.com/locate/jcoa

# Identification and toxicity profiling of degradation impurities of riociguat using tandem mass spectrometry and *in-silico* studies

Rahul S Chodankar [a,*], Anand A. Mahajan [b]

[a] Department of Pharmaceutical Chemistry, Goa College of Pharmacy, 18th June road, Panaji, Goa 403001, India
[b] Department of Pharmaceutical Analysis, Goa College of Pharmacy, 18th June road, Panaji, Goa 403001, India

ARTICLE INFO

*Keywords:*
Riociguat
Stress studies
HPLC
*In-silico* toxicity
LC-QTOF

ABSTRACT

In the current scenario, the safety aspect related to impurities and their permissible level in the formulation has gained worldwide importance. The ICH (International Conference on Harmonization) guidelines and the official books have addressed this issue critically as it has tremendous regulatory implications. The present research work addresses the above-mentioned issue for the drug riociguat and toxicity profiling of its degradation impurities. As per ICH Q1A (R2) guideline, the drug was subjected to various stress conditions wherein the drug generated three unknown degradants from the four that were detected. The degradants were separated and characterized using LC and LC-QTOF/MS studies. Better separation was achieved on Agilent's Zorbax XDB column (150 mm × 4.6 mm, 5 µm) using 10 mM ammonium formate (pH adjusted to 3.7 with formic acid) and acetonitrile in the ratio of 72:28 (v/v). The flow rate was 1.0 mL/min and detection was carried out by using UV detector at 322 nm. The chemical structures of all four degradants and drug were subjected for toxicity prediction using *in-silico* ADMET tools and their relative affinities towards the receptor was compared with riociguat by using molecular docking. The degradants were identified as 3-(diaziridin-3-yl)-1-(2-fluorobenzyl)-1H-pyrazolo[3,4-b] pyridine (DP1), methyl (4,6-diamino-2-(3H-pyrazolo[3,4-b]pyridin-3-yl)pyrimidin-5-yl)(methyl)carbamate(DP2), 2-(1-(2-fluorobenzyl)-1H-pyrazolo [3,4-b]pyridin-3-yl)pyrimidine-4,5,6-triamine(DP3) and 6-amino-2-(1-(2-fluorobenzyl)-1H-pyrazolo[3,4-b]pyridin-3-yl)-7-methyl-7,9-dihydro-8H-purin-8-one (DP4).

## 1. Introduction

Riociguat (RIO) is approved by US-FDA for the treatment of pulmonary hypertension [1]. RIO is a stimulator of guanylate cyclase, which is known to cause relaxation of the vascular smooth muscles. Chemically RIO is Methyl N-[4,6-Diamino-2-[1-[(2-fluorophenyl)methyl]-1H-pyrazolo[3,4-b]pyridin-3-yl]-5-pyrimidinyl]-N-methylcarbamate [2].

RIO has high oral bioavailability due to unrestrained absorption and negligible pre-systematic first pass extraction. RIO undergoes biotransformation (N-demethylation) catalyzed by the various isoforms of the cytochrome P450. The principal metabolite of RIO named M1 is believed to have one-third of its activity. Further, the metabolite M1 gets converted into inactive metabolite M4 by action of uridine diphosphate glucuronosyltransferase. RIO and its metabolites are predominantly excreted through biliary, fecal (48–59%) and renal (33–45%) route [3]. Literature survey revealed couple of bioanalytical methods for the estimation of RIO and its metabolites in plasma [4,5]. Also, methods were available for estimation of RIO in bulk drug and pharmaceutical formulations using UV and HPLC [6–9]. There is a single report about stress study of RIO [10]. However, it lacks in toxicity prediction studies of drug and degradation impurities using *in-silico* tools and comparative receptor binding studies of degradants with that of RIO using molecular docking. The only similarity between present research work with that of reported one is formation of a degradation product having $m/z = 391$ under alkaline stress. The remaining degradation products having $m/z$ values of 351,270 and 315 were unknown. The work presented in the current manuscript involves characterization of all the degradation products using LC-QTOF/MS, prediction of ADMET properties using *in-silico* tools and comparative receptor binding studies of degradants with that of RIO using molecular docking.

*Abbreviations:* HPLC, High performance liquid chromatography; DPs, Degradation products; LC-QTOF, Liquid chromatography-Quadrupole time of flight; RDB, Ring double bond equivalent; mmu, Milli mass unit; RRT, Relative retention time; RT, retention time; ADMET, Absorption, Distribution. Metabolism and Excretion and Toxicity; CYP1A2, Cytochrome P450 Family 1 Subfamily A Member 2; CYP3A4, Cytochrome P450 Family 1 Subfamily A Member 4; $m/z$, mass to charge ratio.

* Corresponding author.
*E-mail address:* Chodankar.rahul@gmail.com (R.S. Chodankar).

https://doi.org/10.1016/j.jcoa.2022.100058
Received 30 March 2022; Received in revised form 10 July 2022; Accepted 11 July 2022

G-CEIP

GOA COLLEGE OF PHARMACY
EXCELLENCE IN PHARMA EDUCATION
50 GOLDEN YEARS

# Certificate of Participation

Presented to

RAHUL CHODANKAR

***in recognition of your participation in the***
*"Research Showcase Presentation (RSP)" at the*
***6th Annual International Conference on IPR***
*Global Trends in IPR: Patenting & Beyond !!*

***held on December 1-2, 2021 at Goa College of Pharmacy, Panaji-Goa***

Umesh Banakar

***Umesh Banakar, Ph.D.***
*Professor*

***Dr. Gopal Krishna Rao***
*Principal*

APPLIED PHARMACEUTICAL ANALYSIS - INDIA

# Certificate of Participation

**Is hereby granted to**

# RAHUL S CHODANKAR

**For presenting a poster on "Development of a stability indicating assay method for determination of Pimozide in the bulk drug"**

**APPLIED PHARMACEUTICAL ANALYSIS (APA) INDIA 2021**

**Virtual Poster Session**

13 November 2021

Boston International Conferences

Adam Brockman, President

## CERTIFICATE OF ANALYSIS

| | | | |
|---|---|---|---|
| Material Name : PIMOZIDE IP/USP | | | |
| Insp. Lot : 12173503<br>Report Dt. : 31.08.2018 | | | Batch No. : PIM/1807006-M<br>AR Number : 2018032362<br>Page No. : 2 / 2 |
| SR. NO. | TESTS | RESULTS | LIMITS |
| | | | secondary peaks, is not greater than 1.5 times the area of the principal peak in the chromatogram obtained with reference solution (b) (0.75 %) |
| 07 | Loss on drying | 0.30 % | Not more than 0.5% |
| 08 | Sulphated Ash | 0.06 % | NMT 0.1 % |
| 09 | Heavy metals | Within limit | Not more than 0.002% |
| 10 | Assay | 99.36 % | Between 99.0% to 101.0% |
| 11 | Bulk density (Tapped) (Inhouse Test) | 0.46 gm/ml | 0.40 gm/ml to 0.50 gm/ml |
| 12 | Particle size (Inhouse Test) | Complies | More than 90% of powder should passed through 100 mesh sieve. |
| 13 | Visible Foreign and Black Particles (Inhouse Test) | Complies | It should be free from foreign and black particles. |

Remarks : Conforms to IP & USP

ANALYSED BY :
DATE :

Q.C.HEAD :
DATE :

# CERTIFICATE OF ANALYSIS

| | | | |
|---|---|---|---|
| Material Name | : PIMOZIDE IP/USP | | |
| Manufacturer | : VASUDHA PHARMA CHEM LIMITED | | |
| Vendor Name | : VASUDHA PHARMA CHEM LIMITED | | |
| Analysis as per | : IP & USP | | |
| Insp. Lot | : 12173503 | Batch No. | : PIM/1807006-M |
| Plant | : INTAS PHARMA.LTD.,VATVA P | AR Number | : 2018032362 |
| Qty. Received | : 2.000 Kg | Mfg. Dt. | : 07/2018 |
| Receipt Dt. | : 28.08.2018 | Exp. Dt. | : 06/2023 |
| Report Dt. | : 31.08.2018 | Spec. No. | : PIMOZ06-3 |
| | | Page No. | : 1 / 2 |

| SR. NO. | TESTS | RESULT | LIMITS |
|---|---|---|---|
| 01 | Description | A white powder. | A white to almost white powder. |
| 02 | Solubility | Insoluble in water, Slightly soluble in ether, and in alcohol, freely soluble in chloroform. | Insoluble in water, Slightly soluble in ether, and in alcohol, freely soluble in chloroform. |
| 03 | Identification | Complies | A.IR graph should concordant with standard IR graph. |
| | | Complies | B.UV Absorption |
| 04 | Apperance of Solution | Complies | Solution is not more intensely coloured than referance solution YS7 |
| 05 | Melting range | 218.2° C | Between 216°C and 220°C |
| 06 | Related Substances | Pimozide Imp. A.B.C.D. and E Not Detected Total Imp. 0.47 % | In the chromatogram obtained with the test solution: the area of any peak due to pimozide impurity A,pimozide impurity B,pimozide impurity C ,pimozide impurity D,pimozide impurity E is not more than the area of the principal peak in the chromatogram obtained with reference solution (b) (0.5 per cent); the sum of the areas of all |

**MSN Life Sciences Private Limited**
Factory : Unit-II, Sy.No. 455/A,455/AA, 455/E and 455/EE, Chandampet (Village),
Shankarampet-R (Mandal),Medak District, Telangana , Pincode: 502255.India.
Phone:+91-8452-334200, Fax:+91-8452 334201 Alternative Fax: +91-40-30438799
www.msnlabs.com

## CERTIFICATE OF ANALYSIS

| | | | |
|---|---|---|---|
| Product | : **RIOCIGUAT** | Customer Name : | **MSN Laboratories PVT LTD. (Formulation Unit-II)** |
| Batch No. | : RGm0070818 | Mfg. Date | : August-2018 |
| Batch Quantity | : 1.550 Kgs | Retest Date | : January-2021 |
| AR No | : FP180290 | Date of Analysis | : 04.09.2018 |
| Reference | : In House | Specification No | : QC-FPRG-001/O3 |

**Storage :Preserve in well closed containers and store at controlled room temperature i.e. between 20°C and 25°C (excursions are allowed between 15°C and 30°C).**

| S.No. | TEST | RESULT | SPECIFICATION |
|---|---|---|---|
| 1.0 | Description | Off-white crystalline powder | White to yellowish crystalline powder. |
| 2.0 | Solubility | Complies | Freely soluble in Dimethylsulphoxide, Soluble in N,N-Dimethyl formamide; Slightly soluble in Tetrahydrofuran and insoluble in water. |
| 3.0 | Identification by | | |
| 3.1 | Infrared absorption | Complies | The infrared absorption spectrum of the sample shall be concordant with that of Riociguat standard spectrum. |
| 3.2 | HPLC | Complies | The major peak retention time of sample shall match with major peak retention time of the standard, as obtained in the Assay by HPLC. |
| 4.0 | Water content by KFR | 0.42% w/w | Not more than 0.50%w/w |
| 5.0 | Residue on ignition | 0.06% w/w | Not more than 0.1% w/w |
| 6.0 | Related substances by HPLC | | |
| 6.1 | Carbamate impurity | 0.03% | Not more than 0.15% |
| 6.2 | Des fluoro impurity | Less than LOQ(0.0186%) | Not more than 0.15% |
| 6.3 | Dimethyl impurity | Less than LOQ(0.0200%) | Not more than 0.15% |
| 6.4 | Highest individual unspecified impurity | 0.04% | Not more than 0.10% |
| 6.5 | Total impurities | 0.13% | Not more than 0.50% |
| 7.0 | Assay by HPLC (On anhydrous basis and solvent-free basis) | 100.2% w/w | Not less than 98.0% w/w and Not more than 102.0% w/w |

MSN Life Sciences Private Limited, Unit-II * Q.A. Dept. * 09/01/2019

FOR REFERENCE ONLY

The product CONFORMS to above specifications

**Compiled by :** G.L **Date :** 09/01/19

**Checked by :** **Date :** 09/01/19

**Head, Quality Control:** **Date :** 09/01/19

**MSN Life Sciences Private Limited**
Factory : Unit-II, Sy.No. 455/A,455/AA, 455/E and 455/EE, Chandampet (Village), Shankarampet-R (Mandal),Medak District, Telangana , Pincode: 502255.India.
Phone:+91-8452-334200, Fax:+91-8452 334201 Alternative Fax: +91-40-30438799
www.msnlabs.com

## CERTIFICATE OF ANALYSIS

| | | | |
|---|---|---|---|
| Product | : **RIOCIGUAT** | Customer Name : | **MSN Laboratories PVT LTD. (Formulation Unit-II)** |
| Batch No. | : RGm0070818 | Mfg. Date | : August-2018 |
| Batch Quantity | : 1.550 Kgs | Retest Date | : January-2021 |
| AR No | : FP180290 | Date of Analysis | : 04.09.2018 |
| Reference | : In House | Specification No | : QC-FPRG-001/03 |

**Storage :Preserve in well closed containers and store at controlled room temperature i.e. between 20°C and 25°C (excursions are allowed between 15°C and 30°C).**

| S.No. | TEST | RESULT | SPECIFICATION |
|---|---|---|---|
| 8.0 | Acetic acid content by HPLC | Not detected | Not more than 5000 ppm |
| 9.0 | Residual solvents by GC (Method-I) | | |
| 9.1 | Methanol | Not detected | Not more than 3000 ppm |
| 9.2 | Acetone | Not detected | Not more than 5000 ppm |
| 9.3 | Isopropyl alcohol | Not detected | Not more than 5000 ppm |
| 9.4 | Acetonitrile | Not detected | Not more than 410 ppm |
| 9.5 | Dichloromethane | Not detected | Not more than 600 ppm |
| 9.6 | Ethyl acetate | 410 ppm | Not more than 5000 ppm |
| 9.7 | Tetrahydrofuran | Not detected | Not more than 720 ppm |
| 9.8 | Toluene | Not detected | Not more than 890 ppm |
| 10.0 | Residual solvents by GC (Method-II) | | |
| 10.1 | N,N-Dimethylformamide | Less than LOQ(106ppm) | Not more than 880 ppm |
| 10.2 | Dimethyl sulphoxide | Not detected | Not more than 5000 ppm |
| 11.0 | Polymorphic identification By PXRD | Complies | The PXRD pattern of sample should exhibit, the presence of 2-Theta value of Riociguat crystalline modification-I Form 6.7,9.1,17.8,20.2,25.6 and 27.3 ± 0.2 theta. |

MSN Life Sciences Private Limited, Unit-II Q.A. Dept. 09/01/2019

The product CONFORMS to above specifications

**Compiled by :** 09/01/19 **Date :**

**Checked by :** 09/01/19 **Date :**

**Head, Quality Control :** 09/01/19 **Date :**

# Goa University

(Establishment by State Legislature by Notification No:LD/10/7/84(D) of year 1984)
Sub P.O. Goa University, Taleigao Plateau, Goa, PIN 403206

**Certificate of similarity check for plagiarism detection**

| | | |
|---|---|---|
| 1 | Name of the Research Scholar | : Mr. Rahul S. Chodankar |
| 2 | Title of the **Thesis** | : Stability Profiling of Certain active Pharmaceutical Ingredients. |
| 3 | Name of the Supervisor | : Dr. Anand A. Mahajan |
| 4 | Dept/School/Institution/Research Centre | : Goa College of Pharmacy |
| 5 | Similar Content Identified in % | : 0% |
| 6 | Software used | : Ouriginal |
| 7 | Date of checking | : 10/05/2023 |

First page of the report of similarity check indicating percentage of similarity is attached.

Similarity check conducted by

Name, Designation and Signature

Mr. Nandkishor K. Bandekar
Asst. Librarian
Goa University

Name & Signature of the Research Scholar: 10/05/2023

Name & Signature of the Research Supervisor: Dr. Anand A Mahajan 10/05/2023

Name & Signature of HOD/Vice Dean (Research):

Name & Signature of Dean (Faculty/School): with seal 19/05/2023

Principal
Goa College of Pharmacy
Panaji Goa

Dr. Gopal Krishna Rao
Dean,
Faculty of Pharmacy,
Goa University,
Taleigao Plateau,
Goa-403206

## Document Information

| | |
|---|---|
| **Analyzed document** | Rahul chodankar.docx (D166419666) |
| **Submitted** | 2023-05-10 07:40:00 |
| **Submitted by** | Nandkishor B. |
| **Submitter email** | asstlib2@unigoa.ac.in |
| **Similarity** | 0% |
| **Analysis address** | asstlib2.unigoa@analysis.urkund.com |

10/5/23

## Sources included in the report

W URL: https://sphinxsai.com/2016/ph_vol9_no3/1/(171-180)V9N3PT.xml 1
Fetched: 2021-10-05 13:32:58

W URL: https://www.academia.edu/46960699/A_novel_stability_indicating_RP_HPLC_method_development_and_... 1
Fetched: 2022-07-18 11:31:53

W URL: https://www.pharmaffiliates.com/en/1361569-10-9-6-amino-2-1-2-fluorophenyl-methyl-1h-pyrazolo-... 2
Fetched: 2021-10-11 11:49:50

## Entire Document